Characterization of the olfactory circuit and computation in an insect *Hieroglyphus* banian

A thesis submitted during 2020 to the University of Hyderabad in partial fulfilment of the requirements for the award

of

Doctor of Philosophy

in

Cognitive Sciences

by

Shilpi Singh



Centre for Neural and Cognitive Sciences School of Medical Sciences

University of Hyderabad, (P.O) Central University, Gachibowli, Hyderabad-500 046 Telangana, India

December 2020



University of Hyderabad

Centre for Neural and Cognitive Sciences, School of Medical Sciences (P.O) Central University, Gachibowli, Hyderabad-500 046
Telangana, India

DECLARATION

I, Shilpi Singh, hereby declare that this thesis entitled, "Characterization of the olfactory circuit and computation in an insect *Hieroglyphus banian*" submitted by me under the guidance and supervision of **Dr. Joby Joseph** is a bonafide research work. I also declare that it has not been submitted previously in part or in full to this University or any other University or Institution for the award of any degree or diploma. I also declare that this is a bonafide work which is free from plagiarism.

A report on plagiarism statistics from the University Librarian is enclosed.

Date: 31.12.2020 Hyderabad Shilpi Singh Registration no: 10CCPC02



University of Hyderabad

Centre for Neural and Cognitive Sciences, School of Medical Sciences (P.O) Central University, Gachibowli, Hyderabad-500 046
Telangana, India

CERTIFICATE

This is to certify that the thesis entitled 'Characterization of the olfactory circuit and computation in an insect *Hieroglyphus banian*' submitted by Ms. Shilpi Singh bearing registration no 10CCPC02 in partial fulfilment of the requirements for the award of Doctor of Philosophy in Cognitive Sciences is a bonafide work carried out by her under my supervision and guidance.

The thesis has not been submitted previously in part or in full to this or any other University or Institution for the award of any degree or diploma.

(**Dr. Joby Joseph**)
Research Supervisor

(**Prof. Ramesh K. Mishra**) Head of the Department/Centre

(**Prof. Prakash Babu**)

Dean of the School



CERTIFICATE

This is to certify that the thesis entitled 'Characterization of the olfactory circuit and computation in an insect *Hieroglyphus banian*' submitted by Ms. Shilpi Singh bearing registration no 10CCPC02 in partial fulfilment of the requirements for the award of Doctor of Philosophy in Cognitive Sciences is a bonafide work carried out by her under my supervision and guidance.

The thesis has not been submitted previously in part or in full to this or any other University or Institution for the award of any degree or diploma.

Parts of this thesis have been:

- A. Published in the following journal: Journal of Comparative Physiology A (2019); 205, 813–838
- B. Presented in the following conferences/workshops:
 - 1. Conference on Frontiers in Olfaction at International Center for Theoretical Physics, Trieste, Italy from 24th–28th July, 2017
 - 2. 39th Annual conference of the Ethological Society of India themed 'National Conference on Ethology and Evolution' at IISER, Mohali from 30th October–1st November, 2015
 - 3. 32nd Annual conference of the Indian Academy of Neurosciences at NIMHANS, Bengaluru, 1st–3rd November, 2014
 - 4. 25th Annual Meeting of Society for Neurochemistry in India (SNCI) at University of Hyderabad, 7th–9th January, 2011
 - 5. Workshop organized by the National Network for Mathematical and Computational Biology (NNMCB) at IISER, Kolkata from 9–10th January, 2016

Further, the student has passed the following courses towards fulfillment of coursework requirement for PhD.

S. no	Course code	Course name	Credits	Pass/Fail
1.	CO801	Formal and Computational Approaches to Cognition (FCAC)	4	Pass
2.	CO802	Empirical bases of cognition	4	Pass
3.	CO803	Language, Philosophy and Cognition (LPC)	4	Pass
4.	CO804	Topics in Cognitive Science: Dissertation oriented readings 'Synchronization in the neuronal systems'	4	Pass
5.	CO805	Statistical methods and research methodology	4	Pass
6.	CO806	Information processing in the nervous system II	4	Pass
7.	CO810	Reading course: Structure and function of the insect nervous system	4	Pass
8.	CO812	Reading course: Computational intelligence and neural networks	4	Pass

(**Dr. Joby Joseph**)
Research Supervisor

(**Prof. Ramesh K. Mishra**) Head of the Department/Centre

(**Prof. Prakash Babu**)
Dean of the School

Dedicated to

Momma, Daddyjee
Priyanka, Prince and Dr. Payal
for not giving up on me through a journey of a lifetime

My mentor, Dr. Joby Without whose support, I would have given up long back

& Myself
Because I deserve this one

Acknowledgements

A decade long rollercoaster of a journey, with a pandemic to top it off, at the end! My PhD has been a learning experience comparable to no other, and in spite of all the ups and downs, it is a defining part of my life because of the *people* who have been with me in this journey.

At the outset, I would like to thank the University of Hyderabad for fostering an environment of 'a spirit of enquiry and questioning', and respectful disagreement. It was a pleasure to spend my time in a naturally beautiful campus, a cauldron of Indian diversity with the best of mentors, students and staff. The common facilities of the university greatly helped me during my PhD work. The nominal tuition and hostel fees along with the fellowship sponsored by them sustained me for many years and made it possible to do my PhD without being a financial burden on my family. I would also like to credit the University environment for my social awakening and sensitization to various issues of the society. This University will always hold a special place in my heart and I credit it for my wholesome growth.

I wish to tender my special thanks to the amazing 'Centre for Neural and Cognitive Sciences'. This department was instrumental in giving me a wholesome exposure to the multidisciplinary nature of Cognitive Science and its environment of open discussion sans any hierarchy enabled me to develop as a matured researcher.

Thanks are also due to Prof. Prakash Babu, the Dean of School of Medical Sciences, with whom I have also interacted when he was the Dean of Student Welfare. In both capacities, he has always been incredibly kind and helpful with all the official work and I am highly obliged to him for it.

I cannot express enough appreciation for the present Head of Centre for Neural and Cognitive Sciences, Prof. Ramesh Mishra, for being very proactive and invested in the growth of the department, for always pushing us to publish more and thus contribute to the research output of the Centre. My sincere thanks are also due to the previous Heads of the Centre, Prof. Vipin Srivastava and Prof. S. Bapiraju, for being the strong foundations on which this department was built. It was under their experienced guidance that I joined this department for my PhD. Prof. S. Bapiraju has been extremely supportive in this regard. Interactions with him have always surrounded me with a positive vibe and strengthened my resolve to do good science.

I also wish to express my heartfelt gratitude to Prof. Aparna Dutta Gupta, my doctoral committee member, who is no longer with us, for her unflinching support and encouragement throughout my PhD journey. All the first solutions for my experiments were made in her lab and her unparalleled aid can never be forgotten

by me. It was from her that I learnt that when one is in a position of authority and means, one should enable the rise of others who are just starting their careers. The support and encouragement which she provided can never be forgotten by me. You will always be missed Ma'am!

I also wish to express my sincere gratitude to Prof. Prajit Basu and Dr. Kiranmayi, whose classes of Philosophy and Neurobiology helped me to broaden my knowledge of Cognitive Science. A big thanks to Dr. Sudipta Saraswati and Dr. Akash for their constant help, support and encouragement. Dr. Sudipta has especially been a treasure-trove of information about how to go about my future career; he goes out of his way to help and discussions with him has always been enlightening. Dr. Akash has always been very approachable and interactions with him always leave a positive and happy vibe. Interaction with these awesome professors has greatly added to my knowledge and experience. These are the people who have helped to make the Department an incredible place to do good science.

By far, my greatest gratitude is reserved for my PhD mentor, Dr. Joby Joseph, who has been immensely patient, encouraging and inspiring throughout my PhD journey. He has been a role model like no other and my gratitude for him cannot be measured in words. He always had my back, no matter what, which allowed me to focus on my work. He has created a lab environment which is conducive to explore not only our specified research area, but also, beyond that, anything which catches our attention. His training has instilled in me the courage to ask questions and the importance of asking worthy research questions. It's said that, 'A teacher affects eternity, he never knows where his influence ends'. This is completely true with respect to my mentor. His constant availability, instant help and advice; and his patience and enthusiasm for science will be treasured by me forever and is the framework which I wish to emulate in future. In addition to learning the ropes of carrying out good science, I have also learnt how to be a kind human being from him. Many thanks, Joby, for being the awesomest mentor I could have asked for!

The past and present office staff of Centre for Neural and Cognitive Sciences Lakshmi, Ramchander, Shalini, Keerthi, Sharada, and Vijay can't be thanked enough for all the assistance which they have provided and continue to be providing in traversing the maze of administrative rigmarole. All of them have been eternally patient and helpful to the numerous queries and doubts I ever had during my journey. Thanks are also due to Ramesh for taking excellent care of our insect room.

I have been extremely fortunate and blessed to be bestowed by amazingly lovely lab mates. I call them my 'second family', because we have together been through numerous heartbreaks, struggles, ups and downs and the frustration of the PhD journey. We have also experienced the ecstasy of success, of publishing papers, of

getting the spikes of those elusive neurons for the first time, of getting beautiful fills of neurons, of finishing PhD at almost the same time (Sandhya and Meenakshi), and of going through the whole rigmarole of the PhD journey together. They are the ones who have shared all of it and can truly empathize with this journey. And they always provided a respite from the daily grind by their support and life lessons. A big shout out to you all—Shalini, Sivaraju, Sandhya, Dr. Meenakshi and Bhavana. You all have been my cheerleader as well as my agony aunts! I can never forget the bird walks, birthday/new year/Christmas/Holi celebrations; food/movie trips; campus food; adda sessions, which I shared with you all.

I extend my heartfelt thanks to Uttam, Dr. Gokul, Shubhodeep, Ananya, Dr. Madhura and Dr. Ashwin; Dr. Hiren, Anuj and Dr. Nidhi for providing me with some of the best memories of my PhD journey. Time spent with you all was filled with fun and laughter. Suchitra, Dr. Vishnu, Dr. Tony, Dr. Neelakanteswar, Ankit, Kamala, Sanjay, Abhilash are other very dear friends from the department who have been immensely helpful, supportive and enjoyable company throughout my PhD.

Anvita and Shalini, words are not enough to express my love and appreciation for the fact that you two have been part of my journey. You have had my back through thick and thin, always supporting me, always encouraging me and always motivating me to do my best. Both of you have been witness to my worst days and my best ones, my love for you is boundless. Thank you very much for being who you are and for being my friends!

Throughout this journey, some of my oldest friends have provided the necessary distraction and companionship. My heartfelt gratitude to my school friends, Malobika and Amrita; friends from Bachelors, Dr. Harmeet, Alpana, Dr. Anamika, Nazma, Dr. Parmita and Arpita; friends from Masters, Dr. Shiksha, Dr. Surya Prakash and Dr. Rakesh; and Dr. Pushpa for always being there, and being understanding, even when I missed all your weddings, childbirths, anniversaries and birthdays. Love and hugs to you all. You are an inseparable part of my life, and all of you make my life more beautiful with the memories of the fun times we spent together.

In the end, I have reserved my heartfelt gratitude for my family, without whose support I'd not have reached this point. Since my childhood, my parents have been the most supporting people behind me. They made sure that education is of highest priority in the family and always pushed us to ascend new heights and milestones. There was no challenge intimidating, no obstacle a stumbling block but rather an opportunity worth giving a shot at. They have been the source of unending encouragement and support in whatever I chose to do. Mom, I aspire to be a strong

woman, like you someday and Daddyjee, the goodness of your heart, inspires me to be a better version of myself always!

I am immensely grateful to my siblings, Priyanka, Prince and Dr. Payal for being the shock absorbers in my life. Especially, in the last two years, my younger sister, Dr. Payal, has been a sounding board for all the highs and lows of PhD life. Soft-spoken jijajee and my niece, Aayanshi, have ensured that I remember to have fun. I can never thank you all enough!

In the end, I extend my gratitude to Science and everybody who is in the quest of rational knowledge—the constant endeavor to unravel the truth and to understand nature. To all the discoveries of the past and many more such discoveries in future—thanks to all those who worked for it and continue working for it!

Contents

Declaration	ii
Certificate	iii
Dedication	vi
Acknowledgements	vii
Table of Contents	xi
Abbreviations	xvi
List of Tables	xviii
List of FiguresList of Figures	ix
Chapter 1 Introduction	1
1.1 Olfaction	1
1.2 Nature of olfactory stimuli	2
1.3 General overview of the insect olfactory circuit	2
1.3.1 First-order olfactory structures—antenna and sensilla	3
1.3.2 First-order olfactory neurons and their properties	5
1.3.3 Second-order olfactory structure—the antennal lobe (AL)	9
1.3.4 Second-order olfactory neurons—interneurons of AL	12
1.3.5 Antennal lobe tracts (ALTs) to the mushroom body and lateral horn.	15
1.3.6 Third-order olfactory structure—mushroom body (MB)	15
1.3.7 Third-order olfactory neurons and their properties—Kenyon cells (K	Cs)18
1.3.8 Third-order olfactory structure—lateral horn and its neurons	19
1.3.9 Fourth-order olfactory neurons—alpha lobe neurons (aLNs) and	beta lobe
neurons (bLNs)	21
1.3.10 Fourth-order inhibitory neurons of the mushroom body	
1.4 The olfactory circuit of Schistocerca americana/Schistocerca gregaria	26
1.5 Objectives of the study	36

Chapter 2 Materials and methods	,38
2.1 Animals	38
2.2 Dissection of animals for experiments	39
2.3 Odorants used during experiments	41
2.4 Set-up for delivery of odor stimuli to the animal	42
2.5 Electrophysiology	42
2.5.1 Electroantennogram (EAG) recording	42
2.5.2 Intracellular recording	43
2.5.3 Extracellular recording	44
2.5.4 Electrical stimulation	45
2.6 Immunohistochemistry of whole mount of brain	45
2.7 Neural tract tracing	47
2.8 Antennal backfills	47
2.9 Confocal microscopy	48
2.10 Processing of antennae for FE-SEM	
2.11 Data analysis	49
2.11.1 Detecting LN and PN spikes from AL interneuron recordings	49
2.11.2 Cross-correlation	49
2.11.3 Calculating power spectrum	50
Chapter 3 Morphological and physiological characterization of the olfactory circuit of grasshopper <i>Hieroglyphus banian</i> through the foorder neurons	ourth-
3.1 Introduction	
3.2 Results	
3.2.1 Types of sensilla found on the antennae of <i>H. banian</i>	
3.2.2 Tracts from the antennal lobe and lobus glomerulus to the higher	
centers	
3.2.3 A novel tract, CT (curved tract)	
3.2.4 Antennal lobe in <i>H. banian</i> has a microglomerular organization	
3.2.5 Morphology and physiology of projection neurons in the antennal lol	be 62

3.2.6	Morphology and physiology of local neurons in the antennal lobe62
3.2.7	Nature of the local field potential in mushroom body66
3.2.8	Features of odor response of Kenyon cells68
3.2.9	Features of lateral horn neurons70
3.2.10	Morphology, types and physiological features of beta lobe neurons73
3.2.11	Morphological, immunohistochemical and physiological features of GGN 76
3.3 Discus	sion
	Is the methodology used to establish similarities between the two species ed and adequate?
	Types of surface sensilla in <i>H. banian</i> closely resemble those in <i>Schistocerca</i> 80
3.3.3	Multiple AL tracts in <i>H. banian</i> —a general trend or an exception81
3.3.4	A novel tract—CT84
3.3.5	Similar neuropils in <i>H. banian</i> and <i>S. americana</i> 84
3.3.6	The tritocerebral tract84
3.3.7	Microglomerular organization of the AL is a feature of family Acrididae85
3.3.8	Interneurons of AL in H. banian closely resemble those in S. americana85
	Conserved anatomical and physiological features of third-order olfactory s—MB and LH
	Conserved anatomical and physiological features of fourth-order olfactory ns—bLNs and GGN
	How different is the olfactory system in vertebrates belonging to different milies?90
3.4 Conclu	usion91
-	roperties of a novel group of bilateral extrinsic neurons of the body in the olfactory circuit of <i>Hieroglyphus banian</i> 98
4.1 Introdu	action98
4.2 Result	s99
4.2.1	Morphological, immunohistochemical and physiological features of MBEN1
	99
4.2.2	Morphological, immunohistochemical and physiological features of MBEN2
	101

4.2.3 Morphological and physiological features of a different bilateral neu	ron 103
4.2.4 Features common to the three bilateral neurons	104
4.3 Discussion	105
4.3.1 Bilateral alpha lobe neurons	106
4.3.2 Bilateral neurons connecting both pedunculi	107
4.3.3 Bilateral neuron with arborization in the superior lateral protocereb	orum (SLP)
	108
4.3.4 Multiplex organization and interaction of olfactory information	108
4.3.5 Unique response pattern of MBENs to odor stimuli	109
4.4 Conclusion	110
Chapter 5 Adaptive modulation of an inhibitory recurrent circuit s serving gain control in the mushroom body network	111
5.1 Introduction	
5.2.1 GGN-IG-KC network in <i>Schistocerca</i>	
5.2.2 IG spikes can be detected unambiguously from GGN membrane potentials.	
5.2.3 IG responds to different odorants with odor-specific temporal pattern	
5.2.4 IG is odor responsive to some odorants even when GGN is not	
5.2.5 IG receives odor input from KCs	
5.2.6 Concentration-dependent odor response properties of IG	
5.2.7 Where is the delay in odor response onset at lower concentration originating?	ns in GGN
5.2.8 KC-IG synapse shows short term plasticity similar to KC-GGN syna	ıpse125
5.2.9 Nature of GGN innervation in the LH	127
5.2.10 Role of neural circuitry involving KC-GGN-IG in processin information	-
5.3 Discussion	131
5.3.1 The odor-response properties of the IG	132
5.3.2 Role of IG in the circuit	135
5.3.3 Nature of GGN innervation in LHN	137
5.3.4 Probable identity of IG	138
5.4 Conclusion	139

Chapter 6 Conclusion	140
Bibliography	144
Anti-Plagiarism Certificate	166
Publications and Conferences	169

Abbreviations

ACh Acetylcholine

AL Antennal lobe

ALT Antennal lobe tract

AN Antennal nerve

APL Anterior paired lateral neuron

aLN α-lobe neuron bLN β-lobe neuron CT Curved tract

EAG Electroantennogram

EPSP Excitatory postsynaptic potential

GGN Giant GABAergic neuron

IG Inhibitor of GGN

IPI Inter-pulse interval

IPSP Inhibitory postsynaptic potential

IR Ionotropic receptor

KC Kenyon cell

lALT Lateral antennal lobe tract

LH Lateral horn

LHN Lateral horn neuron

LOG Lobus glomerulus

LFP Local field potential

LN Local neuron

LPL Lateral protocerebral lobe

mALT Medial antennal lobe tract

mlALT Mediolateral antennal lobe tract

MB Mushroom body

MBEN Mushroom body extrinsic neuron

OR Odorant receptor

ORN Olfactory receptor neuron

OB Olfactory bulb

PSTH Peri-stimulus time histogram

PN Projection neuron

PP Paired-pulse

PPF Paired-pulse facilitation

STA Spike triggered average

tALT Transverse antennal lobe tract

TT Tritocerebral tract

List of Tables

1.1 Classification of insect sensilla	5
1.2 Numerical strength of ORs and ORNs across insect species	6
1.3 Antennal nerve tracts reported in different insect species	9
1.4 Numerical strength of AL glomeruli reported across insect species	11
1.5 LNs and PNs in insect antennal lobe	13
1.6 Antennal lobe tracts (ALTs) across insect species	16
1.7 Kenyon cell numbers and neurotransmitter profile across insect species	18
1.8 Numerical properties of the olfactory circuit of locust	29
3.1 Numerical strength of olfactory pathway neurons in different vertebrates	91
3.2 Comparison of features of the olfactory pathways of S. americana and H. banian	93

List of Figures

1.1 Orientation of brain in the head capsule of insect <i>Hieroglyphus banian</i>	3
1.2 Insect antennal diversity, parts of an antenna and internal structure of an an	tennal
sensillum	4
1.3 Olfactory transduction in the insect sensilla	8
1.4 Anatomical features of the first-order and second-order olfactory centers in Schiste	ocerca
spp. or Locusta migratoria	28
1.5 Morphology of higher-order neurons in <i>Schistocerca</i> spp	34
2.1 Hieroglyphus banian	38
2.2 Animal preparation for dissection	40
2.3 Location of antennal transection for antennal-backfill experiment	47
3.1 External morphology of sensilla found on the antenna of <i>H. banian</i>	55
3.2 Electroantennogram (EAG) varies across the length of the <i>H. banian</i> antennae	57
3.3 Major neuropils in the brain of <i>H. banian</i>	58
3.4 Antennal lobe and lobus glomerulus tracts in <i>H. banian</i>	60
3.5 Morphological and immunohistochemical features of the projection neurons in AL	61
3.6 Physiological properties of AL PNs	63
3.7 Morphological and immunohistochemical features of the local neurons in AL	64
3.8 Physiological properties of LNs	64
3.9. Synaptic interaction between the interneurons of AL	65
3.10 Features of the local field potential (LFP) recorded from the MB	67
3.11 Properties of odor-evoked oscillation in MB LFP	68
3.12 Physiological properties of the Kenyon cell	69
3.13 Kenyon cells respond to odorants in a cell-odor-specific manner	70

3.14 Morphological and physiological characteristics of unilateral third-order lateral horsevers (LUNe)	
neurons (LHNs)	
3.15 Morphological and physiological characteristics of bilateral third-order LHNs	
3.16 Morphological and physiological properties of the fourth-order beta lobe type 1 neuro	
(bLN1)	
3.17 Morphological and physiological properties of the fourth-order beta lobe type 2 neuro	
(bLN2)	
3.18 Morphology and physiological properties of Giant GABAergic Neuron (GGN)	
3.19 GABAergic innervation of the MB	
3.20 Schematic summarizing the olfactory circuit in <i>H. banian</i>	78
4.1 Morphology of mushroom body extrinsic neuron type 1 (MBEN1)1	.00
4.2 Physiology of MBEN1	01
4.3 Morphology of MBEN2	02
4.4 Physiology of MBEN2	03
4.5 Morphology and physiology of another bilateral neuron	04
5.1 Schematic of the KC-GGN-IG olfactory circuit in <i>S. americana</i>	14
5.2 Physiological properties of IG can be derived from GGN membrane potential1	15
5.3 IG responds to odorants in an odor-specific way1	17
5.4 IG is strongly responsive to odors even when the GGN is not	18
5.5 GGN and IG respond to various odorants differently	19
5.6 IG gets its odor-input downstream of Kenyon cells	20
5.7 GGN and IG receive input downstream of KCs	22
5.8 GGN responds to lower concentration of odorant with a delay	23
5.9 Delay in the onset of odor response is observed downstream of mushroom body Keny	on
cells	25
5.10 KC-IG and KC-bLN synapses show paired-pulse facilitation similar to KC-GO	
synapse1	
5.11 Odor-responsive LH neurons are inhibited when MB KCs are electrically stimulated 1	
5.12 Schematic of the KC-GGN-IG circuitry incorporating all the features discovered in t	
	30

5.1 Schematic overview (modelled on published data in <i>Schistocerca</i> spp. and primary data	1 1 T
his study) of the olfactory circuit in <i>H. banian</i> from the second order (antennal lobe) to	the
Fourth order (β-lobe and GGN) including the newly discovered MBENs1	.42
5.2 Schematic of the KC-GGN-IG circuitry incorporating all the features discovered in t	his
study1	43

Chapter 1

Introduction

"My dear young fellow," the Old-Green-Grasshopper said gently, 'there are a whole lot of things in this world of ours you haven't started wondering about yet."

—Roald Dahl

1.1 Olfaction

Olfaction is one of the five sensory modalities which enable us to make sense of the world around us and drives our behavioral responses. It is also one of the oldest sensory systems phylogenetically (Hosek and Freeman 2001; Merrick et al. 2014) and has been well-studied across vertebrates and invertebrates. Since the basic structural design and functional principles of the olfactory circuit are conserved across vertebrates and invertebrates (Hildebrand and Shepherd 1997; Strausfeld and Hildebrand 1999; Ache and Young 2005), principles of olfactory information processing can be studied in invertebrates like insects which provide an accessible and numerically simpler circuit.

The olfactory circuit of insects has thrown light and given insights into many aspects of sensory coding and plasticity (Laurent 2002; Carey and Carlson 2011) and has become an indispensable part of olfactory studies. Olfaction plays an important role in many insect behaviors—foraging for food, mate selection, oviposition, and aggregation, avoiding

unpleasant or dangerous situations. Olfactory circuit has been well-characterized (both anatomically and physiologically) in a wide variety of insect species across orders.

In the following sections, a brief overview of the olfactory circuit in insects from the periphery to the fourth-order levels is presented and the questions which have been addressed in the thesis are outlined at the end of this chapter.

1.2 Nature of olfactory stimuli

Unlike sensory modalities like vision and audition where the stimuli space can be clearly defined and represented by a single parameter (wavelength and intensity of light or frequency and loudness of sound), the olfactory stimuli is highly complex (Grabe and Sachse 2018). The odor space is multidimensional; encompassing an enormous and nearly infinite number of stimuli (Korsching, 2001; Grabe and Sachse 2018). Not only this, the olfactory circuit is sensitive to and adept in identifying and categorizing odor concentrations varying over orders of magnitudes or composed of multimolecular mixtures (Laurent 2002; Grabe and Sachse 2018). Another feature of the odor stimuli is its turbulent nature in space. Odor stimuli are often encountered by animals in highly complex odor plumes, within which the odor landscape can vary widely with intermittent zones of high and low odor concentrations (Murlis and Jones, 1981; Murlis et al. 1992; Riffell et al., 2008). In spite of all this, the olfactory circuit does an impressive feat of detecting, classifying, analyzing and discriminating the chemical volatiles present in the environment.

1.3 General overview of the insect olfactory circuit

The primary olfactory organs of insects, analogous to nose in human, are a pair of antennae located on the head, bearing sensilla. In some insects, olfactory sensilla are also present on the maxillary and labial palps on the mouth (Keil and Hansson 1999). The sensilla bear the

first-order olfactory receptor neurons which relay olfactory information to the antennal lobe (AL) in the brain. The insect brain is divided into protocerebrum, deutocerebrum and tritocerebrum and is generally suspended in the head capsule of the insect anterior to the esophagus (**Fig. 1.1 A and B**). AL is part of the deutocerebrum (Burrows 1996). From the AL, the olfactory information is transmitted to mushroom body and lateral horn in the protocerebrum (Burrows 1996).

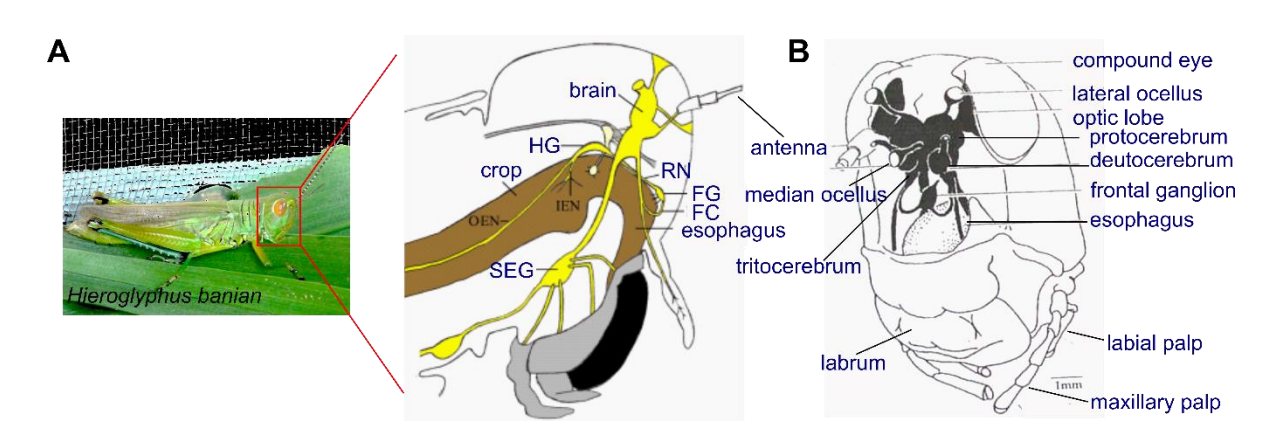


Figure 1.1 Orientation of brain in the head capsule of insect *Hieroglyphus banian*. A) Schematic showing the lateral view of the grasshopper head capsule with reference to the relative positions of the foregut, central nervous system and stomatogastric nervous system. FC: frontal connective; FG: frontal ganglion; HG: hypocerebral ganglion; IEN: inner esophageal nerve; OEN: outer esophageal nerve; RN: recurrent nerve; SEG: subesophageal ganglion; Schematic adapted from Rand et al. (2012) **B**) Schematic showing the frontal view of the orientation of the grasshopper brain inside the head capsule. Adapted from (Burrows 1996)

1.3.1 First-order olfactory structures—antenna and sensilla

Antenna are the primary olfactory organs in insects and can be of many different shapes and sizes, mainly to facilitate the detection of volatile molecules in the environment (**Fig. 1.2 A**). In hemimetabolous insects, they are flagellar while in holometabolous insects, they can be transformed in a wide variety of shapes to facilitate olfaction (Keil and Hansson 1999). An antenna is divided into three main parts—the scapus, the pedicel and the flagellum (**Fig. 1.2 B**). It bears hair-like structures called sensilla which are the smallest functional sensory unit.

In some insects (*Locusta migratoria*, *Gryllus bimaculatus*, *Drosophila melanogaster*, *Aedes aegypti*), olfactory sensilla are also present on maxillary and labial palps on the mouth (Keil and Hansson 1999).

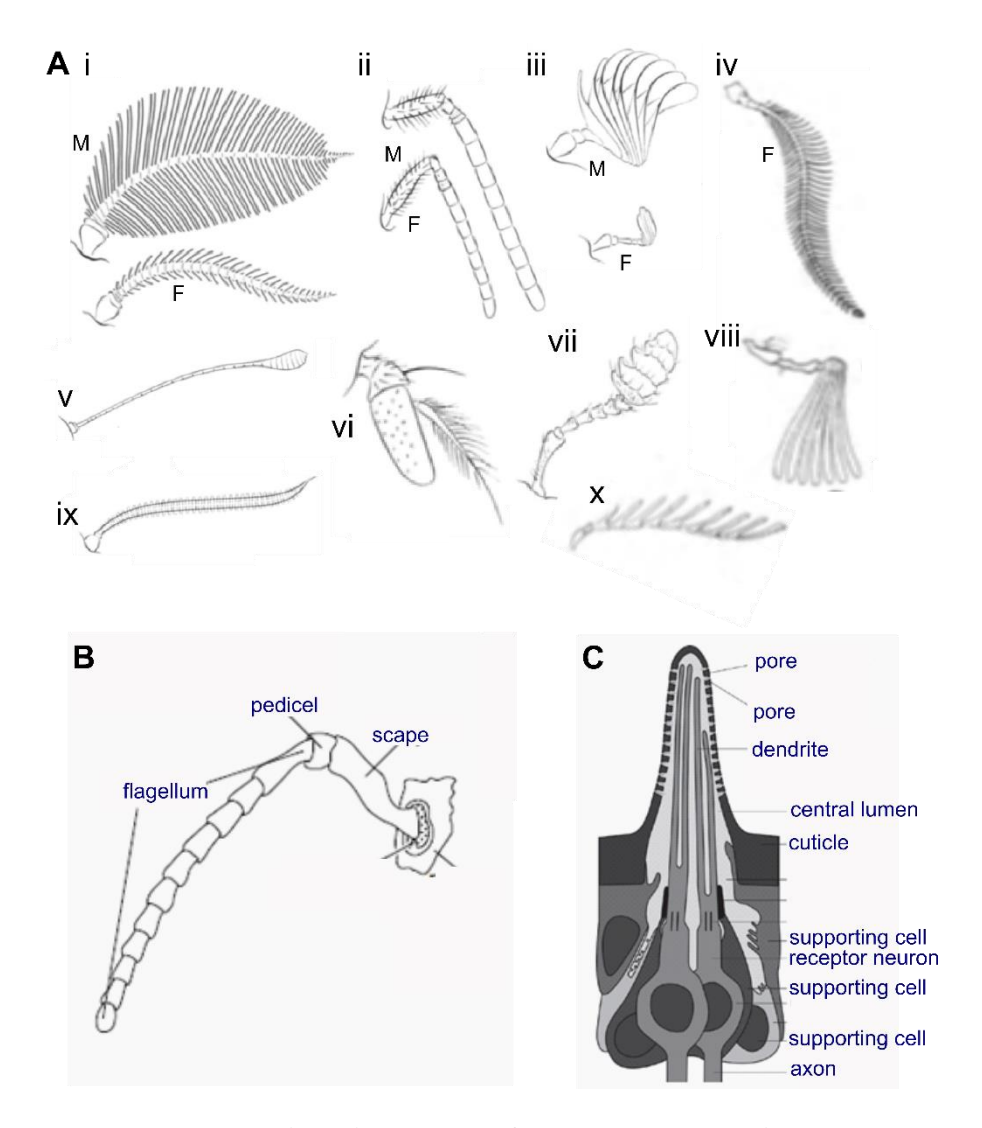


Figure 1.2 Insect antennal diversity, parts of an antenna and internal structure of an antennal sensillum. (A) Antennal diversity across insect species: i) Saturniid moth (Lepidoptera: genus Antheraea) ii) Apis mellifera (Hymenoptera: Apidae) iii) Scarabid beetle (Coleoptera: genus Rhopaea) iv) Cerura vinula (Lepidoptera: Notodontidae) v) Butterfly (Lepidoptera: genus Vanesa) vi) Fleshfly (Diptera: genus Sarcophaga) vii) Cariion beetle (Coleoptera: genus Necrophorus) viii) Melonontha melonontha (Coleoptera: Scarabaeidae) ix) Hawkmoth (Lepidoptera: Sphingidae; genus Pergosa) x) Corymbites pectinicornis (Coleoptera: Elateridae); F: Female; M: Male; Adapted from (Kaissling 1971; Keil and Hansson 1999; Elgar et al. 2018)

(B) Parts of an antenna (example from order Orthoptera); Adapted from (Chapman 1998) **(C)** Longitudinal section of an olfactory sensillum showing its internal organization; Adapted from (Chapman 1998)

In the female moth *Manduca sexta*, eight types of sensilla have been reported, two basiconic, two trichoid, two coeloconic, one auriculate and one styliform complex (Shields and Hildebrand 2001) while nine types have been described in the male *M. sexta* (two basiconic, two trichoid, two coeloconic, two chaetic and one styliform complex; (Lee and Strausfeld 1990)). Five types among the above are olfactory (Shields and Hildebrand 2001). A summary of the different types of sensilla present on the antenna of insects and their function is mentioned in **Table 1.1**.

Table 1.1 Classification of insect sensilla

Basis of classification	Sensilla type	Function
Morphological	Basiconica	olfactory
classification		
(as seen under light microscope)	Coeloconica	olfactory
	Trichodeum	olfactory
(Schenk 1903)		
	Chaetica	taste receptor/
		mechanoreceptor
Based on the structure of	Wall pore-sensilla	generally olfactory
sensilla wall	single- and double-walled	
(as seen in TEM)		
	Tip pore sensilla	mostly gustatory
(Altner 1977; Altner and	single-walled	
Prillinger 1980)		
	No pore sensilla	mechanoreceptors or
	single- and double-walled	thermo/hygroreceptors

Adapted from (Keil and Hansson 1999)

1.3.2 First-order olfactory neurons and their properties

The sensilla house within them the first-order neurons of the olfactory circuit, the bipolar olfactory receptor neurons (ORNs) (**Fig. 1.2 C**). Most olfactory sensilla have 2–5 ORNs (Keil and Hansson 1999) with few exceptions (basiconic sensilla in *Schistocerca gregaria* has 50 ORNs (Ochieng et al. 1998) and the Hymenopteran *Sceliphon spirifex* has 140 ORNs (Martini 1986). Species-specific number of ORNs is tabulated in **Table 1.2**.

Volatile molecules in the atmosphere are detected by the chemoreceptors present on the dendrites of ORNs in sensilla (Fig. 1.3 A and B). The ORNs usually express one of the two classes of chemoreceptors on their dendrites—odorant receptors (ORs) or ionotropic receptors (IRs). Insect ORs were first described for *Drosophila* and are ligand-gated ion channels with seven transmembrane G-protein-coupled receptors (GPCRs) (Clyne et al. 1999; Vosshall et al. 1999; Sato et al. 2008). They form a phylogenetically distinct family different from the mammalian ORs and have an inverted topology (Kaupp 2010). Vertebrate ORs are also distinguished by being metabotropic instead of ionotropic. Insect ORs are heteromultimers with two types of subunits—one of them is the ubiquitous co-receptor called Orco (previously known as Or83b in *Drosophila* and OR2 or OR7 in other insects; (Larsson et al. 2004; Sachse and Krieger 2017) and the other is the odorant-specific, highly divergent OR (Larsson et al. 2004; Sato et al. 2008). The co-receptor Orco, which is conserved across insect species, is important for the trafficking, localization and functioning of the co-expressed OR units (Krieger et al. 2003; Benton et al. 2006). Numerical strength of ORs is specific to a species (Table 1.2).

Table 1.2 Numerical strength of ORs and ORNs across insect species

Insect species	Odorant receptors (ORs)	ORNs
Drosophila	~62	~1200 (Stocker et al. 1990)
melanogaster	(Clyne et al. 1999; Vosshall et al.	
	1999; Robertson et al. 2003)	
Apis mellifera	170 (Robertson and Wanner 2006)	65000 (Esslen and Kaissling 1976)
A. cerana	119 (Park et al. 2015)	_
A. florea	149 (Karpe et al. 2016)	_
Bombus spp.	159 (Sadd et al. 2015)	_
Manduca sexta	_	250000
		(Sanes and Hildebrand 1976)
Bombyx mori	64 (Xiang et al. 2008)	50000
		(Koontz and Schneider 1987)
Aedes aegypti	_	~1600–1900 (Ignell et al. 2005)
P. americana	_	200,000 (Anton et al. 1999)

IRs represent the second family of chemoreceptors found in insects. They are ligand-gated ionotropic glutamate receptors with three transmembrane domains and are highly divergent. The co-receptors of IRs are *IR8a*, *IR25a* and *IR76b* (Benton et al. 2006; Abuin et al. 2011).

Signal transduction in the sensilla: The volatile odorants enter the olfactory sensilla through the numerous pores on its surface (Fig. 1.3 B). Either by diffusion or with the help of olfactory binding proteins (OBPs) in the sensillar lymph, the odorant molecules arrive at the chemoreceptors present on the ORNs' dendrites (Fig. 1.3 B). The binding of the odorant molecules to the receptors on the ORNs opens the ion channels and results in the depolarization of the ORNs (Fig. 1.3 B). Wicher et al. (2008) have also reported that in addition to the ligand-gated activation of the OR, the co-receptor of the complex is also activated by an internal slow metabotropic signaling cascade of cAMP or cGMP. The olfactory signal is then transmitted along the ORN's axons via the antennal nerve (AN) to the next olfactory center—the antennal lobe (Stengl et al. 1999).

The number of AN tracts is species-specific and can vary from 4–10 (**Table 1.3**). For example, in honey bees, four AN tracts are present—T1, T2, T3, T4, each innervating a cluster of glomeruli in the AL. This clustering is represented in separate groups of PNs, uniglomerular or multiglomerular, travelling through the different AL tracts to the MB (Galizia and Sachse 2010).

Odor representation in ORNs and their neurotransmitters: Acetylcholine (ACh) is the main excitatory neurotransmitter released by ORNs' terminals as evidenced by experiments which detected choline acetyltransferase, the ACh-synthesizing enzyme in honey bee ORNs (Bicker and Kreissl 1994; Bicker 1999). Cholinergic ORNs have also been shown in the moth *M. sexta* (Sanes and Hildebrand 1976; Waldrop and Hildebrand 1989; Stengl et al. 1990). In

Drosophila, the synapse between ORN-PN is blocked by an antagonist for nicotinic acetylcholine receptor, implying that the ORN is cholinergic (Kazama and Wilson 2008). Apart from ACh, ORNs also release the neurotransmitter nitrous oxide, though the only evidence reported is from moths (Gibson and Nighorn 2000).

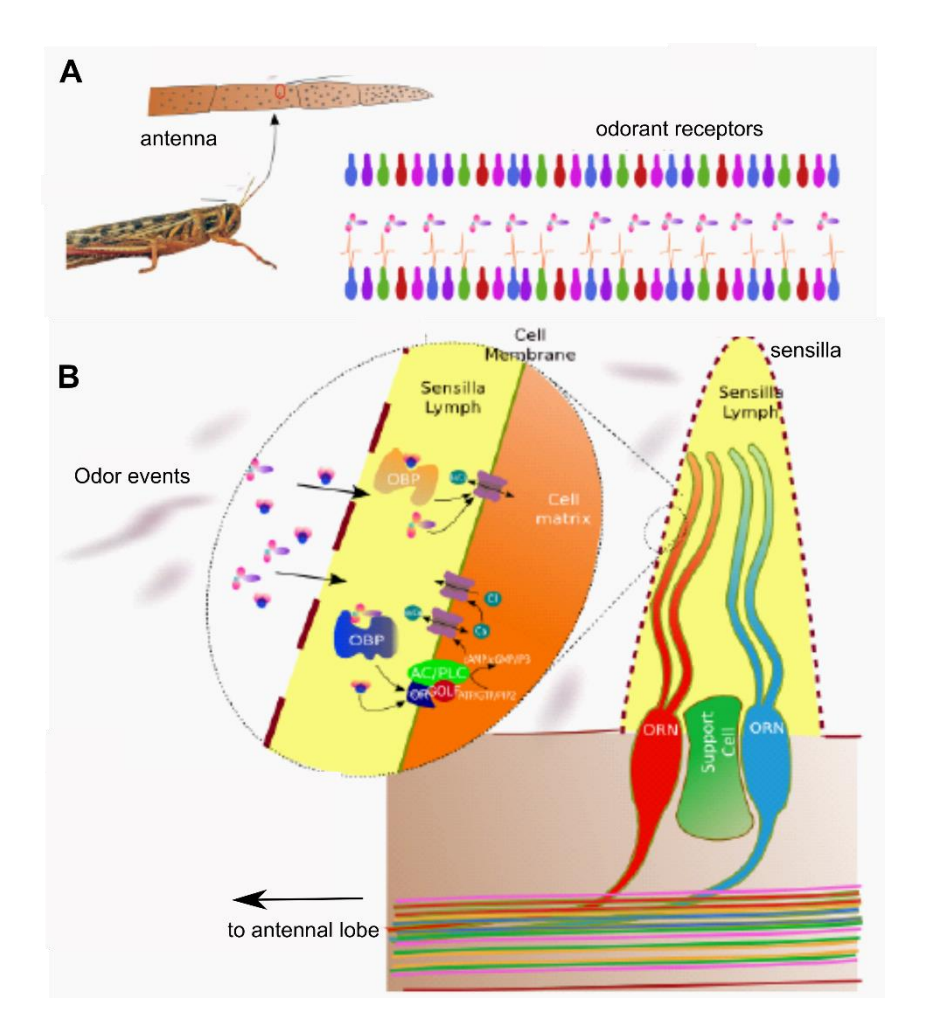


Figure 1.3 Olfactory transduction in the insect sensilla. A) Insect antenna showing the sensilla on its surface. Color coded schematic representing the binding of odorants to different odorant receptor molecules. **B)** An enlarged view of cross-section of a sensilla. Odorants constituting a turbulent plume enter the sensilla on the antenna of the insect through pores present in the cuticle of antenna. They directly diffuse or bind to the odorant binding proteins (OBPs) in the sensillar lymph and are carried to the odorant receptors present on the dendrites of the olfactory receptor neurons. Binding of the odorant/odorant-OBP complex to the odorant receptors leads to the opening of cation-selective channels directly or via second messenger cascade. Influx of positive ions inside the dendrite leads to the depolarization of the ORN and generation of action potential. The signal is then carried by the ORNs' axons to the next olfactory center, antennal lobe. (Image credit: Joby Joseph)

Table 1.3 Antennal nerve tracts reported in different insect species

Insect species	Antennal nerve tracts	
A. mellifera	T1–T4 (to AL); T5–T6 (to antennal mechanosensory and motor center, AMMC) (Suzuki 1975; Flanagan and Mercer 1989; Galizia et al. 1999)	
A. dorsata	T1–T4 (to AL); T5–T6 (to AMMC)	(Mogily et al. 2020)
Bombus terrestris	T1-T6	(Fonta and Masson 1985)
P. americana	T1-T10	(Watanabe et al. 2010)
C. floridanus (nocturnal)	T1-T7	(Zube et al. 2008)
C. sericeus (diurnal, forager)	T1-T7	(Mysore et al. 2009)
C. compressus (nocturnal, forager)	T1-T7	(Mysore et al. 2009)

ORNs in *Drosophila* are spontaneously active even when no odorants are present. Each ORN can respond to most of the odorants and the same odorant can also activate multiple ORNs. Each ORN generally expresses a single functional type of OR (Couto et al. 2005). But these ORs can be broadly tuned or narrowly tuned to the odorant stimuli (Hallem et al. 2004; Hallem and Carlson 2006). ORNs exhibit an increase in firing rate when they encounter an odorant concentration gradient (Hallem and Carlson 2006). Odorants can either increase or decrease the spontaneous firing rate of the ORNs and prolonged presence of the odorant stimuli results in the adaptation of ORNs.

1.3.3 Second-order olfactory structure—the antennal lobe (AL)

The AL is the first-order processing center of the insect olfactory circuit and is analogous to the vertebrate olfactory bulb (OB) in structure and function though it has evolved independently (Strausfeld and Hildebrand 1999; Galizia et al. 2010). The AL is a ubiquitous feature of all insects except few anosmic species where it was lost secondarily (Strausfeld and Hildebrand 1999; Galizia et al. 2010).

It is a part of the deutocerebrum and is composed of dense spheroidal synaptic zones called, glomeruli, the sites of synaptic contact between the ORNs' axons and neurons of the AL (Anton et al. 1999). The glomeruli in insects have a unique number, size and arrangement which are species-specific and vary in range widely across insect species (Galizia et al. 2010) (Table 1.4). The glomeruli/microglomeruli in some insects may be densely packed (*Drosophila*) while it might be arranged around a coarse neuropil in other insects. The ORNs which express the same ORs converge to the same glomeruli in the AL and the number of glomeruli roughly corresponds to the number of functional ORs present in the insect species (Vosshall et al. 2000; Gao et al. 2000). ORNs can be uniglomerular, where all ORNs expressing the same OR type project to a single glomerulus (in most insects) or multiglomerular, where all ORNs expressing the same OR type project to multiple glomeruli/microglomeruli (in locusts) (Anton et al. 1999).

Three types of ALs can be distinguished on the basis of glomerular organization, those of cockroaches and bees, moths and *Drosophila* and locusts (Ignell et al. 2001). The ALs in cockroaches and bees are composed of uniquely identifiable glomeruli, each giving out a pair of PN axons (Ignell et al. 2001). In moths and *Drosophila*, the number of glomeruli is less, uniquely identifiable but innervated by many PNs (Ignell et al. 2001). In locusts, in contrast to all studied insect ALs, the AL is composed of microglomeruli (Ernst et al. 1977; Laurent and Naraghi 1994; Hansson et al. 1996). A comprehensive study of the AL organization in the order Orthoptera revealed that all the three types of glomerular organization mentioned above are present along with some intermediate types (Ignell et al. 2001).

The AL in Hymenoptera (bees, wasps and ants), Lepidoptera (moths) and Dictyoptera (cockroaches) are characterized by sexually dimorphic glomeruli. The males of these orders

have a group of enlarged glomeruli called the macroglomerular complex (MGC) which is involved in processing information from sex-pheromone sensing ORNs (Anton et al. 1999).

Table 1.4 Numerical strength of AL glomeruli reported across insect species

Insect species	Number of glomeruli in AL	
D. melanogaster	43	(Laissue et al. 1999)
Apis mellifera	156–166	(Flanagan and Mercer 1989)
A. dorsata	165	(Mogily et al. 2020)
Manduca sexta	65 OG+3 MGC (macroglomerular complex)	
	(Rospars and Hildebrand 2000; Grosse-Wilde et al. 2011)	
Heliothis virescens	67 OG+4 MGC	(Berg et al. 2002; Løfaldli et al. 2010)
Helicoverpa armigera	76 OG+3MGC	(Zhao et al. 2016)
Bombyx mori	~60 OG+3 MGC	(Kazawa et al. 2009)
Spodoptera littoralis	60 OG+3 MGC	(Couton et al. 2009)
Agrotis infusa	69+3 MGC (male)	; 72+1 (Female) (Adden et al. 2020)
Aedes aegypti	~50	(Ignell et al. 2005)
Butterfly, Pieris brassicae	60	(Rospars 1983)
Periplaneta americana	203 OG+2 MGC	(Watanabe et al. 2010)
Ant, Camponotus floridanus (nocturnal)	464	(Zube et al. 2008)
(nocturnar)		
C. sericeus (diurnal, forager)	~492	(Mysore et al. 2009)
	710	0.5
C. compressus (nocturnal, forager)	~510	(Mysore et al. 2009)
Torugor)		
C. japonicas (female workers	~438	(Nishikawa et al. 2008)
and unmated queens)		

Glomerular odor response: A spatio-temporal pattern of activity is seen in the glomerular organization when an odor stimulus is present. Glomeruli may be narrowly tuned or broadly tuned to an odorant and can show different patterns of activity—excitation, inhibition, off response to a stimulus, response which exceeds the odor duration or which ceases before the odor stimulus stops (de Bruyne et al. 2001; Galizia et al. 2010).

1.3.4 Second-order olfactory neurons—interneurons of AL

The AL in insects is characterized by two main types of neurons—projection neurons and local neurons (**Table 1.5**). The cell bodies of these neurons are present at the periphery of the AL (Anton et al. 1999). In moths and honeybees (Arnold et al. 1985), they are found in three separate clusters while in locusts they are found in a single cluster called the anterior cell group (Ernst et al. 1977). The PN clusters in moths are termed lateral, mediolateral and anteroventral (Homberg et al. 1988). In *Periplaneta*, there are two cell groups of approximately 1000 cell bodies (Ernst et al. 1977).

The only output neurons of the AL are the projection neurons (PNs) which are analogous to the mitral and tufted cells found in the vertebrate olfactory bulb (Hildebrand and Shepherd 1997). The PNs project to the next higher centers—the MB and the LH. PNs in insects are of two types—uniglomerular and multiglomerular. They are found in honey bees, moths and *Drosophila* (Galizia et al. 2010). On the contrary, all reported PNs in locusts are multiglomerular.

Uniglomerular PNs are mostly cholinergic in bees (mALT), moths (lALT) and *Drosophila* (Kreissl and Bicker 1989; Homberg et al. 1995; Yasuyama and Salvaterra 1999). In locusts, the mALT stains for acetylcholinesterase (AChE) (Leitch and Laurent 1996; Homberg 2002). Multiglomerular PNs have been also shown to be GABAergic in bees (Schäfer and Bicker 1986), moths (Hoskins et al. 1986). In *Drosophila*, PNs of the ventral cell cluster projecting to the LH through the lALT are reported to be GABAergic (Okada et al. 1999).

Table 1.5 LNs and PNs in insect antennal lobe

Insect species	PNs (uniglomerular/	LNs
	multiglomerular)	
S. americana	830; mPNs; cholinergic	300; GABAergic
	(Laurent and Naraghi 1994)	(Laurent and Naraghi 1994)
D. melanogaster	150–200; uPNs and mPNs;	~100 ipsilateral; ~100 bilaterally
	cholinergic and GABAergic	projecting; GABAergic and cholinergic
	(Stocker et al. 1997;	(Ng et al. 2002; Wilson and Laurent
	Yasuyama and Salvaterra	2005; Shang et al. 2007; Okada et al.
	1999; Ng et al. 2002; Lai et	2009; Chou et al. 2010)
	al. 2008; Okada et al. 2009;	
	Tanaka et al. 2012a)	
M. sexta	~900; uPNs and mPNs	~360 (Homberg et al. 1988)
	cholinergic and GABAergic	-
	(Homberg et al. 1988)	
P. americana	~700; uPNs and mPNs	~300 (Anton et al. 1999)
	(Anton et al. 1999)	
A. mellifera	~1090; uPNs and mPNs;	~4000; GABAergic and histaminergic
	cholinergic and GABAergic	
	(Schäfer and Bicker 1986;	(Witthöft 1967; Dacks et al. 2010)
	Kirschner et al. 2006; Zwaka	
	et al. 2016)	
B. impatiens	_	~3000; GABAergic and histaminergic
		(Dacks et al. 2010)

PNs get their odor input from ORNs (excitatory), LNs (inhibitory) and other PNs (excitatory or inhibitory as the case may be for individual insect species) and they synapse on to other PNs and LNs. No evidence of PN-ORN synapse has been found, as of now (Galizia et al. 2010). PNs in insects exhibit a baseline firing rate even in the absence of stimuli (honey bees, (Abel et al. 2001; Galán et al. 2006); moths, (Christensen et al. 1998); *Periplaneta*, (Boeckh et al. 1987); locusts, (Laurent and Naraghi 1994); *Drosophila*, (Wilson et al. 2004). And they respond to most odorants with temporal patterns of excitation, inhibition or a combination of both (Christensen et al. 1998; Sachse and Galizia 2002; Wilson and Laurent 2005; Bhandawat et al. 2007; Silbering and Galizia 2007; Schlief and Wilson 2007; Olsen and Wilson 2008).

The second type of neuron which is present in the AL is local neuron (LN). The LNs are axon-less neurons whose arborizations are restricted within the AL. On the basis of arborization in the AL, three types of LNs have been described ((Anton et al. 1999) and references therein):

- 1. Multiglomerular LNs, with homogenous arborization throughout the AL, found in moths, *Apis mellifera*, *Periplaneta americana*, *D. melanogaster* and locusts
- 2. Multiglomerular LNs, with heterogenous arborization, found in the moth *M. sexta*, *A. mellifera* and *P. americana*
- 3. Oligoglomerular LNs, with arborization restricted to few glomeruli, found in the moths *M. sexta* and *S. littoralis*

LNs get their odor input from ORNs and PNs and output on to other LNs, PNs and ORNs (Anton et al. 1999). LNs have been shown to be predominantly GABAergic in nature. This has been shown in honey bees (Schäfer and Bicker 1986), moths (Hoskins et al. 1986), *Drosophila* (Jackson et al. 1990; Buchner 1991), cockroaches (Malun 1991; Distler et al. 1998) and locusts (Leitch and Laurent 1996; Ignell et al. 2001). Some LNs in *A. mellifera* have also been shown to be histaminergic (Bornhauser and Meyer 1996). Cholinergic and glutamatergic LNs have been reported in *Drosophila* (Ramaekers et al. 2001; Shang et al. 2007). In many insects, LNs express a variety of neuropeptides (allatostatin, allatotropin, tachykinins, FMRF-amide or RF-amide) either along with GABA or by themselves alone (Galizia et al. 2010). LNs are characterized by sharp sodium action potential in honey bees, moths and flies while they show visually, low variable amplitude, broad spikelets, putatively calcium-mediated in locusts. *P. americana* are reported to have both kinds of LNs (Galizia et al. 2010). Apart from the PNs and LNs, the AL is also innervated by centrifugal neurons and glia cells.

Odor coding in the AL: The ORNs make synapses with both PNs and LNs in the AL. The PNs represent the odor stimuli by a spatio-temporal code distributed across the AL. Each

odorant is represented by a subset of PNs spiking in response to it and the subset that is active changes dynamically over the duration of odorant stimuli (Laurent 1996; Wilson and Mainen 2006). Each PN responds to the odorant by a unique representation consisting of excitation, inhibition or quiescence or a combination of all these. The inhibition of the PNs by the LNs in each cycle causes subsets of PN spikes to get synchronized dynamically (Laurent 1996; Wilson and Mainen 2006). The PNs' response to odorants shows features at two timescales—fast and slow, that is independent of stimulus feature timescales, indicating the possibility of temporal coding. Fast timescale is mediated by the GABA inhibition of PNs by LNs (~50 ms), through the ionotropic GABA A receptors and is responsible for causing the PNs to transiently synchronize during each odor cycle (MacLeod and Laurent 1996; Bazhenov et al. 2001a; Raman et al. 2010). The slow timescale is thought to be mediated by the GABA B type receptors and is responsible for the temporal patterns which are seen in the PNs odor response.

1.3.5 Antennal lobe tracts (ALTs) to the mushroom body and lateral horn

The axons of the AL PNs form the only output channels from the AL to higher olfactory areas—the MB and the LH. The number of these ALTs varies from species to species but the major ALT is the medial antennal lobe tract (mALT). Apart from mALT, transverse ALT, lateral ALT and mediolateral ALT have been reported in different insect species. **Table 1.6** gives details about the number and types of ALTs reported in different insect species.

1.3.6 Third-order olfactory structure—mushroom body (MB)

The mushroom bodies are multimodal structures found in the protocerebrum of annelids and all groups in phylum Arthropoda except crustaceans and the most basal group of insects, the Archaeognatha (Strausfeld et al. 1998, 2009; Farris and Sinakevitch 2003). Dujardin identified them for the first time in 1850 in honey bees. Mushroom bodies form paired

neuropil structures, the size of which differs across insect taxa. In addition, the size can also vary across different castes in social insects (Strausfeld et al. 1998). Mushroom bodies are so called because of their distinctive mushroom-shaped cup-like area (calyx) with a stalk (pedunculus). In Hymenoptera and *Periplaneta*, each half of the brain has two MB calyces which are fused at the base to form a single pedunculus (Strausfeld et al. 1998).

Table 1.6 Antennal lobe tracts (ALTs) across insect species

Insect species	Number of antennal lobe tracts to MB and LH		
S. americana	1, mALT	(Laurent and Naraghi 1994)	
S. gregaria	1, mALT	(von Hadeln et al. 2018)	
L. migratoria	1, mALT	(Ernst et al. 1977)	
Tetrix subbulata	2, mALT and lALT	(Ignell et al. 2001)	
D. melanogaster	4, mALT, mlALT, lALT, tALT		
	mALT, formed of cholinergic ul	PNs	
	mlALT, formed of cholinergic uPNs and GABAergic mPNs		
	(terminates only in LH)		
	-		
	lALT, formed of uPNs and mPNs		
	(Stock	er et al. 1990; Tanaka et al. 2012b)	
M. sexta	5, mALT, lALT, dALT, mlALT	, dmALT	
		(Homberg et al. 1988)	
H. virescens	5, mALT, lALT, tALT, mlALT,		
		(Ian et al. 2016)	
B. mori	3, mALT, mlALT, lALT		
		nzaki et al. 2003; Seki et al. 2005)	
P. americana	5, mALT, 3 mlALT, lALT	(Malun et al. 1993)	
A. mellifera	5, mALT, 3 mlALT, lALT	(Kirschner et al. 2006)	
Bombus terrestris	2, mALT and lALT	(Strube-Bloss et al. 2015)	
C. floridanus	5, mALT, 3 mlALT, lALT	(Zube et al. 2008)	
Harpegnathos saltator	5, mALT, 3 mlALT, lALT	(Rössler and Zube 2011)	
Atta vollenweideri	5, mALT, 3 mlALT, lALT	(Rössler and Zube 2011)	
Aedes aegypti	3, mALT, mlALT, lALT	(Ignell et al. 2005)	
mALT: medial antennal lobe tract; mlALT: mediolateral ALT; lALT: lateral ALT; tALT:			

mALT: medial antennal lobe tract; mlALT: mediolateral ALT; lALT: lateral ALT; tALT: transverse ALT; dmALT: dorsomedial ALT; uPNs: uniglomerular PNs; mPNs: multiglomerular PNs

The calyx is the zone of synaptic interactions between the intrinsic neurons of the MB, the Kenyon cells and other afferent input from different regions of the brain (Strausfeld et al. 2009). The calyx in Hymenoptera is subdivided into three regions—the lip, collar and basal ring. This subdivision corresponds to the six bands seen in the alpha lobe (Mobbs and Young 1982; Rybak and Menzel 1993). Each subdivision receives input from a particular sensory modality. The lip receives olfactory input; the collar, visual input and the basal ring receives both chemosensory and visual input (Mobbs and Young 1982; Mobbs 1984; Homberg 1984; Gronenberg 1986). The cell bodies of the KCs reside in the area dorsal to the calyx. Their axons form a bundled tract running along the length of the pedunculus and bifurcating into two branches which form the two output lobes of the MB—the vertical lobe, also known as the alpha lobe and the medial lobe, also known as the beta lobe (Strausfeld et al. 1998). In *Drosophila*, there is an additional pair of α ' and β ' lobes (Strausfeld et al. 2003). Some insects like honey bees and *Drosophila* also have an extra lobe called the γ -lobe (Strausfeld 2002; Farris et al. 2004). Lepidopteran insects like M. sexta, B. mori and H. virescens have an additional lobe called 'Y' in addition to α , β , α ', β ' and γ (Rø et al. 2007; Fukushima and Kanzaki 2009; Farris et al. 2011) (**Table 1.7**).

MB in insects have been likened to be analogous to a number of higher centers in the vertebrate brain; the piriform cortex, the cerebellum or the hippocampus (Strausfeld et al. 1998; Campbell and Turner 2010; Farris 2011). Similar to the piriform cortex which gets its olfactory input from the mitral cells of the olfactory bulb; MB receives its major olfactory input from the PNs of AL. MB has also been shown to play a role in some forms of olfactory discrimination and olfactory learning and memory (Galizia et al. 2010). Apart from its olfactory functions, the MB is also involved in sleep and decision making (Joiner et al. 2006; Zhang et al. 2007a). An excellent review by Modi et al. (2020) states that the expand-

converge architecture, which was the foundation for the development of the Marrs-Albus model of a learning network, is a feature also found in the mushroom body.

The predominant input to the calyces of MBs is olfactory though in some insect species (particularly Hymenopterans and Coleopterans), gustatory and/or visual input (in one species of gyrinid beetle) is present in addition to olfactory input (Strausfeld et al. 2009).

Table 1.7 Kenyon cell numbers and neurotransmitter profile across insect species

Insect species	No of KCs/ neurotransmitter profile/ output lobes of MB	
P. americana	~175,000	(Neder 1959)
	Aspartate, glutamate, taurine positiv	ve (Sinakevitch et al. 2001)
	α and β	(Li and Strausfeld 1997)
S. americana	~50000; Non-GABAergic	(Leitch and Laurent 1996)
	α and β	(Laurent and Naraghi 1994)
A. mellifera	~170000	(Witthöft 1967)
	Glutamate-positive subpopulation	(Bicker et al. 1988)
	α and β	(Kenyon 1896a)
D. melanogaster	~2500	(Stocker 1994)
	Aspartate, glutamate, taurine positiv	ve (Strausfeld et al. 2003)
	Produce NO	(Schürmann 2000)
	GABA and acetylcholine-negative	(Yasuyama et al. 2002)
	$\alpha, \alpha', \beta, \beta', \gamma$	(Crittenden et al. 1998)
B. mori	~2000	(Fukushima and Kanzaki 2009)
	α , γ , β , β ', α ' and Y	(Fukushima and Kanzaki 2009)

1.3.7 Third-order olfactory neurons and their properties—Kenyon cells (KCs)

KC population varies widely across insect species (**Table 1.7**). In *Drosophila*, KCs are of three morphological types based on the lobes they innervate— α/β or α'/β' or γ (Crittenden et al. 1998) while four morphological types have been reported in the moth, *B. mori* (Fukushima and Kanzaki 2009)

Odor-evoked activity in KCs is characterized by few spikes against a baseline rate close to zero. This has been shown in *S. americana*, *A. mellifera* and *Drosophila* (Laurent and Naraghi 1994; Wang et al. 2004; Szyszka et al. 2005). KCs show both population sparseness

and lifetime sparseness (Laurent 2002; Olshausen and Field 2004) and their odor response is driven by coincident, synchronous input from PNs (Perez-Orive et al. 2002; Szyszka et al. 2005; Turner et al. 2008; Demmer and Kloppenburg 2009; Honegger et al. 2011). This synchronous input from the PNs results in the local field potential in the MB to show characteristic oscillatory synchronization (Laurent and Naraghi 1994; MacLeod and Laurent 1996).

1.3.8 Third-order olfactory structure-—lateral horn and its neurons

The PNs' axons, after arborizing in the MB calyx, travel further to terminate in an area known as the lateral horn (LH). The LH in insects is thought to be analogous to the vertebrate amygdala (Friedrich 2011; Fişek and Wilson 2014). Extensive morphological data for LHNs is available for *D. melanogaster* (Fişek and Wilson 2014; Dolan et al. 2019; Frechter et al. 2019) and *S. americana* (Gupta and Stopfer 2012). LHN fill has also been shown in the moth *B. mori* (Namiki et al. 2013). The LH receives direct olfactory input from AL PNs by the lALT and mlALT in many insects and a delayed input by the mALT which first projects to the MB calyx.

Fisek and Wilson (2014) classified *Drosophila* LHNs in two spatially separated cell clusters—type 1 (dorsomedial to LH) and type 2 (ventrolateral to LH). Type 1 LHNs innervate the superior medial protocerebrum while type 2 LHNs innervate superior lateral protocerebrum. The two types have different response patterns to odor stimuli—type 1 neurons are broadly tuned with stereotyped odor responses and receive olfactory input from many glomeruli; type 2 LHNs are narrowly tuned receiving input from approximately one (or few) glomeruli. Type 2 LHNs also receive strong odor-evoked inhibition from the inhibitory PNs. However, recent studies have discovered a much larger number of LHNs, not

classifiable in the above two classes alone (Aso et al. 2014b; Dolan et al. 2019; Frechter et al. 2019).

On the basis of primary neurite, morphology and cell type, Frechter et al. (2019) reported that there are ~1400 LHNs of >165 cell types in *Drosophila*. Of these, ~40% are local LH neurons (LHLNs) and ~60% are LH output neurons (LHONs). In contrast to MB Kenyon cells, which have sparse odor response which is probabilistic across animals, LHNs in *Drosophila* have stereotyped odor response across animals (Fişek and Wilson 2014; Frechter et al. 2019). They respond three times more on an average to odors when compared to AL PNs and thus are thought to be better classifiers of odorants. The study also found that the ventral LH in *Drosophila* is a multimodal center receiving thermosensory, hygrosensory and mechanosensory inputs in addition to olfactory inputs. On the other hand, the dorsal LH is predominantly olfactory. The neurotransmitter profile of LHNs is widely diverse. LHONs can be cholinergic, GABAergic and/or glutamatergic (Dolan et al. 2019). On the other hand, LHLNs are GABAergic and/or glutamatergic (Dolan et al. 2019). LHNs in *Drosophila* project to superior medial, superior lateral protocerebrum and also to the ventral nerve cord (Tanaka et al. 2004, 2012b; Jefferis et al. 2007; Ruta et al. 2010; Fişek and Wilson 2014).

The primary role of LHNs appears to be in memory-independent behaviors like predator avoidance, appetitive or aversive responses to favorable or unfavorable food/mates (Schultzhaus et al. 2017). In addition, LHNs also play a role in learned behavioral responses mediated by the MB. One study showed that multiple unique sexually dimorphic behaviors can be elicited by LHNs in response to the same pheromone in *Drosophila* (Ruta et al. 2010).

The LH is implicated to play a role in encoding innately meaningful odors since it has been shown in *Drosophila* that chemical ablation of MB with hydroxyl urea hampers olfactory learning but does not affect innate or experience-independent odor responses (Belle

and Heisenberg 1994; Kido and Ito 2002). A study by Dolan et al. (2019) and Frechter et al. (2019) provide clear evidence (anatomical, functional and behavioral) for the involvement of the LH in olfactory innate behavior. LHNs also drive valence and motor behaviors (Dolan et al. 2019; Lerner et al. 2020). Another study by Varela et al. (2019) reported the role of LHNs in mediating behavioral responses to CO2 in *Drosophila*.

1.3.9 Fourth-order olfactory neurons—alpha lobe neurons (aLNs) and beta lobe neurons (bLNs) $\,$

The extrinsic neurons of the MB form the fourth-order neurons of the olfactory circuit. These neurons are called extrinsic because they provide axonal output to areas outside the MB (in the protocerebrum and deutocerebrum; (Kenyon 1896a, b; Li and Strausfeld 1997). These neurons are postsynaptic to MB KCs (Schürmann 1987) with dense dendritic arborization in the output lobes of the MB or recurrently to the MB calyces (Gronenberg 1987). Two types of extrinsic neurons are known—one with dense arborization in the beta lobe (bLNs) and the other with arborization in the alpha lobe (aLNs). The efferent neurons of the lobes respond to sensory modalities like visual motion, auditory and tactile, in addition to olfaction (Li and Strausfeld 1997, 1999; Strausfeld et al. 2009).

By far, bLNs in *Drosophila* and *S. americana* have been extensively studied. Apart from these two species, bLNs have been investigated in the cricket, *Acheta domesticus* and the cockroach, *P. americana*. In comparison, aLNs have only been studied in *A. mellifera*, *A. domesticus* and *P. americana*.

In *P. americana*, two types of extrinsic neurons (simple and complex) have been reported (Li and Strausfeld 1997). Simple extrinsic neurons have one set of dendritic arborization in one of the MB lobes with one or more terminal arbors. Complex extrinsic neurons have one dendritic arbor inside the MB and the other outside the MB. All the

extrinsic neurons reported respond to more than one sensory modality. Two simple aLNs have dendritic arbor in the alpha lobe of MB and a single axonal projection in the inferior lateral protocerebrum. The third aLN has diffused terminals lateral to the MB and dendrites in the alpha lobe. Complex aLN have two dendritic arbors—one in alpha lobe and the other in the medial protocerebrum. Two complex and one simple bLNs have also been described (Li and Strausfeld 1997). Recurrent extrinsic beta lobe neurons (simple and complex types), with dendritic arborization in one lobe and axonal terminals in another lobe have been reported in (Li and Strausfeld 1999) where they also reported three bLNs with dendritic arborization in the superior lateral protocerebrum. Approximately 30 beta lobe neurons and 60 alpha lobe extrinsic neurons are possibly present in *Periplaneta* (Li and Strausfeld 1999).

In *Drosophila*, 34 MB output neurons (MBONs) of 21 types have been reported (Aso et al. 2014b, a). They compartmentalize the MB lobes into 15 discrete compartments each innervated by a unique group of dopaminergic neurons (Aso et al. 2014b; Owald et al. 2015). They can be cholinergic, GABAergic or glutamatergic (Aso et al. 2014b). MBONs in *Drosophila* have been implicated in reward learning pathways driving avoidance behavior and courtship behavior.

In the moth *Agrotis segetum*, neuron 72 is reported which connects the MB with the lateral accessory lobe (LAL; (Lei et al. 2001)). The cell body of this neuron is located lateral to the alpha lobe in the inferior medial protocerebrum, and it has dense arborization in the heel (junction between the pedunculus and beta lobe) of the ipsilateral beta lobe. After innervating the ipsilateral blobe, the neurite of this neuron crosses the midline of the brain through the LAL commissure to arborize and terminate in the contralateral LAL with varicose processes. All odors which were tested elicited an excitatory response in this neuron (Lei et al. 2001).

In *A. mellifera*, 7 clusters of alpha lobe neurons (A1–A7) numbering ~400 neurons have been described (Rybak and Menzel 1993). The seven clusters are further subdivided into unilateral (A1, A2, A4 and A5), recurrent (A3d and A3v) and bilateral (A6 and A7) neurons on the basis of their arborization patterns (Rybak and Menzel 1993). One of the most studied aLN is the Pe-1 (pedunculus extrinsic neuron; (Rybak and Menzel 1993; Mauelshagen 1993) which connects the pedunculus with lateral protocerebral lobe and the ring neuropil around the alpha lobe (Rybak and Menzel 1998). Pe-1 is a multimodal neuron responding to olfactory, mechanosensory and visual stimuli and involved in multisensory integration and olfactory learning associated plasticity (Mauelshagen 1993; Rybak and Menzel 1998; Iwama and Shibuya 1998; Menzel and Manz 2005; Okada et al. 2007). Extrinsic neurons (EN) of the A1, A2, A4, A5, A7 clusters have been shown to encode valence for rewarded odors (Strube-Bloss et al. 2011). A3v and A3d MBONs which are inhibitory are proposed to integrate context and cue values (Filla and Menzel 2015).

In the cricket *A. domesticus*, Schildberger (1984) reported one MBEN with dense innervation in the ipsilateral alpha lobe. The cell body of this aLN is located dorsal to the MB with fine and dense arborization in the alpha lobe and varicose and diffuse terminals in the lateral protocerebrum. The neuron exhibits spontaneous baseline firing and is multimodal in nature, responding to light, sound and mechanical stimulation of antenna and cerci.

1.3.10 Fourth-order inhibitory neurons of the mushroom body

Inhibitory neurons in the neural circuitry are involved in integrating the inputs and shaping the outputs (Zhu and Lo 2000). Similar to other sensory modalities, inhibitory neurons are indispensable for the stability, autonomy and independence of the circuit and play a major role in odor information processing. The MB in insects is innervated by many such neurons. These have been studied in *A. mellifera* (Bicker et al. 1985; Schäfer and Bicker 1986; Rybak

and Menzel 1993; Grünewald 1999b, a; Zwaka et al. 2018), *P. americana* (Weiss 1974; Yamazaki et al. 1998; Nishino and Mizunami 1998; Strausfeld and Li 1999; Takahashi et al. 2017, 2019), *D. melanogaster*, *M. sexta* (Homberg et al. 1987) and *S. americana/gregaria* (Papadopoulou et al. 2011). One distinctive inhibitory neuron reported in locust species (*S. americana* and *gregaria*, *Melanoplus femurrubrum*) which innervates the MB is the giant GABAergic neuron or GGN. In *D. melanogaster*, a similar neuron is called anterior paired lateral neuron (APL). On the other hand, *P. americana*, bees, and moths have multiple GGN-like neurons (4, ~ 50, and ~ 150, respectively).

In Drosophila, a pair of APL neurons have been described which are GABAergic and densely arborize in the calvees of the MB, pedunculi and all the lobes (Jefferis et al. 2001; Liu and Davis 2009; Papadopoulou et al. 2011). The APL in *Drosophila* is different from the GGN in Schistocerca in one respect. GGN arborizes only in the alpha lobe out of the two output lobes—alpha and beta, while in *Drosophila*, the APL arborizes in all the output lobes. The odor response of APL is similar to that of GGN. It is a non-spiking neuron which responds to odor stimuli with depolarization of its membrane potential and the DC component of the depolarization increases with the increasing concentration of the odorant (Papadopoulou et al. 2011). APL receives its odor input from the MB KCs in the lobes and feedbacks to the MB calyx (Papadopoulou et al. 2011; Lin et al. 2014). The suppression of APL enhances olfactory learning and shows a depression in activity after learning (Liu and Davis 2009). APL also plays a role in sparse coding of odors in MB by acting on GABA A receptors on KCs (Lei et al. 2013). The APL has been shown to play a role in enhancing learned odor discrimination (Lin et al. 2014), olfactory reversal learning (Wu et al. 2012), sustain anesthesia-sensitive memory formation (Pitman et al. 2011) and memory consolidation (Haynes et al. 2015). APL in Drosophila is octopaminergic as well as GABAergic and helps in modulating the formation of anesthesia-resistant memory (Wu et al.

2013). In aversive olfactory learning, the APL is disinhibited by dopaminergic neurons to allow for efficient learning (Zhou et al. 2019).

In *A. mellifera*, Grunewald (Grünewald 1999b) reported ~55 GABAergic feedback neurons (FNs) whose cell bodies are located in the lateral protocerebral lobe. They are classified into four types (FN1, FN2, FN3 and FN4) on the basis of their branching pattern in the alpha lobe layer and the MB sub compartment. They form part of the alpha lobe neurons, termed A3v by Rybak and Menzel (1993). The FNs innervate all the calycal compartments of the MB and project to ipsilateral alpha lobe (bands 1–3), beta lobe and the pedunculus. Individual FNs arborize in a specific layer of the alpha lobe and their corresponding calycal sub compartment (lip, collar or basal ring). FNs in *A. mellifera* are spiking neurons which have a baseline spiking activity and they respond to odor stimuli with excitatory phasic-tonic activity (Grünewald 1999a). The odor-evoked activity of these neurons decreases when a reward is paired with an odor (Grünewald 1999a). Boitard et al. (2015) reported that FNs facilitate olfactory reversal learning.

In the cockroach *P. americana*, 4 GGN-like neurons, designated calycal giants (CGs; CG1, CG2a, CG2b, and Non-spiking CG) have been identified (Weiss 1974; Nishino and Mizunami 1998; Takahashi et al. 2017). All of them are GABAergic (Yamazaki et al. 1998), three are spiking and one of them is non-spiking. Type 1 CG is multimodal and shows disinhibition in response to stimuli (Nishino and Mizunami 1998). The NS-CG is probably analogous to the GGN in locusts. The 4 CGs innervate different regions of the MB, the largest CG innervates the basal region while the two smaller CGs and the NS-CG innervate the lip region of the MB calyx. Since these two regions of the MB receive olfactory input from two different clusters of uniglomerular PNs in AL, it is postulated that two separate but

interactive streams of inhibitory control is active which helps in differential odor information processing (Takahashi et al. 2017, 2019).

1.4 The olfactory circuit of Schistocerca americana/Schistocerca gregaria

One of the most widely studied insect olfactory systems is that of the locusts—*S. americana* and *S. gregaria* in the order Orthoptera (family Acrididae). Another widely studied locust species is *L. migratoria*. The *Schistocerca* spp. are robust to electrophysiological recordings and are amenable to various invasive techniques available today. With the exception of *Drosophila*, an unparalleled model organism with its repertoire of genetic tools and honey bees and moths, which are indispensable for behavioral studies, the locusts are one of the best model organisms for electrophysiological investigation. Many computational models have also been constructed on the basis of the available data in *Schistocerca* to explain the computational principles underlying olfaction (Rabinovich et al. 2000, 2001; Bazhenov et al. 2001b, a; Kee et al. 2015; Sanda et al. 2016).

A wide literature is available in terms of olfactory coding and anatomy (especially at S. **Table** the higher orders) in americana. 1.8 enumerates the reported numerical/miscellaneous features of the neurons of the locust olfactory pathway. In addition, a comprehensive study of the olfactory circuit has also been done in S. gregaria. Literature shows that these two species are very similar to each other (Burrows 1996; Song 2004; Farivar 2005), therefore the available data with respect to the olfactory circuit in both these species will be used interchangeably throughout this thesis.

The brain of *Schistocerca* spp. is bilaterally symmetrical. In *S. americana*, the first-order neurons of the olfactory pathway, the ORNs are housed in olfactory sensilla on the antennae (**Fig. 1.4 A**). In locusts, sensilla basiconica and trichodea have ORNs which express

odorant receptors and Orco. Different types of olfactory sensilla house different numbers of ORNs—basiconica has up to 50 ORNs, coeloconica has 1–4 ORNs and trichodea has 1–3 ORNs (Ochieng et al. 1998). S. basiconica in locusts is unusual in housing a large number of ORNs (~50). Recently, it was shown that the same OR type is expressed in more than one ORN in the same sensilla (Pregitzer et al. 2017) which is different from the case found in other insects where the ORNs in the same sensilla express the same OR type (Jiang et al. 2019).

The 50,000 excitatory and cholinergic ORNs in *Schistocerca* (Laurent 1996) are spontaneously active, firing at a baseline rate of ~5 Hz (Joseph et al. 2012). When an odorant binds to the ORs in the ORNs, it results in changes of the baseline firing rate of the ORNs. They respond to odorants with periods of excitation or inhibition. 119 OR types have been reported in *S. gregaria* (Pregitzer et al. 2017). And according to this study, the same sensilla can have ORNs expressing different OR types, unlike other insect species. But it is still debatable if the same ORN expresses more than one type of OR (Hansson et al. 1996).

The number of ORNs increases in *S. gregaria* during its development from nymphal to adult stage, concomitant with an increase in the number of microglomeruli, thus increasing the converging input to the AL though the number of PNs remain constant (Anton et al. 2002).

Each ORN innervates 1–3 microglomeruli (Masson and Mustaparta 1990; Laurent et al. 1998). And they synapse onto both PNs and LNs in the AL (Leitch and Laurent 1996). There are ~1000 microglomeruli in the *Schistocerca* AL, one of the highest reported in any insect species (**Fig. 1.4 B**). The microglomerular organization of the AL is a unique feature of the family Acrididae of order Orthoptera (Ignell et al. 2001). Each glomerulus in the locust is innervated by more than one ORN. The microglomeruli are very small in size, measuring

about 25 µm in diameter (Ernst et al. 1977; Anton et al. 2002) and they are the only site of synaptic interaction in the AL. According to Ernst et al. (1977), up to 8 neurons (ORNs, PNs and LNs) synapse within a single microglomerulus in the AL (*Locusta migratoria*).

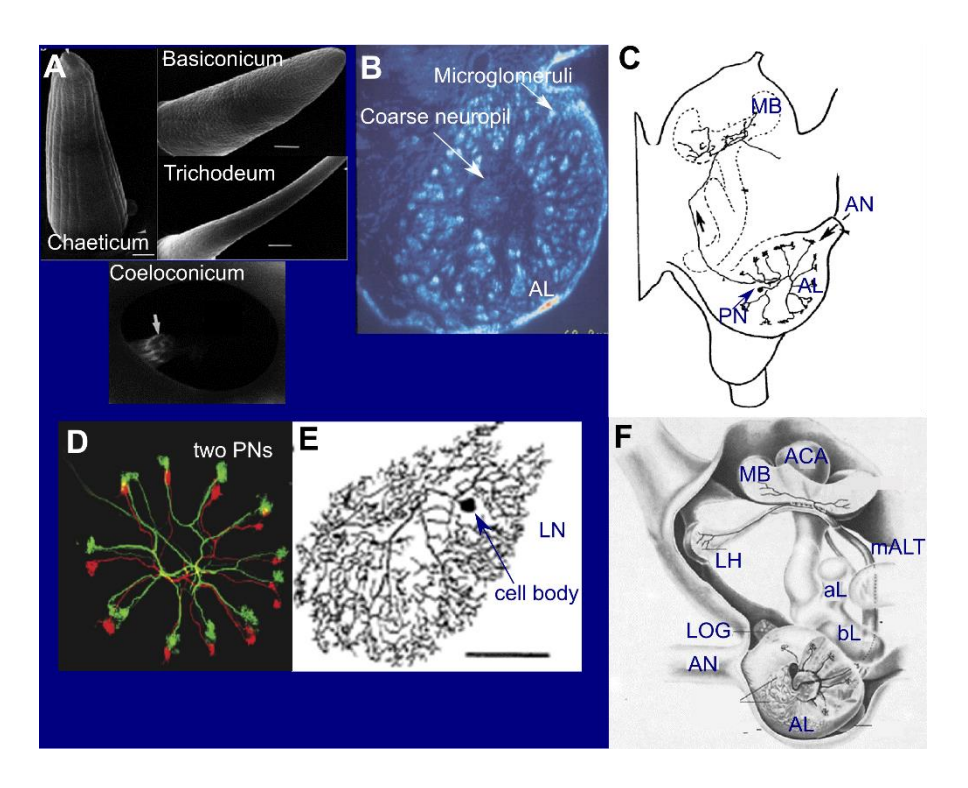


Figure 1.4 Anatomical features of the first-order and second-order olfactory centers in Schistocerca spp./Locusta migratoria (A) Different types of sensilla present on the antenna; Adapted from (Ochieng et al. 1998) (B) Microglomerular organization of the AL; (Laurent and Naraghi 1994) (C) PN in the AL; (Laurent and Naraghi 1994) (D) Two intracellularly-filled PNs in the same preparation, showing their multiglomerular arborization in the same set of AL microglomeruli; (Farivar 2005) (E) Wide spread arborization of a LN in the AL; (MacLeod and Laurent 1996) (F) AL tract—mALT, carrying the axons of the AL PNs to MB and LH; (Ernst et al. 1977); AL: antennal lobe; AN: antennal nerve; LOG: lobus glomerulus; ACA: accessory calyx; MB: mushroom body; LH: lateral horn; aL: alpha lobe; bL: beta lobe; LN: local neuron; PN: projection neuron; mALT: medial antennal lobe tract

The AL of *Schistocerca* comprises of 830 PNs and 300 LNs (Laurent and Naraghi 1994). PNs are multiglomerular, each arborizing in 10–20 microglomeruli (Laurent and Naraghi 1994; Laurent et al. 1998) (**Fig. 1.4 C and D**).

Table 1.8 Numerical properties of the olfactory circuit of locust

Neuronal	Numerical strength/miscellaneous feature/value		
element/feature			
Brain volume/ total number of cells	~6 mm ³ /~360,000	(Burrows 1996)	
OR types ORNs	119, S. gregaria 50000, L. migratoria	(Pregitzer et al. 2017) (Ernst et al. 1977; Laurent 1996)	
	,	C	
AL glomeruli	~1000 microglomeruli; ~8 cells per microglomeruli (Ernst et al. 1977; Laurent and Naraghi 1994)		
AL PNs	~830, multiglomerular (Laurent and Naraghi 1994; Leitch and Laurent 1996; Laurent et al. 1998; Anton et al. 2002) Baseline spike rate 2.5–4 spks/s (Perez-Orive et al. 2002; Joseph et al. 2012)		
	2012) Odor response ~20 spks/s ~907, multiglomerular, <i>S. gregaria</i> (2002)	(Perez-Orive et al. 2002) (Ernst et al. 1977; Anton et al.	
	Each PN innervates 10–20 microglo Cell bodies are located in ventral cel	· · · · · · · · · · · · · · · · · · ·	
AL LNs	300; axon-less, GABAergic, non-spiking (Masson and Mustaparta 1990; Laurent and Davidowitz 1994; Laurent 1996; Leitch and Laurent 1996; MacLeod and Laurent 1996)		
Tracts to MB	1, medial ALT (mALT)	(Laurent and Naraghi 1994)	
KCs	50000; ~2.3 spikes/s odor response; baseline~0 (Laurent and Naraghi 1994; Leitch and Laurent 1996; Perez-Orive et al. 2002, 2004; Stopfer et al. 2003)		
MB LFP power/plasticity	20 Hz/Yes (Laurent and Narag	thi 1994; Stopfer and Laurent 1999)	
LHNs Output lobes of MB	~8 types 2, Alpha (vertical) and beta (medial)	(Gupta and Stopfer 2012) (Laurent and Naraghi 1994)	
blobe neurons (bLNs)	7 morphological types; type 1—one bLN; type 2—12 to15 bLNs (MacLeod et al. 1998; Gupta and Stopfer 201		
GGN	1/GABAergic/non-spiking (Leitch and Laurent 1996; Papadopoulou et al. 2011)		
IG	1/inhibitory/spiking	(Papadopoulou et al. 2011)	

The cell bodies of the PNs are located in the ventral cell group (*S. gregaria* (Anton et al. 2002)). They are the only output from AL to higher olfactory centers—MB and LH (Laurent and Naraghi 1994). An electron microscope study of the AL tract to MB, comprising of the axons of PN shows them to be cholinergic as they stain strongly against the antibody acetylcholinesterase (Homberg 2002). A previous study (Leitch and Laurent 1996) using EM-immunocytochemical labelling with anti-GABA antibody of the *Schistocerca* brain revealed the presence of a variety of synaptic connections in the AL (GABA-positive to GABA-positive; GABA-positive to GABA-negative; GABA-negative to GABA-negative to GABA-negative).

PNs exhibit baseline spontaneous firing similar to the ORNs and this activity originates from the ORNs baseline spontaneous firing (Joseph et al. 2012). The PNs respond to different odorants with different spatio-temporal patterns of firing, which again originate from the temporally structured input from the ORNs (Laurent and Davidowitz 1994; Laurent et al. 1996; Raman et al. 2010).

Odor response is driven by transient synchronized firing of PN subsets which dynamically change during the course of odor presentation (Laurent and Davidowitz 1994; Laurent and Naraghi 1994; Laurent et al. 1996; Wehr and Laurent 1996). This synchronization of PNs during odor response is executed by the fast reciprocal/recurrent synaptic connection between inhibitory LNs and excitatory PNs (MacLeod and Laurent 1996; Bazhenov et al. 2001). The identity, concentration and timing of the odor pulse are represented by the dynamic subsets of active PNs during the odor presentation (Laurent et al. 1996; Stopfer et al. 2003; Brown et al. 2005). The odor response of PNs often outlasts the duration of the odor input (Perez-Orive et al. 2002; Brown et al. 2005). The activity of PNs during odor response increasingly becomes decorrelated. This has been shown in the zebra

fish olfactory bulb where during the course of duration of the odor stimuli, the odor response of mitral/tufted cells in the olfactory bulb becomes increasingly dissimilar (Friedrich and Laurent 2004).

The LNs in *Schistocerca* are GABAergic, axon-less and non-spiking (Laurent 1996; Leitch and Laurent 1996; MacLeod and Laurent 1996). They arborize throughout the AL neuropil (MacLeod and Laurent 1996) (**Fig. 1.4 E**). The non-spiking feature of *Schistocerca* LN is unique to this family as the LNs in bees and moths show Na+ action potential. The odor response of LNs in *Schistocerca* is characterized by short-amplitude spikelets, putatively calcium-mediated (Laurent 1996). The inhibition of PNs by LNs is also responsible for the synchronization of dynamic ensembles of AL PNs which leads to the oscillation observed in the LFP of MB (Laurent and Davidowitz 1994; Laurent and Naraghi 1994; Laurent et al. 1996; MacLeod and Laurent 1996; Wehr and Laurent 1996). The synchronized activity of PNs during odor response is abolished when the GABA A receptors are blocked by picrotoxin, a chloride channel blocker (Benson 1993; MacLeod and Laurent 1996) which has been shown to be effective in insects as well (Waldrop et al. 1987).

The odor information is relayed by the PNs in AL to the MB and LH by the mALT. There is only one reported ALT in *Schistocerca* spp. (Laurent and Naraghi 1994) (**Fig. 1.4 E**). The MB in *Schistocerca* is made up of a single cup-like structure called the calyx (**Fig. 1.5 Ai**), unlike the double calyces in cockroaches and honey bees but similar to the single calyx in *Drosophila*. The ~50000 KCs (diameter 4–8 μm) in the MB of *Schistocerca* project their dendrites in the calyx of the MB while their cell bodies are densely packed dorsal to the cup of calyx (**Fig. 1.5 Ai**). The axons of the KCs run ventrally, forming the pedunculus of the MB and bifurcate into two branches forming the alpha and beta lobes (Laurent and Naraghi 1994; Leitch and Laurent 1996) (**Fig. 1.5 Aii**). The pedunculus of MB is divided into three

fiber bundles, two from primary calyces and one from the accessory calyx (Weiss 1981). KC axons are spiny throughout their length and form en-passant synapses among themselves as well as with fiber of other neurons (both GABAergic and non-GABAergic) (Leitch and Laurent 1996). No subdivision of the MB in locust has been shown yet like those reported in honey bee, cockroach and *Drosophila*. The only segregation is seen in the organization of the pedunculus which has been shown to be organized in tubes when stained against NADPH-diaphorase (a marker for nitrous oxide) and in the alpha lobe where 6 tubes were stained (OShea et al. 1998) (Fig. 1.5 Aiii). The stratification in alpha lobe is postulated to be due to innervation by extrinsic neurons (OShea et al. 1998).

The MBs in *Schistocerca* also have a well-developed accessory calyx which receives afferent input from gustatory center, the lobus glomerulus (LOG). The LOG neurons are located dorso-lateral to the AL at the junction of the deutocerebrum and tritocerebrum (Ernst et al. 1977).

The odor-evoked synchronized input from the AL PNs results in the LFP in the calyx to be oscillatory with a power of 20–30 Hz (Laurent and Naraghi 1994). This oscillatory synchronization of the MB LFP is generated by the synchronized input from the AL PNs (MacLeod and Laurent 1996). The KCs are characterized by a baseline close to zero (Laurent and Naraghi 1994). Their odor response threshold is also very high. They fire only when synchronized input from multiple PNs reach it during a small time-window of each oscillation cycle. It thus acts like a coincidence detector. Its response consists of ~2.3 spikes (Laurent and Naraghi 1994; Perez-Orive et al. 2002, 2004; Stopfer et al. 2003; Jortner et al. 2007). In addition, since the identity of a given subset of PNs which are active during any particular odor instant keeps changing, it results in the change in the KCs which are active during any particular point.

The odor information is represented by a dense spatio-temporal code in the AL and this representation is transformed into a sparse code in the MB on the background of synchronized oscillatory activity. According to Macleod et al. (1998), the information encoded in MB is read by neurons downstream of KCs, the bLNs. Seven distinct morphological types of beta lobe extrinsic neurons have been reported in S. americana, of which type 1 and type 2 are commonly encountered in recordings (MacLeod et al. 1998; Gupta and Stopfer 2014). The cluster of bLN cell bodies is located in the lateral protocerebral lobe. Only a single neuron of type 1 bLN is present in each half of the brain (Fig. 1.5 Bi). It projects to the beta lobe, pedunculus and LH. It is GABA-negative. 12–15 type 2 bLNs have been reported and they project to the beta lobe, alpha lobe, pedunculus and also feed back to the calyx of MB (Gupta and Stopfer 2014) (Fig. 1.5 Bii). The bLNs respond to all odorants with vigorous firing rate and Macleod et al. (1998) report that the specificity of these neurons to distinguish between different odors is compromised when the synchronized oscillatory activity in MB is obstructed. Thus, the bLNs are sensitive to the synchronized activity of KCs. The synapse between bLN and KC has been shown to undergo Hebbian spike-timing dependent plasticity (STDP) on a timescale of \pm 25 ms. According to Cassaener and Laurent (2012), these synapses are susceptible to modulation by the reinforcement inducing neurotransmitter octopamine. This is thought to help in forming associations between different stimuli. Gupta and Stopfer (2014) have shown that the bLNs are also sensitive to the spike timing of KCs and respond to odor stimuli accordingly.

The transformation from dense representation of odor stimuli to sparse representation in the MB is attributed to the global inhibition of the KCs by a giant GABAergic neuron (GGN; (Papadopoulou et al. 2011), a neuron with wide spread arborizations in the calyx of MB, in addition to the alpha lobe and LH (Leitch and Laurent 1996; Papadopoulou et al. 2011) (Fig. 1.5 C). The GGN is GABAergic, with depolarizing odor response which

corresponds positively to increasing concentration strengths. GGN is reciprocally inhibited by another neuron called the IG (Inhibitor of GGN). The identity and role of IG in the circuit is unknown (Papadopoulou et al. 2011).

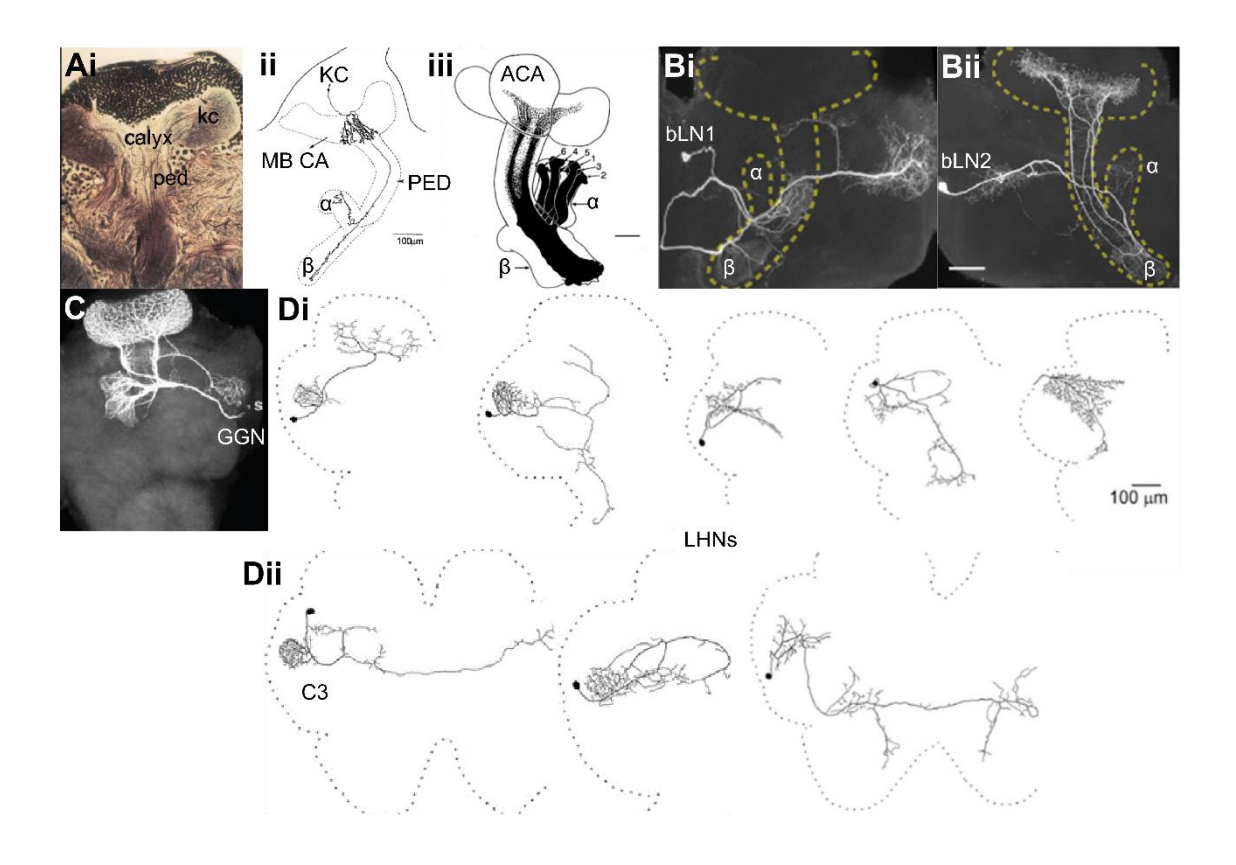


Figure 1.5 Morphology of higher-order neurons in *Schistocerca* spp. (A) Mushroom body structure and neuronal element. (i) Cell bodies of Kenyon cells are packed together densely, dorsal to the calyx of MB. Adapted from (Laurent and Naraghi 1994) (ii) A single KC, with its dendrites arborizing in the calyx and axon traversing ventrally before branching in the alpha and beta lobes. Adapted from (Laurent and Naraghi 1994) (iii) Tubular organization of the pedunculus and alpha lobe revealed by staining against NADPH-diaphorase (a marker for nitrous oxide). Adapted from (OShea et al. 1998) (B) Beta lobe neurons (i) type 1 bLN with cell body in the medial protocerebrum (ii) type 2 bLN with cell body in the lateral protocerebrum. Adapted from (Gupta and Stopfer 2014) (C) Giant GABAergic neuron. Adapted from (Papadopoulou 2010) (Di and ii) A variety of morphological types of lateral horn neurons. Adapted from (Gupta and Stopfer 2012)

The odor information from the PNs in AL is also fed to an area in the lateral protocerebrum called the LH (Ernst et al. 1977; Laurent and Naraghi 1994). The LH is analogous to the vertebrate amygdala (Friedrich 2011; Fisek and Wilson 2014). The LH in Schistocerca is an unstructured neuropil unlike the one in moths where it is formed of two linked toroids at a particular depth (Ian et al. 2016). The LH neurons show a wide diversity in morphology. Gupta and Stopfer (2012) reported at least eight different morphological types of LHNs, one of which projects to the MB (C3) (Fig. 1.5 Di and Dii). C3-like LHN, which has arborization in the LH and projects back to MB calyx, has also been reported in the moth, B. mori (Namiki et al. 2013). Another set of LHNs reported were bilateral in nature, crossing the midline of the brain and projecting to the contralateral side. All the LHNs respond to odorant stimuli with an increased firing rate. Gupta and Stopfer (2012) reported that the LHNs do not play a role in innate odor coding as reported in other insect species. Rather they play a role in bilateral coding (bilateral LHNs), multimodal integration and concentration coding. They also refuted the established notion prevalent until that time that the sparsening of odor response in KCs of MB is enabled by the feedforward inhibition from the LHNs (Perez-Orive et al. 2002) and postulated that this role is played by the GGN (Gupta and Stopfer 2012; Komarov et al. 2017). Since the LHNs responded to all the odors tested, they asserted that LHNs do not encode information about innately relevant odors.

Finally, across insect species including *Schistocerca* spp., neurons connecting the mushroom body structures bilaterally have not been identified. Though there have been reports of memory transfer between the two sides (Sandoz and Menzel 2001), it has now been shown that there is no evidence for such a bilateral transfer of olfactory memory (Vijaykumar et al. 2019).

With the aim of standardizing a species of grasshopper that is reasonably large and widely distributed in South Asia, *Hieroglyphus banian* was chosen for exploring the details of the olfactory circuit. It is known as a major paddy pest (Das et al. 2002; Mandal et al. 2007). It is easily available and we were able to breed it in the lab to have a steady supply without depending on the natural conditions outside. In the wild, it is found for approximately three months. In addition, it belongs to the family Acrididae of the order Orthoptera. As mentioned before, the olfactory circuits of a few insects from this family, namely *S. americana*, *S. gregaria* and *L. migratoria* have been investigated to different extents of detail due to their accessibility. In particular, the olfactory circuit of *S. americana* provides a robust system to study olfaction, and the advantage of 'uniquely identifiable neurons' which are amenable to various ways of manipulations. All this has helped to elucidate many principles of operation in the olfactory circuit.

1.5 Objectives of the study

The principal objectives of this study are outlined below:

- To characterize the anatomy and physiology of the neurons of the olfactory circuit in the grasshopper *H. banian*
- To compare the findings with a well-studied grasshopper *S. americana* and identify if the differences between olfactory circuit arise at early or late stages in the olfactory pathway, when the two species diverge at the subfamily level
- To identify novel circuits in the olfactory pathway
- To dissect the workings of a microcircuit formed by a pair of recurrent inhibitory olfactory neurons at the fourth-order level reported in *S. americana* and elucidate its role in the mushroom body circuit

1.6 Layout of the thesis

Chapter 2 describes the methods used to obtain the data.

Chapter 3 presents the data from the first-order to the fourth-order neurons in the olfactory pathway of grasshopper *H. banian* and compares it to the published data in *S. americana*.

Chapter 4 mentions and describes a class of novel bilateral MB extrinsic neurons discovered in *H. banian*.

Chapter 5 elucidates and tries to dissect the role of IG (Inhibitor of GGN) neuron in the olfactory circuit, using a unique indirect method to investigate its odor-response properties.

Chapter 6 summarizes the findings of the thesis.

A note on the terminology used in this thesis: The standardized terminology as specified by the Insect Brain Name Working Group (Ito et al. 2014) has been followed throughout the thesis, with the exception being alpha and beta lobes (which have been termed as vertical and medial lobes respectively, for all insect species in the updated nomenclature). The reason for retaining the old terminology for the output lobes of the mushroom body is to avoid any ambiguity as the published papers in *Schistocerca* use the old names.

Chapter 2

Materials and methods

2.1 Animals

We used adult *Hieroglyphus banian* (common name: rice grasshopper) of both sexes (**Fig. 2.1 A and B**) bred in-house in a crowded colony for our experiments. The grasshoppers were reared under controlled condition in the insect room maintained at the Centre for Neural and Cognitive Sciences, University of Hyderabad. The animals were kept at 70% relative humidity and 29°C temperature throughout the year. The insect room was maintained at 14h/10h light/dark cycle and the animals were provided with fresh wheat shoots (*Triticum aestivum*) everyday *ad libitum*.

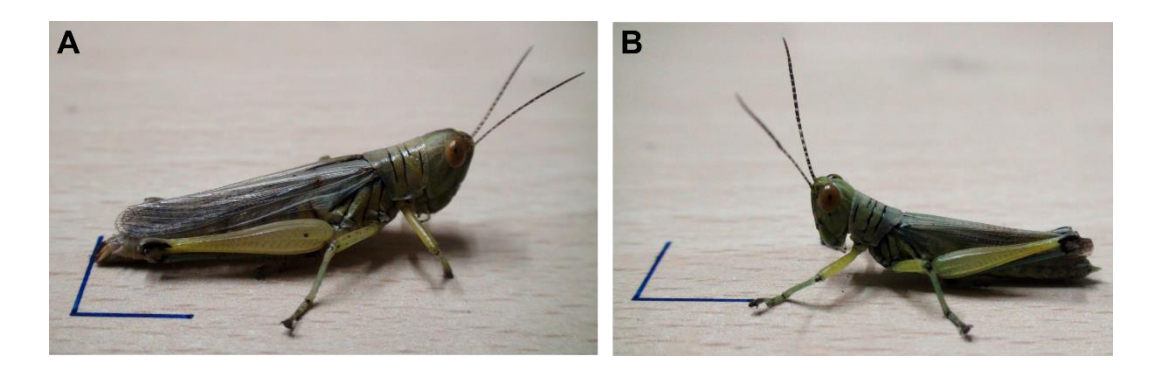


Figure 2.1 Hieroglyphus banian (A) Female H. banian (B) Male H. banian Scale bar: 1 cm

2.2 Dissection of animals for experiments

All the experiments were performed in vivo at 25°C and the methodology followed was as described in Laurent and Naraghi (1994) and Singh and Joseph (2019). At first, the wings and legs of the animal were removed to prevent movement during experiments; it was then placed in a small plastic holder (width similar to the animal's body-width) and secured with tape (Fig. 2.2 A). This plastic holder with the animal in it was stuck securely on a raised platform made of modelling clay (Mungyo Codiform, non-air hardening modelling material, Korea) fixed on a Petri plate (diameter 120 mm). The head of the animal was placed on a plastic head-stage such that the face was approximately at 45° (Fig. 2.2 B). A wax cup was subsequently built around the head of the animal to hold the insect physiological saline (Ringer's) during dissection and recording. Both the antennae of the animal were threaded through small tubes made of PTFE which were in turn threaded through wider plastic rings. The outer plastic rings were stuck on each side of the animal to the wax cup using wax (Fig. 2.2 C and D). This was done to prevent movement of the antennae from disrupting the recording process. Next, quick-hardening glue called epoxy (Fevitite, Pidilite Industries Ltd.) was mixed and inserted in the space between the inner tube and the base of the antennae such that the epoxy covered the surface of the base of the antennae as well as inside the inner tube. The inner tubes were gently pushed towards the base of the antennae and left as such for one hour for hardening completely. This tube held the antenna at the base. It was pushed outwards later on during dissection to provide extra space for having better access to the brain.

The wax cup was filled with insect physiological saline Ringer's and the cuticle of the head capsule was cut using a custom-made small axe (fabricated from a piece of razor blade fixed to a toothpick using epoxy). After removing most of the cuticle from the top of the head, the inner tubes covering the antenna were gently pushed outwards and the cuticle

covering the antennal base was carefully removed (**Fig. 2.2 E**). The fat bodies and air sacs on top of the brain were removed carefully using forceps, until the brain was exposed. Next, we removed the gut to reduce the movement of the brain. In order to remove the gut, at first its connection with the mouth, anterior to the brain, was sectioned using ophthalmic scissors.

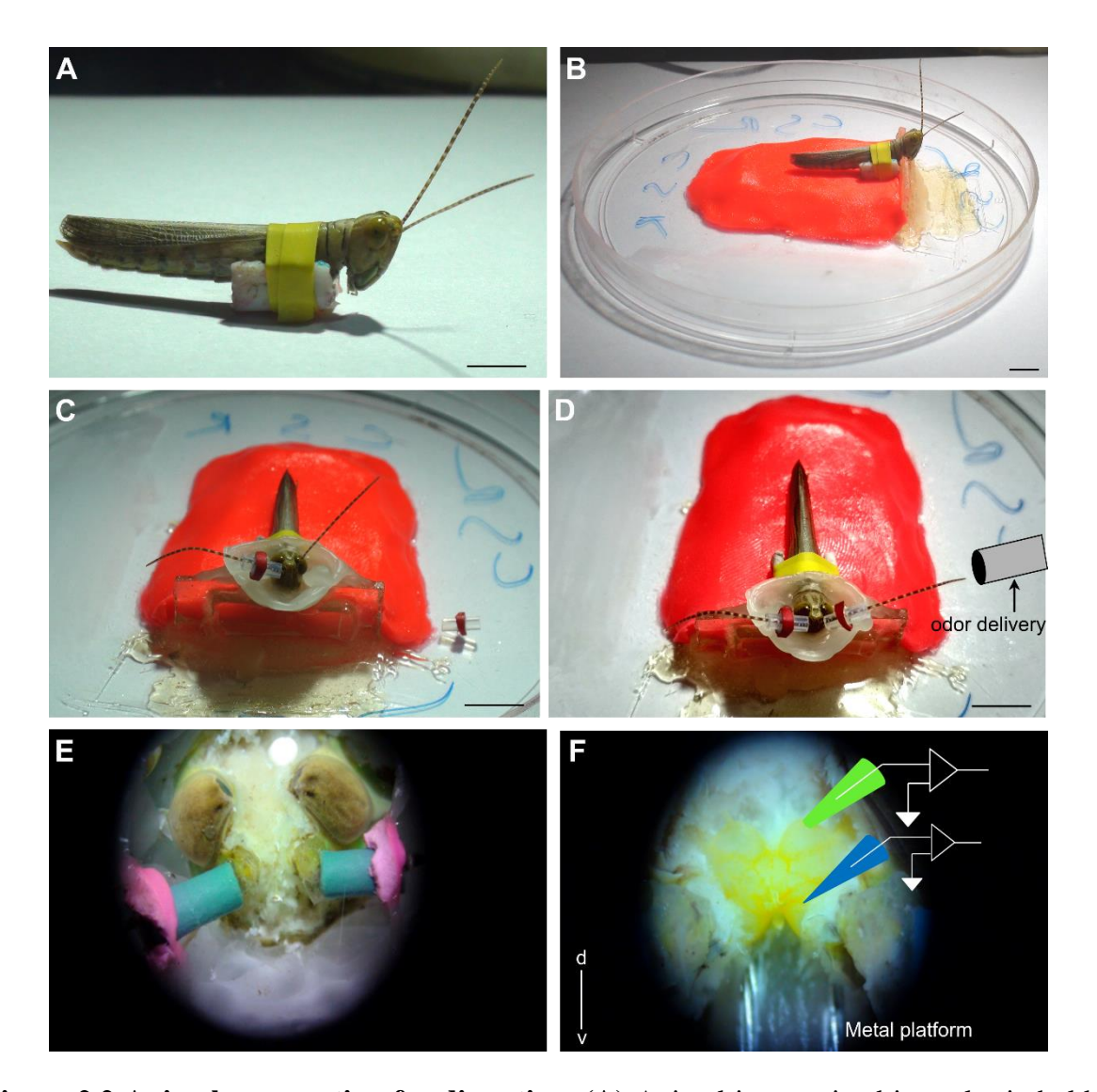


Figure 2.2 Animal preparation for dissection. (**A**) Animal is restrained in a plastic holder using insulating tape. (**B**) The restrained animal is fixed on a clay platform which is stuck on a Petri dish. The head of the animal is rested on a plastic head-stage. (**C**) The antennae of the animal are threaded through a small PTFE tube inserted into an outer plastic ring. The outer plastic ring is stuck to the wax cup which is built around the head of the animal. The wax cup holds the insect physiological saline during electrophysiology experiments. (**D**) Odor delivery set up near the animal. (**E**) The mounted animal with the cuticle of the head capsule removed. The fat bodies (whitish in the picture) can be seen. (**F**) The exposed brain after the fat bodies and air sacs are removed. The metal platform beneath the brain can also be seen. Scale bars: 1 cm for (**A**), (**C**), (**D**); 0.5 cm for (**B**)

A T-shaped slit was then made in the lower abdominal segment, dorsally, and the gut was pulled out through the slit carefully. The abdomen was tied tightly with a thread immediately, to prevent the leakage of body fluid and saline through the slit. The intracranial muscles posterior to the brain were also removed. Subsequently, a platform was made by twisting a wire, shaping it wide enough to fit the width of brain and covered thinly with wax. This metal platform was gently pushed below the brain, and raised upwards slightly to elevate the brain (**Fig. 2.2 F**). The protruding end of the wire platform was stuck to the wax cup and the extra part was cut off carefully using a metal-cutting plier.

Finally, a very small amount of protease (P5147, Sigma-Aldrich, India) was dabbed softly on top of the brain of the animal using forceps, left for ~30 seconds and then washed off vigorously using saline. The protease helps to soften the protein sheath covering the brain. Fine forceps were then used to tug at the protein sheath gently until the sheath detached from the brain. The sheath was removed gradually and the brain was exposed to access the neurons inside.

Composition of Ringers' saline: Glucose, Trehalose, 6.3 mM HEPES, 140 mM Sodium chloride, 1 mM Magnesium chloride, 5 mM Potassium chloride, 5 mM Calcium chloride, 4 mM Sodium bicarbonate, Sucrose, pH ~7.1 (Laurent and Naraghi 1994).

2.3 Odorants used during experiments

We used the odorants 2-Octanol (oct2ol), 1-Hexanol (hex), Octanoic acid (octac), Geraniol (ger), 1-Octanol (oct1ol) and mineral oil (MO) in our experiments. All the odorants and mineral oil were procured from Sigma-Aldrich, India. In few experiments, freshly cut wheat grass (*Triticum aestivum*) was also used. The odorants were used at concentrations of 0.1/1/10/100 % and the dilutions were made in mineral oil v/v.

2.4 Set-up for delivery of odor stimuli to the animal

The procedure outlined by Brown et al. (2005) was followed for setting up the odor delivery system. The odorants were delivered to the antenna of the animal by means of PTFE tubing kept three cm away from it (**Fig. 2.2 D**). A continuous stream of dry air flowed through the PTFE tubing at a speed of ~0.75 L/min and the odorants were delivered in this stream of dry air using computer-controlled valve system at a speed of ~0.1 L/min. A large vacuum pipe (diameter 16 cm) was placed behind the antennae to prevent the odorants from lingering in the airspace after delivery. The odorants (5 mL of each) were kept in glass bottles of 30 mL capacity. The bottles were fitted with a silicon stopper into which two hypodermic needles (Romsons, 18 G x 1.5"; 1.25x38 mm) were pierced such that the sharp ends were inside the bottle. The other ends were fitted with PTFE tubing, one meant for applying air pressure into the bottle and the other for pushing the odorant out into the continuous air stream.

2.5 Electrophysiology

Three types of electrophysiological recordings were carried out to study the properties of neurons of the olfactory circuit—electroantennogram (EAG), extracellular recordings and, intracellular recordings. In a few experiments, electrical stimulation was used to stimulate neurons and record from post-synaptic neurons. After intracellular recordings, the neurons were filled with dyes to observe their morphological characteristics.

2.5.1 Electroantennogram (EAG) recording

EAG recording was carried out from the tip (distal two segments), middle and basal (proximal two segments) parts of the animal's antenna using custom-made blunt borosilicate glass electrodes. The impedance of the electrodes was $<10M\Omega$ after filling with saline. Silver/silver chloride (Ag/AgCl) wire was used as a reference electrode and it was inserted in the ipsilateral eye of the animal. The signal recorded from the antenna was amplified by

Axopatch 200B (Axon Instruments) amplifier and bandpass filtered between 0.7–300 Hz. It was acquired at a sampling rate of 15 kHz using an acquisition system (USB National Instruments) and stored in a computer for offline analysis.

2.5.2 Intracellular recording

Custom-made sharp borosilicate glass microelectrodes (with filament, inner diameter 0.5 mm, outer diameter 1 mm, length 10 cm, catalog no BF-100-50-10, Sutter Instrument, Novato, CA, USA) pulled using a Flaming/Brown micropipette puller (model P-97; Sutter Instrument Co., Novato, CA, USA) were used for intracellular recording from different areas of the brain. The microelectrodes were backfilled with 0.2 M potassium chloride (KCl) solution made in 1X phosphate buffered saline (PBS). The electrodes with impedance ranging between 60– $200~M\Omega$ were used for recording intracellularly. Electrodes with higher impedances (>200 M Ω) were used to target Kenyon cells in the mushroom body. In most of the experiments, the electrodes were also filled with a dye (2% Neurobiotin; SP-1120, Vector Labs) prior to backfilling with 0.2 M KCl solution.

An Ag/AgCl ground wire was also inserted in the saline to act as a reference electrode for our recordings. The analog signal recorded from a neuron was first amplified by a head stage amplifier (HS-9AX0.1, Axon Instruments) by 0.1X. It was then amplified by another amplifier (Axoclamp 900A, Molecular Devices) 10X or 5X times and low pass Bessel filtered at 4 kHz. It was converted to digital form at a sampling rate of 10 kHz by Clampex 10.3 software and Digidata 1440A interface (Molecular Devices). Finally, it was stored in a computer for offline analysis.

We positioned the electrodes in the area of interest (AL/MB/LH/ beta lobe/LPL) using the coarse-movement switch of micromanipulators (MP-225, Sutter Instrument) and then searched the tissue using fine movement of the manipulators watching for membrane

potential features, characteristic of the neuron of interest. After recording from the neurons, they were filled with the dye Neurobiotin (2%), iontophoretically by injecting 1–4 nA current at 2 Hz pulse for 20–60 minutes.

LNs in AL were identified by the shape and amplitude of the action potential recorded. LNs are reported to be devoid of sodium action potential (Laurent and Davidowitz 1994; Laurent 1996) and LN spikes have shorter amplitude as compared to PN spikes. They were detected when three times the standard deviation of the membrane potential was used as a threshold while doing offline analysis.

PNs in AL were recognized by the characteristic sodium spikes produced by them which are sharp and have large amplitudes. They were detected when six times the standard deviation of the membrane potential was used as threshold while doing offline analysis.

KCs were recorded from the cell body layer of the MB instead of the calyx, in order to avoid recording from PNs or other protocerebral neurons, which innervate the MB calyx. They were targeted with high impedance electrodes as they have very high input resistance. GGN was identified by the characteristic large discrete IPSPs and odor-induced depolarizing response to Hexanol 100% in its membrane potential.

We targeted the areas where LHNs' and bLNs' arborizations are known to be present and they were identified by their vigorous odor responses. LHNs were also characterized by the sub-threshold oscillations in their odor response. The final identities of all neurons were confirmed by confocal imaging of the dye-filled neurons after the experiments.

2.5.3 Extracellular recording

Custom-made blunt borosilicate glass microelectrodes pulled using the micropipette puller were used to make extracellular recordings of LFP from the MB calyx and cell body layer.

The electrodes used had an impedance of $<10 \text{ M}\Omega$ after they were filled with insect saline. The signal recorded was processed as mentioned in section 2.5.2, amplified by 1000X. The signal was bandpass Bessel filtered between 0.1–80 Hz and acquired at a sampling rate of 10 kHz by the digitizer (Digidata 1440A) before storing it in the computer for offline analysis.

2.5.4 Electrical stimulation

In few experiments involving GGN (chapter 5), MB KCs were electrically stimulated using custom-made twisted wire tetrodes electroplated with a gold solution, to reach the impedance of 220 k Ω at 1 kHz. These twisted wire tetrodes were electrically stimulated using a custom-made optically isolated electrical stimulator at strengths of ~15 μ A TTL triggered for 4 ms from the acquisition setup (Evans 1982). In order to induce a response in GGN membrane potential indirectly, by electrically stimulating the MB KCs, the strength of the current injected in the MB cell body layer was adjusted, until EPSP was observed in the GGN membrane potential.

2.6 Immunohistochemistry of whole mount of brain

The brains with dye-filled (2% Neurobiotin) cells were perfused with Ringers' physiological saline for a minimum of 4–6 hours after filling. They were then dissected out and immediately put in 4% paraformaldehyde (PFA) made in 1X phosphate buffered saline (PBS; 1X in distilled water; Himedia, RM7385) for 4 hours for fixation. This was followed by three washes of PBS for 30 minutes each and membrane permeabilization in 3% Triton® X-100 (Sigma, T8787) in PBS (PBST) for one hour. Subsequently, they were incubated with fluorescent streptavidin-conjugated Alexa Fluor 488 or 568 or 633 (S11223 or S11226 or S21375; Invitrogen) added to the PBST solution (1:1000 dilution) for five days, with intermittent shaking. After five days, the solution was decanted off and the brains were washed in PBS thrice for 30 minutes each. The brains were then run through an ascending

alcohol series for dehydration (30, 50, 70, 80, 90, 100%) for 20 minutes each. Finally, they were cleared and mounted in methyl salicylate (M-6752; Sigma-Aldrich, India) in concavity slides (Himedia, GW089). The whole mounts of brains were covered with a glass coverslip and the edges sealed with transparent nail polish (Lotus/Lakme) to prevent the methyl salicylate from leaking out. They were kept in horizontal slide boxes covered with aluminum foil to protect from light and stored at 4°C until the day of confocal imaging.

Anti-GABA and nc82 immunohistochemistry: Anti-GABA immunohistochemistry for determining the GABAergic nature of dye-filled cells and nc82 immunohistochemistry against the synaptic density protein bruchpilot for delineating the synaptic areas of the brain was carried out on brains with dye-filled cells. After the brains were fixed in 4 % PFA and washed thrice in PBS as described above, they were immersed in PBST (to permeabilize the membrane) containing 10% normal goat serum (NGS; 1:10 dilution; for blocking nonspecific binding of antibody) for one hour. The brains were then incubated with rabbit polyclonal anti-GABA primary antibody (1:1000; A-2052, Sigma-Aldrich, India) and/or mouse monoclonal nc82 (1:1000; DSHB, Iowa city, IA; donated by E. Buchner) and stored at 4°C for five days, with intermittent shaking. After five days, the solution was decanted off and the brains were washed thrice with PBST (for one hour each). Thereafter, they were incubated in the secondary antibodies' goat anti-rabbit/anti-mouse Alexa Fluor 488 or 568 or 633 IgG (A-11008 or A-11011 or A-21070; Invitrogen) at 1:1000 dilution in PBST for another five days, with intermittent shaking. After five days, the brains were washed in PBST and PBS as described above and dehydrated in an ascending alcohol series. Finally, they were cleared and mounted in methyl salicylate for confocal imaging.

2.7 Neural tract tracing

Dextran biotin (DB; D7135, Invitrogen) and dextran tetramethylrhodamine (DTMR; D3308, Invitrogen) were used for neural tract tracing. These were inserted in the areas of interest (AL or MB calyx or beta lobe in different preparations) using fine forceps after dissection and washed with saline thereafter to prevent the extra dye from getting absorbed in other areas. For DB, the brain is processed similar to the method described in section 2.6 (for Neurobiotin). Since DTMR is fluorescent, it does not require a secondary for visualization, but rest of the post dye-insertion process is same as that for Neurobiotin.

2.8 Antennal backfills

For visualizing the glomerular structure of the AL in *H. banian*, the animal was fixed on a Petri dish as described in section 2.2 and the antennae was cut with ophthalmic scissors at the level of the scape, the basal segment (**Fig. 2.3**). The stump was then filled with the dye dextran biotin and covered with Vaseline to avoid desiccation. It was left as such at 4°C for ~12 hours, and the brain was dissected the next day and processed similar to the tissues for neural tract tracing (section 2.7).



Figure 2.3 Location of antennal transection for antennal-backfill experiment. The antenna was cut at the basal segment called scape (red line in the image) and the stump was filled with the dye dextran biotin. Scale bar: 1 mm; Adapted from Roonwal (1952)

2.9 Confocal microscopy

The brains with dye-filled neurons or tracts were imaged using confocal laser scanning microscope (CLSM; Leica TCS SP2, Leica microsystems or Zeiss LSCM NLO 710) with an objective of 10X or 20X. The tissues were scanned at a resolution of 1024X1024 or 512X512 pixels. The wavelengths of the excitation lasers used were either 488 or 545 or 633 and their gain and intensity were adjusted manually. After imaging, the confocal stacks were processed using three public domain software, Fiji ImageJ 1.47v (National institute of Health, Bethesda, MD) (Schindelin et al. 2012), Inkscape 0.92.5 and GIMP 2.10.8 to make the final images. All the images are projections along the z-axis of a stack of multiple optical slices. They were only modified for brightness and contrast.

In cases where the images of dye-filled neurons were not clear when the z-projections were made, they were reconstructed using the simple neurite tracer plug-in (chapter 3, **Fig. 3.14** and **3.15** and chapter 4, **Fig. 4.5**) (Longair et al. 2011) in Fiji ImageJ 1.47v. In some cases, two or more images were stitched together using the 'image stitching' plug-in (Preibisch et al. 2009) in Fiji ImageJ 1.47v to make a composite image.

2.10 Processing of antennae for FE-SEM

The morphological details about the different types of sensilla present on the antennae of *H. banian* were explored by scanning it in a Field Emission Scanning Electron Microscope (FE-SEM; Zeiss Ultra 55). The processing of antennae for FE-SEM was done according to the procedure outlined by Ochieng et al. (1998). Briefly, the antennae, cut at the base, were fixed in 70% ethanol and kept at room temperature for three days. Subsequently, they were dehydrated through an ascending ethanol series of 80%, 90% and 100% for 30 minutes each. The dehydrated antennae were stored in 100% ethanol at 4°C until the day of imaging. Before imaging, the ethanol was pipetted out from the Eppendorf tubes containing the antennae and

the antennae were dried using hot air dryer for two minutes. They were then air-dried for 15 minutes. The antennae were fixed on a platform and sputter-coated with gold palladium for 90 seconds before being imaged at 3/20 kV EHT in FE-SEM.

2.11 Data analysis

All the electrophysiological data were analyzed using custom-made programs written in MATLAB (MathWorks). The plots were then processed in Inkscape 0.92.5 and GIMP 2.10.8.

2.11.1 Detecting LN and PN spikes from AL interneuron recordings

LN spikes were detected by using three times the standard deviation of the membrane potential as a threshold, while six times the standard deviation of the membrane potential was used as threshold for detecting PN spikes. The difference between the average resting membrane potential and the peak of the spikes was taken as the amplitude of the PN and LN spikes and their widths were calculated as width at half of the spike's peak amplitude. PN and LN spikes differ from each other in their spike amplitude and width.

2.11.2 Cross-correlation

Unbiased cross-correlation function in MATLAB was used to compute and plot the cross-correlation between the LFP recorded from the cell body layer and calyx of MB.

Cross-correlation between the KC membrane potential and LFP from the calyx of MB was calculated using the xcorr() function in MATLAB. The procedure followed was similar to the one outlined by Laurent and Davidowitz (1994) and Perez Orive et al. (2002). The cross-correlogram was created by taking 200 ms windows of the waveform shifted every 50 ms and then stacked together.

2.11.3 Calculating power spectrum

The fft() function in MATLAB was used to calculate the LFP spectrum recorded from the MB calyx. The square of the absolute value of the Fourier transform was used while computing the power spectrum and the area under the curve of the power spectrum in a particular band was used to calculate the power in that band.

Chapter 3

Morphological and physiological characterization of the olfactory circuit of grasshopper *Hieroglyphus banian* through the fourth-order neurons

3.1 Introduction

Insects constitute one of the most diverse phylogenetic groups on earth, one million species belonging to 30 orders have been described as of now and many continue to be discovered still (Grimaldi et al. 2005). A mindboggling 400 million years of evolution has resulted in them dominating every possible favorable or extreme ecological niche (Grimaldi et al. 2005). As described in chapter 1, olfaction plays a major role in many insect behaviors critical for its procreation and survival. The olfactory circuit has been well-elucidated to varying degrees of details in a number of insect species, especially from the seven orders Diptera (*Drosophila*), Hymenoptera (bees and ants; particularly *Apis mellifera*), Lepidoptera (moths; particularly *Manduca sexta*), Blattoria (cockroach; *Periplaneta americana*), Orthoptera (crickets and grasshoppers/locusts; particularly *Schistocerca americana/gregaria* and *Locusta migratoria*), Hemiptera and Coleoptera (beetles) (Martin et al. 2011).

One question of interest is how conserved the olfactory circuit is across insects at different taxonomic levels. In general, it is well-established that the basic plan of organization is similar across insect species from different orders (Hildebrand and Shepherd 1997;

Strausfeld et al. 1998; Strausfeld and Hildebrand 1999; Ache and Young 2005; Wilson and Mainen 2006; Galizia and Rössler 2010). However, differences have been found at the peripheral (ORNs, antenna) or initial stages of olfactory processing centers, in terms of innervation pattern or organization of neurons within a particular area (antennal lobe, PNs and LNs) (Galizia and Sachse 2010; Hansson and Stensmyr 2011; Martin et al. 2011). Moreover, a number of studies have compared the olfactory circuit at different levels between insect species from different orders, genus, families (Brockmann and Brückner 2001; Ignell et al. 2001; Rössler and Zube 2011; Bisch-Knaden et al. 2012; Kollmann et al. 2016; Schultzhaus et al. 2017). Extensive comparative studies are available for the first and second-order olfactory structures, some are also available for the third-order level; nonetheless studies at the fourth-order level are rare. Besides, there is no study which gives information about how similar or different the olfactory circuit would be between species which belong to different subfamilies, especially at the higher orders. This information would enable us to predict or make an informed guess about similarities or dissimilarities we could expect in species belonging to different subfamilies.

Among insects, a number of orthopteran species like *S. americana*, *S. gregaria* and *L. migratoria* have been widely used to investigate the olfactory circuit—morphologically as well as physiologically. They have proved to be very useful in elucidating the basic principles of olfaction, not only in insects but have broadly helped to understand human olfaction as well. In fact, the olfactory circuit in *S. americana* has been dissected through the fourth-order neurons which is a rarity as fourth-order olfactory neurons have only been studied in very few insect species, namely *P. americana*, *A. mellifera*, *D. melanogaster*, *Acheta domesticus* (as detailed in chapter 1).

The species *S. americana* which has been so well-studied is not found in India. In order to study the olfactory circuit of a grasshopper species which is endemic to India, we tried to rear few grasshopper species collected from the wild in lab conditions. Of the species which we tried to culture; we were able to successfully breed *H. banian* and maintain its culture. Both *S. americana* and *H. banian* belong to the same family but different subfamilies which separated from each other approximately 57 million years ago (Song et al. 2018). *H. banian* is an Acrididae species belonging to the subfamily Hemiacridinae (Dirsh 1956; Cigliano et al. 2018) while *Schistocerca* belongs to Cyrtacanthacridinae (Kirby 1910; Cigliano et al. 2018). *H. banian* is native to the Indian subcontinent and Vietnam while *S. americana* is found in North America (Cigliano et al. 2018).

The two species differ in other aspects as well. The former has a single breeding season in a calendar year (Mandal et al. 2007) while *S. americana* has two breeding seasons per year (Kuitert and Connin 1952). Both the species differ in their host plant preferences, even though both are generalists and polyphagous by nature. *S. americana* feeds primarily on citrus plants, corn, soybean, bean and several species of grasses (Capinera 1993; Squitier and Capinera 1996). On the other hand, *H. banian* is an infamous paddy pest. It also feeds on a number of other species from the Poaceae and Cyperaceae families (Das et al. 2002; Mandal et al. 2007). Since olfaction mediates in giving rise to all the above-mentioned behaviors, we expected to find differences at the anatomical or physiological level between the olfactory circuit of the two species. To this end, we studied the olfactory circuit of the grasshopper *H. banian*, and compared its olfactory circuit (both anatomically and physiologically) through the fourth-order neurons to that of the well-studied locust *S. americana*.

We carried out intracellular recordings from individual neurons constituting the olfactory pathway of *H. banian* to characterize their responses to odorants and filled them

with dyes post-recording to delineate their morphological features. The odor-evoked population response of neurons from mushroom body, a learning and memory center was studied using extracellular recordings. The connectivity between different olfactory areas was investigated using mass dye fills. Major synaptic neuropils and inhibitory elements of the brain were examined using specific antibodies. In addition, the sensilla on the antenna which is the primary olfactory organ was explored using FE-SEM. All the methods used in this chapter to obtain the results, namely FE-SEM, neural tract tracing using mass dye fills, extracellular and intracellular recordings, immunohistochemistry, confocal imaging and image processing, electrophysiological data analysis using MATLAB are described in detail in Chapter 2.

Our results show that the olfactory circuits of the two species, *H. banian* and *S. americana* are conserved, both physiologically and anatomically, through the fourth-order neurons. Details about the olfactory pathway of *S. americana* can be found in chapter 1. We also found that in *H. banian*, there are three antennal lobe tracts (lateral ALT, mediolateral ALT and transverse ALT) in addition to the major ALT—the medial ALT (mALT). Only mALT has been reported in *S. americana* or its related species *S. gregaria*. There might be differences at the peripheral levels in terms of number of olfactory receptors or branching patterns of olfactory receptor neurons or projection neurons' dendrites between the two species, which we did not investigate in the present study. However, we found that at the higher levels (third and fourth orders—LHNs, KCs, bLNs and GGN), the neurons of the olfactory pathway are highly conserved in terms of their morphological and physiological features. We have also discovered a new tract between MB and LH (Singh and Joseph, 2019). In short, we can say that the olfactory circuit of two species belonging to different subfamilies would be highly conserved.

3.2 Results

3.2.1 Types of sensilla found on the antennae of *H. banian*

The antenna of HB is of filiform type (**Fig. 3.1 A**) subdivided into three parts—scape, pedicel and base. A previous study reported the number of segments on each antenna and compared it between male and female *H. banian* (Coleman and Kunhi Kannan 1911; Roonwal 1952). The counting of the antennal segments was repeated and found to be similar to the previously reported data. There were 28–30 segments in adult female *H. banian* and 28–29 in adult males. Coleman and Kuhni Kannan (1911) reported 25–26 in males and 27–28 antennal segments in females in the penultimate stage.

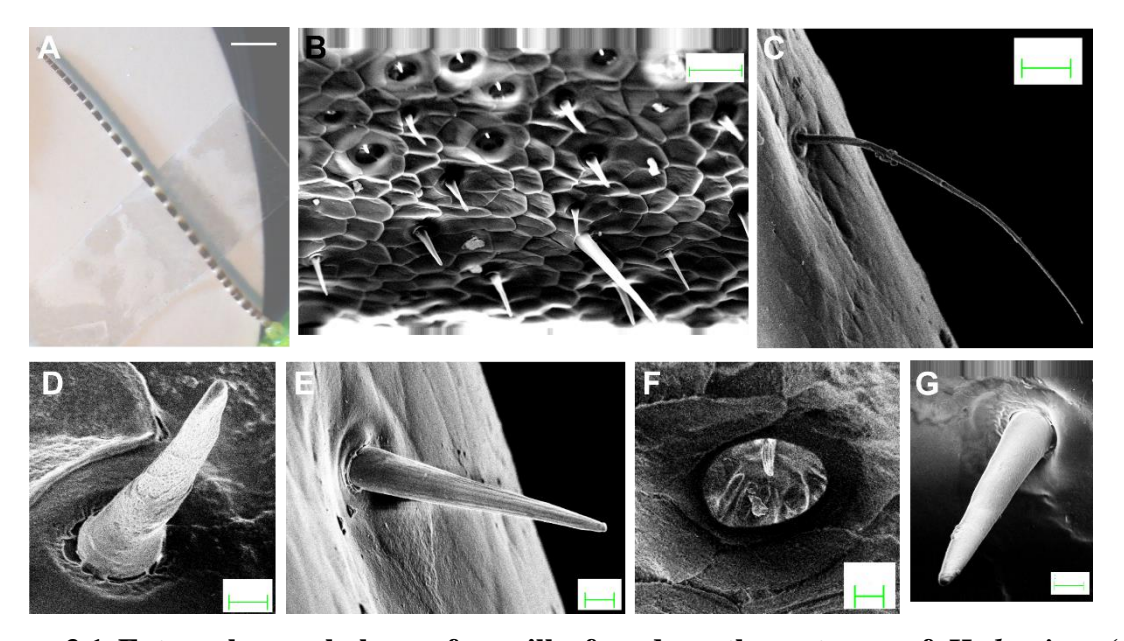


Figure 3.1 External morphology of sensilla found on the antenna of H. banian. (A) External morphology of the antenna. The antenna in H. banian is of filiform type with three segments commonly found in all insects—scape, pedicel and flagellum. The number of segments in male and female vary from 28–30. (B) A portion of antennal surface showing the different kinds of sensilla present on it. (C) A mechanosensory sensillum, observed on the basal segment of the antenna. It is poreless and longer than other types of sensilla. (D) Sensillum basconicum, characterized by numerous pores on its antennal surface. (E) Sensillum chaeticum, marked by longitudinal ridges on its surface. (F) Sensillum coeloconicum, the shortest among all the sensilla types. It is located inside a pit on the antennal surface and has longitudinal grooves on its surface. (G) Sensillum trichodeum, with pores on its surface but the density was less when compared to sensillum basiconicum. Images (B–G) are from the same animal. Scale bars: 2 mm (A), 20 μ m (B, C), 2 μ m (D, F, G), 3 μ m (E)

Similar to other insect species, in *H. banian*, any given segment of the antenna bears sensilla of different types on it (**Fig. 3.1 B**). A putative mechanosensory sensillum was observed on the basal segment of the antenna (**Fig.3.1 C**). This sensillum was longer as compared to the other sensillar types which were observed on the *H. banian* antenna and very narrow in width. It did not have pores on its surface. In addition, four types of surface sensilla were found on the antenna of *H. banian* (**Fig. 3.1 D-G**). Sensillum basiconicum (**Fig. 3.1 D**), has numerous pores on its surface and is located in a shallow depression on the antennal surface. Sensillum chaeticum (**Fig. 3.1 E**) is distinguished by longitudinal grooves on its surface. Sensillum coeloconicum (**Fig. 3.1 F**) is located in a pit on the antennal surface and has longitudinal ridges on its surface. It is the shortest of all the sensillar types. Sensillum trichodeum (**Fig. 3.1 G**) also has pores on its surface but the density was less when compared to S. basiconicum. The presence of pores on the surface of the sensilla points to their putative role in olfaction.

The population response of the ORNs (electroantennogram, EAG) in response to different odorants was recorded from the tip, middle and basal segment of the antenna (**Fig. 3.2**). The EAG recorded varied in strength across the three regions in compliance with the density of olfactory sensilla on the antennal surface, where the tip has the maximum density and the base, the least. In addition, the strength of EAG amplitude recorded from a particular location varied across different odorants and also across different concentrations of the same odorant (**Fig. 3.2 A and B**).

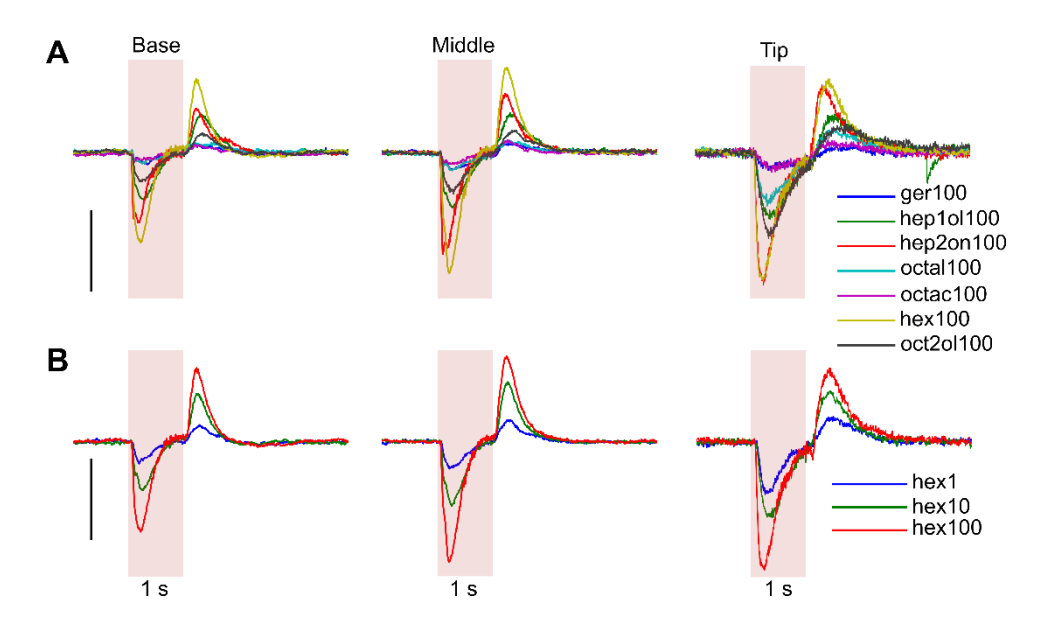


Figure 3.2 Electroantennogram (EAG) varies across the length of the *H. banian* antennae. (A) EAG recorded from the base, middle and tip of the antenna of the same animal varied in strength for the same odorant. The odor-response was strongest at the tip and weakest at the base. The EAG amplitude also varied in strength for different odorants. Some of the odorants elicited stronger responses than others. Scale bar: $300 \, \mu V$ (B) The population odor-response also varied for different concentrations of the same odorant, indicating the recruitment of larger numbers of olfactory receptor neurons or currents per receptor neuron at higher concentrations. Scale bar: $300 \, \mu V$

To characterize the synaptic neuropils, present in the brain of *H. banian* and the presence of GABAergic elements, the whole brain of *H. banian* was immunostained with nc82 and anti-GABA primary antibodies (**Fig. 3.3 A and B**). The observable synaptic neuropils were optic lobe, mushroom body calyx, alpha lobe, beta lobe, antennal lobe, pedunculus, lateral horn, and central complex (protocerebral bridge and central body).

3.2.2 Tracts from the antennal lobe and lobus glomerulus to the higher olfactory centers

In dye-fills from the AL, four antennal lobe tracts (ALTs) were observed (**Fig. 3.4 A**). Of these, three have been observed for the first time in any insect species from family Acrididae of order Orthoptera. They are the lateral ALT (lALT), mediolateral ALT (mlALT) and the transverse ALT (tALT). The naming convention for these tracts is as described by Ito et al. (2014). The major ALT is the medial ALT (mALT), through which the majority of the AL

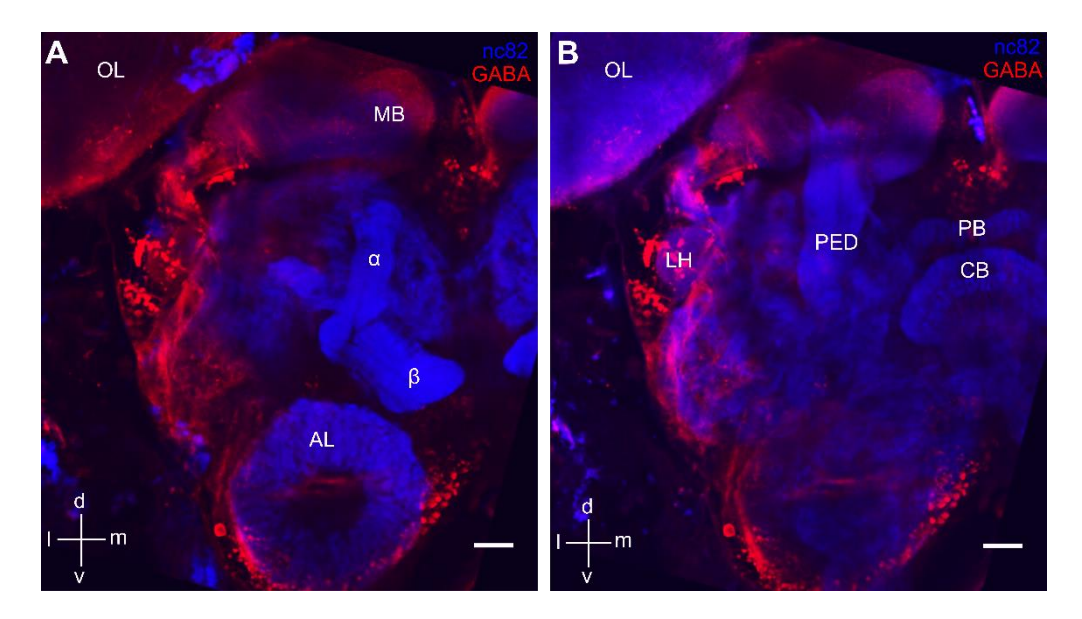


Figure 3.3 Major neuropils in the brain of H. banian. Major neuropils (areas of synaptic densities) discernible in H. banian brain when immunostained with nc82 (blue, antibody against synaptic density protein bruchpilot) and anti-GABA (red). (A) Antennal lobe (AL), alpha lobe (α), beta lobe (β), lateral horn (LH), mushroom body (MB), optic lobe (OL), pedunculus (PED) (B) central body (CB) and protocerebral bridge (PB). The axons of the intrinsic neurons of the MB travel through the PED to bifurcate and arborize in α and β lobes, the two output lobes of the MB. AL, MB and LH form part of the olfactory circuit, while OL is involved in processing visual information. The PB and CB are part of the central complex, an area involved in processing polarized light. Scale bars: 100 μ m

PN axons project to the higher olfactory centers. The mALT exits the AL dorso-laterally, and runs across the protocerebrum dorsally to project first to the MB calyx and then to the LH. Its trajectory is similar to that reported in other orthopteran species (Ignell et al. 2001). Two more tracts exiting from a location lateral to the mALT were observed. The lateral most of these is the lALT (named according to the convention followed by (Ito et al. 2014)) which after exiting the AL, projects to the LH. It does not project to the MB. The other tract which was designated the mediolateral ALT (mlALT), travels to the LH first and then to the MB. Apart from the mALT, lALT and the mlALT, another tract, transverse ALT (tALT) was also observed. The tALT branches out from the mALT, at the level of the central complex and travels laterally to project to the LH. Both lALT and tALT project only to the LH.

The cell bodies of lobus glomerulus (LOG) are located dorsolateral to the AL, at the juncture of the deutocerebrum and the tritocerebrum (**Fig. 3.4 B**). The LOG receives gustatory input from the sensilla on the maxillary palps (Ernst et al. 1977). The tritocerebral tract (TT), which is formed of the axons of LOG neurons, travels ventrally for a short distance and then bifurcates into two branches—dorsal and ventral. The dorsal branch travels for a short distance dorso-medially and exits from the same location as the mALT forming the TT while the ventral branch travels for a short distance to arborize in the tritocerebrum.

The TT travels along the lateral margin of the mALT up to the medial protocerebrum (Fig. 3.4 A). It diverges from it there and travels further, dorsally to terminate in the accessory calyx.

3.2.3 A novel tract, CT (curved tract)

Dye fills from the calyx of MB also revealed a novel tract not reported in any insect species (Fig. 3.4 Ci, Cii). This tract, which we termed as CT (for curved tract) begins near the area where cell bodies of the LH are generally found. It runs between the LH and MB. We observed this tract in five separate preparations, when dye was injected in the MB calyx. The complete tract was filled in only one sample, but even in other samples with partial fills, this tract could be recognized unambiguously. The tract runs ventromedially from the LH for some distance and turns in the medial direction towards the pedunculus but does not innervate it. From there, it runs in a slightly dorsomedial direction up to the mALT and turns once more, this time in the dorsal direction. It continues slightly dorsolaterally to reach the MB to terminate in the calyx at a point between the mALT and the pedunculus. We did not observe terminals of the CT near LH, however a branch was observed in the superior lateral protocerebrum dorsal to the LH. The details of CT in the circuit need to be explored further.

A schematic representing all the AL tracts, TT and CT is shown in Fig. 3.4 D.

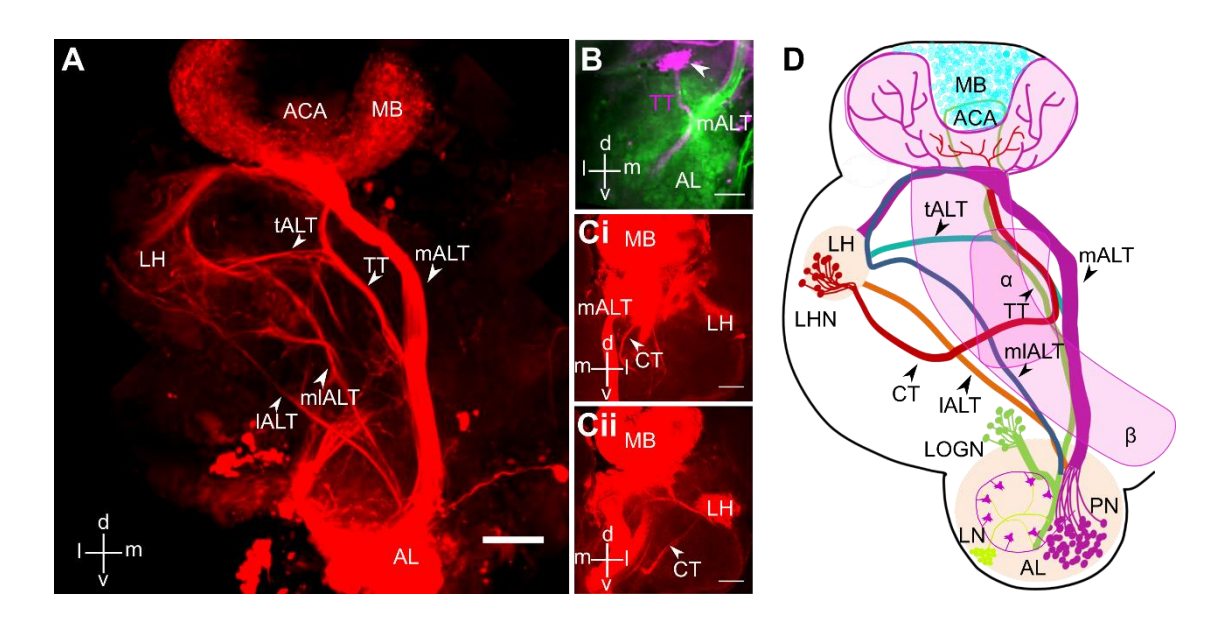


Figure 3.4 Antennal lobe and lobus glomerulus tracts in H. banian. (A) AL tracts to MB and LH. Dye-fill from the AL reveals multiple tracts projecting to the higher olfactory centers, MB and LH. Medial antennal lobe tract (mALT), transverse ALT (tALT), mediolateral ALT (mlALT) and lateral ALT (lALT) are the four ALTs observed in H. banian. mALT projects to both MB and LH, tALT and lALT project to the LH alone while mlALT projects to LH first and then to the MB calyx. The major tract—mALT exits the AL dorso-medially and projects to the MB calvx before travelling further and terminating in the LH. The tALT branches out from the mALT and terminates in the LH, bypassing the MB calyx completely. In addition, two ALTs-IALT and mlALT, which exit from the AL adjacent to the exit point of the mALT, project directly to the LH; lALT terminates in LH but mlALT runs further to terminate in the MB calyx. The tritocerebral tract (TT) is also identifiable in this figure. TT originates from the lobus glomerulus (LOG) cell bodies in the tritocerebrum and terminates in the accessory calyx of the MB. (B) Origin of the TT. The TT is formed by axons of the LOG neurons (arrowhead), which are located dorso-lateral to the AL, at the junction of the deuto- and tritocerebrum. The TT travels ventrally for a short distance and then bifurcates into two branches. One branch runs ventro-laterally to arborize in the tritocerebrum, while the other travels dorso-medially and exits from the same point as the mALT, running along its lateral margin. (Ci) and (Cii) A novel tract, designated CT (for curved tract) is visible in fills from the MB calyx. This tract runs between the LH and MB and has not been reported in any insect species so far. (D) Schematic showing all the AL tracts, CT and TT in the same figure. Images (A-C) are from different animals. Scale bars: $100 \mu m$

3.2.4 Antennal lobe in *H. banian* has a microglomerular organization

The microglomerular nature of the AL in *H. banian* is revealed by dye fill from the antenna (**Fig. 3.5 A**). A central dark region, known as the coarse neuropil, is seen which is devoid of ORN innervation. This central region is surrounded by numerous microglomeruli which appear as bright spots in the image. In some microglomeruli fibers of the ORNs terminating in them are also distinguishable.

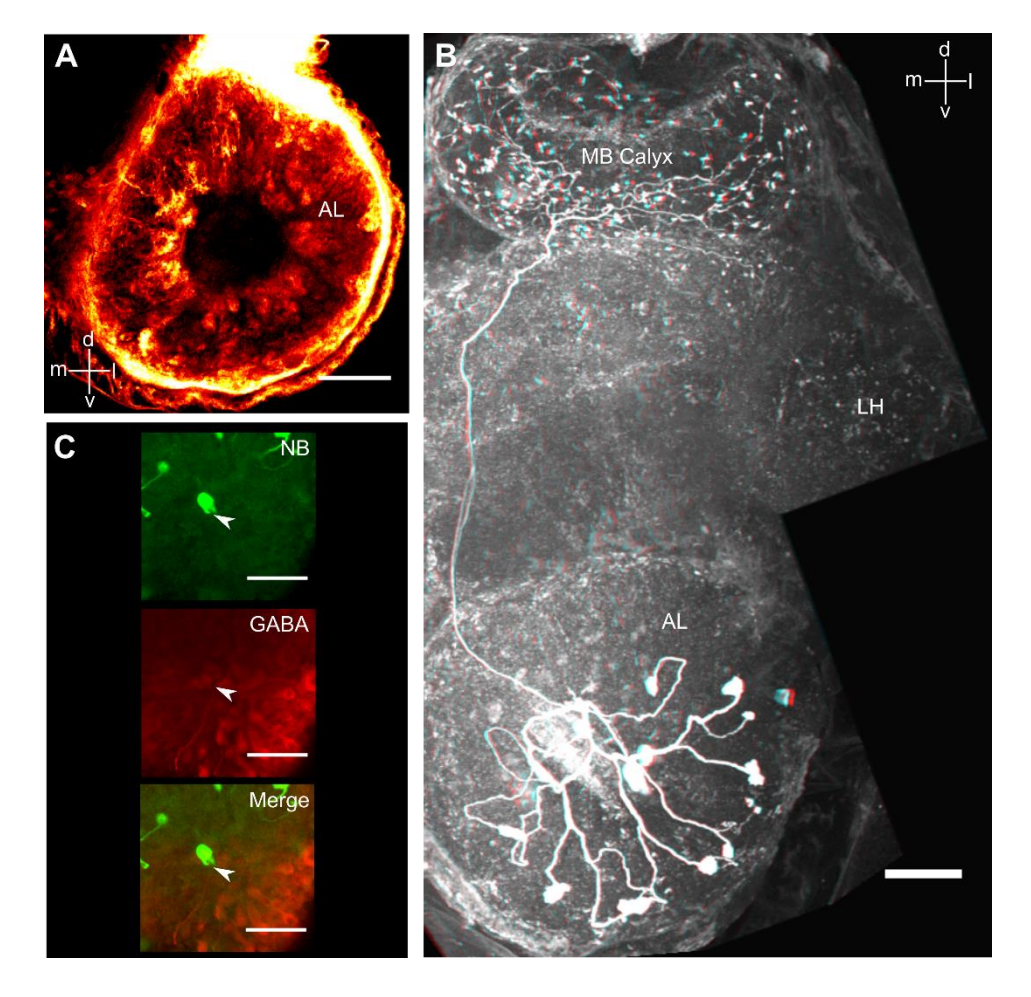


Figure 3.5 Morphological and immunohistochemical features of the projection neurons in AL. (A) Microglomerular nature of the AL. Dextran biotin fill from the antenna reveals the microglomeruli arrangement of the AL. A dark core devoid of ORN terminals, called the coarse neuropil, is surrounded by a bright area with discernible fibers of ORNs. (B) Morphology of AL PN. It is multiglomerular, with multiple neurites radiating outwards and terminating in neuropils. A single axon from each PN exits the AL dorso-medially, running dorsally across the protocerebral lobe and arborizing in the MB calyx densely and widely. The axon travels further, laterally and terminates in the LH. The varicose terminals are indicative of its output nature in the MB and LH. (C) Anti-GABA immunohistochemistry of this PN revealed it to be GABA-negative. Scale bar: 100 μm

3.2.5 Morphology and physiology of projection neurons in the antennal lobe

The projection neuron (PN) in the AL of *H. banian* is multiglomerular (**Fig. 3.5 B**). The dendrites of the PN bifurcate into many branches and terminate in different microglomeruli in the AL. The axon of the PN exits the AL dorso-laterally and travels to the MB calyx first and then to the LH. It arborizes densely in the MB calyx. This PN was GABA-negative (**Fig. 3.5 C**).

The same PN responds to different odorants with different spatio-temporal patterns of activity (**Fig. 3.6 A**). The set of PNs we recorded from responded to all odorants presented. These temporal patterns are characterized by periods of excitation, inhibition and quiescence.

Intracellular recordings from different PNs showed that they responded with different patterns of activity to the same odorant (**Fig. 3.6 B**). The pattern of activity varied across time and space and was composed of periods of excitation, inhibition and quiescence. All PNs recorded showed spontaneous baseline spiking activity.

3.2.6 Morphology and physiology of local neurons in the antennal lobe

Intracellular fill of a local neuron (LN) is shown in **Fig. 3.7** (**A and B**). LN in *H. banian* has a big cell body and no axon. The neurites of the LN are dense and widely distributed throughout the AL volume. They end in dense terminals indicative of the microglomeruli in AL (arrow). Anti-GABA immunohistochemistry of the LN showed it to be GABAergic in nature (**Fig. 3.7 B**). A cluster of GABA-positive neurons, putatively LNs, was observed in the anterior lateral AL when anti-GABA immunohistochemistry of the whole brain was done (**Fig. 3.7 C**).

Different LNs respond to the same odorant with different temporal patterns of activity (Fig. 3.8). The multiphasic activity consists of depolarization or hyperpolarization of the

membrane potential, sometimes superimposed by short amplitude spikelets, presumably calcium-mediated. Some LNs have a weak odor response (LNs 3, 4 and 5) while others show an off response (LNs 6 and 7).

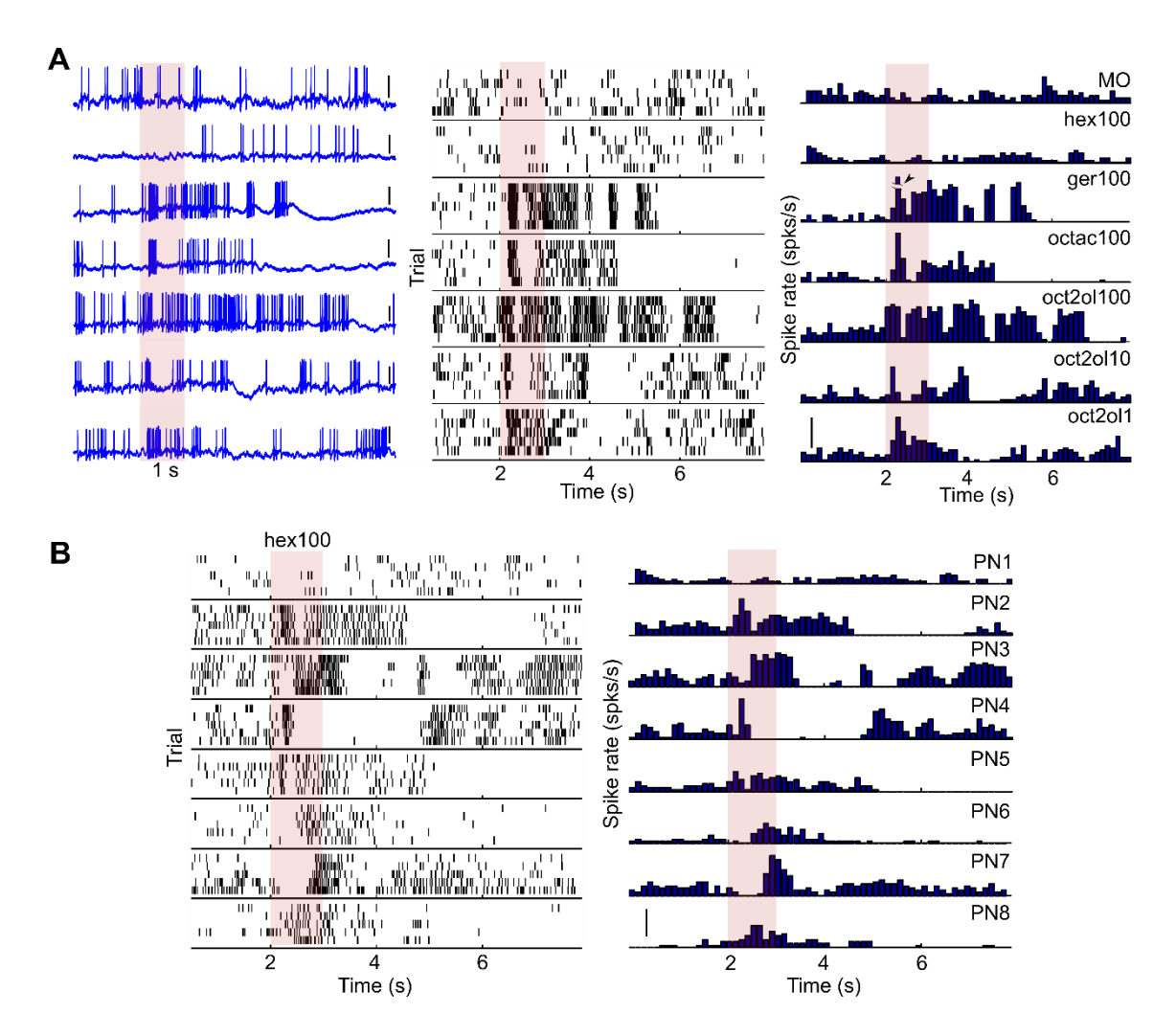


Figure 3.6 Physiological properties of AL PNs. (**A**) AL PN responds to different odorants with different temporal patterns of activity. The response is characterized by periods of excitation, inhibition and quiescence. MO: mineral oil, hex100: 1-Hexanol 100%, ger100: Geraniol 100%, octac100: octanoic acid 100%, oct2ol100/10/1: 2-Octanol100%, 10%, 1%. Single traces are shown first, followed by rasters in the middle panel and peri-stimulus time histogram (PSTH). Scale bar: 5 mV (raw traces); 20 spks/s (PSTH); arrowhead: ~62 spks/s. (**B**) Odor response of different PNs to the same odorant. The same odorant (hex100) elicits non-identical patterns of odor response in 8 different PNs. Scale bar: 20 spks/s (PSTH)

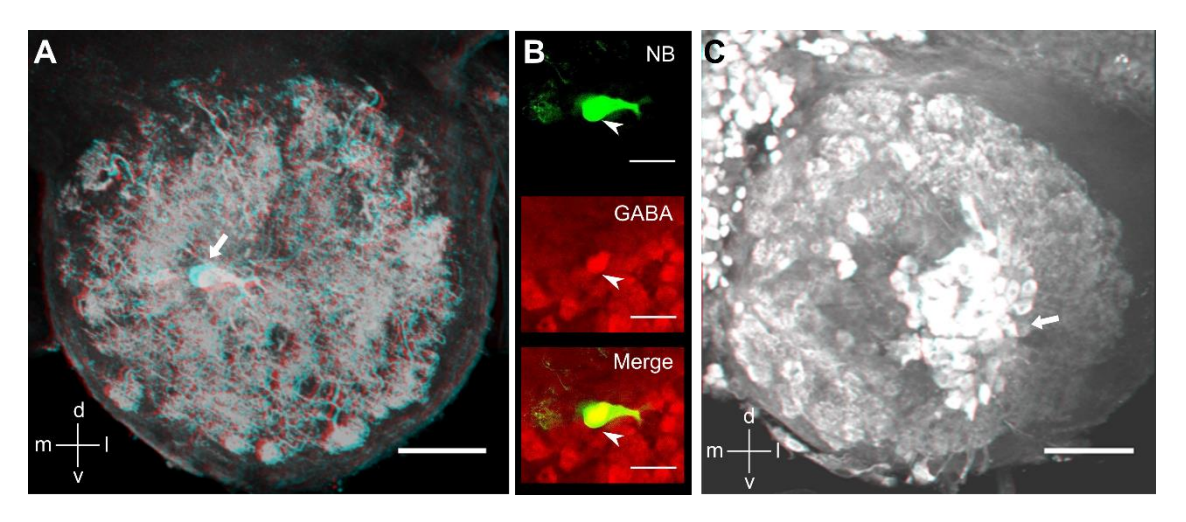


Figure 3.7 Morphological and immunohistochemical features of the local neurons in AL. (A) LN in *H. banian* is axon less with wide and profusely ramifying arborizations throughout the AL area and a large cell body (arrow). These arborizations often terminate in the microglomerular structures, reflective of local units of synaptic interactions between PNs and ORNs. Scale bar: 100 μm. **(B)** Anti-GABA immunohistochemistry shows that this LN is GABAergic in nature. Scale bar: 50 μm **(C)** A cluster of GABA-positive cell bodies (putatively of LNs) can be observed in the anterior lateral area of the AL. Scale bar: 100 μm

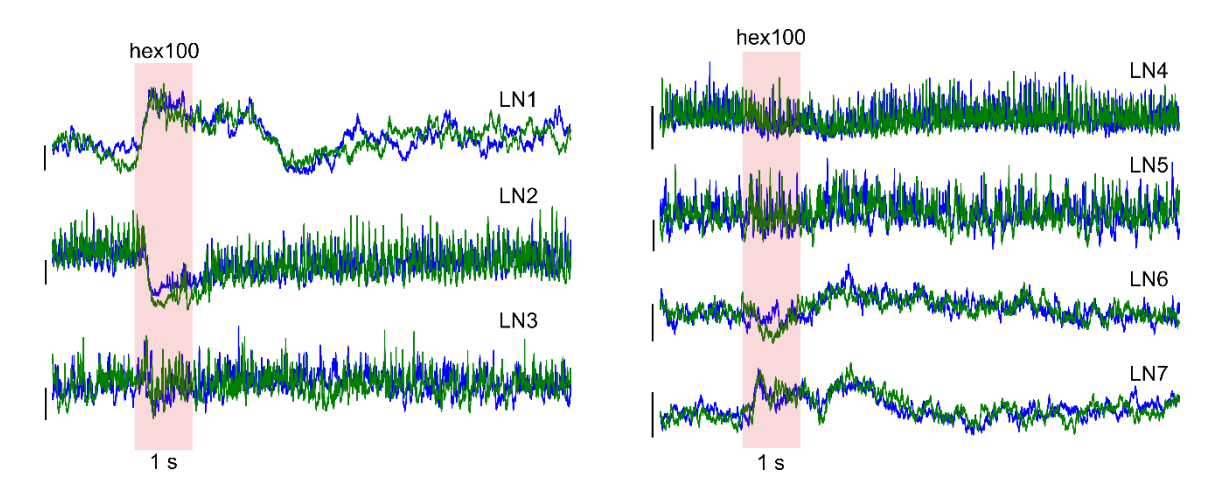


Figure 3.8 Physiological properties of LNs. Intracellular recordings from seven different non-spiking cells in AL, putatively of LNs, show multiphasic responses to the same odorant. Blue and green traces represent two trials from the same LN to show that the responses are consistent. LN1 has putative calcium spikes riding on top of the depolarizing response to 1-Hexanol 100% while LN2 has a hyperpolarizing response to the same. LNs 3, 4 and 5 show weak response to the odorant. LN 6 has an off-response. LN 7 responds to the same odorant with depolarization of the membrane potential followed by hyperpolarization and an off-response. Scale bar: 20 mV

Paired intracellular recordings between three pairs of PNs and LNs show correlated or anti-correlated patterns of activity (Fig. 3.9 Ai-iii). These patterns of activity point to possible synaptic interactions between the two types of AL interneurons. A probable LN to PN synaptic connection can be observed in two pairs (Fig. 3.9 Ai and Aiii). When the LN responds with odor-evoked depolarization of the membrane potential, hyperpolarization of the PN membrane potential is detected after a delay which implies that the LN might be inhibiting the PN (Fig. 3.9 Aiii). The third pair does not seem to have a correlated change in activity, implying thereby that the two interneurons might not be synaptically connected (Fig. 3.9 Aii).

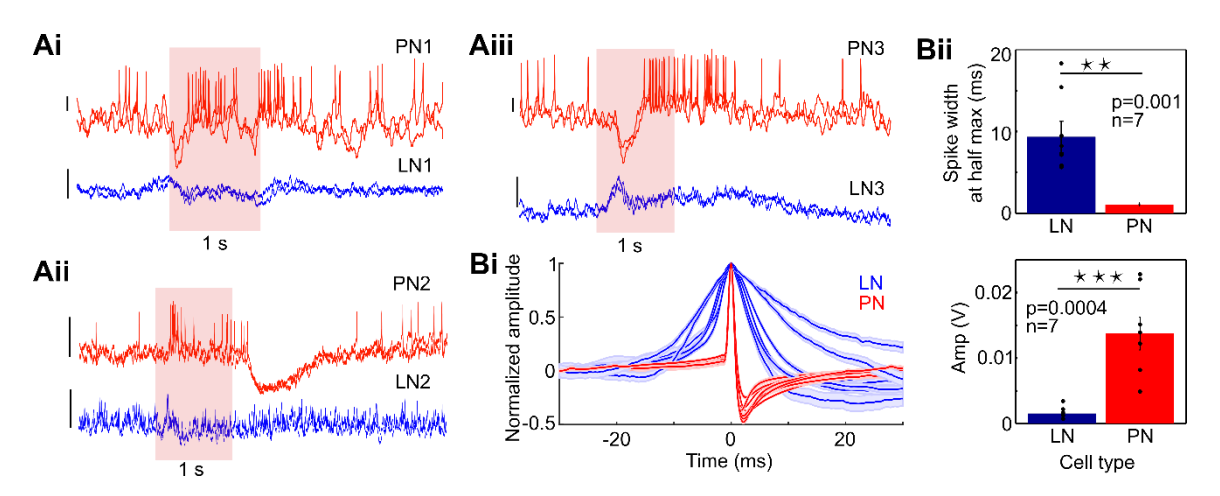


Figure 3.9 Synaptic interaction between the interneurons of AL. Paired intracellular recordings between PNs and LNs show that they have different kinds of synaptic interactions between them. (Ai) and (Aiii) have correlated or anti-correlated change of activity while (Aii) does not seem to have PN-LN synaptic connection between them. Scale bar: 2 mV (Bi) Distinguishing the source of spikes recorded from the AL. Spikes from PN look very different from those recorded from the LNs in the AL of *H. banian*. PN spikes are narrow in width, with prominent after-hyperpolarization phase and higher amplitude (red trace), while those from LNs are shorter in amplitude and wider in width, without a prominent after-hyperpolarization (blue trace). The shaded region around the traces indicates mean \pm SEM. (Bii) Statistical analyses of spike-width at half maximum (top panel) between LN and PN shows that spike-width of LN is significantly larger than that of PN (p=0.001, n=7, unpaired t-test); Bottom panel: Spike amplitude (Amp) of PN is significantly larger than that of LN (p=0.0004, n=7, unpaired t-test)

The spikes of PNs and LNs recorded intracellularly from the AL can be distinguished from each other by their features. PN spikes are narrower in width (p=0.001, n=7, unpaired t-test) and have larger amplitudes (p=0.0004, n=7, unpaired t-test) while those of LNs are significantly wider and shorter in amplitude (**Fig. 3.9 Bi and Bii**). These differences arise because the spikes in PNs are sodium-channel mediated while those in LNs are putatively calcium-channel mediated (Laurent et al. 1996).

3.2.7 Nature of the local field potential in mushroom body

Odor-evoked oscillations are observed in the LFP recorded from the cell body layer and primary calyx of the MB. The LFP recorded from the two layers of the MB are correlated negatively and are anti-phasic in nature, both during odor response and during baseline (**Fig. 3.10 A and B**). The recording location of the two electrodes is shown in the schematic (**Fig. 3.10 C**). This negative correlation is consistent with the distinctive arrangement of the population of MB intrinsic neurons, the KCs (**Fig. 3.10 C**).

The strength of the odor-evoked oscillations increases over repeated presentations of the same odorant (**Fig. 3.11 A and B**). The predominant frequency of the odor-evoked oscillation is ~25 Hz (**Fig. 3.11 B**) and the strength of the LFP power in different bands during odor response also changes across trials (**Fig. 3.11 C**). The LFP power in the higher band (15–40 Hz) increases in strength over repeated presentations while the lower frequencies (1–5 Hz) decrease in strength simultaneously. The LFP power remains constant at baseline (**Fig. 3.11 C**).

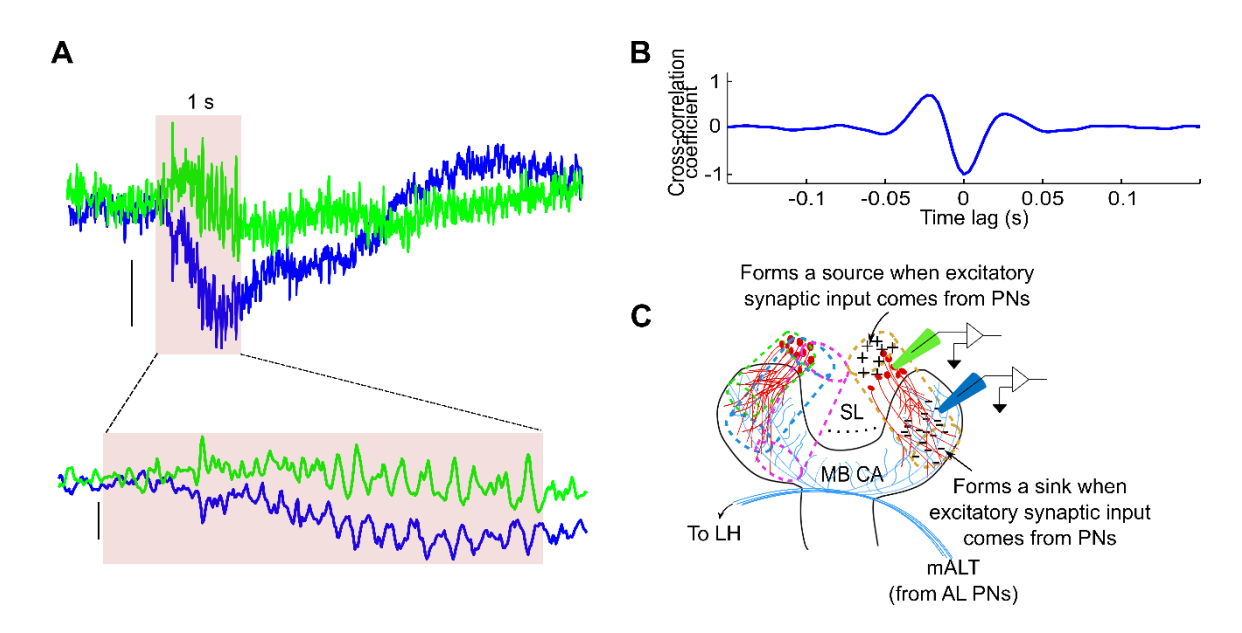


Figure 3.10 Features of the local field potential (LFP) recorded from the MB. (A) Top panel: Odor-evoked oscillations are observed in the LFP, simultaneously recorded from the cell body layer/soma layer (SL, green trace) and the MB calyx (MB CA, blue trace). The recording locations of the two electrodes are shown in the schematic (C). Bottom panel: Magnified view of the duration during which odor stimuli was applied to show that the LFP recorded from the two areas is anti-correlated and out of phase to each other. Scale bar: 100 μV (B) Cross-correlation analysis of the two traces reveals that the LFP traces recorded from the SL and the MB CA are negatively correlated and out of phase to each other. (C) A source-sink pair is formed by the columnar arrangement of MB KCs. KCs' cell bodies are arranged dorsal to the MB calyx (SL), and their dendrites project in the calycal area (MB CA), the synaptic area. Multiple column-like structures are formed by any closely placed cluster of KCs (black dots represent the fact that any area in the MB can form columns). This can give rise to an open field arrangement observed in many brains and brain parts (Johnston and Wu 1994). The synchronized excitatory synaptic input from the AL PNs is delivered via the mALT to the KCs in the synaptic area, the calvx and this gives rise to the formation of a source-sink pair. The synaptic flow spreads throughout the MB calyx (Jortner et al. 2007) forming a sink while the SL forms the source of the electrical dipole. Thus, the LFP recorded from the two layers are negatively correlated and out of phase to each other when observed in a narrow band.

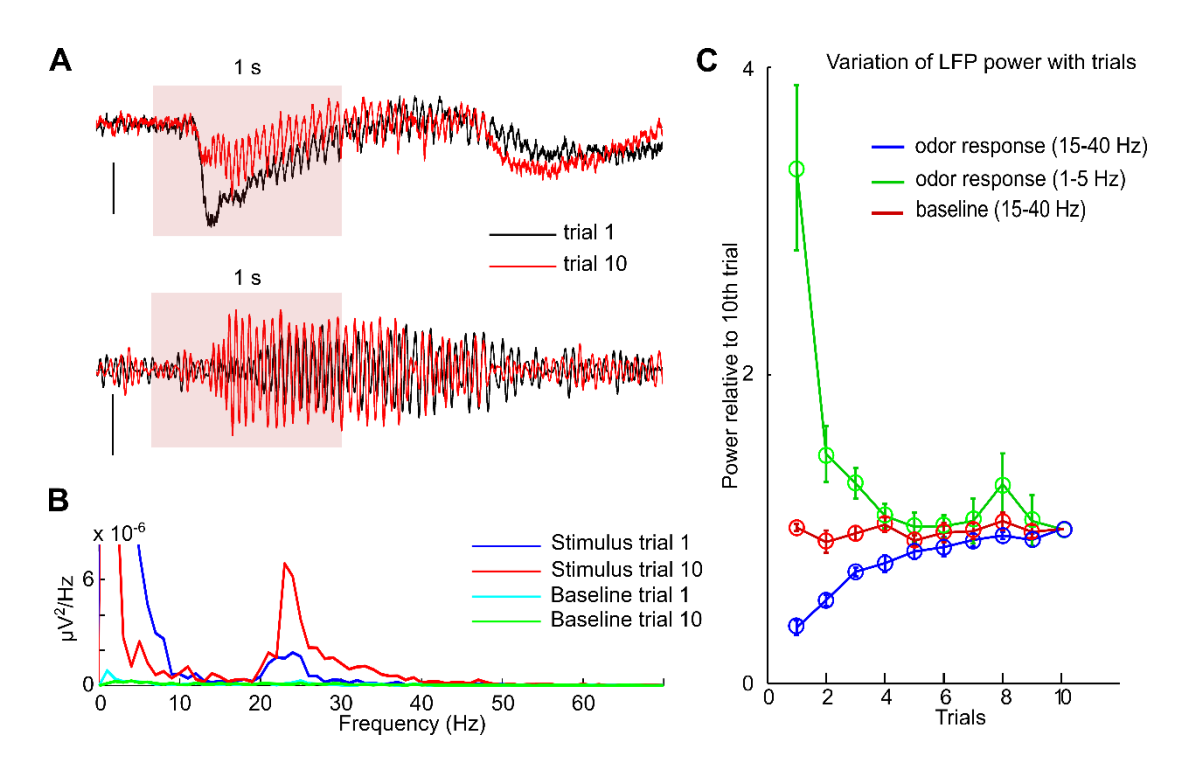


Figure 3.11 Properties of odor-evoked oscillation in MB LFP. (A) The strength of the LFP oscillations increases over repeated presentations of the same odor stimuli. Top panel: Raw data (Scale bar: 0.5 mV). Bottom panel: the same data filtered between 15–40 Hz. Scale bar: 0.2 mV (**B**) The power spectrum of the LFP compared between the 1st trial and the 10th trial during odor presentation and baseline. The power of the odor-evoked LFP oscillations increases in amplitude during 10th trial when compared to the 1st trial. The predominant frequency during odor response when oscillations occur is ~25 Hz. Baseline power remains unchanged between 1st and 10th trial. (**C**) **Plasticity of MB LFP**. The power of MB LFP relative to the 10th trial changes during the course of repeated presentations of the same odor stimuli. This change also differs between different frequency bands. The strength of the lower frequencies (1–5 Hz, green trace) decreases from 1st to 10th trials whereas the higher frequency components of the LFP (15–40 Hz, blue trace) increases in strength during the same duration. Baseline frequency (red trace) remains unchanged during the same period.

3.2.8 Features of odor response of Kenyon cells

The intrinsic neurons of the MB, KCs, respond to odorants with sparse spiking and odor-evoked subthreshold membrane oscillations (**Fig. 3.12 A**). The odor-evoked subthreshold membrane oscillations in KC membrane potential are periodically synchronized with the odor-evoked oscillations in the LFP recorded from the MB primary calyx (**Fig. 3.12 B**).

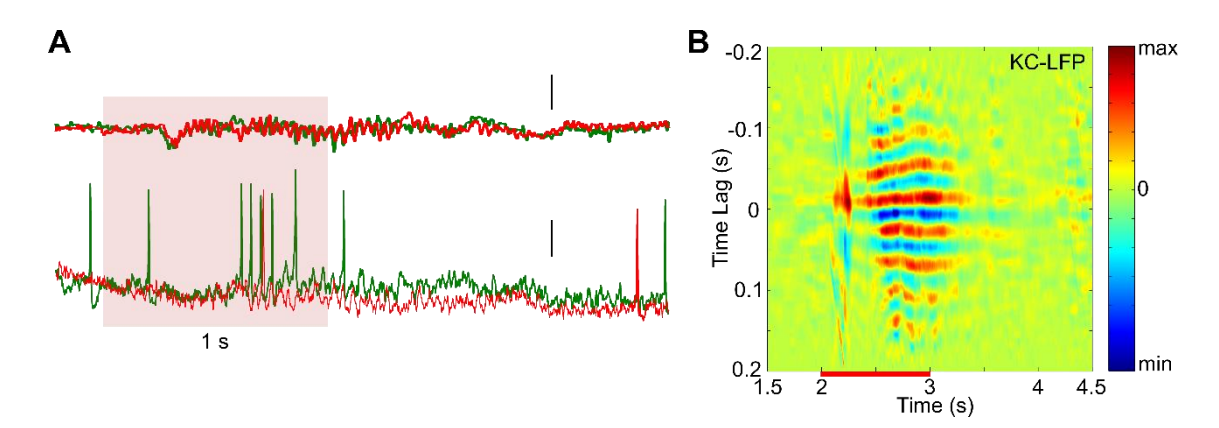


Figure 3.12 Physiological properties of the Kenyon cell. (A) KC, the intrinsic neuron of the MB, responds with subthreshold oscillations to odor stimuli. Red and green traces are two trials from the same recording session. Top panel: Simultaneously recorded LFP from the MB calyx, showing odor-evoked oscillations. The KC is characterized by low baseline firing rate with odor response consisting of sparse firing and subthreshold membrane oscillations. Scale bar: $200~\mu V$ (LFP), 1mV (KC) (B) Cross-correlation between KC membrane potential and the MB LFP reveals that the KC membrane potential is synchronized with the LFP during odor response.

Different KCs respond to the same odorant with different patterns of activity (**Fig. 3.13**). In addition, the same KC also responds with different patterns of spiking activity to different odorants. The baseline rate of KCs is very low and their odor response consists of sparse spiking.

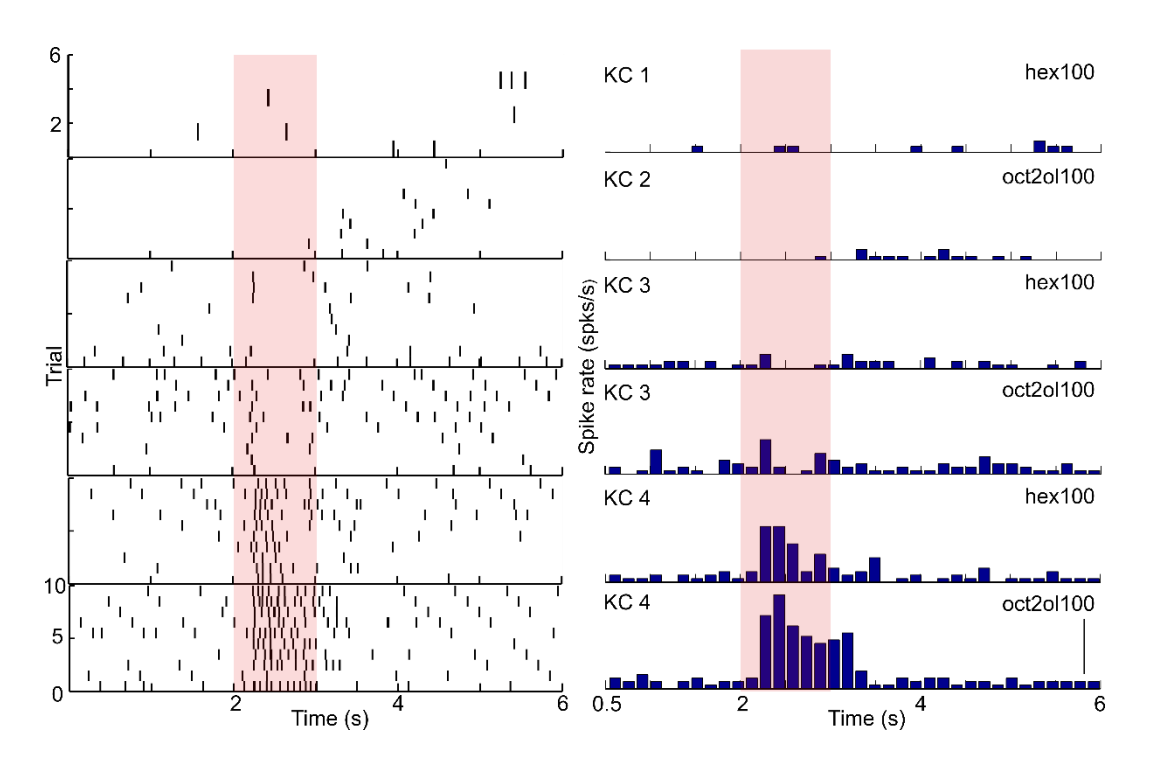


Figure 3.13 Kenyon cells respond to odorants in a cell-odor-specific manner. Intracellular recording from four different KCs across three animals shows that different KCs respond to different odor stimuli with non-identical response patterns. Additionally, they have low baseline rate with sparse response to odor stimuli. Scale bar: 10 spikes/s

3.2.9 Features of lateral horn neurons

The LHN cell bodies are located in the lateral protocerebral lobe and can be seen in fills from the calyx of MB (**Fig. 3.14 A**).

LHNs can be of widely differing morphologies as seen from six fills from the region (Fig. 3.14 Bi-Ei and Fig. 3.15 Ai, Bi). All these neurons have either dense or sparse arborization in the LH. They also arborize in areas other than the LH, like the superior lateral

protocerebrum. Some of them can be bilateral and project in the contralateral half of the brain (**Fig. 3.15**). The LHN shown in **Fig. 3.15** (**Ai**) is morphologically similar to the LHN termed C3 in *S. americana*, reported by Gupta and Stopfer (2012).

Odor responses of LHNs consist of increase in firing rate as compared to the baseline rate. They responded to all the odorants tested with different patterns of activity (Fig. 3.14 Bii–Eii and Fig. 3.15 Aii, Bii).

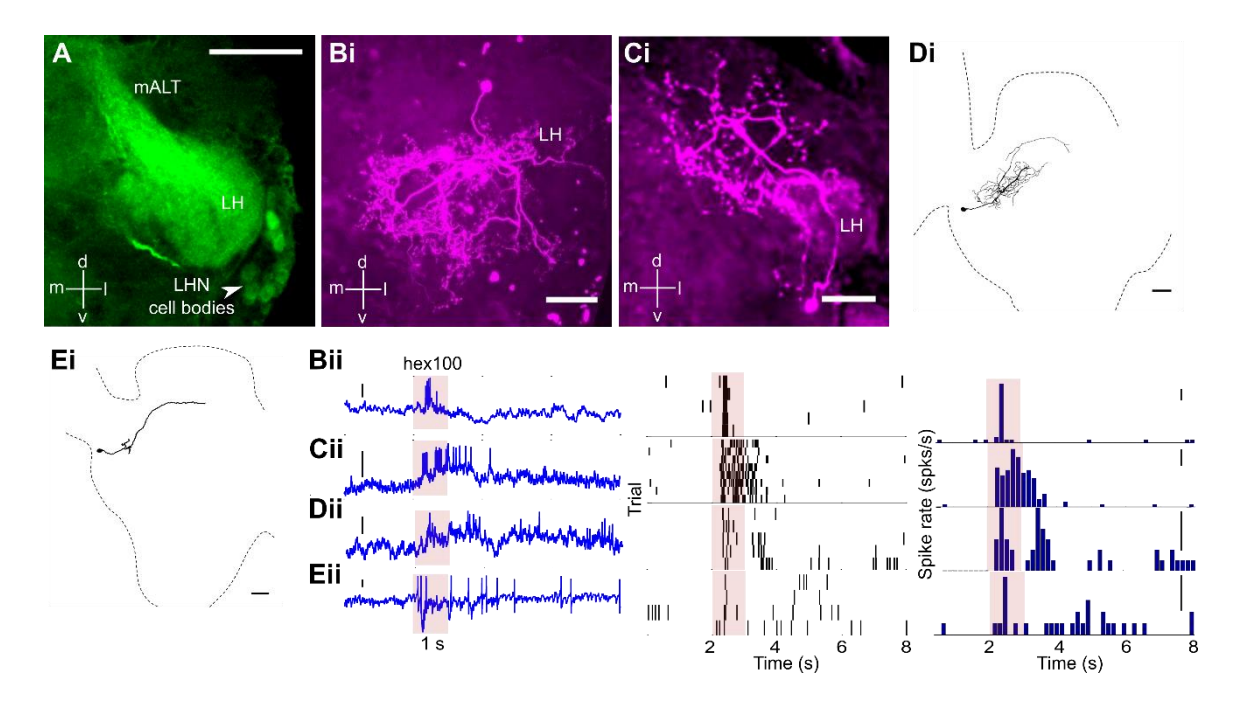


Figure 3.14 Morphological and physiological characteristics of unilateral third-order lateral horn neurons (LHNs). (**A**) Dye-fill from the MB calyx reveals a cluster of LH neurons in the lateral protocerebrum (arrowhead). Scale bar: 100 μm (**Bi**)–(**Ei**) Four distinct morphological types of unilateral LHNs, with either sparse or dense arborizations in the LH. (**Bi**) and (**Ci**) are z-projection made from a confocal stack. (**Di**)–(**Ei**) are tracings drawn from the original confocal stack. Scale bar: 100 μm. (**Bii**)–(**Eii**) **Odor responses of the four LHN types to different odorants.** LHNs respond to most odorants with an increased firing rate. The odor responses (raw traces, rasters and PSTH) corresponding to the dye-filled LHNs are shown in (**Bii–Eii**). Scale bar: (**Bii**) 5 mV, (**Cii–Eii**) 2 mV; (**Bii–Eii**) 5 spikes/s for PSTH

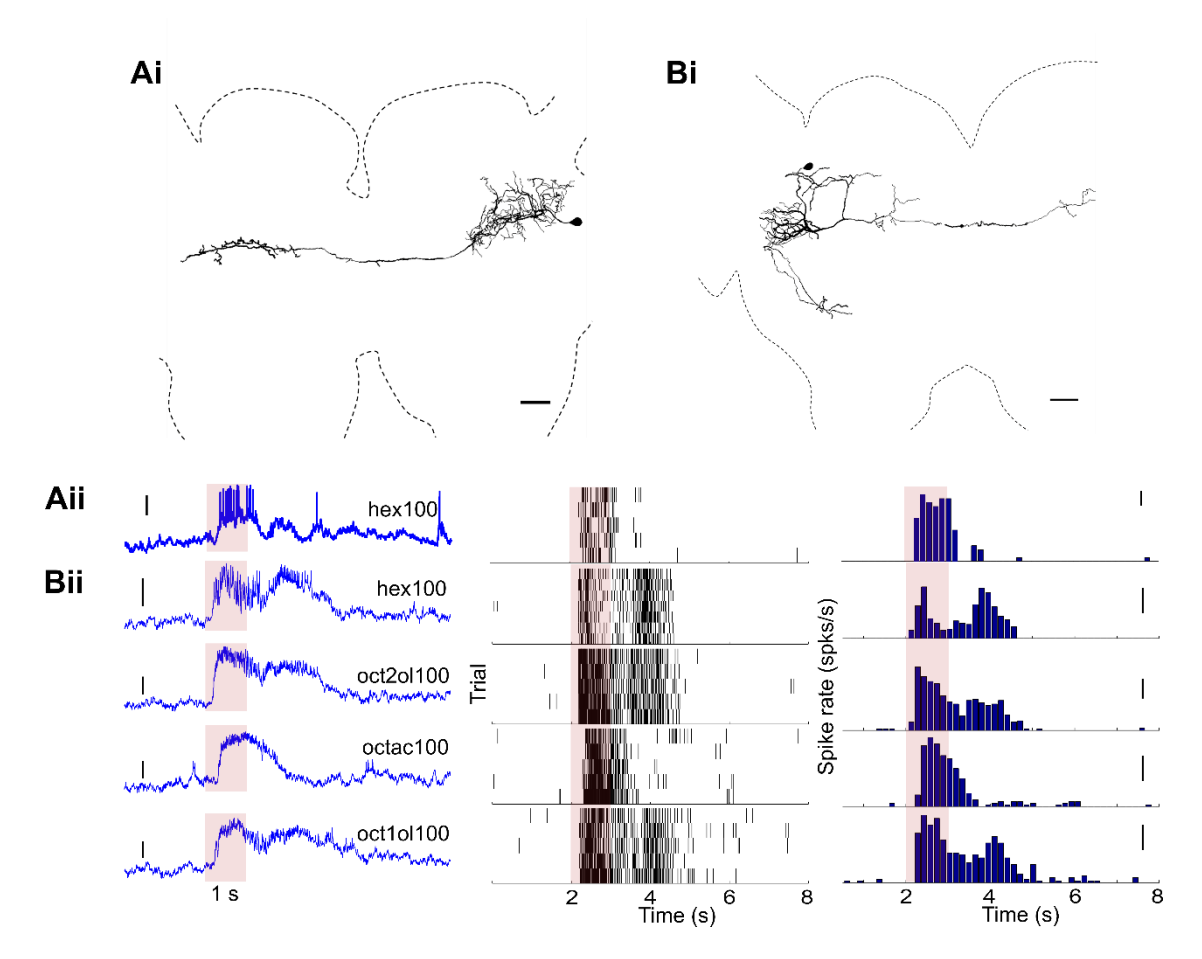


Figure 3.15 Morphological and physiological characteristics of bilateral third-order LHNs. (**Ai**)–(**Bi**) Two distinct morphological types of bilateral LHNs with either sparse or dense arborizations in the LH. The images are tracings drawn from the original confocal stack. Scale bar: 100 μm. (**Aii**)–(**Bii**) **Odor responses of the two bilateral LHNs to different odorants.** Bilateral LHNs also respond to most odorants with an increased firing rate. The odor responses (raw traces, rasters and PSTH) corresponding to the dye-filled LHNs are shown in (**Aii**–**Bii**). Scale bar: (**Aii**) 2 mV, (**Bii**) 5 mV for raw traces; (**Aii**) 5 spikes/s, (**Bii**) 20 spikes/s for PSTH

3.2.10 Morphology, types and physiological features of beta lobe neurons

Dye-fill from the beta lobe of the MB reveals a cluster of 13–16 bLNs in each half of the *H. banian* brain (**Fig. 3.16 A**).

In the locust *S. americana*, 7 morphological types of bLNs have been reported (MacLeod et al. 1998; Gupta and Stopfer 2014). In *H. banian* we were able to successfully fill two types—1 and 2. bLN1 has its cell body in the medial protocerebrum, near the midline of the brain and it projects to the LH and pedunculus of MB, in addition to beta lobe (**Fig. 3.16 B**). It has sparse arborization in the superior protocerebral area and is GABA-negative. Odor response of bLN1 consists of vigorous increase in the firing rate (**Fig. 3.16 C**). It responds to all odorants tested and has a spontaneous baseline spiking rate.

We report two subtypes of bLN2 (**Fig. 3.17**). Both the subtypes have their cell bodies in the cluster of bLNs in the lateral protocerebral lobe and both project to the beta lobe, alpha lobe, pedunculus and feedback to the MB calyx. The difference between the two arises in the manner of their arborization in the MB calyx. One subtype arborizes in the MB calyx and spreads out horizontally there (**Fig. 3.17 A**). The other subtype seems to arborize in the accessory calyx of MB (**Fig. 3.17 B**). Both subtypes of bLN2 respond to all the odorants tested with increased spiking rate and their odor responses lasted longer than the duration of the odor pulse (**Fig. 3.17 C and D**).

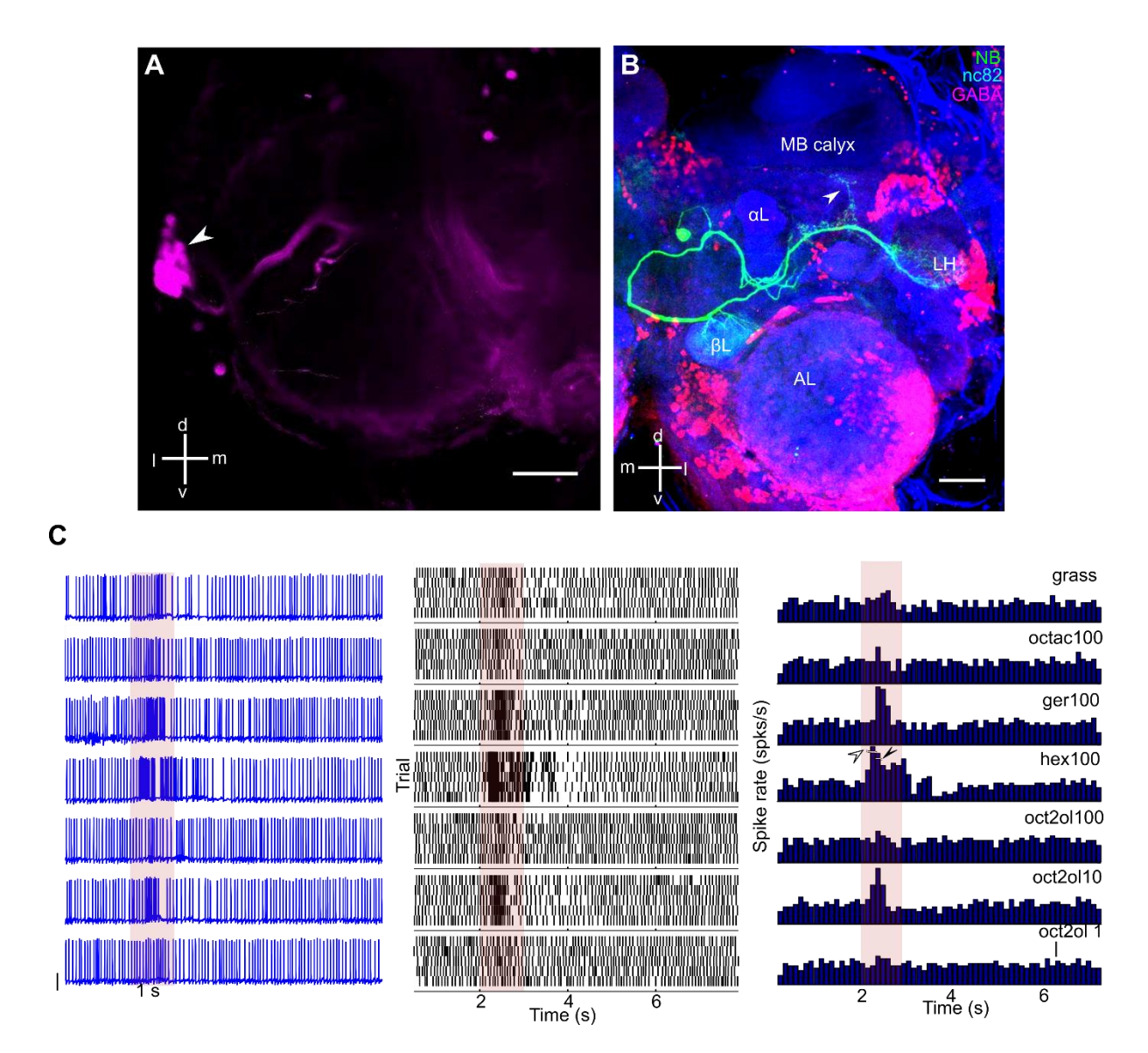


Figure 3.16 Morphological and physiological properties of the fourth-order beta lobe type 1 neurons (bLN1). (A) A cluster of 13–16 bLNs is seen in the lateral protocerebral area (arrowhead) in dye-fills from the beta lobe. Scale bar: 100 μm (**B**) Morphology of bLN type 1. The cell body of bLN1 is located in the medial protocerebrum and it has dense arborizations in the beta lobe, pedunculus and the LH. bLN1 is GABA-negative. A small branch from the main branch also arborizes in the superior protocerebrum (arrowhead). The synaptic densities are demarcated by immunostaining against bruchpilot antigen (blue) and the GABAergic elements are shown in magenta. Scale bar: 100 μm (**C**) bLN1 is characterized by spontaneous firing at baseline and it responds to all odorants tested with vigorous increase in firing rates. Scale bar: 10 mV (raw traces); 20 spks/s (PSTH); open arrowhead ~130 spks/s, closed arrowhead ~60 spks/s

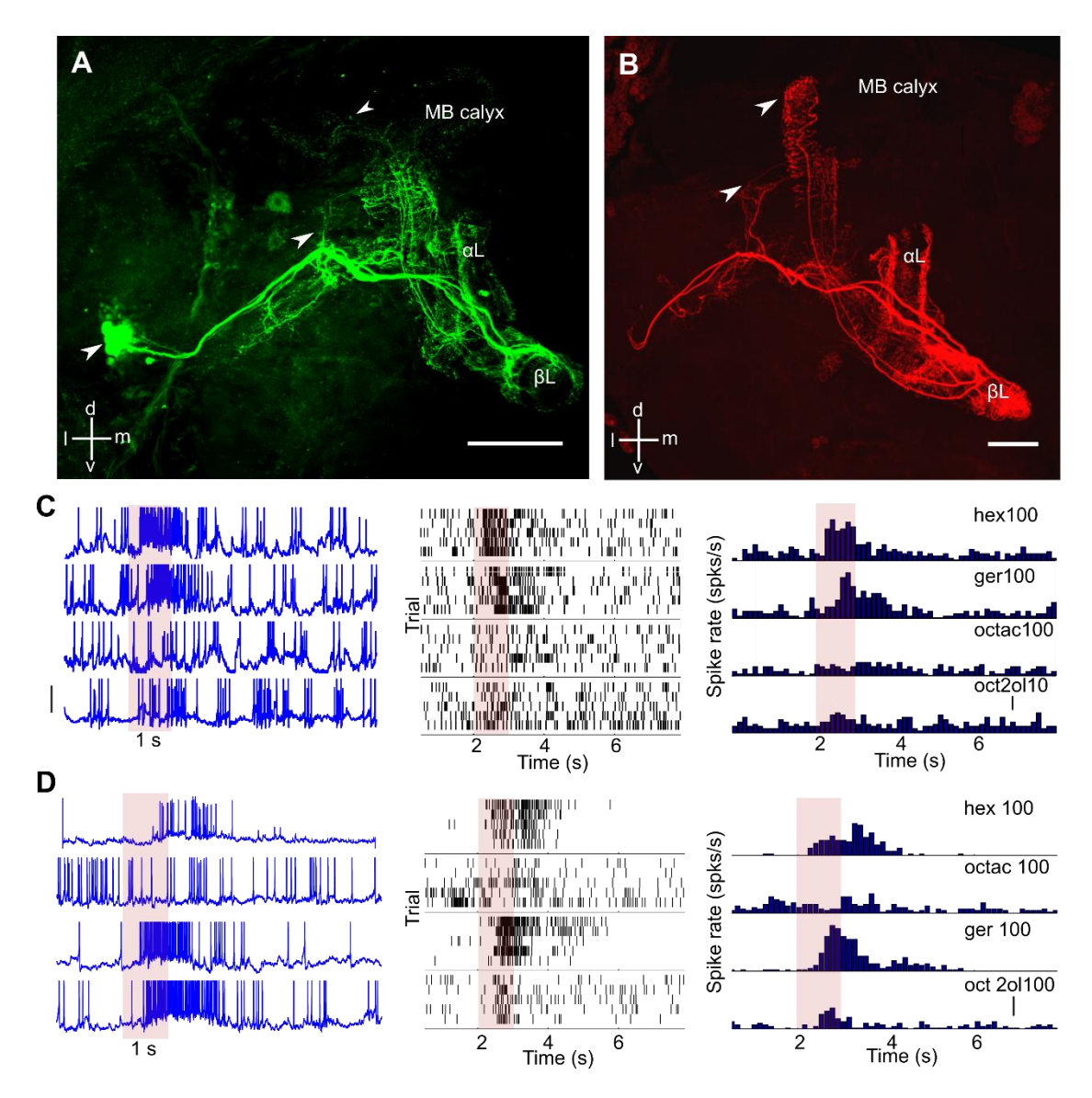


Figure 3.17 Morphological and physiological properties of the fourth-order beta lobe type 2 neurons (bLN2). (A) and (B) Two subtypes of bLN2. Both the subtypes have their cell bodies in the lateral protocerebrum and arborize in the beta lobe, alpha lobe, pedunculus and the MB calyx. They differ in their pattern of arborization in the MB calyx. While subtype 1 (A) arborizes in the primary calyx, subtype 2 (B) arborizes in the accessory calyx. (C) Odor response of bLN2 subtype 1 (shown in A). This bLN2 is characterized by spontaneous baseline firing which increases in rate when the odor stimuli are presented. It responds to different odorants with different patterns of activity. (D) Odor response of bLN2 subtype 2 (shown in B). This bLN2 is also characterized by baseline spontaneous firing with vigorous increase in firing rate during odor response. It responds to the different odorants tested with different temporal patterns. Scale bar: 10 mV (raw traces); 20 spks/s (PSTH)

3.2.11 Morphological, immunohistochemical and physiological features of GGN

The giant GABAergic neuron (GGN) is a large inhibitory neuron whose cell body is located in the lateral protocerebral lobe and it projects to the MB calyx, LH, and alpha lobe (**Fig. 3.18 A**). It has dense and widespread arborization in the MB calyx and it is GABA-positive (**Fig. 3.18 B**).

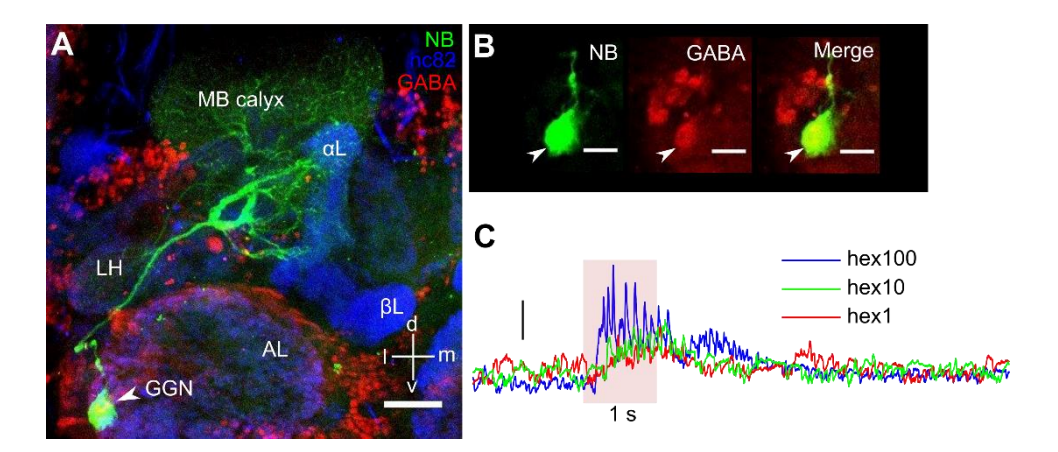


Figure 3.18 Morphology and physiological properties of Giant GABAergic Neuron (GGN). (A) Intracellular fill of GGN. GGN has its cell body in the lateral protocerebral lobe and arborizes densely in the MB calyx, alpha lobe, and LH. The synaptic densities are demarcated by nc82 immunostaining (in blue) while red represents GABA-positive profiles. Scale bar: $100 \,\mu\text{m}$ (B) GGN is GABA-positive. Scale bar: $50 \,\mu\text{m}$ (C) GGN responds to odors with depolarization of the membrane potential, which is superimposed with EPSPs and IPSPs. The odor response of GGN increases in strength with increasing log concentration of the same odorant. Scale bar: $10 \,\text{mV}$

GGN is devoid of spiking activity and its odor response is characterized by the depolarization of the membrane potential superimposed with EPSPs and IPSPs (**Fig. 3.18 C**). The amplitude of the depolarization increases with log concentration increase of the odorant. The baseline as well as the odor response of the GGN is also characterized by a distinct unitary IPSP, which is reported in *S. americana* to be due to the input from another inhibitory neuron IG (Inhibitor of GGN; (Papadopoulou et al. 2011). The properties and effects of IG on GGN and its role in the olfactory circuitry are discussed in Chapter 5 of this thesis.

Anti-GABA immunohistochemistry of the whole brain shows that the GABAergic innervation in the MB is segregated into two distinct layers (arrowheads; **Fig. 3.19 A**). It is not clear if the source of both the segregated layers of GABAergic innervation in the MB is due to GGN, or if two different sources give rise to it. Dye fills from the MB calyx also revealed a single fiber originating from a single large somata in each half of the brain, thus indicating that there is only one GGN per brain hemisphere (**Fig. 3.19 B**).

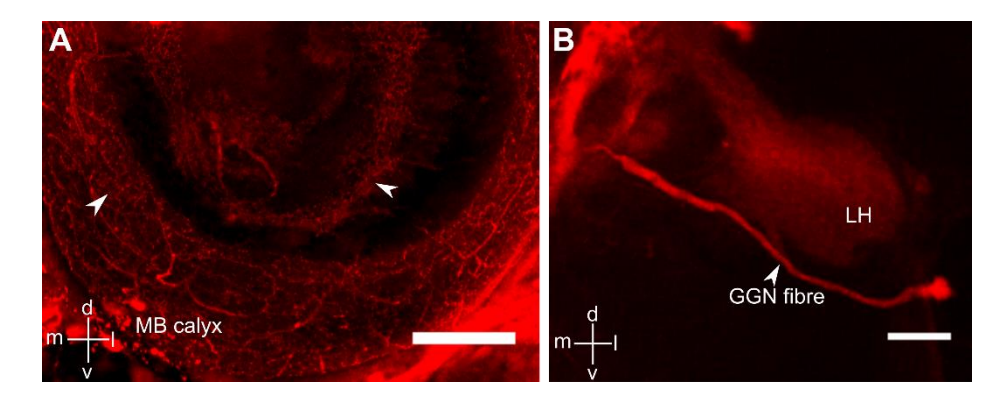


Figure 3.19 GABAergic innervation of the MB. (A) Anti-GABA immunohistochemistry of the whole brain shows two distinct layers of GABAergic innervation in the MB calyx (arrowheads). Scale bar: $100 \, \mu m$ (B) A single GGN-like fiber originating from a large somata located in the LPL, reminiscent of GGN, is seen in one half of the brain in samples where dye was injected in the MB calyx. This points out to the fact that only one GGN is present in each half of the brain. Scale bar: $50 \, \mu m$

A schematic summarizing the data presented in this chapter is shown in Fig. 3.20.

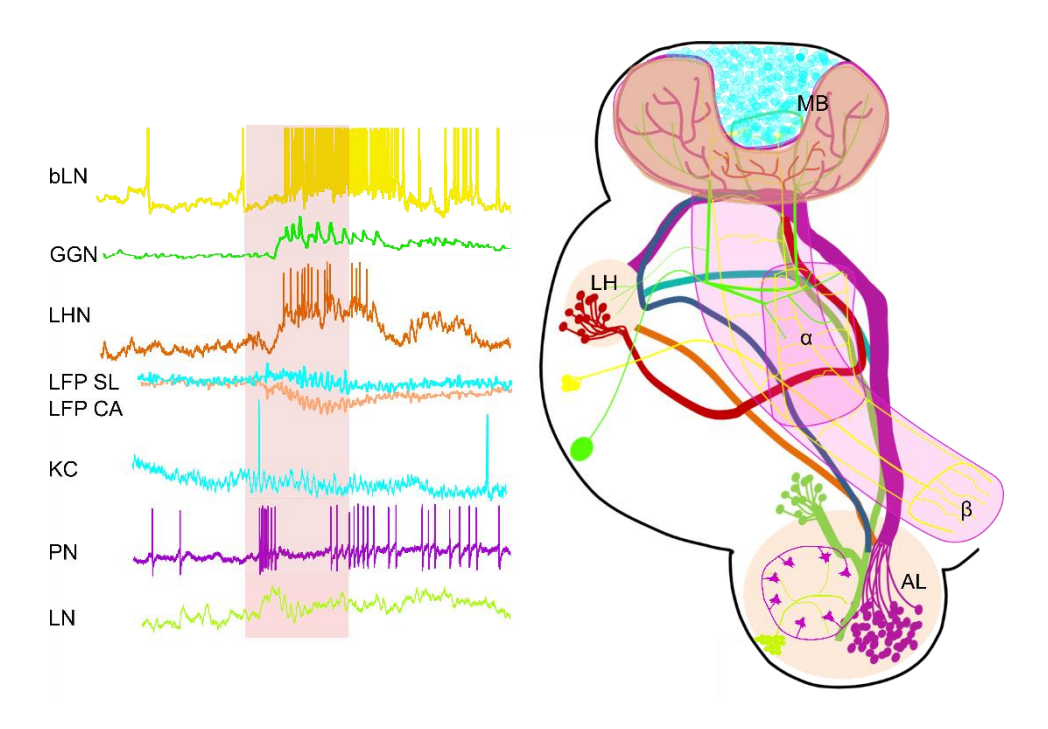


Figure 3.20 Schematic summarizing the olfactory circuit in *H. banian*. Schematic illustrating the AL tracts to MB, the tract between LH and MB and the representative response properties of olfactory neurons recorded from different areas involved in olfactory information processing in *H. banian*. AL: antennal lobe; α: α-lobe of MB; β: β-lobe of MB; bLN: beta lobe neuron; GGN: giant GABAergic neuron; KC: Kenyon cell; LH: lateral horn; LHN: lateral horn neuron; LN: local neuron; LFP CA: local field potential recorded from the MB calyx; LFP SL: local field potential recorded from the MB soma/cell body layer; MB: mushroom body; PN: projection neuron

3.3 Discussion

The main results from this part of the thesis are the comparison of the similarities and differences in the olfactory circuits between two grasshopper species, the well-studied *S. americana* (not found in India) and *H. banian* (endemic to the Indian subcontinent) from the second-order through the fourth-order neurons. Both these species from the order Orthoptera belong to different subfamilies which were separated ~57 million years ago (Song et al. 2018). Our data from *H. banian* when compared with the published literature in *S. americana* reveals that the two species are conserved in terms of anatomy and physiology through the fourth-order level of the olfactory circuit.

This study, for the first time, throws light on the olfactory circuit of the grasshopper *H. banian*. Apart from it, this study also elucidated the following novel features in Orthoptera:

- 1) Additional antennal lobe tracts, not reported in Acrididae species
- 2) Novel tract, designated CT, between lateral horn and mushroom body
- 3) Negative correlation of LFP recorded from cell body layer and calyx of MB
- 4) Dissimilar changes in different frequency bands constituting the LFP oscillations in MB in response to repeated odor presentations
- 5) New morphological types of lateral horn neurons
- 6) A new subtype of bLN2

3.3.1 Is the methodology used to establish similarities between the two species justified and adequate?

We used intracellular recordings, dye-fills, immunohistochemistry to compare the olfactory circuits of the two species and establish that they resemble each other through the fourth-order neurons. These techniques have been used widely to reach to the same conclusion in different species. Intracellular recordings and dye-fills have been used to establish homology of auditory neurons between locusts and bush crickets (Römer et al. 1988). These techniques have also been used to confirm similarity of protocerebral neurons and descending neurons in numerous moth species (Kanzaki et al. 1991a, b; Kanzaki and Shibuya 1992; Mishima and Kanzaki 1999; Lei et al. 2001; Iwano et al. 2010; Namiki et al. 2018). Extensive anatomical and physiological studies using genetic lines expressing fluorescent dyes in specific neurons have been used in *Drosophila* to discover and characterize neurons of the olfactory pathway (Wong et al. 2002; Lai et al. 2008; Tanaka et al. 2012b; Frechter et al. 2019). Boyan et al. (1993) suggested that in order to establish homology between neurons, lineage analysis of the neurons is obligatory. But, lineage analysis of neurons or neuronal studies in genetically

labelled lines is not always feasible and many studies bear evidence to the fact that intracellular recordings and dye fills are justified in establishing similarity of neurons (Kanzaki et al. 1991b; Kanzaki and Shibuya 1992; Lei et al. 2001; Namiki and Kanzaki 2011; Rössler and Zube 2011; Tanaka et al. 2012b). Moreover, new antennal lobe tracts were discovered in *Drosophila* and the moth *Heliothis virescens* by utilizing tract tracing method of mass dye fills (Tanaka et al. 2012b; Ian et al. 2016). Therefore, the use of these techniques to compare two species is justified and adequate.

3.3.2 Types of surface sensilla in *H. banian* closely resemble those in *Schistocerca* spp.

In *H. banian*, the males undergo six moults and females seven. With each moult, the number of antennal segments increases and consequently the number of sensilla as well (Coleman and Kunhi Kannan 1911; Roonwal 1952). The types of surface sensilla which we found on the antenna of *H. banian* namely, basiconica, coeloconica, trichodea and chaetica are also found in *S. gregaria* (no reports in *S. americana*; (Ochieng et al. 1998). These types have also been reported in other acridid species like *Locusta migratoria* (Altner et al. 1981) and *Hypochlora alba* (Bland 1982).

Sensilla types are important for housing the first-order neurons of the olfactory circuit, the olfactory receptor neurons (ORNs). Of the four types of surface sensilla, basiconica, coeloconica and trichodeum have been shown to be olfactory in nature by means of physiological recordings (Ochieng and Hansson 1999). In *S. gregaria*, the ORNs housed in sensilla basiconica have been shown to respond to aggregation pheromone volatiles (Hansson et al. 1996).

Two types of sensilla coeloconica have been reported in insects including Acrididae species. One type which has a cuticular pore is chemosensitive in *L. migratoria* while the other type with non-porous wall responds to hygro- and thermostimulation (Boeckh 1967;

Altner et al. 1981). ORN recordings from coeloconica sensilla have been shown in *S. gregaria* (Ochieng and Hansson 1999). Coeloconica sensilla have also been reported in the cockroach *P. americana*, where the ORNs housed are chemo-, hygro- and thermosensitive (Altner et al. 1977).

Chaetica is reported to house gustatory or mechanoreceptors (Ochieng et al. 1998). To confirm the same property of these sensilla in our species, we need to do a physiological investigation of the sensilla type.

We have not investigated the stage-related (nymphal vs adult) changes in the sensillar types as reported in *S. gregaria* (Ochieng et al. 1998), neither have we characterized their internal morphology. In addition, physiological characterization also needs to be done as we have classified and identified the sensillar types only on the basis of external morphology.

3.3.3 Multiple AL tracts in *H. banian*—a general trend or an exception

One of the critical finds of this study was the presence of additional tracts from the AL to the MB and LH in *H. banian*. Multiple AL tracts are not a new discovery as such, because they have been reported in many holometabolous (Blattodea) insect species and hemimetabolous (Diptera, Hymenoptera, Lepidoptera) insect species as well (Galizia and Rössler 2010; Tanaka et al. 2012b; Ian et al. 2016). On the other hand, only mALT has been reported in *S. americana/gregaria* and *L. migratoria* (Ernst et al. 1977; Laurent and Naraghi 1994; Hansson and Anton 2000; Ignell et al. 2001; Anton et al. 2002; Galizia and Rössler 2010). Across the order Orthoptera, the only other ALT (IALT) reported is in the species *Tetrix subulata* from the family Tetrigidae (Ignell et al. 2001). Thus, this is the first report of the presence of tALT, mlALT and lALT in addition to mALT in an Acrididae species.

The presence of additional ALTs raises questions about their significance as has been discussed about the same in other species of insects (Galizia and Rössler 2010). For instance,

in the honey bee, it is proposed that the mALT and the lALT form part of a dual olfactory pathway to the higher olfactory centers, the MB and LH (Kirschner et al. 2006). This is because the mALT projects to the MB first and then the LH, while in the case of lALT, the sequence of projecting to the higher centers is flipped—LH first and then the MB. Both these tracts in the honeybee have similar number of PN axons running through them, while in our case, the lALT has significantly fewer PN axons than the mALT. In honey bees and ants, uniglomerular PNs project through lALT and mALT while multiglomerular PNs project through the three mlALTs (Kirschner et al. 2006; Zube et al. 2008; Rössler and Zube 2011). In the moths, Manduca sexta and Heliothis virescens, mALT and lALT are composed of both uniglomerular PNs and multiglomerular PNs while mlALT is composed of only multiglomerular PNs (Homberg et al. 1988; Helge et al. 2007; Ian et al. 2016). The nature of neurotransmitter of PNs in different tracts also varies in some species. GABAergic PNs have been reported in many PNs of the mlALT tract in M. sexta and H. virescens (Hoskins et al. 1986; Berg et al. 2009). In honey bees, GABAergic (mALT, mlALT; (Schäfer and Bicker 1986), cholinergic (mALT; (Kreissl and Bicker 1989), and taurine-reactive PNs have been reported (IALT; (Schäfer et al. 1988; Kreissl and Bicker 1989). We did not explore the neurotransmitter profile of the different tracts in *H. banian*.

In *H. banian*, according to the terminology used by Ignell et al. (2001), we named the lateral-most tract as the lALT. This tract in *H. banian* originates at a location medial to the mlALT and projects only to the LH. This is in contrast to the lALT reported in *A. mellifera* (Kirschner et al. 2006), other Hymenopterans (Rössler and Zube 2011), and the Lepidoptera *Heliothis virescens* (Ian et al. 2016), where the lALT projects to LH first and then to the MB. In *H. banian*, this trajectory is followed by the mlALT.

At the level of subfamily divergence, both *M. sexta* from subfamily Sphinginae (Homberg et al. 1988) and *Heliothis virescens* from subfamily Heliothinae (Ian et al. 2016) have five ALTs. On the other hand, *Bombyx mori* from the subfamily Bombycinae is reported to have only three tracts (Kanzaki et al. 2003; Seki et al. 2005). The honey bee *Apis mellifera* (subfamily Apinae) has five tracts (Kirschner et al. 2006) while the bumble bee *Bombus terrestris* from sub family Bombyinae has only two (Strube-Bloss et al. 2015). The ants *Camponotus floridanus*, *Harpegnathos saltator* and *Atta vollenweideri* (subfamilies Formicinae, Ponerinae, and Myrmicinae respectively) all have five ALTs (Zube et al. 2008; Rössler and Zube 2011). This comparison points to a conserved number of ALTs in species from the same family. This would imply that either this is not true for the family Acrididae where variable number of ALTs are present across different species or earlier studies have missed these tracts in other Acrididae.

What is the need for multiple ALTs? Galizia and Rössler (2010) suggested that the presence of multiple ALTs points to higher complexity in organization, as primitive insects like bristletails and silverfish which have no MBs have a single ALT (mALT). A single tract is also reported in basal coleopteran species (Galizia and Rössler 2010). They proposed that since all the PNs in the family Acrididae are multiplemerular, therefore only one ALT is present. The presence of multiple tracts might indicate the presence of different types of PNs (uniglomerular or multiplemerular) or to separate channels for processing olfactory information. The latter case is proposed for the presence of multiple ALTs in the bee *Apis mellifera* where the uniglomerular PNs in the different mlALTs, have different physiological properties and process different aspects of odor information (Abel et al. 2001; Müller et al. 2002; Kirschner et al. 2006; Peele et al. 2006; Galizia and Rössler 2010).

Thus, the question regarding multiple ALTs is still open to debate. One probable reason as to why these were not discovered in *S. americana* or other Acrididae species may be the presence of fewer fibers running through them which were not stained. In our case too, we did not observe all the tracts in all the successfully filled samples.

3.3.4 A novel tract—CT

We discovered a new tract running between the LH and the MB. This has not been reported in any insect species, as far as we know, and further studies would be required to elucidate its function in the circuit. From our data, it looks as if the tract is running from the LH to the MB. If this is the case, then it would be the first evidence of this kind of connection in any insect species which is not a standard set of LHNs. What, then, would be the significance of such a connection is still open for exploration, though it would be interesting from the point of view of olfactory processing, since the MB is a center involved in learning and memory while LH is involved in innate behavior. In vertebrates, it has been shown that there are extensive functional connections between the amygdala and the hippocampus in human subjects, the former analogous to the LH in insects and the latter to the MB, as has been suggested (Phelps 2004; Zheng et al. 2019).

3.3.5 Similar neuropils in H. banian and S. americana

The neuropils which were visualized in the brain of *H. banian* are similar to the ones reported in *S. americana* which is expected, since the basic anatomical structures and primary regions are conserved across insect species (Ito et al. 2014).

3.3.6 The tritocerebral tract

The tritocerebral tract in *H. banian* is very similar to that reported in other insect species which have an accessory calyx. TT has not been shown in *S. americana* but it is reported in *S. gregaria* (Homberg et al. 2004) and *Locusta migratoria* (Ernst et al. 1977). The trajectories

followed by the TT in all the three species are similar. The TT is ubiquitous across insect species and terminates in the accessory calyx (when it is present) or a location between the MB calyces when it is absent (Farris 2008). The TT is implicated to play a role in gustation as it receives its input from the sensilla present on the maxillary palps (Ernst et al. 1977).

3.3.7 Microglomerular organization of the AL is a feature of family Acrididae

The AL in *H. banian* also displays a microglomerular organization as reported in *S. americana* (Laurent and Naraghi 1994) and its sister species *S. gregaria* (Anton and Hansson 1996) and *L. migratoria* (Ernst et al. 1977). Microglomerular organization of the AL is a characteristic feature of insect species in the families Acrididae and Gryllidae though it arose independently in the two suborders (Ignell et al. 2001). In general, the size and organization of glomeruli is a characteristic feature of a particular insect taxon (Ignell et al. 2001). The presence of unique glomeruli is considered to be a primitive feature, present in lower Orthopterans and Blattodea (sister order of Orthoptera) whereas microglomerular organization is said to be a complex feature of AL, indicating a compartmentalization of anatomical and functional entities (Ignell et al. 2001). The conserved nature of glomerular organization has also been shown across 22 different families in the order Coleoptera (beetles) (Kollmann et al. 2016).

3.3.8 Interneurons of AL in H. banian closely resemble those in S. americana

The PN in *H. banian* is morphologically similar to the one found in *S. americana* and *S. gregaria* (Laurent and Naraghi 1994; Anton and Hansson 1996; Ignell et al. 2001). This is in line with the types found in other grasshopper/locust species from the order Orthoptera (Laurent 1996; Ignell et al. 2001; Galizia and Rössler 2010). The PNs in all these species are multiglomerular with 10–20 radially orienting dendrites in the AL and a single axon exiting from the AL to project to the MB and LH. However, since we discovered new ALTs in *H. banian*, a comprehensive survey of PN types is required to conclusively prove that all PNs in

H. banian are multiglomerular. The physiological properties of the PNs in *H. banian* are also similar to the ones shown by PNs in *S. americana*. They show cell-specific odor-evoked spatio-temporal response properties to different odorants (Laurent and Davidowitz 1994; Wehr and Laurent 1996; Perez-Orive et al. 2002; Mazor and Laurent 2005) and are characterized by Na+ spikes as described by Distler (1990). At the level of the subfamily, PNs in *Bombyx mori* and *Manduca sexta* also exhibit similar morphological types (Namiki and Kanzaki 2011).

The second type of interneuron in *H. banian*, the LN, is also similar to the one found in *S. americana*. Both of them have dense arborization throughout the volume of the AL, are GABA-positive and respond to odor stimuli with small amplitude spikes, putatively Camediated (Laurent and Davidowitz 1994; Laurent 1996; Leitch and Laurent 1996; MacLeod and Laurent 1996).

3.3.9 Conserved anatomical and physiological features of third-order olfactory centers—MB and LH

LFP frequency: The odor-evoked oscillations in the LFP recorded from the MB calyx in *H. banian* have a predominant frequency of ~25 Hz which is similar to that reported in *S. americana* (Laurent and Naraghi 1994; Laurent 1996). We were unable to find an instance of comparison of predominant LFP frequencies between species which diverge at the subfamily level. The reported predominant frequencies of MB LFP varies widely across insect species, from ~10 Hz in *Drosophila* (Tanaka et al. 2009), ~17 Hz in the wasp *Polistes fuscatus* (Stopfer et al. 1999), to ~35 Hz in the moth *M. sexta* (Ito et al. 2009) and it is still unresolved if there is any significance of the predominant frequencies of LFP for olfactory information processing. The reason for the wide variability of the predominant frequency present in LFP recordings may be due to the difference in timescales of the synaptic currents, their strength and spatial scale involved.

Spatial variation of phase of LFP in mushroom body: We have shown that the LFP recorded from the primary calyx of MB is negatively correlated and out of phase to that recorded from the cell body layer (Fig. 3.10). This feature can arise because of the anatomical arrangement of the KCs in the MBs of insects, where the cell bodies of KCs are present in the cell body layer, dorsal to the calyx and the KC dendrites arborize in the calyx forming parallel columns (Laurent and Naraghi 1994; Strausfeld et al. 2003; Jones et al. 2009; Rybak 2012; Schuermann 2016). The synaptic input coming from the AL PNs in the MB calyx makes it act like a source while the cell body layer forms the sink of an electrical dipole-like arrangement. This kind of source-sink arrangement with dipolar currents is also found in neocortex, cerebellum and hippocampus of mammalian brains (Johnston and Wu 1994). As a result of this kind of arrangement, the LFP recorded from the cell body layer and MB calyx is negatively correlated and out of phase to each other (Johnston and Wu 1994; Herreras 2016). The spatial variation of phase of MB LFP should be taken into account when interpreting phase relationships between intracellularly recorded neurons from different areas and MB LFP (recorded from cell body layer or calyx).

Correlated slow plasticity in LFP: Consistent with reports in *S. americana*, the oscillatory components in the MB LFP around 25 Hz increase in power with repeated odor presentations. However, we have also shown that the lower frequency components of the LFP decrease in strength while the higher frequency components increase in strength during repeated presentations of odor stimuli. The slow plasticity in the AL that is shown to be the reason for ~25 Hz LFP power build up in *S. americana*, may also be accompanied by similar effects. Thus, it is important to realize that the LFP in MB calyx, which to a great extent reflects the PN input to the KCs has to be interpreted by taking this additional observation correlated with the slow plasticity in AL.

KC response: The KCs in *H. banian* display sparse spiking at the baseline and they respond to odorants with few spikes and subthreshold membrane oscillations similar to that reported in *S. americana* (Laurent and Naraghi 1994; Perez-Orive et al. 2002; Broome et al. 2006; Jortner et al. 2007). We were unsuccessful in filling any KC in *H. banian*. But KCs across insect species have been shown to be broadly similar in morphology with the cell bodies located dorsal to the calyx and dendrites in the calyx. Their axons run through the pedunculi and bifurcate to project in the MB output lobes (Strausfeld et al. 1998). Additionally, KCs have been classified into different classes based on the calycal areas innervated by them (details in Chapter 1).

Lateral horn neurons' morphology and physiology: The LHNs in *H. banian* seem to be composed of a diverse array of morphological types, similar to that reported in *S. americana* (Gupta and Stopfer 2012). We filled and recorded six neurons with either dense or sparse arborization in the LH area. Out of the six, one is morphologically similar to one of the 10 (C3) reported in *S. americana* (Gupta and Stopfer 2012). Three roles for LHNs have been proposed by Gupta and Stopfer (2012), bilateral coding, multimodal integration and concentration coding. The multimodal nature of LHN neurons has not been investigated in the present study. LHNs have also been reported from a number of other insect species. One type reported in *Schistocerca* is morphologically similar to the one LHN reported in the moth *Bombyx mori* (Namiki et al. 2013). This points out to the fact that in spite of the wide diversity in LHN morphological types, a rigorous study might reveal similar kinds across insect species, probably performing similar functions. But studies comparing LHNs morphology and physiology between species of different subfamilies are nonexistent.

3.3.10 Conserved anatomical and physiological features of fourth-order olfactory neurons—bLNs and GGN

In *H. banian*, we discovered two morphologically distinct types of bLNs—type 1 and type 2. Both of these correspond to the two types reported in *S. americana* in terms of morphology as well as physiologically (MacLeod et al. 1998; Cassenaer and Laurent 2007; Gupta and Stopfer 2014). Apart from the above two types, five more morphological types of bLNs have been reported in *S. americana* (Gupta and Stopfer 2014), but we did not encounter them in our preparations. This may be due to the difficulty in locating these types as they were rarely encountered in *S. americana* as well (Gupta and Stopfer 2014). The bLN2 count in our species is slightly more than that reported in *S. americana* (Gupta and Stopfer 2014). From our bLN2 fills, we observed that there might be two subtypes of bLN2 with difference in their patterns of arborization in the MB calyx. This might have implications in terms of different bLN2 subtypes feeding back to different subsets of KC populations and thereby modulating its output differentially.

GGN in *H. banian* is morphologically and physiologically similar to the one reported in *S. americana* (Leitch and Laurent 1996; Papadopoulou et al. 2011) and *S. gregaria* (Homberg et al. 2004). Both of them have arborizations in the alpha lobe, LH, and MB calyx. Both are GABAergic in nature and their odor response is characterized by depolarization of the membrane potential superimposed by EPSPs and IPSPs (Papadopoulou et al. 2011; Gupta and Stopfer 2012, 2014). In *P. americana*, GGN-like neurons are called calycal giants (CGs). Of the four found in them, 3 are spiking and one non-spiking (NS-CG). All of them are GABAergic in nature and project to different areas of the MB, feeding back to it. The NS-CG might be homologous to GGN in locusts as both are similar in morphology and physiology (Takahashi et al. 2017). In our samples with anti-GABA immunohistochemistry, we could discern two distinct and segregated layers of GABAergic zones of innervation. This kind of

segregated GABAergic innervation in MB has also been reported in *S. americana* (Gupta and Stopfer 2012). In *P. americana* too, it has been reported that the CG's innervation in the MB is segregated in different zones. In this case, it has been attributed to innervation by two different groups of AL uniglomerular PNs (Takahashi et al. 2017).

3.3.11 How different is the olfactory system in vertebrates belonging to different subfamilies?

In order to assess the similarities and differences of the olfactory circuit between species in vertebrates, we compared humans (subfamily: Homininae) with mouse, rat (both belonging to subfamily Murinae) and rabbit as substantial information is available only for these four species. The information which we could gather from literature is enumerated in **Table 3.1.**

We can see from the table that at the peripheral level, there are some differences in the number of olfactory receptors and the number of glomeruli per olfactory bulb (OB). In addition, the mouse, rat and rabbit olfactory circuits are characterized by the presence of a sex-specific organ, the vomeronasal organ which is absent in humans. At the second-order processing center, the OB, there are differences in the number of different neuronal types but overall, the basic architecture is conserved across mammalian systems (Sinakevitch et al. 2018) as is the case in insects. It was not possible to compare at the higher orders as studies at that level are difficult to come by.

Table 3.1 Numerical strength of olfactory pathway neurons in different vertebrates

	Rat	Mouse	Human	Rabbit
Order/ Subfamily	Rodentia/	Rodentia/	Primates/	Lagomorpha
	Murinae	Murinae	Homininae	
OR genes	1576	1375	437	
intact+pseudogenes	(1284+292)	(1194+181)	(295+142)	
	(Zhang et al.	(Zhang et al.	(Zhang et al.	
	2007b)	2007b)	2007b)	
ORs	~1300	≈1200	≈350	_
	(Zhang et al.	(Zhang et al.	(Maresh et al.	
	2007b)	2007b)	2008)	
ORNs	21,000,000	5,200,000		50,000,000
	(Kawagishi et	(Kawagishi et		(Allison and
	al. 2015)	al. 2014)		Warwick 1949)
Glomeruli: ORN	3:1	2/3:1	16:1	_
		(Maresh et al.	(Maresh et al.	
		2008)	2008)	
Glomeruli in OB	4200	≈3700	≈5500	6300
	(Royet et al.	(Richard et	(Maresh et al.	(Royet et al.
	1998)	al. 2010)	2008)	1998)
Mitral cells	56200	≈33000	~50935	59600
	(Royet et al.	(Richard et	(Bhatnagar et	(Royet et al.
	1998)	al. 2010)	al. 1987)	1998)
Tufted cells	160000	73200		130,000
	(Meisami and	(Burton		(Allison and
	Safari 1981)	2016)		Warwick 1949)
Granule cells		$\approx 10^6$		_
		(Richard et		
		al. 2010)		
Periglomerular	_	297500	_	_
cells (inhibitory)		(Parrish-		
		Aungst et al.		
		2007)		

3.4 Conclusion

Taking together all the evidences that we presented for the grasshopper *H. banian* (subfamily Hemiacridinae), with respect to the anatomical and physiological characteristics of the olfactory circuit and comparing them to that in the locust *S. americana* (subfamily Cyrtacanthacridinae), we see that the olfactory circuit of the two species are conserved through the fourth-order level (**Table 3.2**).

The biggest takeaway from this study is that we can expect two species from different subfamilies to be highly similar at the higher orders. Though more studies to establish the applicability of this principle to species from different orders as a general rule is required, this points to the conserved nature of olfactory circuit at higher levels in species which have not been studied yet. For example, we can expect that the olfactory circuit at the fourth-order level would be similar between the hymenopterans *Bombus terrestris* and *Apis mellifera*, which belong to two different subfamilies (Bombinae and Apinae respectively) or between the mosquitoes *Anopheles gambiae* and *Aedes aegypti* (Subfamilies Anophelinae and Culicinae respectively).

This study also introduces a new model organism which can be used to investigate information processing in the olfactory circuit. This model organism is a nice complement to the well-studied *S. americana* in which a number of computational principles underlying olfactory processing have been studied. The accessibility and tractability of *H. banian* can be used to carry out studies in the Indian subcontinent without the introduction of an alien locust species *S. americana*.

Table 3.2 Comparison of features of the olfactory pathways of S. americana and H. banian

	Anatomical features		Physiological features	
	Reported in S. americana	H. banian (Present study)	Reported in S. americana	H. banian (Present study)
Sensilla types and recordings (representative of ORNs)	Reported in sister species S. gregaria	Similar types— coeloconica, chaetica, basiconica and trichodea	Respond to different odors with wide variety of odor-specific patterns	Not measured
	(Ochieng et al. 1998)	(Singh and Joseph 2019)	Baseline spontaneous firing present	
			(Hansson et al. 1996; Ochieng and Hansson 1999; Raman et al. 2010; Joseph et al. 2012)	
Organization of antennal	Large no. of	Large no. of		
lobe glomeruli	microglomeruli	microglomeruli		
	(Laurent and Naraghi 1994)	(Singh and Joseph 2019)		
AL tracts to MB	Only mALT reported (Laurent and Naraghi 1994)	Bulk tract tracing from AL reveal 3 more tracts in addition to mALT- lALT, mlALT and tALT (Singh and Joseph 2019)		
AL PN	Multiglomerular; a single axon runs to the MB and then to the LH. It arborizes densely in the MB calyx and the LH.	Multiglomerular; a single axon runs to the MB and then to the LH. It arborizes densely in the MB calyx and the LH.	Multiphasic-cell-odor specific responses which often include strongly inhibited phases	Multiphasic-cell-odor specific responses which often include strongly inhibited phases

	(Laurent and Naraghi 1994)	(Singh and Joseph 2019)	Spontaneous spiking activity at baseline (Laurent and Davidowitz 1994; Laurent and Naraghi 1994; Laurent et al. 1996; Wehr and Laurent 1999)	Spontaneous spiking activity at baseline (Singh and Joseph 2019)
AL LN	Wide arborization in AL, axonless and GABA- positive (Leitch and Laurent 1996; MacLeod and Laurent 1996)	Wide arborization in AL, axonless and GABA-positive (Singh and Joseph 2019)	No sodium action potentials but spikelets of varying shapes and amplitudes (Laurent and Davidowitz 1994; Laurent 1996)	No sodium action potentials but spikelets of varying shapes and amplitudes (Singh and Joseph 2019)
МВ КС	Cell body in cell-body layer and putative dendrites in synaptic layer (calyx). The axons run through the pedunculus and bifurcate to terminate in α-lobe and β-lobe. (Laurent and Naraghi 1994)	Not filled	Low baseline rate Sparse spiking with subthreshold oscillations during odor response (Laurent and Naraghi 1994)	Low baseline rate Sparse spiking with subthreshold oscillations during odor response (Singh and Joseph 2019)
Features of MB LFP			Have oscillations ~25 Hz which is correlated to the subthreshold oscillation in the KC membrane potential	Have oscillations ~25 Hz which is correlated to the subthreshold oscillation in the KC membrane potential

			(Laurent and Naraghi 1994; Perez-Orive et al. 2002)	
			Slow plasticity in the LFP power in 5-55 Hz band	Slow plasticity in the LFP power and we show that while LFP power in 15-40
			(Stopfer and Laurent 1999)	Hz band increases similar to <i>S. americana</i> , it decreases in 1-5 Hz band
			Not reported	Different features of LFP recorded from the cell body layer and synaptic layer
			Not reported	LFP from cell body layer and synaptic layer are negatively correlated
				(Singh and Joseph 2019)
LH neuron	Variety of morphological types	Variety of morphological types (one of which corresponds to the	Responds with increased firing rate to most odors	Responds with increased firing rate to most odors
		reported type; Fig 6 gi is similar to C3 in Gupta and Stopfer (2012)	(Gupta and Stopfer 2012)	(Singh and Joseph 2019)
	(Gupta and Stopfer 2012)	(Singh and Joseph 2019)		
bLN type1	Cell body in the medial	Cell body in the medial	Baseline spontaneous	Baseline spontaneous
	protocerebrum with arborization in the beta	protocerebrum with arborization in the beta	firing present	firing present

	1 1 1 1 1 1 1 1 1 1 1 1 1 1 1 1 1 1 1 1	1 1 1 1 1 1 1 1 1 1 1 1 1 1 1 1 1 1 1 1	In the state of	D 1
	lobe, pedunculus and LH	lobe, pedunculus and LH	Responds to most odors	Responds to most odors
			with increased firing rates	with increased firing rates
	GABA-negative	GABA-negative	and no strong inhibitory	and no strong inhibitory
			phases like those observed	phases like those observed
	(MacLeod et al. 1998;	(Singh and Joseph 2019)	in PNs	in PNs
	Gupta and Stopfer 2014)			
			(MacLeod et al. 1998;	
			Gupta and Stopfer 2014)	
bLN type2	Cell bodies in the lateral	Cell bodies in the lateral	Baseline spontaneous	Baseline spontaneous
oErv type2	protocerebrum with	protocerebrum with	firing present	firing present
	arborization in the alpha	arborization in the alpha	ining present	ining present
	lobe, beta lobe,	lobe, beta lobe,	Desmands to most odors	Desmands to most adoms
			Responds to most odors	Responds to most odors
	pedunculus and MB calyx	pedunculus and MB calyx	with increased firing rates	with increased firing rates
			often lasting beyond the	often lasting beyond the
	12–15 cell bodies	13–16 cell bodies	odor duration and no	odor duration and no
			strong inhibitory phases	strong inhibitory phases
	(MacLeod et al. 1998;	(Singh and Joseph 2019)	like those observed in PNs	like those observed in PNs
	Gupta and Stopfer 2014)			
			(MacLeod et al. 1998;	(Singh and Joseph 2019)
			Gupta and Stopfer 2014)	
bLN type3–7	Diverse morphological	Not encountered	Data not presented	_
T ST	types		1 1 1 1 1 1 1 1 1 1 1 1 1 1 1 1 1 1 1 1	
	i cypes			
	(Gupta and Stopfer 2014)			
Property of KC-bLN			Synapse between KC-bLN	Not tested
synapse			shows modifiable Hebbian	1vot tested
synapse			spike-timing dependent	
			plasticity (STDP)	
			(Cassenaer and Laurent	
			2007, 2012)	

GGN	Large cell body in the lateral protocerebrum with	Large cell body in the lateral protocerebrum with	Non-spiking neuron	Non-spiking neuron
	innervations in MB calyx,	innervations in MB calyx,	Responds to odors with	Responds to odors with
	alpha lobe and the LH	alpha lobe and the LH	depolarization of the resting membrane	depolarization of the resting membrane
	GABA-positive	GABA-positive	potential superimposed with EPSPs and IPSPs	potential superimposed with EPSPs and IPSPs
	(Leitch and Laurent 1996;	(Singh and Joseph 2019)		
	Papadopoulou et al. 2011)		Strength of depolarization increases with increasing concentration gradient of odors	Strength of depolarization increases with increasing concentration gradient of odors
			Reliable IPSPs in resting membrane potential as well as during odor response	Reliable IPSPs in resting membrane potential as well as during odor response
			(Papadopoulou et al. 2011)	(Singh and Joseph 2019)

Chapter 4

Properties of a novel group of bilateral extrinsic neurons of the mushroom body in the olfactory circuit of *Hieroglyphus banian*

4.1 Introduction

Olfactory circuits across animals are characterized by a bilaterally symmetrical organization similar to other sensory systems. This kind of organization is critical for building reliable internal representation of the outside world but how and where the two sides interact is still inconclusive (Sandoz and Menzel 2001; Komischke et al. 2003). Though it has been shown in rats and humans that olfactory memory can be transferred from one hemisphere to the contralateral hemisphere, the exact neural circuitry underlying such transfer is still unknown (Kucharski and Hall 1987, 1988; Bromley and Doty 1995; Mainland et al. 2002; Yan et al. 2008). One possible neural element executing such transfer may be the existence of bilateral neurons in the brain which could probably mediate such transfer across brain hemispheres.

In insects, the mushroom bodies are the areas which are reported to play critical roles in olfactory learning and memory (Heisenberg 2003; Davis 2004). Until now, bilateral neurons connecting both the mushroom bodies have not been reported in any insect species. In this chapter, we are reporting a novel class of bilateral neurons, innervating areas of both the mushroom bodies (we call them MB extrinsic neurons or MBENs). All of them have cell

bodies in superior lateral protocerebrum, at the boundary of the MB, and they exhibit steady, nearly rhythmic baseline firing rate with weak odor response.

The results described in this chapter have been obtained by using intracellular recordings and intracellular dye fills (detailed in Chapter 2). Confocal imaging of the dye-filled tissues and post-imaging analysis was done using the software Fiji. The successfully filled samples were taken back in alcohol series to do anti-GABA immunohistochemistry.

When 2D projections obtained from confocal z-stacks were not clear for representation, the plug-in 'simple neurite tracer' in Fiji was used to reconstruct the morphology of the neuron (**Fig. 4.5**). Physiological data were analyzed and plotted offline using custom programs written in MATLAB.

4.2 Results

4.2.1 Morphological, immunohistochemical and physiological features of MBEN1

The cell body of type 1 MBEN is located ventrolateral to the MB calyx in the superior lateral protocerebrum (Fig. 4.1 Ai). It gives off a neurite which travels medially towards the pedunculus of the ipsilateral side for some distance and then turns ventral slightly and runs across the pedunculus ventromedially. Before running across the ipsilateral alpha lobe, few branches from the main neurite ramify in the superior intermediate protocerebrum (SIP) and the superior lateral protocerebrum (arrowheads, Fig. 4.1 B). After crossing over the ipsilateral alpha lobe, the major neurite bifurcates into two branches (Fig. 4.1 Ai and Aii). One branch runs along the dorso-medial margin of the ipsilateral alpha lobe and ramifies densely in the anterior parts (Fig. 4.1 C). The other branch continues further, crosses the midline of the brain at the level of the central complex, and then ascends dorsolaterally towards the contralateral alpha lobe (Fig. 4.1 Aii). It bifurcates again and one branch runs along the dorsomedial margin of the contralateral alpha lobe and enters it, arborizing

profusely in the anterior part. The other branch runs further across the alpha lobe, its termination could not be discerned from the image. Anti-GABA immunohistochemistry of this neuron revealed that it is non-GABAergic in nature (**Fig. 4.1 D**).

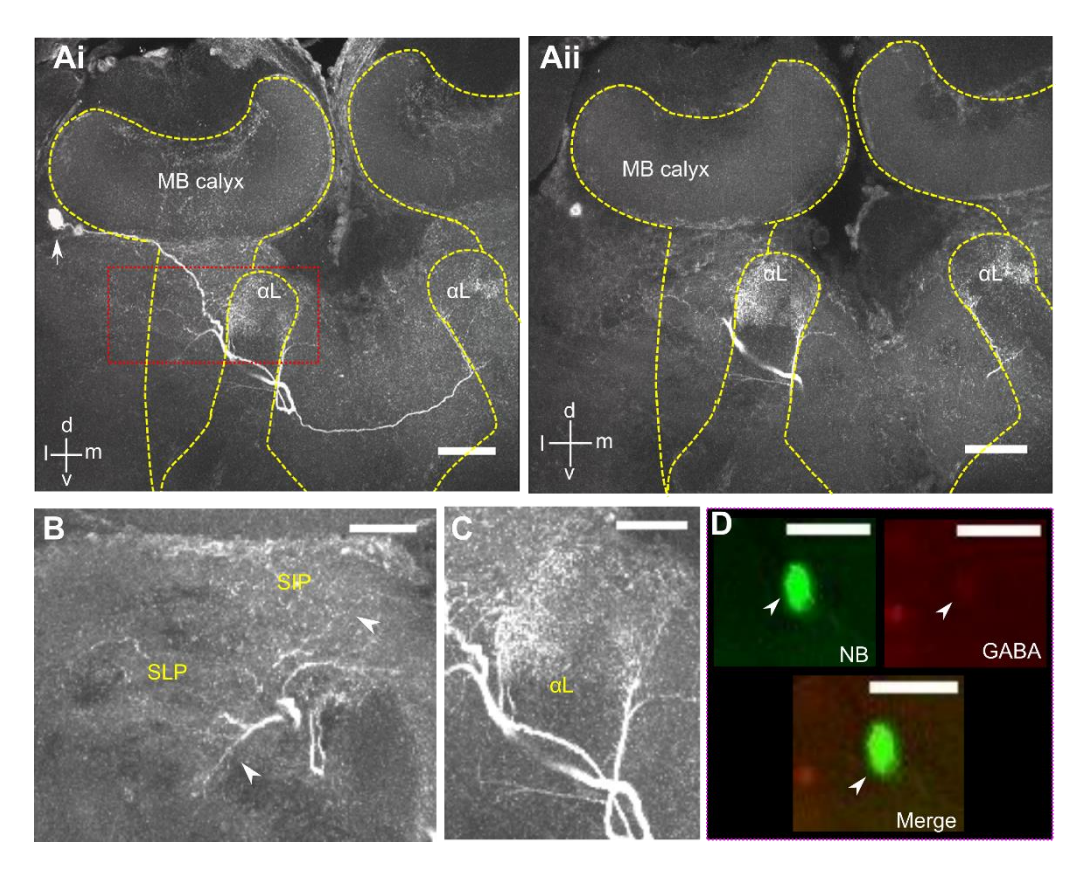


Figure 4.1 Morphology of mushroom body extrinsic neuron type 1 (MBEN1). (Ai and Aii) The cell body of MBEN1 is located ventrolateral to the MB calyx in the superior lateral protocerebrum (arrow in Ai). A single thick efferent neurite emanates from the cell body, runs medially for a short distance and then turns ventromedially, crossing over the ipsilateral alpha lobe. Before crossing the alpha lobe, this neurite gives off few branches which ramify in the ipsilateral superior lateral protocerebrum and superior intermediate protocerebrum, (Ai, red box) and arrowheads in (B). The main branch bifurcates after crossing the ipsilateral alpha lobe. One branch turns backwards and runs dorsally to innervate the anterior part of the ipsilateral alpha lobe (Ai, red box) and (C). The other branch crosses the midline of the brain at the level of the central complex, reaches the contralateral alpha lobe and ramifies in its anterior part. (D) Anti-GABA immunohistochemistry of this dye-filled neuron showed it to be GABA-negative. Scale bars: 100 μm for (Ai and Aii); 50 μm for (B, C and D)

The physiological response of MBEN1 to five different odorants was not very different from the baseline activity (**Fig. 4.2**). Baseline activity of this neuron was characterized by constant spontaneous firing. The presence of odorant caused only a slight change in the baseline firing rate.

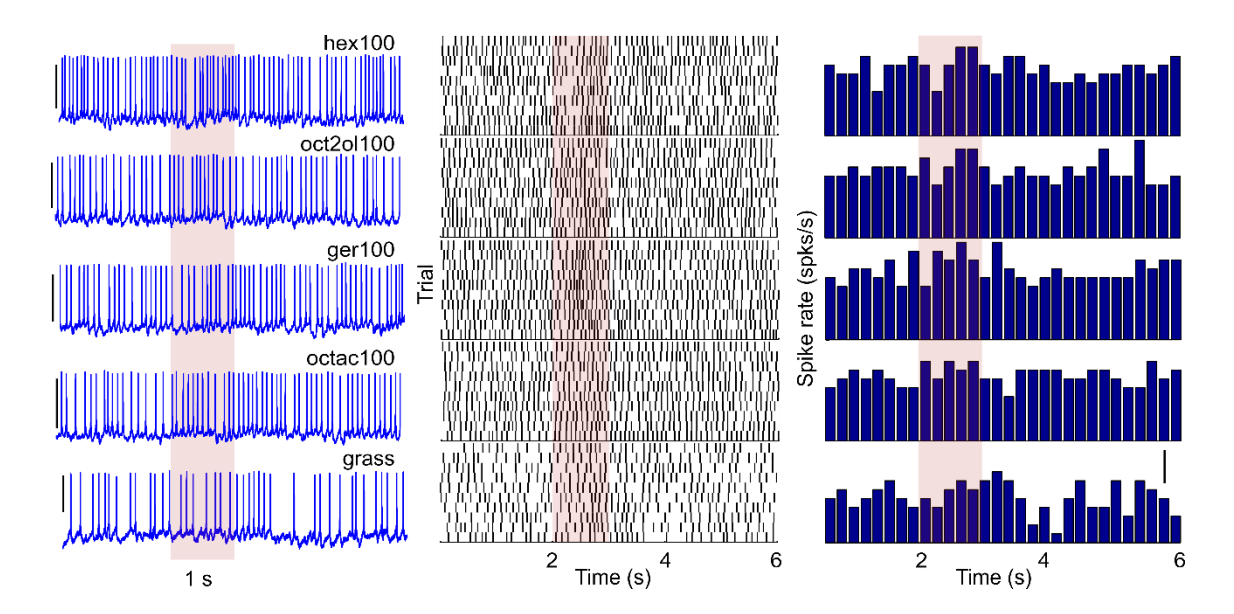


Figure 4.2 Physiology of MBEN1. Physiological response of MBEN1 to four different odorants and grass. This neuron showed a constant baseline spontaneous spiking which increased only sparingly when the odor stimuli were presented. In general, grass resulted in a lower level of response compared to the pure odorants. Scale bars: 0.01 mV for raw traces of pure odorants in first column; 5 mV for raw trace of grass; 2 spikes/s for PSTH in third column

4.2.2 Morphological, immunohistochemical and physiological features of MBEN2

The second morphological type of MBEN has its cell body in a location similar to that of MBEN1 (ventrolateral to the MB calyx, in the superior lateral protocerebrum; **Fig. 4.3 A**). The major efferent neurite of the neuron first runs medially for a short distance, it then turns in the ventral direction and runs ventromedially across the ipsilateral pedunculus and the alpha lobe. It bifurcates into multiple branches at this point. The major neurite continues further in the ventromedial direction and after reaching the level of the central complex, it makes a U-turn. Multiple branches from the U-junction enter the ipsilateral pedunculus and

arborize densely (**Fig. 4.3 A**). The arborization is reticulate in structure and at least two finger-like arborization pattern could be discerned in the pedunculus reminiscent of the arborization pattern of the PE1 extrinsic neuron in the alpha lobe of honey bee (Rybak and Menzel 1993, 1998; Mauelshagen 1993).

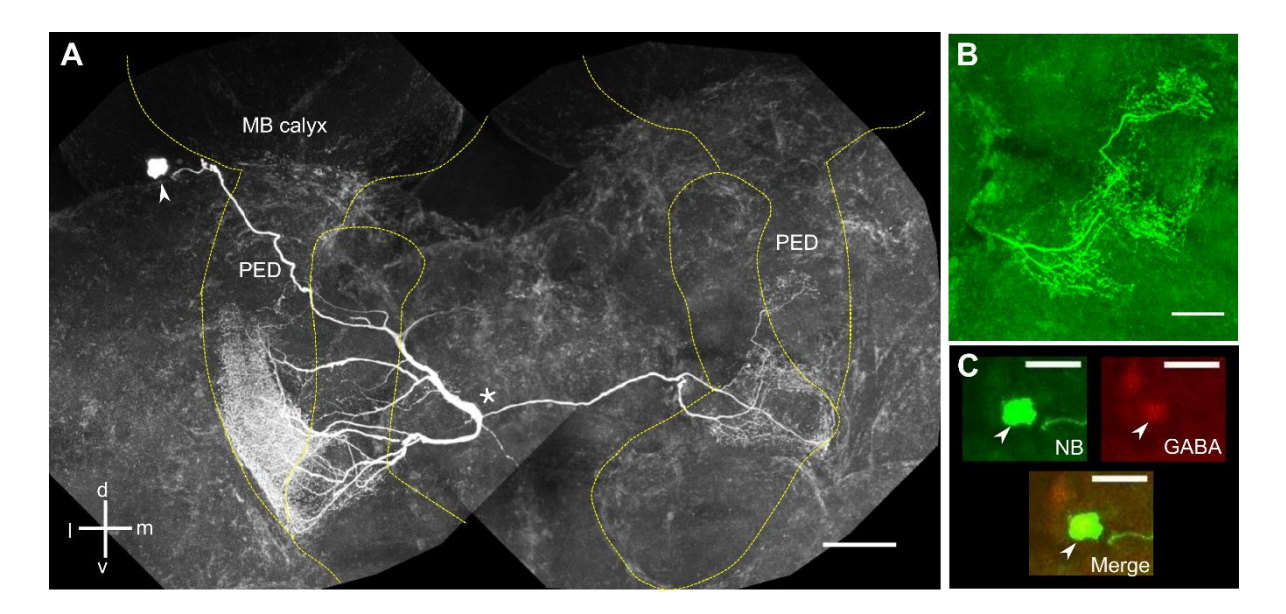


Figure 4.3 Morphology of MBEN2. (A) MBEN2 has its cell body in the superior lateral protocerebrum, ventrolateral to the calyx of the MB. The major neurite from the cell body runs ventromedially and runs across the ipsilateral pedunculus and alpha lobe, bifurcating into multiple branches at various locations. It takes a U-turn at the level of the central complex, branching into a number of neurites which enter the ipsilateral pedunculus. They innervate the ipsilateral pedunculus densely and in a reticulate formation. A thin neurite from the U-junction (star) of the major neurite runs medially and crosses the midline at the level of the central complex. It reaches the contralateral pedunculus and branches into many sub-branches. These enter the contralateral pedunculus and ramify in three distinct rows (B). The ipsilateral pedunculus has denser innervation compared to the contralateral pedunculus. The innervations in the contralateral pedunculus have varicose structure, putatively implying output area. (C) Anti-GABA immunohistochemistry of this neuron shows it to be GABA-positive. Scale bars: 100 μm for (A); 50 μm for (B), (C)

One small branch from the U-junction where the main branch bifurcates, runs in the medial direction, crossing the midline of the brain at the level of the central complex and reaches the contralateral pedunculus (**Fig. 4.3 A and B**). The neurite arborizes in the contralateral pedunculus in three distinct zones. The arborization does not appear reticulate

here; rather it is diffused (**Fig. 4.3 B**). Anti-GABA immunohistochemistry of MBEN2 showed it to be GABA-positive (**Fig. 4.3 C**).

The physiological feature of MBEN2 consisted of constant spontaneous firing at the baseline (**Fig. 4.4**). Odor response to three different odorants showed brief excitation. For the odorant 2-octanol, we could not discern any change from the baseline spontaneous firing rate.

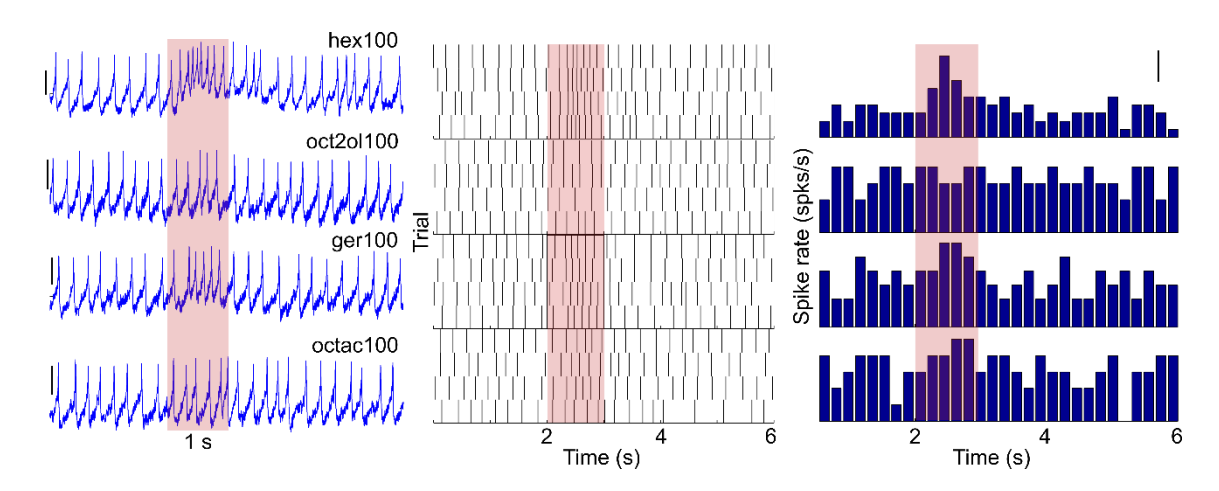


Figure 4.4 Physiology of MBEN2. This neuron showed constant baseline spontaneous firing. Odor response to the odorants hexanol, geraniol and octanoic acid showed a slight increase in firing rate. Scale bars: 2 mV for raw traces; 2 spikes/s for PSTH

4.2.3 Morphological and physiological features of a different bilateral neuron

The third type of bilateral neuron also has its cell body ventrolateral to the MB calyx in the superior lateral protocerebrum (**Fig. 4.5 A**). Its major neurite travels medially for a short distance and then turns ventromedially. The neurite runs across the ipsilateral pedunculus and the alpha lobe crossing the midline of the brain at the level of the central complex. On the contralateral side, it travels dorsally for some distance before turning and running laterally. It ramifies in the contralateral superior lateral protocerebrum (**Fig. 4.5 A**).

The physiological feature of this bilateral neuron consisted of a regular firing rate which increased briefly when an odorant stimulus was presented to it (Fig. 4.5 B).

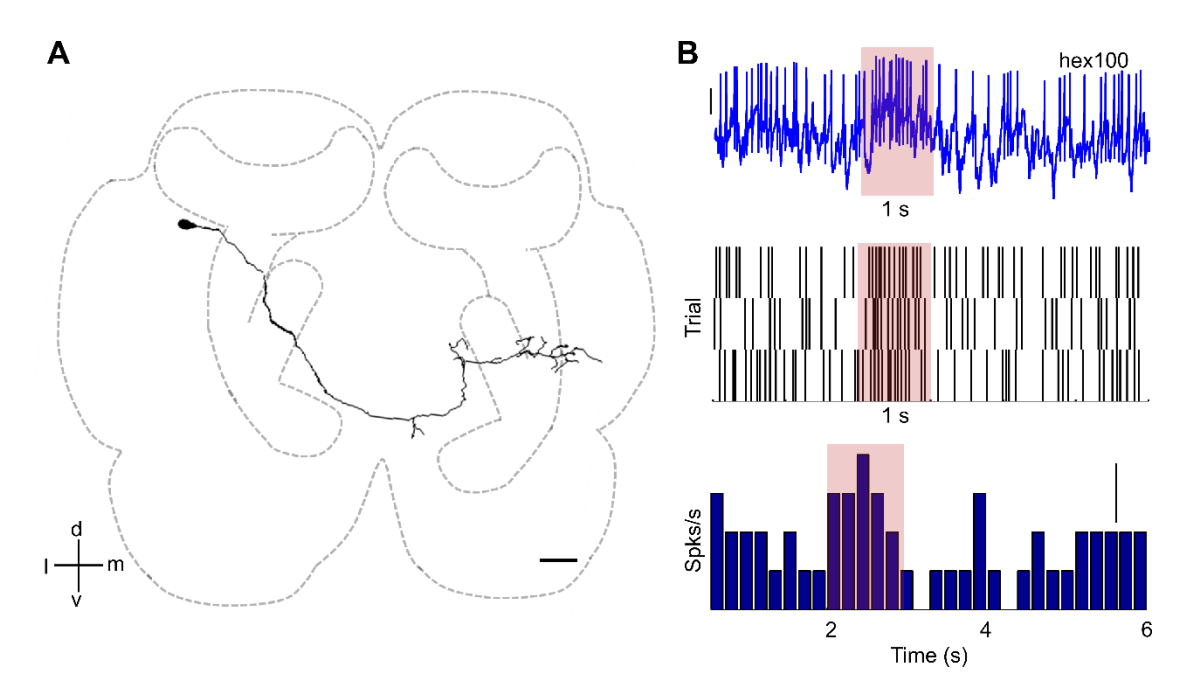


Figure 4.5 Morphology and physiology of another bilateral neuron. (A) This bilateral neuron has its cell body in the same location as the two MBENs described before, that is, in the superior lateral protocerebrum, ventrolateral to the calyx of the MB. Its major neurite runs ventromedially towards the midline of the brain and crosses it at the level of the central complex, with no side branches. After crossing the midline, it arborizes in the superior lateral protocerebrum of the contralateral side. Scale bar: $100 \, \mu m$ (B) This neuron responded to the odorant hexanol by a brief increase in firing rate and it exhibited spontaneous baseline firing. Scale bars: $2 \, \mu V$ for raw trace; $2 \, \text{spikes/s}$ for PSTH

4.2.4 Features common to the three bilateral neurons

All the three bilateral neurons have their cell bodies in a similar location, that is, ventrolateral to the MB calyx, in the superior lateral protocerebrum. All three of them appear to follow the same trajectory in the beginning—ventromedially, crossing over the ipsilateral pedunculus and alpha lobe. In addition, the major neurite of all three of them cross the midline of the brain at the level of the central complex. Two of them (MBEN1 and MBEN2) innervate downstream of MB, the third-order olfactory center.

4.3 Discussion

This part of the work reports a novel set of bilateral neurons discovered in *H. banian*. The following findings are new with respect to the observed data:

- 1. A set of three new morphological types of bilateral neurons, with their cell bodies in the same location. One of them arborizes in both alpha lobes; the second one has arborization in both pedunculi while the third bilateral neuron has sparse arborization in the contralateral half of the brain but no arborization in the ipsilateral half.
- 2. Of the three, two types have dense arborization downstream of KCs, the third-order neurons intrinsic to the MB. In spite of their dense innervation, they show weak responses to odor stimuli, which is surprising considering that all known fourth-order neurons in the olfactory circuit show vigorous responses to odor stimuli.
- 3. One MBEN is GABA-positive while another one is GABA-negative.

What can be the possible function of these kinds of bilateral neurons and what roles do they play in the circuit? Behavioral studies in insects (Martin 1965; Louis et al. 2008) and mammals (Rajan et al. 2006; Porter et al. 2007) have indicated the interplay of information from both halves of the brains in olfactory-guided behaviors like tracking odor plumes. This helps in making decisions faster and more accurately as information from both sides is available to the animal. In one study carried out in human subjects, bilateral input was deemed to be better than unilateral for odor recognition memory (Bromley and Doty 1995). The question then arises as to where such integration of information from both halves of the brain may occur. In humans, Bromley and Doty (1995) have reported that since peripheral projections are unilateral, the underlying mechanism for odor recognition

memory may be carried out in the higher order anterior olfactory nucleus, which has neurons with contralateral projections and fibers.

In insects, too, such role of bilateral integration of olfactory information is attributed to bilateral neurons in the circuit. The bilateral integration of olfactory information may occur at the third-order by LH neurons (as postulated by (Gupta and Stopfer 2012) or at the output level of the MB (alpha and beta lobes) or by other bilateral protocerebral neurons (Lei et al. 2001). Since the mushroom bodies are higher centers for olfactory learning and memory in insects (Heisenberg 2003; Davis 2004), bilateral connection between them might play a role in integrating olfactory information from both halves of the brain. However, until now, no examples of bilateral neurons having neurites in both the mushroom bodies or their output lobes have been reported in any insect species. Thus, this report of bilateral MBENs in the present study is the first example of such neurons in the insect olfactory circuit.

On the basis of the innervation areas, the three bilateral neurons reported in this study can be divided into the following types:

4.3.1 Bilateral alpha lobe neurons

These kinds of neurons have been reported in honey bees (A6 and A7 clusters; (Rybak and Menzel 1993) and the moth *Agrotis segetum* (Lei et al. 2001). Their arborization in the alpha lobe seems to be restricted in bands. Though the cell bodies of A6 cluster in honey bee are located in a similar location to the one in *H. banian* (ventral to the calyx), their innervation in the alpha lobes is different. A6 cluster in honey bees is divided into two types. A6-type 2 neurons innervate around the alpha lobe on the ipsilateral side and in the ventral part of alpha lobe on the contralateral side. A6-type 1 and A7 cluster bilateral neurons in honey bee and the bilateral alpha lobe neuron in *Agrotis segetum* innervate only

the ipsilateral alpha lobe. While in *H. banian*, the bilateral MBEN1 innervates both the alpha lobes densely (**Fig. 4.1**).

4.3.2 Bilateral neurons connecting both pedunculi

The pedunculi in insects is formed by the axons of the KCs (Fahrbach 2006). The axons in the pedunculus have been shown by electron microscopic studies to have axon-axon synapses between them along their length (Leitch and Laurent 1996; Strausfeld and Li 1999). What could be the possible role of neurons connecting the two pedunculi? What kind of information processing might they be involved in? The dense reticulate arborization which we see for MBEN2 (**Fig. 4.3 A and B**) may probably help in comparing olfactory information between the two sides. Since the neuron is GABA-positive, it is possible that it inhibits the information flow from the KCs to the lobes.

One study in cockroach reported the presence of a GABAergic bilateral afferent neuron supplying neurites to the pedunculus (Strausfeld and Li 1999). The neuron responded to mechanical stimuli and was postulated to mediate in providing information about movement of the antenna and body to KCs. Other unilateral extrinsic neurons with arborization in the pedunculus have also been reported (Li and Strausfeld 1999). But neurons with arborizations in both the pedunculi have not been reported in any insect species as of now.

In the family Acrididae, bilateral neurons associated with the olfactory pathway have only been reported in *S. americana*. Two morphological types of bilateral lateral horn neurons (termed C3 and C7) have been suggested to play a role in bilateral integration of odor information (Gupta and Stopfer 2012).

4.3.3 Bilateral neuron with arborization in the superior lateral protocerebrum (SLP)

The SLP in many insects is innervated by protocerebral neurons (Lei et al. 2001). It might be the area involved in integrating information from the neurons of the olfactory pathway and neurons innervating premotor areas in the thoracic area (Lei et al. 2001). One of the three bilateral neurons in this study projects to the SLP (**Fig. 4.5**). However, at this juncture, it is difficult to reach to a conclusion about this as more data is required.

4.3.4 Multiplex organization and interaction of olfactory information

The KCs in mushroom bodies of most insects are organized in concentric zones of modality specific, segregated zones—the lip, collar and basal ring (Mobbs and Young 1982; Mobbs 1984). This laminar organization extends along the length of the KCs' axons in the pedunculi and the two lobes—alpha and beta (Strausfeld et al. 2009).

Both longitudinal and transverse arborization pattern of the MBENs may indicate the possibility that these neurons sample different populations of KCs to give rise to modality-specific processing of information or playing a role in learning and memory (Li and Strausfeld 1997). Evidence for the significance of such segregated arborization in the MBs comes from two studies, one in cockroach (Mizunami et al. 1998) and the other in *Drosophila* (O'Dell et al. 1995). We observe this kind of segregated arborization pattern of neurites in MBEN2 (**Fig. 4.3 A and B**). This neuron displayed longitudinal segregated arborization in the ipsilateral pedunculus and transverse ramification of neurites in three distinct zones in the contralateral pedunculus. However, further study to explore its multimodal nature is required to conclusively make a claim that it plays a role in modality-specific processing of information or in learning and memory.

4.3.5 Unique response pattern of MBENs to odor stimuli

Physiologically, the odor responses of the MBENs are unlike the ones found in other fourth-order neurons of the locust olfactory circuit. In *S. americana* (Papadopoulou et al. 2011; Gupta and Stopfer 2014) and *H. banian* (as reported in chapter 3 of this thesis; (Singh and Joseph 2019) all reported fourth-order neurons like the bLNs and GGN show vigorous odor responses. In *Apis mellifera*, the extensively studied unilateral alpha lobe neuron, the PE1 also shows vigorous odor responses (Rybak and Menzel 1993, 1998; Mauelshagen 1993). On the contrary and to our surprise, the bilateral MBENs in *H. banian* show weak responses to odor stimuli. Further study is required to explore the reason and mechanism behind this observation.

Most unilateral alpha lobe neurons in insects have been shown to respond to multimodal stimuli (in cricket *Acheta domesticus*, (Schildberger 1984); in cockroach *P. americana*, (Li and Strausfeld 1997); in moth *Agrotis segetum* (Lei et al. 2001)). The multimodal nature of the MBENs has not been investigated in this study and needs to be explored in further studies.

Another distinguishing physiological character observed in these neurons is that they exhibit constant spontaneous firing at baseline. Constant spontaneous baseline frequency is defined as baseline frequency with relatively small statistical variation over long duration (Homberg and Erber 1979). Alpha lobe neurons with this kind of baseline activity have been reported in honey bees (Homberg and Erber 1979). Physiologically, the response of these neurons to stimuli varied widely, from no response to multimodal responses.

Neurons manifesting constant spontaneous frequency have also been reported in the protocerebrum of Lepidoptera (Schümperli 1975), around the MB in honey bees (Erber 1978) and in the optic ganglia of the bee (Homberg and Erber 1979). The neurons reported

by Erber (1978) responded to multimodal stimuli. One intracellular recording from a protocerebral neuron in the moth *Agrotis segetum* also showed constant spontaneous baseline activity (Lei et al. 2001).

The significance of this type of baseline activity is still open to interpretation. Considering that the change in the baseline activity due to stimuli is very low, Erber (1978) postulated that these kinds of neurons might act as synchronizing and gating elements between different synaptic areas.

4.4 Conclusion

With the data in hand, we can say that there are a group of bilateral neurons, downstream of KCs, which though innervating densely in the output regions of the MB, the higher-order olfactory integration center, have weak response to odor stimuli. This is unlike any other known fourth-order neurons in the grasshopper olfactory circuit. The roles which these kinds of neurons play in the circuit needs to be investigated further.

Chapter 5

Adaptive modulation of an inhibitory recurrent circuit sub-serving gain control in the mushroom body network

5.1 Introduction

Sensory stimuli in the environment can give rise to either of two responses in the nervous system across animals—excitation or inhibition. And the balance between these two neuronal responses is maintained by inhibitory neurons which is highly critical to keep the system stable, running and giving rise to meaningful behavior.

One of the ways by which the inhibitory neurons execute this is by gain control, implemented by an excitatory-inhibitory (E-I) recurrent network, a ubiquitous coding mechanism across sensory systems of animals. Gain control or negative feedback circuit is a mechanism by which the response of a neuron (restricted by output range) is modulated to represent a stimulus varying across magnitudes of intensity. The question then arises as to how does a gain control network adapts itself across different conditions or what regulates the behavior of the inhibitory neurons involved in gain control. This role is postulated to be played by recurrent inhibitory (I-I) networks which are well placed to provide dynamic regulation of a gain control network resulting in flexible response to changing stimuli (Kapfer et al. 2007 and references therein). Nevertheless, how these networks embedded

within the neuronal circuit give rise to behavior is still ambiguous because of the difficulties in studying these circuits in isolation.

An instance of a recurrent inhibitory local circuit embedded within a gain control network is reported in the locust *Schistocerca americana* (Papadopoulou et al. 2011). The I-I recurrent network is formed by the GGN-IG (Inhibitor of GGN) pair embedded in an E-I recurrent network formed by the KCs and GGN. Even though the MB KCs receive a barrage of excitatory input from the PNs in the AL in response to odor stimuli, they respond with very few spikes (sparse code) (Laurent and Naraghi 1994; Perez-Orive et al. 2002). The inhibitory GGN is responsible for the sparse odor response of MB KCs (Papadopoulou et al. 2011). GGN is, in turn, reciprocally inhibited by an inhibitory neuron IG, whose identity is unknown. It is only known that it is a spiking neuron, unlike GGN whose odor responses consist of depolarization of the membrane potential superimposed by EPSPs and IPSPs (Papadopoulou et al. 2011). Therefore, we explored the role of a recurrent inhibitory network (GGN-IG) involving an unidentified neuron (IG) embedded within a gain control network (KC-GGN) in the grasshopper olfactory circuit, using *Hieroglyphus banian*.

The results in this chapter have been obtained through intracellular recordings from the GGN, AL PN, LHN and bLN in response to odor stimuli and electrical stimulation of MB KCs. LFP recordings from the MB calyx or EAG from the antenna were simultaneously recorded in most of the cases. The details are laid out in Chapter 2.

We recorded intracellularly from GGN while simultaneously recording LFP from the MB. We used the data from GGN recording to detect the odor-response properties of IG indirectly. We show that IG is odor-responsive, receives its input from the MB KCs and is responsible for fine tuning the response of GGN to odor stimuli. We also show that KC-IG

synapse shows short term plasticity similar to KC-GGN synapse by undergoing paired-pulse facilitation (PPF).

5.2 Results

5.2.1 KC-GGN-IG network in *Schistocerca*

A schematic based on the published data about the GGN circuitry is depicted in **Fig. 5.1**. GGN gets its olfactory input from the KCs in the alpha lobe where it has fine arborizations, putatively of dendrites and feeds back to the MB calyx (Papadopoulou et al. 2011). The KC-GGN synapse shows paired-pulse facilitation, a kind of short-term synaptic facilitation, in response to repeated odor presentations with an inter-pulse interval less than 1 s. The membrane potential recorded from the GGN shows unitary IPSPs which come from an unidentified neuron called IG. GGN and IG have reciprocal inhibitory connections (Papadopoulou et al. 2011). However, the features of IG and its role in the circuit are still unexplored. Similar to the GGN in *S. americana*, *H. banian* also has a single large inhibitory neuron in the lateral protocerebral lobe feeding back to the MB calyx. The morphology and physiology of GGN in *H. banian* is similar to the one in *S. americana* and is described in detail in chapter 3 of this thesis.

5.2.2 IG spikes can be detected unambiguously from GGN membrane potential

Papadopoulou et al. (2011) reported in their study that GGN-IG have a monosynaptic connection as all the IPSPs in GGN membrane potential can be attributed to IG input. It also follows thereby that there are no IPSPs which cannot be accounted for by IG input. Thus, there is a one-to-one relationship between the IPSPs in GGN membrane potential and the IG spikes.

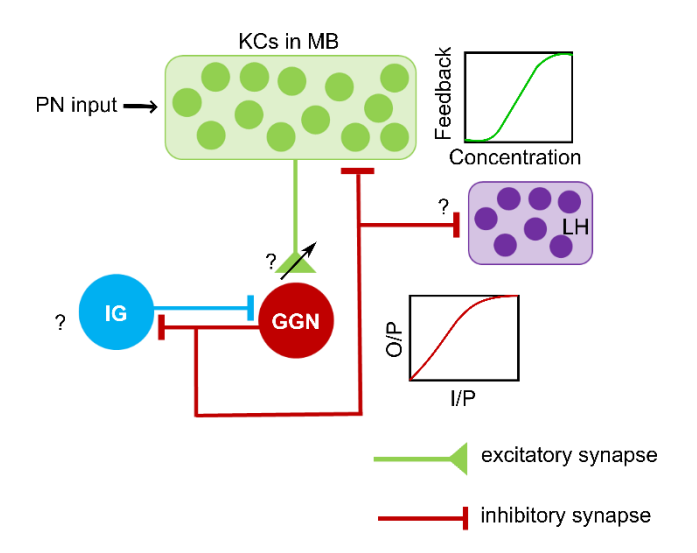


Figure 5.1 Schematic of the KC-GGN-IG olfactory circuit in *S. americana*. Schematic based on published data in *S. americana* (Papadopoulou et al. 2011), showing the known information related to GGN in the olfactory pathway. GGN gets its olfactory input from the KCs in MB and it forms an inhibitory feedback loop with MB. The KC-GGN synapse shows a form of short-term plasticity known as paired-pulse facilitation in response to repeated odor stimulation (arrow at KC-GGN synapse). The neurites of GGN also ramify in the lateral horn but the nature of its innervation is not known. The schematic also shows the inhibitory neuron reciprocally-connected with the GGN, IG (Inhibitor of GGN) whose identity and role in the olfactory circuit are still unexplored. AL antennal lobe; KC: Kenyon cell; LH: lateral horn; MB: mushroom body; PN: projection neuron; I/P: input; O/P: output.

Taking this as the basis, we reasoned that if we could reliably detect the IPSPs from the GGN membrane potential, we could possibly be able to extract the physiological properties of IG, which as of now, has not been identified anatomically. To that end, we recorded intracellularly from GGN and all the unitary IPSPs in the membrane potential of GGN were used to detect the features of IG indirectly (Fig. 5.2 A). All such IPSPs, putatively coming from IG, were detected from the GGN membrane potential and used to construct raster plots and PSTH for IG (Fig. 5.2 B, top two panels). The raster and PSTH of detected IG spikes show that it responds to the odorant hexanol. In order to be sure about the efficacy of our detection method, we also plotted the histogram of inter-spike intervals of IG spikes detected from the GGN membrane potential (Fig. 5.2 B, bottom panel). It showed a Poisson distribution, indicative of the fact that our detection method is reliable.

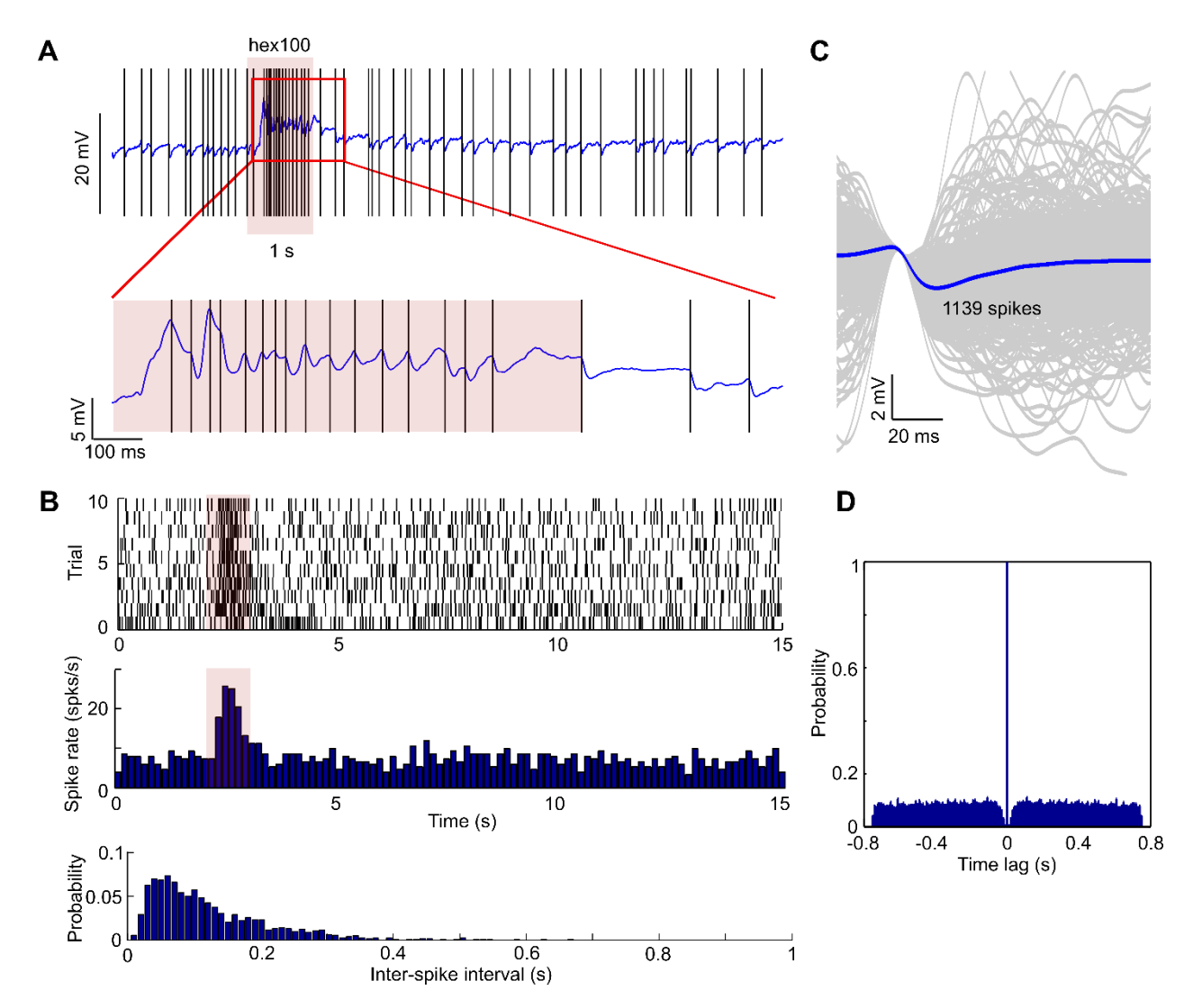


Figure 5.2 Physiological properties of IG can be derived from GGN membrane potential. (A) GGN membrane potential during baseline and odor response is characterized by distinctive IPSPs (indicated by black vertical lines). IG is the source of the IPSPs in GGN membrane potential (Papadopoulou et al. 2011). The IPSPs in the membrane potential of GGN can be used as a surrogate to detect the odor-response properties of IG. Bottom panel shows a magnified image of the GGN membrane potential with IPSPs (indicated by black vertical lines) during odor response. (B) Each IPSP in the membrane potential of GGN is detected to construct a raster plot and PSTH. The bottom panel is a plot of the histogram of inter-spike intervals of IG. It shows a Poisson-like distribution, indicative of reliable IG-spike detection from the GGN membrane potential. (C) Spike-triggered sweeps of 1139 IPSPs in the GGN membrane potential have the same shape and all of them are aligned at the starting point. Blue trace is the mean of the 1139 IPSP events while gray represents the individual events. (D) Auto-correlogram of IG spikes showing refractory period

A spike-triggered average of 1139 IPSPs in the GGN membrane potential align at the initiation point and they have a characteristic IPSP shape (**Fig. 5.2 C**). Autocorrelogram of IG spikes shows the refractory period (**Fig. 5.2 D**).

5.2.3 IG responds to different odorants with odor-specific temporal patterns

We probed the odor-response properties of IG to different odorants. For this, we recorded from GGN in response to different odorants and plotted the IG spikes detected from its' membrane potential as described in the previous section. We found that IG responded to all the odorants tested with an increase in firing rate and it was characterized by odor-specific temporal patterns (**Fig. 5.3 A**). The duration of the response, the intensity of the response and the pattern varied across different odorants but was same across animals (**Fig. 5.3 B**). For example, in response to the odorant hexanol, it responded with two bursts of increase in firing rate while for geraniol, octanoic acid and 2-octanol, it responded with variable intensities of a single burst of firing rate across different animals.

5.2.4 IG is odor-responsive to some odorants even when GGN is not

A surprising observation was made with the odorant geraniol. For this odorant, the GGN did not respond with any visible depolarization of its membrane potential (**Fig. 5.4 A and B**). But in spite of that, we noticed that IG responded to the odorant with increased spike rate. To explore this, we compared the average membrane potential of GGN before odor response and during odor response for a number of odorants (**Fig. 5.5**). We observed that average membrane potential of GGN was more during odor response when compared to the baseline. But for some odorants, geraniol and octanoic acid, the mean membrane potential of GGN was less than the baseline. Next, we plotted the average spike-rate of IG before and during odor response. In contrast to GGN, IG had increased spike-rate to all the tested odorants when compared to the baseline (Wilcoxon signed rank test). So, the likely source

of inhibition that hyperpolarizes GGN is from IG though we cannot rule out other sources of inhibition at this juncture.

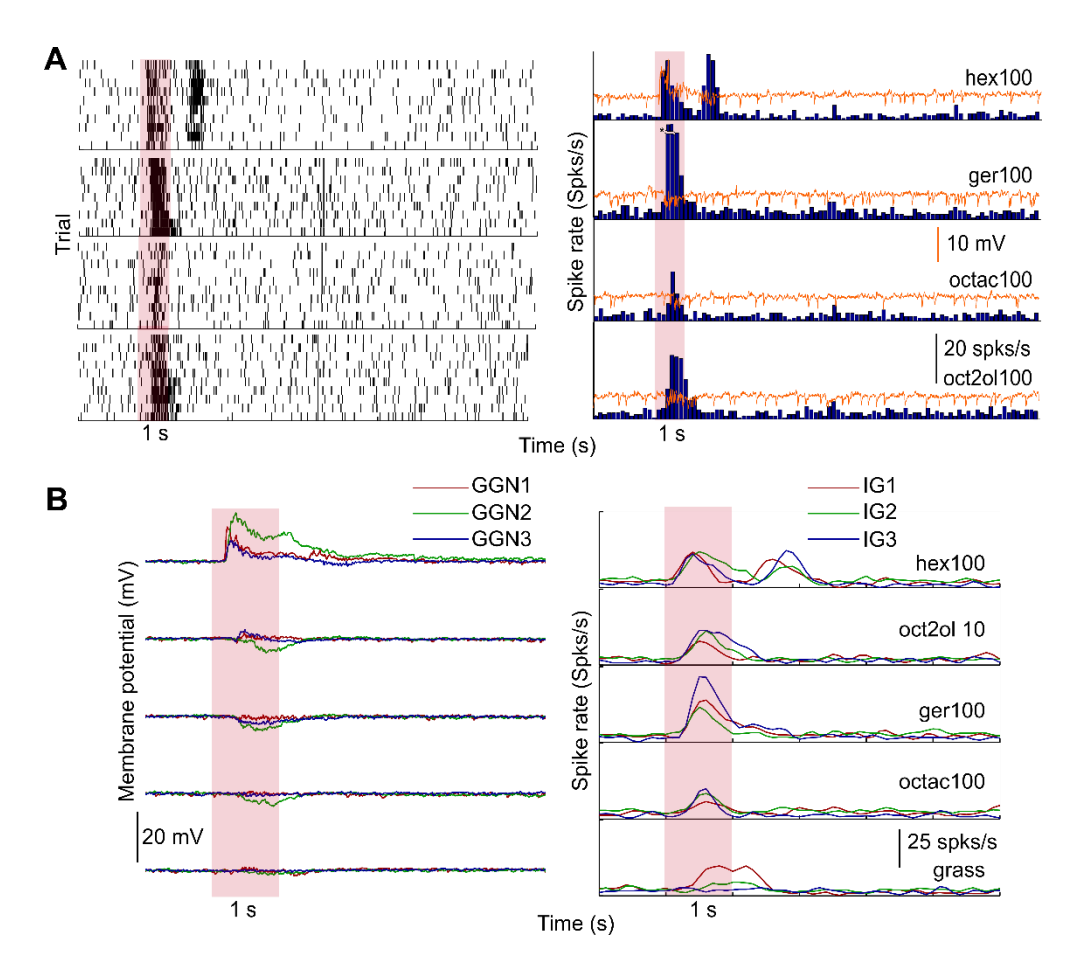


Figure 5.3 IG responds to odorants in an odor-specific way. (A) Raster plots and PSTH constructed from the detectable IPSPs in the membrane potential of GGN (orange trace superimposed on the PSTH) recorded from the same animal shows that IG responds to all the odorants tested. The response consists of an increase in firing rate, the pattern of which differs from odorant to odorant. Asterisk = 45 spikes/s (B) GGN and IG show the same pattern of activity for the same odorant across three different animals.

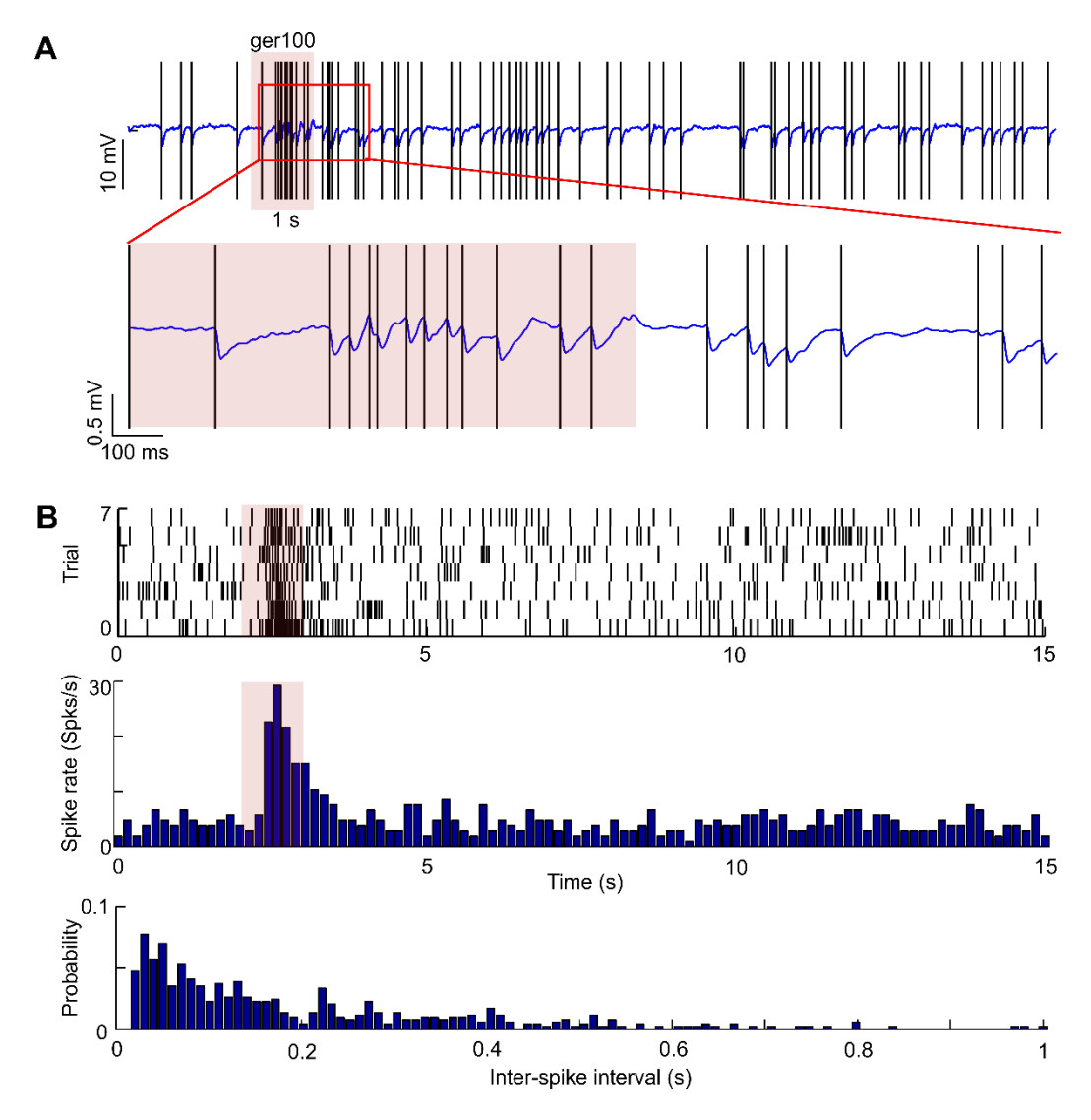


Figure 5.4 IG is strongly responsive to odors even when the GGN is not. (A) The GGN membrane potential is not depolarized in response to the odorant geraniol. Bottom panel shows a magnified view of GGN membrane potential during odor duration. (B) The IG response plotted using the detectable IPSPs (vertical black lines in A) show that IG is strongly responsive to geraniol even though GGN does not show a net depolarization. The bottom panel is the inter-spike interval plot for IG spikes indicating that it follows a Poisson distribution.

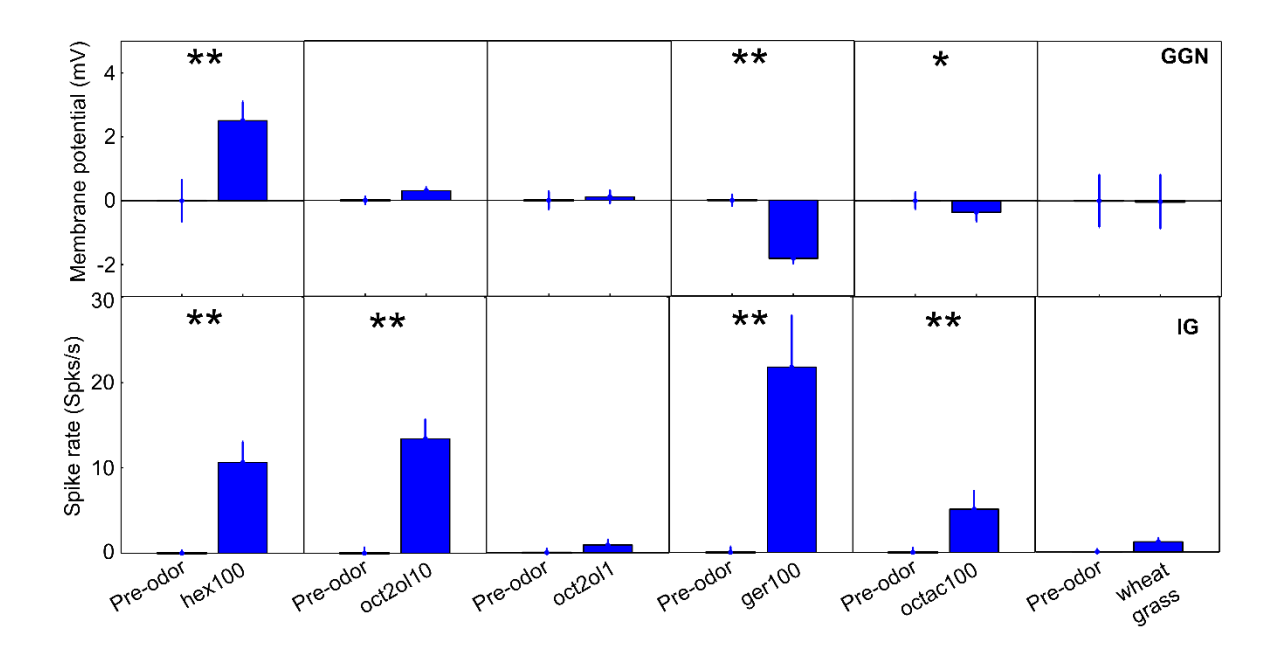


Figure 5.5 GGN and IG respond to various odorants differently. Mean membrane potential of GGN (top panel) goes below the baseline in response to some odorants (ger: geraniol; octac: octanoic acid) while, the spike rate of IG always increases in response to all odorants tested (bottom panel). In all cases, it is mean \pm SEM (Wilcoxon signed rank test).

5.2.5 IG receives odor input from KCs

The fact that IG responded to odor stimuli with increase in firing rate even when GGN was inhibited (**Fig. 5.4 and 5.5**) points to the fact that IG is receiving odor input from a source other than GGN. In order to investigate the source of odor input to the IG other than GGN, we electrically stimulated the immediate upstream source of odor input to GGN, the KCs in MB. In an intracellular recording session from the GGN, the odor input was presented first and after five seconds, the KCs in the MB were electrically stimulated with an electrical pulse of 15 µA strength TTL triggered for 4 ms. We observed EPSP-like depolarization of the GGN membrane potential, consistent with the successful stimulation of the MB KCs (**Fig. 5.6 A**). Superposed on this depolarization, a large barrage of IPSPs could be seen. The IPSPs in the GGN membrane potential, indicative of IG spiking, were detected and plotted as rasters and PSTH as before (**Fig. 5.6 B**). We noticed that in response to electrically

stimulated MB KCs, there was an increase in spiking activity of the IG, similar to when the odor stimuli were presented. This is consistent with a circuit in which IG receives odor input downstream of MB KCs.

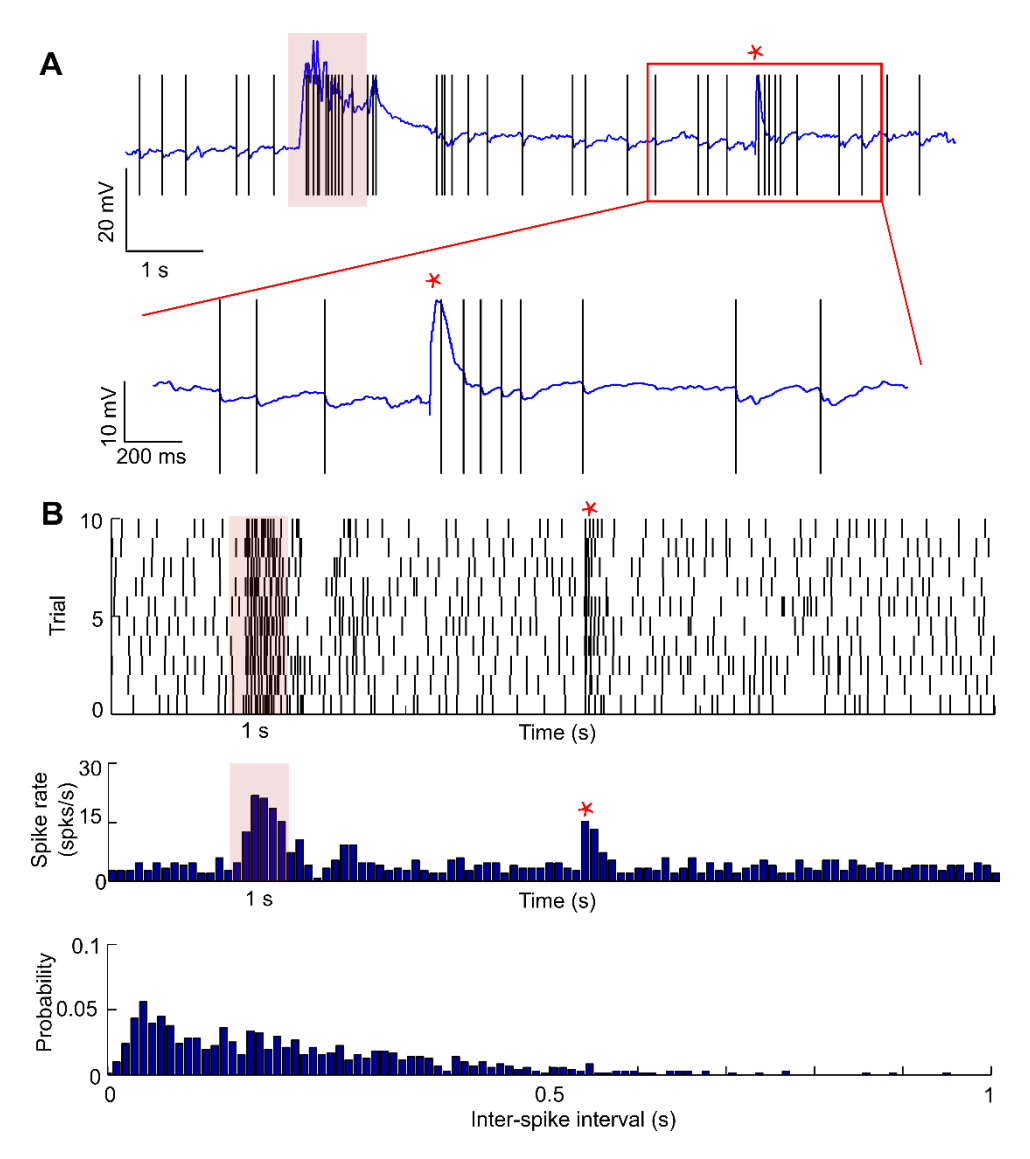


Figure 5.6 IG gets its odor-input downstream of Kenyon cells. (A) Top panel shows the membrane potential recorded from the GGN with odor stimulation period indicated in pink. The response in GGN due to electrical stimulation of KCs (red star) is magnified and shown below. Electrical stimulation of the KCs (red star) causes large summed EPSP in GGN and increased spiking activity of the IG riding on top of it. (B) The IPSPs detected in the GGN membrane potential are plotted as rasters and PSTH of the IG response. IG exhibits increase in firing rate in response to odor as well as when KCs in MB were electrically stimulated (red star). The ISIs for detected IG spikes show a Poisson distribution (bottom panel), consistent with reliable detection of IG spikes from GGN membrane potential.

Since both GGN and IG receive olfactory input downstream of MB KCs, we should be able to see depolarization in the GGN membrane potential before the excitatory input from MB KCs causes spikes in IG. And after the IG spikes, we should observe an IPSP in GGN membrane potential in response to the inhibitory input from IG. We used the IG spike as the trigger point and plotted the STA for three different animals (**Fig. 5.7 A**). We see a depolarizing component in the GGN membrane potential just before the IG spikes (arrows), representing the excitatory input from MB KCs to GGN. And after the IG spike, we observe an IPSP in the GGN membrane potential representing the inhibitory input of IG to the GGN (**Fig. 5.7 A**). The EPSP in the IPSP-triggered GGN membrane potential precedes the IG IPSP. This is consistent with the circuit. Mean of the GGN membrane potential calculated for a time window of 10 ms during baseline, before the IG spikes and after the IG spikes reveals that the depolarization of GGN membrane potential before IG spike and hyperpolarization after it is significant when compared to the baseline GGN membrane potential (p = 0 for animals 1 and 2, $p = 6.1126e^{-22} \approx 0$ for animal 3; one-way ANOVA) (**Fig. 5.7 B**).

5.2.6 Concentration-dependent odor-response properties of IG

GGN in *S. americana* is reported to show odor concentration-dependent increase in response strength (Papadopoulou et al. 2011). When we tested the same in *H. banian*, we also observed concentration-dependent increase in strength of the GGN odor-response (**Fig. 5.8 Ai**). This kind of concentration-dependent increase in odor response can also be seen in the LFP recorded from the MB and the oscillatory power calculated from the LFP (**Fig. 5.8 Aii**). Odor-response of IG also shows a concentration-dependent increase in its spike-rate (**Fig. 5.8 Aiii**). However, there is an interesting difference between the concentration-dependent odor-induced activities of GGN and IG at lower concentrations (**Fig. 5.8 B**).

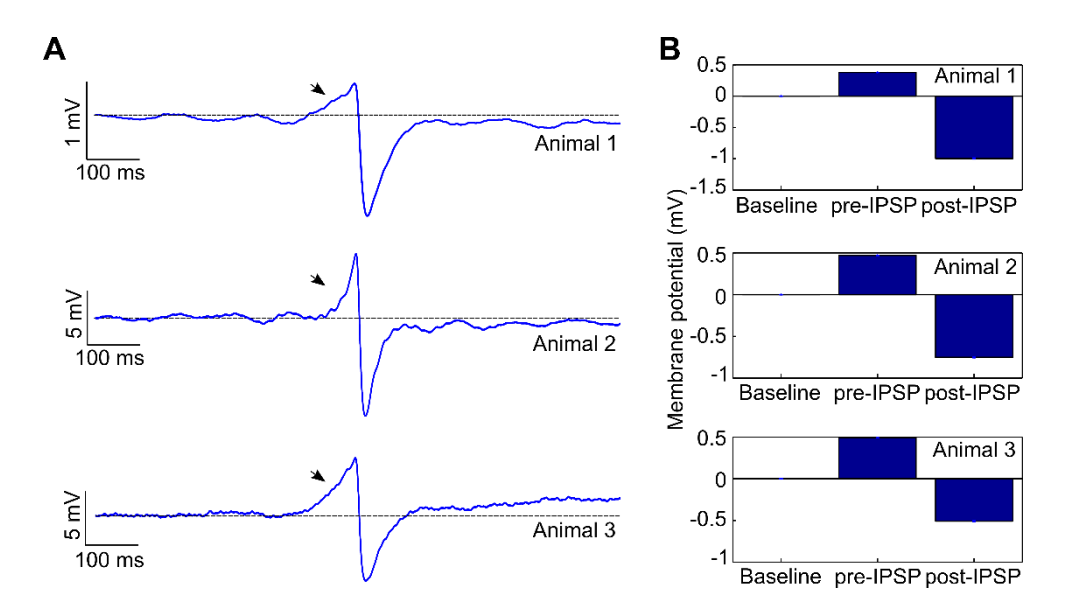


Figure 5.7 GGN and IG receive input downstream of KCs. (A) Spike-triggered average from the IG spikes in GGN membrane potential (from three different animals) shows that there is an excitatory input from MB KCs coming into GGN (arrows) just before the IG spikes. After the spiking of IG, an IPSP is observed in the GGN membrane potential, indicating the inhibitory input which GGN gets from IG. This is consistent with the fact that both GGN and IG are downstream of KCs. (B) Bar graphs comparing the mean GGN membrane potential at baseline, pre-IPSP and post-IPSP (10 ms time window for each) reveals that the depolarization of GGN membrane potential before IG spike and hyperpolarization after it is significant when compared to the baseline GGN membrane potential (p = 0 for top and middle panels, p = $6.1126e^{-22} \approx 0$ for bottom panel; one-way ANOVA). All bar graphs are mean \pm SEM.

At lower concentration of odorant, the odor-response onset in GGN is delayed by up to 1000 ms in some cases (**Fig. 5.8 Ai and B, middle panel**). This delay in odor-response onset at lower concentration of odor stimuli is not observed in IG firing rate (**Fig. 5.8 Aiii and B, third panel**). Data from five animals for three different concentrations of odorants shows that this is a consistent and significant feature of GGN response to odors at lower concentrations (**Fig. 5.8 B**). It also shows that GGN is inhibited below the baseline at lower concentration of odor stimuli (n=5, p=0.0652, Kruskal-Wallis test; **Fig. 5.8 B, first panel**). The delay in onset of GGN odor-response at low concentration of odor stimuli (n=5, p=0.0108, Kruskal-Wallis test) is consistent with inhibition from IG spikes which do not

show a decrease at lower concentration of odor (n=5, p=0.0919, Kruskal-Wallis test) (**Fig. 5.8 B**). The delay was calculated by taking the intercept of odor-response onset with the baseline (**Fig. 5.8 C**).

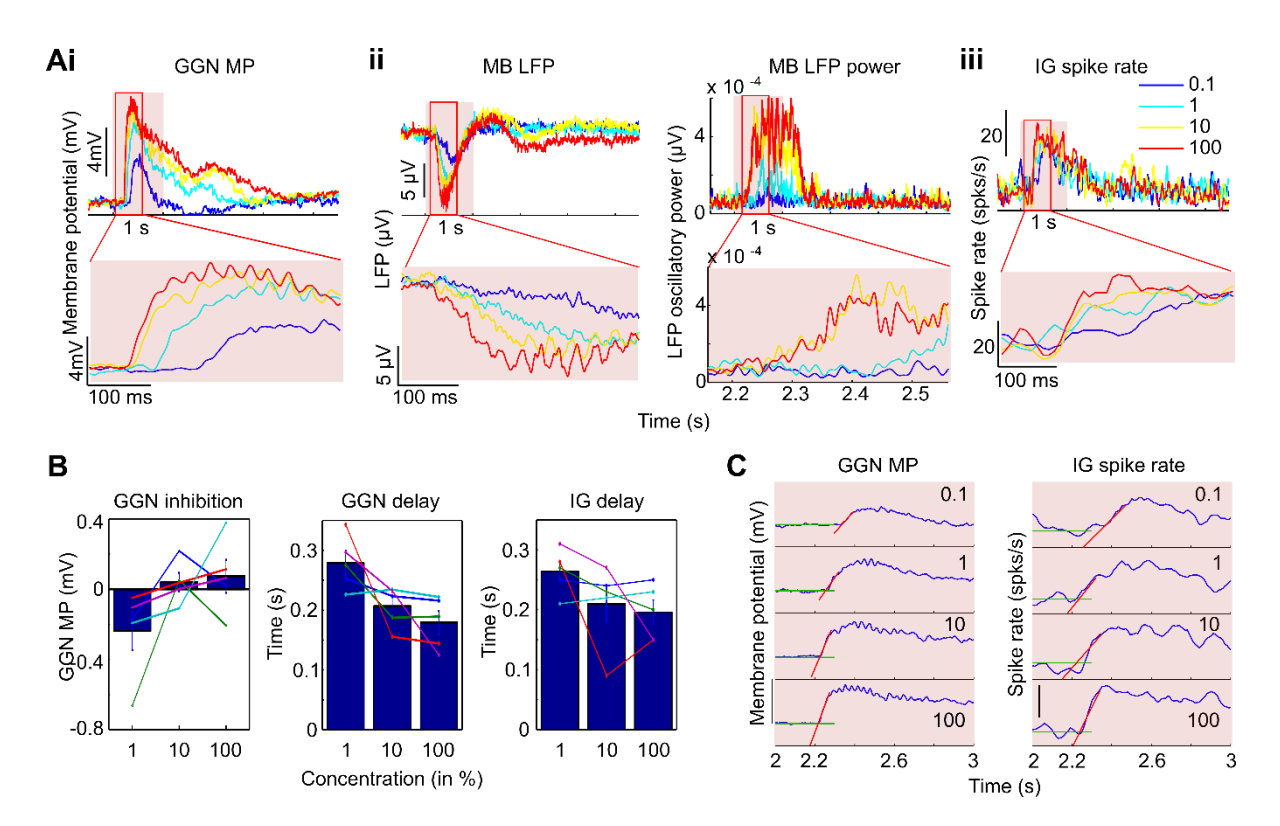


Figure 5.8 GGN responds to lower concentration of odorant with a delay. (Ai) GGN shows a concentration-dependent increase in its odor-response. At lower concentrations, the odor response of GGN starts after with a delay of ~1000 ms. (Aii) Odor concentrationdependent increase is also seen in the LFP response recorded from the MB calyx and the strength of the oscillatory power calculated from the MB LFP. (Aiii) IG also shows a concentration-dependent increase in its odor-response. Bottom panel is the magnified portion of the top panel. (B) Histogram of GGN membrane potential shows that it is inhibited below the baseline at lower concentrations (n=5, p=0.0652, Kruskal-Wallis test). Here, mean of the GGN membrane potential 100 ms before the intercept was compared with mean of the membrane potential 100 ms during the odor onset. The delay in odor-response onset for lower concentrations of odor stimuli is significantly more for GGN (middle panel; n=5, p=0.0108, Kruskal-Wallis test) than the same in IG (right panel; n=5, p=0.0919, Kruskal-Wallis test). This is consistent across five different animals. (C) Intercepts of GGN membrane potential and IG spike-rate to calculate the delay in odor-response onset at lower concentrations. Intercepts of GGN are at 2.3271, 2.2451, 2.2201 and 2.2133 s from top to bottom. Scale bars: 10 mV, 20 spks/s

5.2.7 Where is the delay in odor-response onset at lower concentrations in GGN originating?

Next, we wanted to find out if the delay in odor-response onset which we observed in the GGN response to odorants at lower concentrations was also exhibited by other neurons of the olfactory pathway. To investigate this, we recorded the population odor response of the first-order ORNs from the antenna of the animal, simultaneously recording intracellularly from different neurons of the olfactory pathway—PN, LHN, bLN and GGN (Fig. 5.9 A, B, C and D). The EAG (which represents the summed population odor response of the ORNs) in each of these cases shows no delay in odor-response onset at any of the concentrations which we tested (Fig. 5.9 A, B, C and D, top panels). The same is true for LHN and PN (Fig. 5.9 A and B, bottom panel). But in the case of bLN and GGN, we observe that at lower concentrations of the odorant, the odor-response in both these neurons starts after a delay (Fig. 5.9 C and D, bottom panels). This delay in odor-response onset may thus be generated as threshold in KCs or downstream of it, as the upstream neurons do not show this feature at lower concentrations.

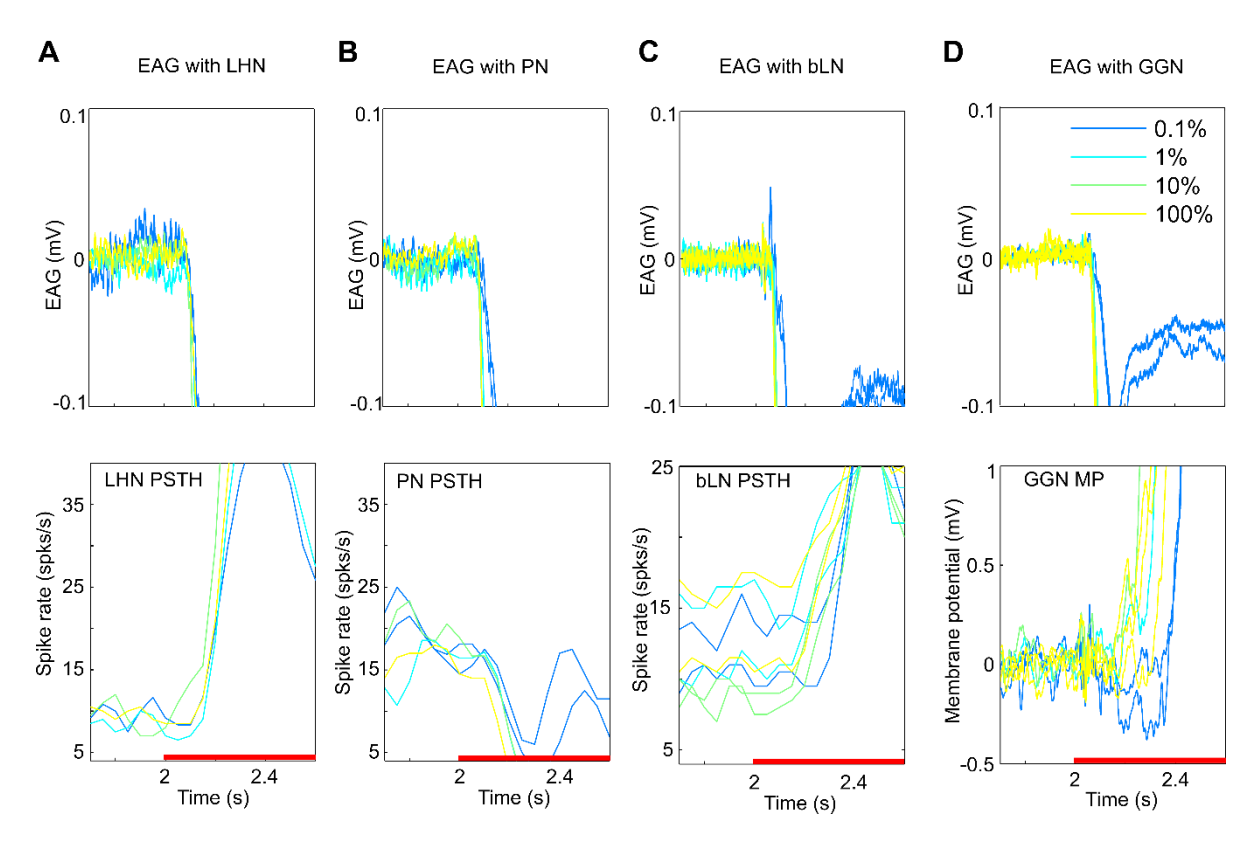


Figure 5.9 Delay in the onset of odor response is observed downstream of mushroom body Kenyon cells. Paired EAG recordings (top panel) with intracellular recording (bottom panel) from the PN (A), LHN (B), bLN (C) and GGN (D). There is no delay in the odorresponse onset of ORN population response represented by the EAG at lower concentrations of odor stimuli in any of the preparations. Delay in onset of odor response at lower concentration is not visible for PN and LHN as well. But bLN and GGN, both downstream of KCs exhibit delay in odor-response onset at lower concentrations of odor stimuli. Red bars: odor pulse; MP: membrane potential

5.2.8 KC-IG synapse shows short term plasticity similar to KC-GGN synapse

The synapse between KC and GGN exhibits a form of short-term plasticity known as paired-pulse facilitation (PPF) in *S. americana* (Papadopoulou 2010). We tested for the same in *H. banian*. When the MB KCs were electrically stimulated by two pulses separated by inter-pulse intervals ranging from 10 to 1000 ms, the depolarizing response of the GGN recorded intracellularly was enhanced for the second pulse in a delay-dependent manner (**Fig. 5.10 A**). Thus, the KC-GGN synapse in *H. banian* also undergoes PPF.

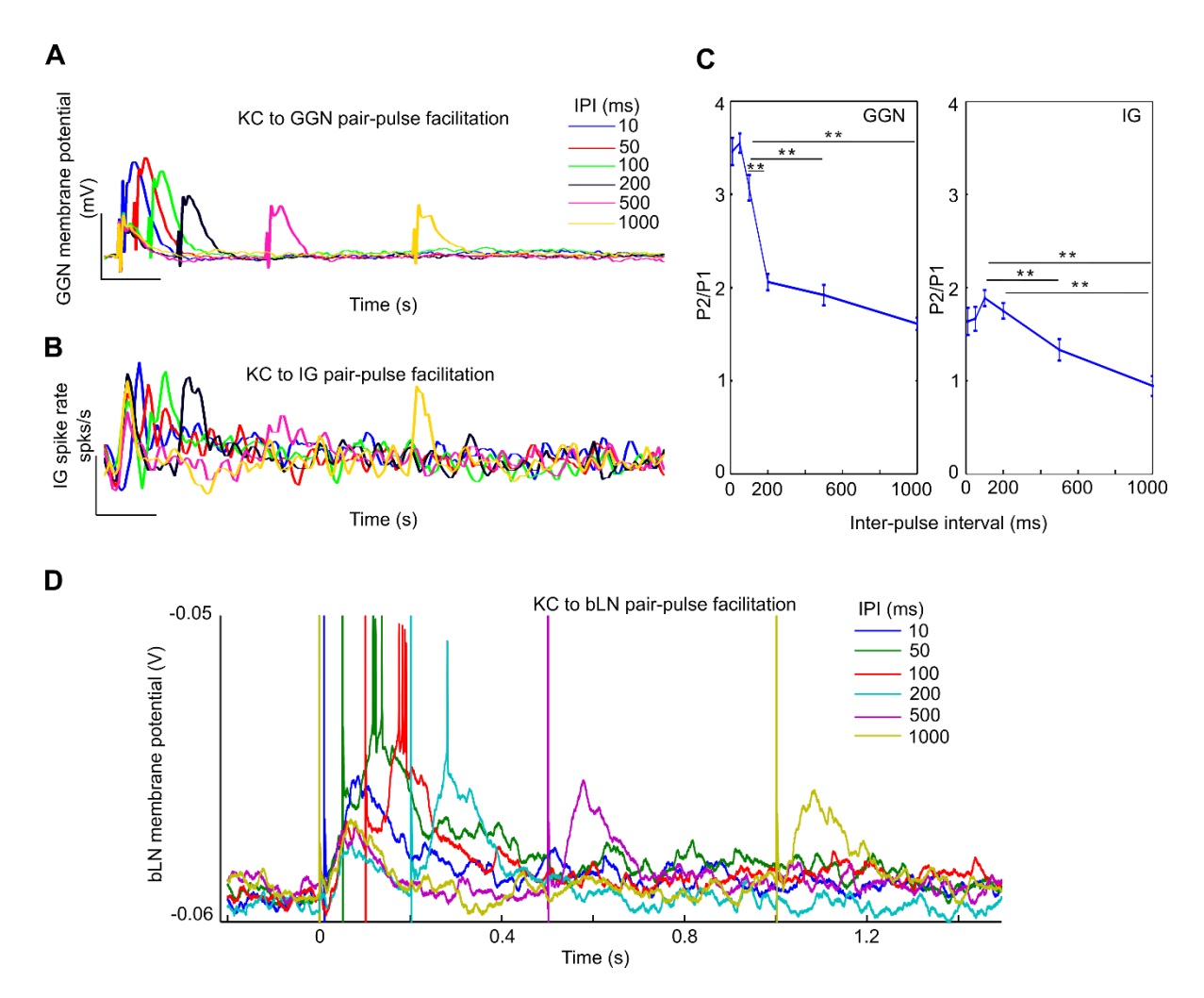


Figure 5.10 KC-IG and KC-bLN synapses show paired-pulse facilitation similar to KC-GGN synapse. (A) The stimulation of KCs in MB with two electrical pulses separated by an inter-pulse interval (IPI) less than 1 s results in the GGN response to show facilitation in response to the second pulse (paired-pulse facilitation). This was tested for different delays between the two pulses, all of which caused facilitation of GGN response. Scale bars: 10 mV, 250 ms (B) The IG spikes detected from the GGN membrane potential during paired-pulse electrical stimulation of MB KCs also show facilitation for different IPIs (less than 1 s). Scale bars: 20 spks/s, 250 ms (C) Ratio of the amplitude of the GGN EPSP for the different IPIs (P2/P1) shows that the increase in the strength of the EPSP for the second pulse is significant (N=18, one-way ANOVA, p=3.45563*10⁻²⁸). Post hoc test reveals that facilitation from the PP ratio decays from 3.5 to 1 in ~1 s. The ratio of the change in IG spike-rate in response to the paired-pulse stimulation of MB KCs is also significantly more for the second pulse when compared to the first (N=18, one-way ANOVA, p=2.53052*10⁻¹ ⁰⁷). Post hoc test shows facilitation of the paired-pulse ratio decays from 1.9 to 1 in \sim 1 s. (**D**) bLN, another neuron downstream of KCs, also shows paired-pulse facilitation in response to electrical stimulation of MB KCs by two pulses with an IPI less than 1 s.

We also tested whether the KC-IG pair exhibits a similar kind of plasticity. Since we did not have access to the subthreshold activity of IG, we tested if the spike-rate of IG undergoes facilitation. We observed a similar pattern of PPF at KC-IG synapse as well (Fig. 5.10 B). The paired-pulse (PP) ratio (change in response amplitude between subsequent and previous pulse, P2/P1) calculated for both KC-GGN and KC-IG synapse and plotted with respect to the inter-pulse interval shows characteristic trend of classical PPF (Fig. 5.10 C) (Jackman and Regehr 2017). The calculated PP ratio for KC-IG pair does not directly correspond to synaptic facilitation because of the non-linearities present in the change from membrane potential to spike-rate. Still, it is a qualitative indicator of the plasticity of KC-IG transfer function. Statistical analysis of the PP ratio reveals that the facilitation observed is significant in both the cases (for GGN: N=18, one-way ANOVA, p=3.45563*10⁻²⁸; for IG: N=18, one-way ANOVA, p=2.53052*10⁻⁰⁷) (Fig. 5.10 C). Post hoc test reveals that facilitation from the PP ratio decays from 3.5 to 1 in ~1 s in the case of GGN while in the case of IG, the decay is from 1.9 to 1 in ~1 s (Fig. 5.10 C).

Additionally, we explored whether this form of plasticity could be a common feature of all neurons downstream of KCs. For this, we carried out the same experiment for bLNs and we found that KC-bLN synapse also exhibits PPF (**Fig. 5.10 D**). Since all these neurons are downstream of KCs, the mechanism governing the facilitation process may be presynaptic in nature.

5.2.9 Nature of GGN innervation in the LH

We also wanted to explore the connectivity of GGN in LH, the second area where it has arborization. This was not investigated in *S. americana* (Papadopoulou et al. 2011) but the possibility has been mentioned in a computational modelling chapter by Komarov et al. (2017). To this end, we recorded intracellularly from the LH neurons (n=11) and observed

its response both to odor stimuli and to electrical stimulation of MB KCs (**Fig. 5.11 A**). The odor response of LHNs was inhibited by the electrical stimulation of the MB KCs. There are three types of neurons which have innervation in the LH—GGN, AL PNs and bLN type 1. Of these, only GGN is inhibitory and has arborization in the LH (Papadopoulou et al. 2011). This would imply that if we electrically stimulated KCs while recording from LH neurons and saw inhibition of LHNs, then it is likely that GGN is the source of inhibition of LHNs.

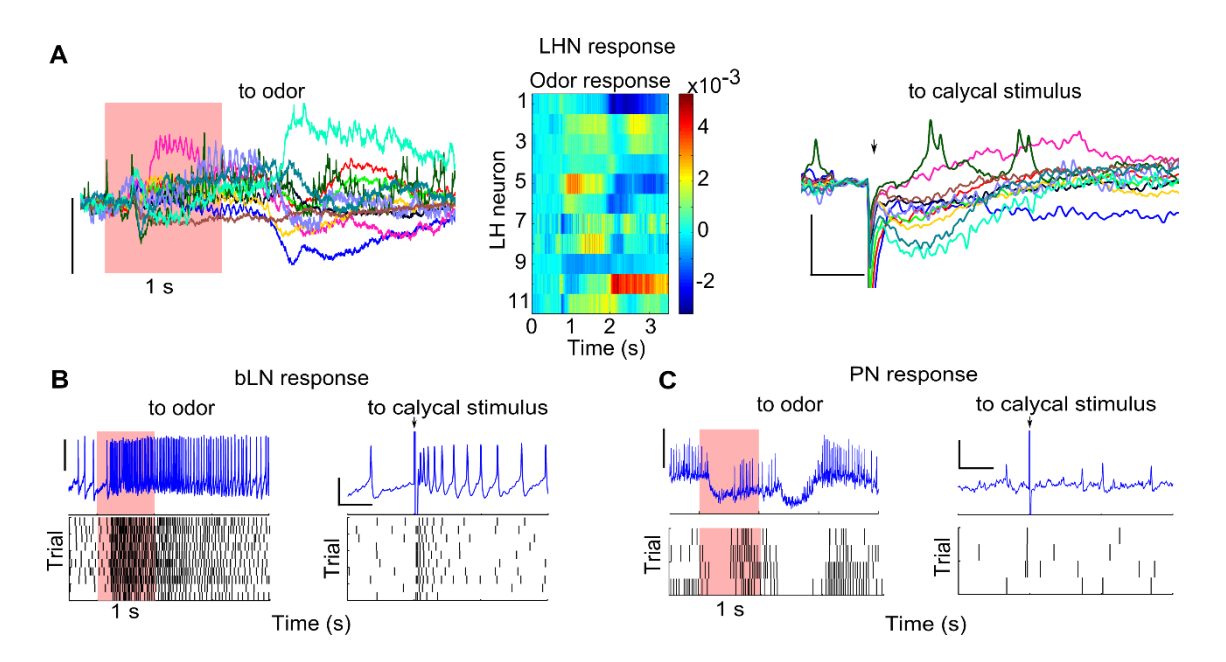


Figure 5.11 Odor-responsive LH neurons are inhibited when MB KCs are electrically stimulated. (A) LHNs (N=11) recorded from the same animal show that they respond to the same odorant (hexanol) with a variety of patterns (left panel). The odor response of the 11 LHNs is represented as a heat map in the middle panel. The odor-induced spiking activity of the same 11 LHNs is inhibited when KCs in MB are electrically stimulated (right panel). Scale bars: 4 mV, 2 mV, 50 ms (B) A putative bLN recorded in the same preparation, responds to odor stimulus (right panel). It also shows increased spiking activity in response to electrical stimulation of the MB KCs (left panel). Scale bar: 10 mV (both panels) (C) A putative PN recorded from the AL in the same animal, responds to odor stimulus (right panel). When the MB is electrically stimulated, it shows no change in baseline activity (left panel). Scale bar: 5 mV (both panels); 100 ms

To test this, we recorded from a set of LH neurons and electrically stimulated the KCs. The neurons recorded were tested for characteristic excitatory response to odor (Fig.

5.11 A, left and middle panels). When KCs were electrically stimulated, most of the neurons recorded from the LH showed hyperpolarization (**Fig. 5.11 A, right panel**).

To test that the electrical stimulation was reliably activating KCs, we recorded from bLN (neuron downstream of KCs) in the same preparation and it responded both to odor and calycal stimulation with increased firing rate (Fig. 5.11 B). To make sure that our calycal stimulation was not activating PNs (neurons upstream of KCs, which give input to the LHNs), we recorded from PN intracellularly and observed that there were no antidromic spikes generated in it (Fig. 5.11 C). This is consistent with the fact that bLN is downstream of MB KCs and our electrical stimulus is successful in causing response only in downstream neurons, and not the upstream neurons, thereby eliminating the possibility of the LHNs getting any input from the PNs. This, in turn, implies that the inhibition of LHNs in response to electrically stimulated MB KCs, could be due to downstream neurons of MB KCs, likely GGN.

5.2.10 Role of neural circuitry involving KC-GGN-IG in processing of odor information

We show that IG responds to odor stimuli and the synapse between KC-IG shows pairedpulse facilitation similar to that between KC-GGN. In addition, GGN may possibly play a
role in inhibiting LHNs. The GGN-IG microcircuit likely acts to fine tune the gain-control
function of GGN in the MB circuitry (Fig. 5.12 A). GGN is inhibited by the IG at lower
concentrations of odorant, delaying the onset of its odor response This in turn allows the
MB KCs to be more sensitive to the weak input of odor stimuli since the feedback inhibition
from GGN is delayed. At higher concentrations of odorants, as the odor response of the
GGN kicks in, it inhibits the IG and decreases its reciprocal inhibition onto GGN. This
results in the inhibitory feedback from the GGN providing global inhibition to MB KCs
without a delay, thus controlling the output gain of the circuit. The existence of short-term

plasticity in the circuit at both the KC-GGN synapse and the KC-IG synapse may enable the system to dynamically change the sensitivity of the system (MB KCs) at both lower and higher concentrations of the odor stimuli to allow it to operate over a range of concentrations. We propose that the KC-GGN-IG circuit and associated plasticity behaves as an *input-dependent* adaptive gain control system (**Fig. 5.12 A and B**).

We reconstructed the GGN-IG circuitry associated with the MB KCs by incorporating all the known information about the circuitry (from *S. americana*) and the new observations in *H. banian* (**Fig. 5.12 A and B**).

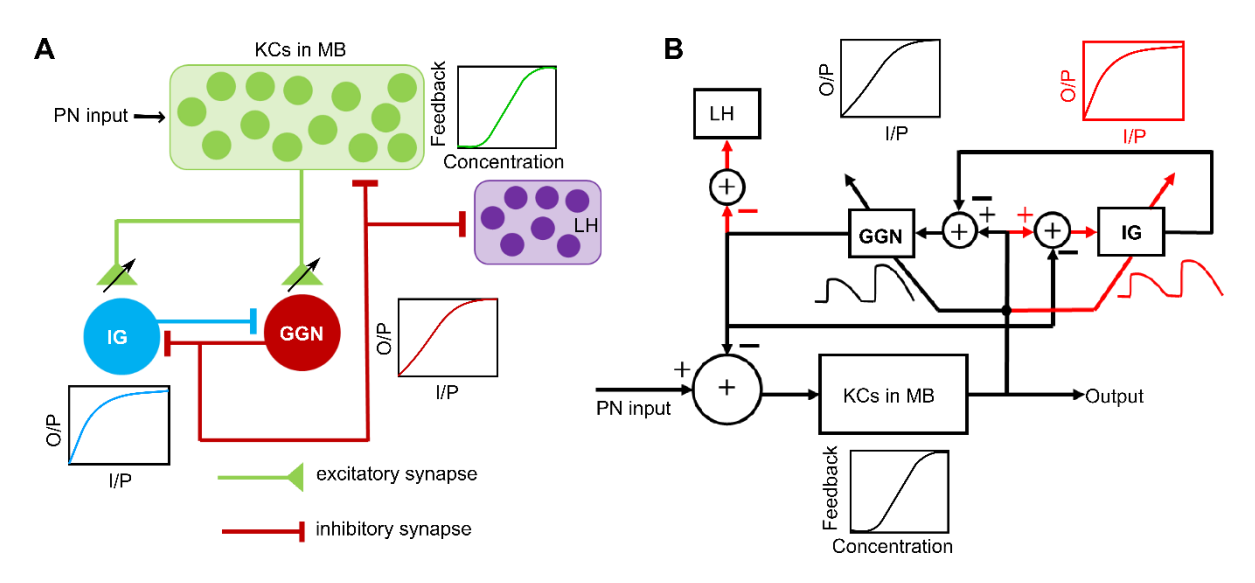


Figure 5.12 Schematic of the KC-GGN-IG circuitry incorporating all the features discovered in this study. (**A**) Neural circuit schematic of the KC-GGN-IG circuit in *H. banian*. IG receives its odor input from the KCs in MB. Both KC-GGN and KC-IG synapses show paired-pulse facilitation and GGN is the likely source of inhibitory input to LHNs (**B**) Block schematic of the KC-GGN-IG circuit. The sections in black represent the information known from the study in *Schistocerca* while those in red are the new data from the present study in *H. banian*. LH: lateral horn; KC: Kenyon cell; GGN: giant GABAergic neuron; IG: Inhibitor of GGN; MB: mushroom body; PN: projection neuron in antennal lobe; I/P: input; O/P: output

5.3 Discussion

KC-GGN-IG circuit was first described in the locust *S. americana* (Papadopoulou 2010; Papadopoulou et al. 2011; **Fig. 5.1 A**) and recently explored by Ray et al. (2020). In one of the experiments described, GGN membrane potential always showed a delayed IPSP after the KC was stimulated (Papadopoulou 2010). The source of this inhibition was found to be another inhibitory neuron which was serendipitously chanced upon while doing paired intracellular recordings from GGN. The set of paired recordings from GGN and IG showed that IG is a spiking neuron and that the two are reciprocally connected, inhibiting each other. It was also reported that IG received input from KC (Papadopoulou 2010; Ray et al. 2020). But the role of IG in the network remains unclear. With an aim to explore this gap in the KC-GGN-IG circuit, we investigated the same in our species, *H. banian*, in which we have established the presence of a similar GGN (chapter 3).

The major findings of this part of the study are as follows:

- 1. IG odor-response pattern can be derived from the membrane potential of GGN.
- 2. IG responds to odorants and this response is concentration dependent and can have a net hyperpolarizing influence on GGN membrane potential under certain stimulus conditions.
- 3. IG, like GGN, gets its odor input from the olfactory pathway via KCs.
- 4. KC-IG and KC-bLN synapses shows paired-pulse facilitation similar to KC-GGN synapse.
- 5. GGN can be the likely source of inhibition for lateral horn neurons.
- 6. Inhibition of GGN by IG can hyperpolarize GGN at lower concentration, consistent with decreasing the negative feedback to the MB calyx, to enhance the detection of weak odor stimuli by MB KCs.
- 7. PPF makes this negative feedback circuit an *input-dependent* adaptive gain control circuit.

5.3.1 The odor-response properties of the IG

The IG was reported for the first time as an inhibitory neuron inhibiting GGN in *S. americana*. As there was no successful morphological fill, the identity of IG remains elusive. But it was reported that this neuron has neurites in the beta lobe (Papadopoulou 2010) and GGN-IG have monosynaptic connection between them. In addition, the authors also mentioned that all the IPSPs observed in the GGN membrane potential could be accounted for as the inhibitory input coming from the IG.

Keeping all this information about IG and GGN-IG connection in mind, we struck upon an idea that we could possibly get information about IG from the GGN membrane potential even without getting the actual IG in the picture. The odor-response properties of IG in *H. banian* which we discovered by using a novel method are consistent with those reported for the IG in *Schistocerca*. IG in *H. banian* also exhibits spontaneous firing at baseline and responds to odors (**Fig. 5.2**, **5.3**; (Papadopoulou et al. 2011)). We have now shown that IG responds to all odorants tested in an odor-specific manner with different patterns of activities (**Fig. 5.3**). Given the conserved architecture and morphology of the olfactory circuit at higher centers, it would be our prediction that this would be true in *Schistocerca* as well.

As mentioned in the result section 5.2.4, IG shows odor response to some odorants even when the GGN is not depolarized in response to the odorant (**Fig. 5.4**). The mean membrane potential of GGN showed hyperpolarization in response to some odorants to which the IG displayed an increased firing rate (**Fig. 5.5**). This observation led us to explore and make the finding that the IG in *H. banian* receives odor-input from its immediate upstream center, the MB (**Fig. 5.6**). The same was reported in a different manner in *S. americana*. Here, the excitatory EPSP in the GGN membrane potential in response to

electrical stimulation of a KC was not a pure EPSP, rather it was followed by delayed inhibition. This observation of delayed inhibition was taken to be coming from the KC input to another inhibitory neuron, in this case IG (Papadopoulou 2010). Our data is also supported by a recent study in which a computational model with all KCs-to-IG connection reliably reproduces the odor-elicited spiking pattern in the IG (Ray et al. 2020).

We predicted that if IG is receiving input from KCs, then it should be reflected in the spike triggered average of the GGN membrane potential. And that's what we observed when triggered average of GGN membrane potential was computed from the IG spike. We detected depolarization of the GGN membrane potential just before the IG spike, indicating that the excitatory input from the KCs excites both GGN and IG, prior to the inhibition of the GGN by the IG (Fig. 5.7). When we went back and checked if this feature (the depolarizing input before the IG spikes) was present in the published figure of STA of GGN membrane potential in *S. americana*, we found the same feature though there was no mention of this observation in the study (Papadopoulou et al. 2011).

Testing the response of GGN and IG to increasing concentration gradient of odors showed that the magnitude of their response increased correspondingly (Fig. 5.8). We also observed that the GGN response at lower concentration was marked by a significant delay which was not seen in the IG odor response. This delay was seen only in neurons downstream of KCs and not upstream (Fig. 5.9). This concentration-dependent delay was absent from EAG recordings from antenna and PN membrane potential. All these point to the fact that the delay in odor response at lower concentrations may be due to KCs properties.

The synapse between KC-GGN shows paired-pulse facilitation. When KCs were stimulated by two electrical pulses with an inter-pulse interval of less than 1 s, the amplitude

of the depolarization recorded from the GGN in response to the second pulse was more than the first (Papadopoulou 2010). PPF is one form of short-term plasticity which occurs when a pair of inputs with an inter-pulse interval (IPI) of less than a second from the presynaptic neuron depolarize the postsynaptic neuron. The postsynaptic neuron responds to the second pulse with an increase in amplitude when compared to the first. In S. americana, the PPF ratio is highest at IPIs of 50 and 250 ms with a dip in between (Papadopoulou 2010). The author explained this as being ecologically significant since 250 ms is within the range at which KCs fire two spikes (Perez-Orive et al. 2002). The author hypothesized that this form of plasticity could play a role in lateral inhibition of KCs, by amplifying the effect of the second pulse on GGN's inhibitory output which would result in KCs being inhibited. It was also hypothesized that PPF helped the GGN to overcome the inhibition from IG and amplify its overall effect on MB KCs, during odor response. In our experiments, we found that both KC-GGN synapse and KC-IG synapse undergo PPF with a single peak as in a classical PPF-IPI plot (Jackman and Regehr 2017) (Fig. 5.10 A, B and C). Our data shows that maximum facilitation at the KC-GGN synapse occurs when the IPI is 50 ms and we also observed that there is no peak at 200 ms. We are not sure why this difference exists between these reports. Thus, the explanation that facilitation at KC-GGN synapse follows the KC firing probability for odor stimuli, resulting in inhibition of KCs needs to be tested by other means. Facilitation was also observed at the KC-bLN synapse (Fig. 5.10 D). Thus, we see that all the synapses showing facilitation are downstream of KCs, therefore the mechanism underlying PPF is probably at the presynaptic level.

The IG has high baseline rate, both in *S. americana* and *H. banian*. According to Papadopoulou (2010), it is probably due to IG receiving input from all KCs. On the contrary, Ray et al. (2020), proposed that the ~zero baseline rate of KCs cannot account for the high baseline spontaneous firing rate of the IG. Their experiment of removing both the

antennae was also unable to silence the IG at rest. They proposed that the source of spontaneous firing of IG might be either intrinsic or neurons other than PNs or KCs.

We have thus been able to deduce the odor-response properties of IG without having to be dependent on the identification of IG morphologically. Discovering the IG would definitely add to our understanding of microcircuits.

As described in the introduction to this thesis, GGN-like feedback neurons have been reported in other species like *Drosophila* (Anterior Paired Lateral neuron, APL), *P. americana* (Calycal giants, CGs) and *A. mellifera*. But none of them have reported an IG-like neuron. The physiological recordings which are reported in the literature also, do not mention the characteristic IPSP in the GGN-like neurons in these other species. Therefore, the GGN-IG circuit seems to be a microcircuit unique to the grasshopper family.

5.3.2 Role of IG in the circuit

After establishing the odor-response properties of the IG, we tried to investigate its role in the recurrent inhibitory network formed by it. Recurrent networks constitute a ubiquitous architectural motif in cortical organization and so, not surprisingly, have been shown to play a role in various functions like, short-term memory, modulation of neuronal excitability with attention and generation of spontaneous activity during sleep (Shu et al. 2003 and references therein). The flip-flop mechanisms of these networks can generate numerous states of activity, a basic feature of cortical networks (both locally and long-distant). They can give rise to a network 'on-off' scenario which can be put into action by fluctuating synaptic inputs coming in (Shu et al. 2003).

Results from our study definitely point in this direction; we can say that the IG acts like a switch for the GGN in the olfactory circuit. The KC-GGN-IG network self-tunes itself

to respond to odors at different concentration levels. At lower concentrations, the IG inhibits the GGN such that the feedback inhibition of GGN on MB KCs is delayed and the KCs become more sensitive to the lower concentrations of the odorant. At higher concentrations, the GGN becomes more active than the IG and inhibits IG. As a result, the feedback inhibition by the GGN on to the MB KCs is enhanced and the KCs respond to the odorant at a firing rate presumably optimal in some way for the system. One would imagine that a nonlinearity in the GGN response function could achieve the role that we attribute to the IG, namely suppressing GGN inhibitory feedback to KC during weak drive from KC. But this is not so and this role is played by IG. Thus, it is still unclear as to why this function should be mediated by another neuron (IG) in the circuit.

The ability to show PPF at the KC-GGN synapse in this context is consistent with the above explanation. If the KCs start getting activated more, then the negative feedback via GGN should increase and PPF at KC-GGN synapse enables this. However, PPF at KC-IG synapse does not fit in to such a simple story.

The importance of dynamic regulation of neuronal processes cannot be emphasized enough, especially when these processes play key roles in learning and memory or even in internal representation of the outside world which needs to be constantly updated according to changing environment and guide perception and consequent behavior. In the insect brain, mushroom body is the higher center implicated to play critical roles in olfactory learning and memory (Heisenberg 2003; Davis 2004). The olfactory stimuli pose a difficult problem for the nervous system because of its multidimensional and fluctuating nature (Murlis et al. 1992; Laurent 2002; Grabe and Sachse 2018). Still, it is able to detect, discriminate and classify odor stimuli.

Inhibitory circuits play an important role in integrating inputs and modulating outputs in the nervous system (Zhu and Lo 2000). At the MB level, GGN is one such inhibitory neuron which enables gain control in the olfactory circuit of the grasshoppers. Inhibitory-inhibitory recurrent connection may modulate frequency transition in response to stimulus intensity (Shin and Cho 2013). A model replicating recurrent inhibitory network within a gain control framework can result in stable changes of frequency over a large range of inputs (Manor et al. 1999).

Recurrent inhibitory networks have been reported in the stellate cells of MEC (medial entorhinal cortex) layer II in young adult rats where they are postulated to play a role in grid formation (Couey et al. 2013). They have also been reported in the burst-firing cells in the deep layers of the superior colliculus in rabbit (Zhu and Lo 2000). This kind of network is also found in the avian midbrain. The somatosensory barrel cortex of the rat also recruits a recurrent inhibitory microcircuit to modulate its excitatory response to stimuli (Kapfer et al. 2007). This highly sensitive recurrent inhibitory circuit enables a single pyramidal neuron to modulate the overall cortical excitability. Not only these, but these recurrent inhibitory networks also form part of rhythmic pattern generators in the motor circuit (Manor et al. 1999). It is understood to play a role in acting like a switch alternating between controlling antagonistic muscle groups.

What could be the possible way in which the GGN-IG inhibitory recurrent network enable functioning of olfactory learning and memory in the mushroom body circuit is yet to be investigated but the above examples do give us some pointers.

5.3.3 Nature of GGN innervation in LHN

The inhibitory effect of the GGN on LHN is in line with the observation that the GGN fibers in LH exhibit varicosities indicative of its output nature. This innervation has been reported

in *S. americana* (Ray et al. 2020) and corresponds to our observation of the GGN neurite in *Hieroglyphus* as well. The possibility of such a feedforward inhibitory connection from GGN to LHN has also been mentioned (but not shown) in a computational modelling chapter by Komarov et al. (2017). We show that electrically stimulating the KCs in MB result in the inhibition of LHNs (n=11; **Fig. 5.11**). The only known olfactory input to the LHNs apart from GGN is from AL PNs and bLN type 1. But of these, GGN is the only inhibitory neuron. Thus, by principles of elimination, we reach to the probable conclusion that GGN could be the neuron inhibiting LHNs downstream of KCs.

In *Drosophila*, where extensive work has been done on LHNs, it has been reported that GABAergic PNs inhibit LHNs and this long-range GABAergic inhibition is said to result in fine tuning of courtship behavior (Wang et al. 2014). In another study, parallel inhibition of LHNs by inhibitory PNs leads to distinct processing of different kinds of odors—pheromones or fruit (Liang et al. 2013). We do not know of existence of inhibitory PNs in the *Schistocerca* or *H. banian* olfactory circuit. Moreover, we have observed that our calycal cell body stimulation does not cause spikes in PNs, thereby supporting our conclusion of GGN being the likely source of LHN inhibition.

5.3.4 Probable identity of IG

The neurites of GGN are found in the alpha lobe, LH and MB and its output areas (axonal termination) are in MB (Papadopoulou et al. 2011) and the LH (as shown in this study). Papadopoulou et al. (2011) postulated that the arborization in the alpha lobe might be the input area of GGN as it has fine neurites and might probably be the area where IG gives input to GGN. Alpha lobe is innervated by the KCs, LHNs, and bLNs. Of these, only a subset of bLN type 2 have been shown to be GABAergic (Gupta and Stopfer 2014). In addition, it has been reported that IG has neurites in the blobe (Papadopoulou 2010). Taking

this together, is it possible that IG is a type of bLN type 2? However, multiple attempts to find the bLN inhibiting GGN were unsuccessful.

In *Drosophila*, the GGN-homolog, APL has been shown to receive inhibitory inputs from dopaminergic neurons (Zhou et al. 2019). Is it possible that the IG in *H. banian* is also a dopaminergic neuron not discovered yet? This is a question which requires further study as of now.

5.4 Conclusion

Taken together, in this part of the thesis, we were able to discover the odor-response properties of IG from GGN in *H. banian* and have postulated a role of IG in olfactory information processing. However, the behavioral relevance of this microcircuit needs to be probed in future studies. It would also be exciting to discover the identity of IG for future explorations. In addition, the inhibitory connection of GGN-LHN needs to be explored in paired intracellular recording of GGN-LHN, to conclusively prove the inhibition of LHN by GGN. The network motif formed by KC-GGN-IG is one of the very few examples of input-dependent adaptive gain control reported across animal species so far.

Chapter 6

Conclusion

We have characterized the olfactory circuit of the grasshopper *Hieroglyphus banian* from the second-order to the fourth-order neurons, both anatomically and physiologically and discovered a novel class of bilateral mushroom body extrinsic neurons. The schematic of the complete circuit is shown in **Fig. 6.1**.

We compared the findings with the well-established species *Schistocerca americana* and found that the two species belonging to different subfamilies are highly conserved at the higher levels. The species *H. banian*, endemic to South Asia can now be used to explore olfactory information processing and its principles at any level of the olfactory circuit. We have also characterized the odor-response properties of IG and its role in the inhibitory recurrent circuit effecting gain control in the mushroom body network. These findings are represented in **Fig. 6.2**.

In summary, following are the important findings of this study:

- Olfactory circuit of *Hieroglyphus banian* was characterized from the second-order to the fourth-order neurons.
- Olfactory circuit of species from different subfamilies is conserved physiologically and anatomically through the fourth order.
- Three new antennal lobe tracts were discovered in *H. banian*, not reported in any other species of family Acrididae.
- A new tract between LH and MB was discovered.
- A set of three new morphological types of bilateral neurons was discovered.

- Of the three, two types have dense arborization downstream of Kenyon cells, and are a novel class of bilateral MBENs, not reported in any insect species, as far as we know.
- In spite of having dense arborization, the MBENs show weak responses to odor stimuli, in contrast to vigorous odor responses of other known fourth-order neurons in the olfactory circuit.
- IG (Inhibitor of GGN) responds to odor.
- IG receives odor input downstream of KCs, similar to the GGN.
- KC-GGN, KC-IG and KC-bLN synapses undergo paired-pulse facilitation.
- The KC-GGN-IG circuit functions as an *input-dependent* adaptive gain control circuit.
- GGN can be the source of inhibition of the lateral horn neurons.

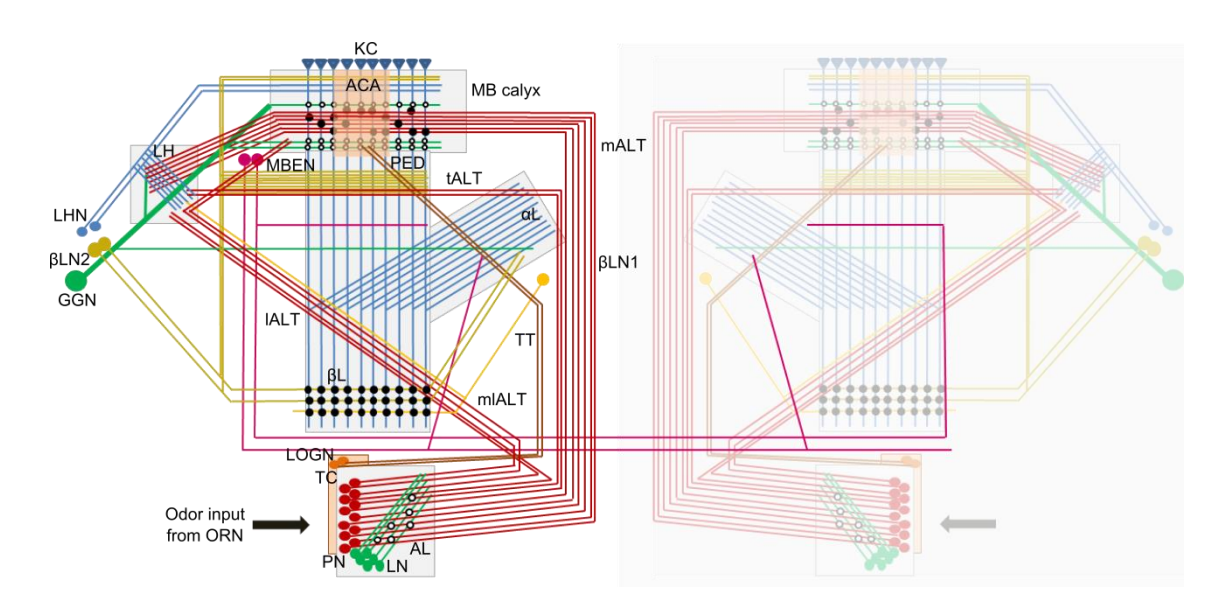


Figure 6.1 Schematic overview (modelled on published data in Schistocerca spp. and primary data in this study) of the olfactory circuit in H. banian from the second order (antennal lobe) to the fourth order (β-lobe and GGN) including the newly discovered MBENs (chapters 3 and 4). The olfactory circuit in H. banian begins with the first-order ORNs, housed in sensilla on the antenna. The ORNs make synapses on the PNs and LNs present in the second relay center, the AL. The PNs are the only output from AL and they relay the olfactory information through multiple tracts (mALT, lALT, mlALT and tALT) to the KCs in MB and LH, the third-order centers. The axons of the KCs form the pedunculus of the MB which bifurcates into the α - and β -lobes. The KCs make synapse with the fourthorder neurons in the β -lobe (bLNs) and with the GGN and bLNs in the α -lobe. The Giant GABAergic neuron (GGN) has neurites in the MB calyx, α-lobe and LH. The tritocerebral tract, part of the gustatory circuit, arises from the cell bodies of LOG located dorso-lateral to the AL and terminates in the accessory calyx of MB. Newly discovered bilateral MBENs in H. banian (chapter 4) have their cell bodies near the superior lateral protocerebral lobe and they project either to α-lobes or pedunculi in both halves of the brain. ORN: olfactory receptor neuron; AL: antennal lobe; LN: local neuron; PN: projection neuron; mALT: medial antennal lobe tract; mlALT: mediolateral ALT; tALT: transverse ALT; lALT: lateral ALT; GGN: giant GABAergic neuron; LH: lateral horn; MBEN: mushroom body extrinsic neuron; MB calyx: mushroom body calyx; PED: pedunculus; KC: Kenyon cell; bLN: β-lobe neuron; αL: α-lobe; βL: β-lobe; TT: tritocerebral tract; ACA: accessory calyx; LOG: lobus glomerulus; LOGN: lobus glomerulus neurons; TC: tritocerebrum; open circles: inhibitory synapse; closed circles: excitatory synapse

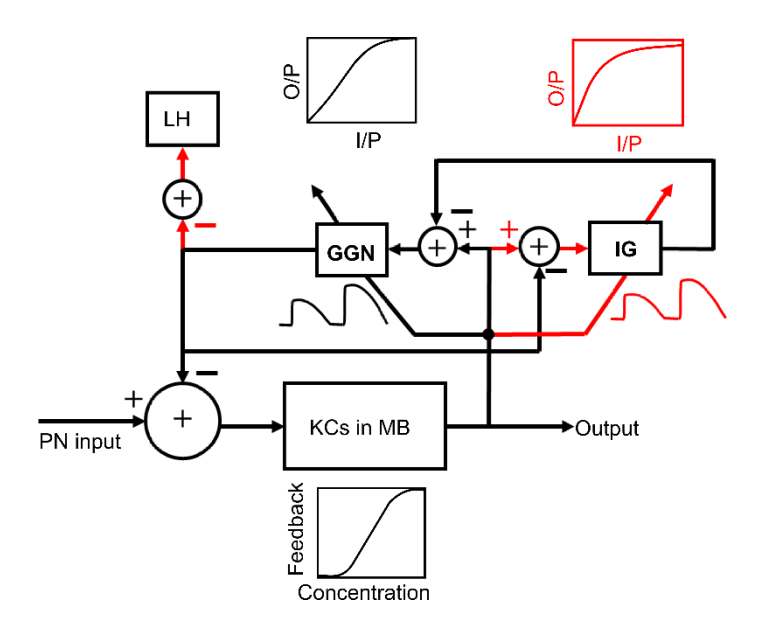


Figure 6.2 Schematic of the KC-GGN-IG circuitry incorporating all the features discovered in this study (in red). LH: lateral horn; KC: Kenyon cell; GGN: giant GABAergic neuron; IG: Inhibitor of GGN; MB: mushroom body; PN: projection neuron; I/P: input; O/P: output

Bibliography

Abel R, Rybak J, Menzel R (2001) Structure and response patterns of olfactory interneurons in the honeybee, *Apis mellifera*. J Comp Neurol 437:363–383

Abuin L, Bargeton B, Ulbrich MH, et al (2011) Functional architecture of olfactory ionotropic glutamate receptors. Neuron 69:44–60

Ache BW, Young JM (2005) Olfaction: Diverse species, conserved principles. Neuron 48:417–430.

Adden A, Wibrand S, Pfeiffer K, et al (2020) The brain of a nocturnal migratory insect, the Australian Bogong moth. Journal of Comparative Neurology **528**:1942–1963.

Allison AC, Warwick RTT (1949) Quantitative observations on the olfactory system of the rabbit. Brain 72:186–197.

Altner H (1977) Insect sensillum specificity and structure: an approach to a new typology. Olfaction Taste 6:295–303

Altner H, Prillinger L (1980) Ultrastructure of invertebrate chemo-, thermo-, and hygroreceptors and its functional significance. In: International Review of Cytology. Elsevier, pp 69–139

Altner H, Routil C, Loftus R (1981) The structure of bimodal chemo-, thermo-, and hygroreceptive sensilla on the antenna of *Locusta migratoria*. Cell Tissue Res 215:289–308

Altner H, Sass H, Altner I (1977) Relationship between structure and function of antennal chemo-, hygro-, and thermoreceptive sensilla in *Periplaneta americana*. Cell Tissue Res 176:389–405.

Anton S, Hansson BS (1996) Antennal lobe interneurons in the desert locust *Schistocerca gregaria* (Forskal): processing of aggregation pheromones in adult males and females. J Comp Neurol 370:85–96

Anton S, Homberg U, Hansson BS (Ed) (1999) Antennal lobe structure. In: Insect olfaction. Springer-Verlag Berlin Heidelberg GmbH, pp 98–127

Anton S, Ignell R, Hansson BS (2002) Developmental changes in the structure and function of the central olfactory system in gregarious and solitary desert locusts. Microsc Res Tech 56:281–291

Arnold G, Masson C, Budharugsa S (1985) Comparative study of the antennal lobes and their afferent pathway in the worker bee and the drone (*Apis mellifera*). Cell Tissue Res 242:593–605.

Aso Y, Hattori D, Yu Y, et al (2014a) The neuronal architecture of the mushroom body provides a logic for associative learning. Elife 3:e04577

Aso Y, Sitaraman D, Ichinose T, et al (2014b) Mushroom body output neurons encode valence and guide memory-based action selection in *Drosophila*. Elife 3:e04580

Bazhenov M, Stopfer M, Rabinovich M, et al (2001a) Model of transient oscillatory synchronization in the locust antennal lobe. Neuron 30:553–567

Bazhenov M, Stopfer M, Rabinovich M, et al (2001b) Model of cellular and network mechanisms for odor-evoked temporal patterning in the locust antennal lobe. Neuron 30:569–581

Belle J de, Heisenberg M (1994) Associative odor learning in *Drosophila* abolished by chemical ablation of mushroom bodies. Science 263:692–695.

Benson JA (1993) The electrophysiological pharmacology of neurotransmitter receptors on locust neuronal somata. In: Comparative molecular neurobiology. Springer, pp 390–413

Benton R, Sachse S, Michnick SW, Vosshall LB (2006) Atypical membrane topology and heteromeric function of *Drosophila* odorant receptors in vivo. PLoS Biol 4:e20

Berg BG, Galizia CG, Brandt R, Mustaparta H (2002) Digital atlases of the antennal lobe in two species of tobacco budworm moths, the oriental *Helicoverpa assulta* (male) and the American *Heliothis virescens* (male and female). J Comp Neurol 446:123–134.

Berg BG, Schachtner J, Homberg U (2009) γ -Aminobutyric acid immunostaining in the antennal lobe of the moth *Heliothis virescens* and its colocalization with neuropeptides. Cell Tissue Res 335:593–605

Bhandawat V, Olsen SR, Gouwens NW, et al (2007) Sensory processing in the *Drosophila* antennal lobe increases reliability and separability of ensemble odor representations. Nat Neurosci 10:1474–1482

Bhatnagar KP, Kennedy RC, Baron G, Greenberg RA (1987) Number of mitral cells and the bulb volume in the aging human olfactory bulb: A quantitative morphological study. Anat Rec 218:73–87.

Bicker G (1999) Histochemistry of classical neurotransmitters in antennal lobes and mushroom bodies of the honeybee. Microsc Res Tech 45:174–183.

Bicker G, Kreissl S (1994) Calcium imaging reveals nicotinic acetylcholine receptors on cultured mushroom body neurons. J Neurophysiol 71:808–810

Bicker G, Schäfer S, Kingan TG (1985) Mushroom body feedback interneurones in the honeybee show GABA-like immunoreactivity. Brain Res 360:394–397

Bicker G, Schafer S, Ottersen OP, Storm-Mathisen J (1988) Glutamate-like immunoreactivity in identified neuronal populations of insect nervous systems. J Neurosci 8:2108–2122.

Bisch-Knaden S, Carlsson MA, Sugimoto Y, et al (2012) Olfactory coding in five moth species from two families. J Exp Biol 215:1542–1551.

Bland RG (1982) Morphology and distribution of sensilla on the antennae and mouthparts of *Hypochlora alba* (Orthoptera: Acrididae). Ann Entomol Soc Am 75:272–283.

Boeckh J (1967) Reaktionsschwelle, Arbeitsbereich und Spezifität eines Geruchsrezeptors auf der Heuschreckenantenne. Z Für Vgl Physiol 55:378–406.

Boeckh J, ERNST K-D, Selsam P (1987) Neurophysiology and neuroanatomy of the olfactory pathway in the cockroach. Ann N Y Acad Sci 510:39–43

Boitard C, Devaud J-M, Isabel G, Giurfa M (2015) GABAergic feedback signaling into the calyces of the mushroom bodies enables olfactory reversal learning in honey bees. Front Behav Neurosci 9:198.

Bornhauser BC, Meyer EP (1996) Histamine-like immunoreactivity in the visual system and brain of an orthopteran and a hymenopteran insect. Cell Tissue Res 287:211–221.

Boyan GS (1993) Another look at insect audition: the tympanic receptors as an evolutionary specialization of the chordotonal system. J Insect Physiol 39:187–200

Brockmann A, Brückner D (2001) Structural differences in the drone olfactory system of two phylogenetically distant *Apis* species, *A. florea* and *A. mellifera*. Naturwissenschaften 88:78–81

Bromley SM, Doty RL (1995) Odor recognition memory is better under bilateral than unilateral test conditions. Cortex 31:25–40

Broome BM, Jayaraman V, Laurent G (2006) Encoding and decoding of overlapping odor sequences. Neuron 51:467–482

Brown SL, Joseph J, Stopfer M (2005) Encoding a temporally structured stimulus with a temporally structured neural representation. Nat Neurosci 8:1568

Buchner E (1991) Genes expressed in the adult brain of *Drosophila* and effects of their mutations on behavior: a survey of transmitter-and second messenger-related genes. J Neurogenet 7:153–192

Burrows M (1996) The neurobiology of an insect brain. Oxford University Press, New York

Burton SD (2016) Novel cell types and circuits in the mouse main olfactory bulb. Carnegie Mellon

Campbell RA, Turner GC (2010) The mushroom body. Curr Biol 20:R11–R12

Capinera JL (1993) Host-plant selection by *Schistocerca americana* (Orthoptera: Acrididae). Environ Entomol 22:127–133

Carey AF, Carlson JR (2011) Insect olfaction from model systems to disease control. Proc Natl Acad Sci 108:12987–12995

Cassenaer S, Laurent G (2012) Conditional modulation of spike-timing-dependent plasticity for olfactory learning. Nature 482:47–52.

Cassenaer S, Laurent G (2007) Hebbian STDP in mushroom bodies facilitates the synchronous flow of olfactory information in locusts. Nature 448:709

Chapman RF (1998) The insects: structure and function, Fifth. Cambridge university press

Chou Y-H, Spletter ML, Yaksi E, et al (2010) Diversity and wiring variability of olfactory local interneurons in the *Drosophila* antennal lobe. Nat Neurosci 13:439

Christensen TA, Waldrop BR, Hildebrand JG (1998) GABAergic mechanisms that shape the temporal response to odors in moth olfactory projection neurons. Ann N Y Acad Sci 855:475–481.

Cigliano MM, Braun H, Eades DC, Otte D (2018) Orthoptera Species File. Version 5.0/5.0. http://orthoptera.speciesfile.org/HomePage/Orthoptera/HomePage.aspx. Accessed 18 Aug 2018

Clyne PJ, Warr CG, Freeman MR, et al (1999) A novel family of divergent seven-transmembrane proteins: candidate odorant receptors in *Drosophila*. Neuron 22:327–338

Coleman L, Kunhi Kannan K (1911) The rice grasshopper (*Hieroglyphus banian* F.). Bulletin Department of Agriculture Mysore (Ent.), Mysore

Couey JJ, Witoelar A, Zhang S-J, et al (2013) Recurrent inhibitory circuitry as a mechanism for grid formation. Nat Neurosci 16:318–324

Couto A, Alenius M, Dickson BJ (2005) Molecular, anatomical, and functional organization of the *Drosophila* olfactory system. Curr Biol 15:1535–1547

Couton L, Minoli S, Kiêu K, et al (2009) Constancy and variability of identified glomeruli in antennal lobes: computational approach in *Spodoptera littoralis*. Cell Tissue Res 337:491–511

Crittenden JR, Skoulakis EMC, Han K-A, et al (1998) Tripartite mushroom body architecture revealed by antigenic markers. Learn Mem 5:38–51.

Dacks AM, Reisenman CE, Paulk AC, Nighorn AJ (2010) Histamine-immunoreactive local neurons in the antennal lobes of the hymenoptera. J Comp Neurol 518:2917–2933.

Das A, Das S, Haldar P (2002) Effect of food plants on the growth rate and survivability of *Hieroglyphus banian* (Fabricius)(Orthoptera: Acridoidea), a major paddy pest in India. Appl Entomol Zool 37:207–212

Davis RL (2004) Olfactory learning. Neuron 44:31–48

de Bruyne M, Foster K, Carlson JR (2001) Odor coding in the *Drosophila* antenna. Neuron 30:537–552.

Demmer H, Kloppenburg P (2009) Intrinsic membrane properties and inhibitory synaptic input of Kenyon cells as mechanisms for sparse coding? J Neurophysiol 102:1538–1550

Dirsh VM (1956) The phallic complex in Acridoidea (Orthoptera) in relation to taxonomy. Trans R Entomol Soc Lond 108:223–270

Distler P (1990) GABA-immunohistochemistry as a label for identifying types of local interneurons and their synaptic contacts in the antennal lobes of the American cockroach. Histochemistry 93:617–626

Distler PG, Gruber C, Boeckh J (1998) Synaptic connections between GABA-immunoreactive neurons and uniglomerular projection neurons within the antennal lobe of the cockroach, *Periplaneta americana*. Synapse 29:1–13.

Dolan M-J, Frechter S, Bates AS, et al (2019) Neurogenetic dissection of the *Drosophila* lateral horn reveals major outputs, diverse behavioural functions, and interactions with the mushroom body. eLife 8:e43079

Elgar MA, Zhang D, Wang Q, et al (2018) Insect antennal morphology: The evolution of diverse solutions to odorant perception. Yale J Biol Med 91:457–469

Erber J (1978) Response characteristics and after effects of multimodal neurons in the mushroom body area of the honey bee. Physiol Entomol 3:77–89.

Ernst KD, Boeckh J, Boeckh V (1977) A neuroanatomical study on the organization of the central antennal pathways in insects. Cell Tissue Res 176:285–308

Esslen J, Kaissling K-E (1976) Zahl und Verteilung antennaler Sensillen bei der Honigbiene (*Apis mellifera* L.). Zoomorphologie 83:227–251.

Evans MH (1982) Optically coupled stimulus isolation headstage. Med Biol Eng Comput 20:648.

Fahrbach SE (2006) Structure of the mushroom bodies of the insect brain. Annu Rev Entomol 51:209–232

Farivar SS (2005) Cytoarchitecture of the locust olfactory system. California Institute of Technology

Farris SM (2011) Are mushroom bodies cerebellum-like structures? Arthropod Struct Dev 40:368–379

Farris SM (2008) Tritocerebral tract input to the insect mushroom bodies. Arthropod Struct Dev 37:492-503

Farris SM, Abrams AI, Strausfeld NJ (2004) Development and morphology of Class II Kenyon cells in the mushroom bodies of the honey bee, *Apis mellifera*. J Comp Neurol 474:325–339.

Farris SM, Pettrey C, Daly KC (2011) A subpopulation of mushroom body intrinsic neurons is generated by protocerebral neuroblasts in the tobacco hornworm moth, *Manduca sexta* (Sphingidae, Lepidoptera). Arthropod Struct Dev 40:395–408.

Farris SM, Sinakevitch I (2003) Development and evolution of the insect mushroom bodies: towards the understanding of conserved developmental mechanisms in a higher brain center. Arthropod Struct Dev 32:79–101.

Filla I, Menzel R (2015) Mushroom body extrinsic neurons in the honeybee (*Apis mellifera*) brain integrate context and cue values upon attentional stimulus selection. J Neurophysiol 114:2005–2014.

Fişek M, Wilson RI (2014) Stereotyped connectivity and computations in higher-order olfactory neurons. Nat Neurosci 17:280

Flanagan D, Mercer AR (1989) An atlas and 3-D reconstruction of the antennal lobes in the worker honey bee, *Apis mellifera* L. (Hymenoptera : Apidae). Int J Insect Morphol Embryol 18:145–159.

Fonta C, Masson C (1985) Organisation neuroanatomique de la voie afferente antennaire chez les bourdons males et femelles (Bombus sp.). Comptes Rendus Séances Académie Sci Sér 3 Sci Vie 300:437–442

Frechter S, Bates AS, Tootoonian S, et al (2019) Functional and anatomical specificity in a higher olfactory centre. eLife 8:e44590.

Friedrich RW (2011) Olfactory neuroscience: Beyond the bulb. Curr Biol 21:R438–R440

Friedrich RW, Laurent G (2004) Dynamics of olfactory bulb input and output activity during odor stimulation in zebrafish. J Neurophysiol 91:2658–2669

Fukushima R, Kanzaki R (2009) Modular subdivision of mushroom bodies by Kenyon cells in the silkmoth. J Comp Neurol 513:315–330.

Galán RF, Weidert M, Menzel R, et al (2006) Sensory memory for odors is encoded in spontaneous correlated activity between olfactory glomeruli. Neural Comput 18:10–25.

Galizia CG, McIlwrath SL, Menzel R (1999) A digital three-dimensional atlas of the honeybee antennal lobe based on optical sections acquired by confocal microscopy. Cell Tissue Res 295:383–394.

Galizia CG, Rössler W (2010) Parallel olfactory systems in insects: anatomy and function. Annu Rev Entomol 55:399–420

Galizia CG, Sachse S (2010) Odor coding in insects. Neurobiol Olfaction 35–70

Galizia CG, Sachse S, Menini A (Ed) (2010) Odor coding in insects. In: The neurobiology of olfaction. CRC Press, Taylor and Francis Group, pp 35–70

Gao Q, Yuan B, Chess A (2000) Convergent projections of *Drosophila* olfactory neurons to specific glomeruli in the antennal lobe. Nat Neurosci 3:780.

Gibson NJ, Nighorn A (2000) Expression of nitric oxide synthase and soluble guanylyl cyclase in the developing olfactory system of *Manduca sexta*. J Comp Neurol 422:191–205.

Grabe V, Sachse S (2018) Fundamental principles of the olfactory code. Biosystems 164:94–101.

Grimaldi D, Engel MS, Engel MS (2005) Evolution of the Insects. Cambridge University Press

Gronenberg W (1986) Physiological and anatomical properties of optical input-fibres to the mushroom body in the bee brain. J Insect Physiol 32:695–704.

Gronenberg W (1987) Anatomical and physiological properties of feedback neurons of the mushroom bodies in the bee brain. Exp Biol 46:115–125

Grosse-Wilde E, Kuebler LS, Bucks S, et al (2011) Antennal transcriptome of *Manduca sexta*. Proc Natl Acad Sci 108:7449–7454.

Grünewald B (1999a) Physiological properties and response modulations of mushroom body feedback neurons during olfactory learning in the honeybee, *Apis mellifera*. J Comp Physiol A 185:565–576.

Grünewald B (1999b) Morphology of feedback neurons in the mushroom body of the honeybee, *Apis mellifera*. J Comp Neurol 404:114–126

Gupta N, Stopfer M (2012) Functional analysis of a higher olfactory center, the lateral horn. J Neurosci 32:8138–8148

Gupta N, Stopfer M (2014) A temporal channel for information in sparse sensory coding. Curr Biol 24:2247–2256

Hallem EA, Carlson JR (2006) Coding of odors by a receptor repertoire. Cell 125:143–160.

Hallem EA, Ho MG, Carlson JR (2004) The molecular basis of odor coding in the *Drosophila* antenna. Cell 117:965–979.

Hansson BS, Anton S (2000) Function and morphology of the antennal lobe: new developments. Annu Rev Entomol 45:203–231

Hansson BS, Grosmaitre X, Anton S, Njagi PGN (1996) Physiological responses and central nervous projections of antennal olfactory receptor neurons in the adult desert locust, *Schistocerca gregaria* (Orthoptera: Acrididae). J Comp Physiol A 179:157–167

Hansson BS, Stensmyr MC (2011) Evolution of insect olfaction. Neuron 72:698-711

Haynes PR, Christmann BL, Griffith LC (2015) A single pair of neurons links sleep to memory consolidation in *Drosophila melanogaster*. Elife 4:e03868

Heisenberg M (2003) Mushroom body memoir: from maps to models. Nat Rev Neurosci 4:266

Helge R, Müller D, Mustaparta H (2007) Anatomical organization of antennal lobe projection neurons in the moth *Heliothis virescens*. J Comp Neurol 500:658–675

Herreras O (2016) Local field potentials: myths and misunderstandings. Front Neural Circuits 10:101

Hildebrand JG, Shepherd GM (1997) Mechanisms of olfactory discrimination: converging evidence for common principles across phyla. Annu Rev Neurosci 20:595–631

Homberg U (1984) Processing of antennal information in extrinsic mushroom body neurons of the bee brain. J Comp Physiol A 154:825–836.

Homberg U (2002) Neurotransmitters and neuropeptides in the brain of the locust. Microsc Res Tech 56:189–209

Homberg U, Brandl C, Clynen E, et al (2004) Mas-allatotropin/Lom-AG-myotropin I immunostaining in the brain of the locust, *Schistocerca gregaria*. Cell Tissue Res 318:439–457

Homberg U, Erber J (1979) Response characteristics and identification of extrinsic mushroom body neurons of the bee. Z Für Naturforschung C 34:612–615

Homberg U, Hoskins SG, Hildebrand JG (1995) Distribution of acetylcholinesterase activity in the deutocerebrum of the sphinx moth *Manduca sexta*. Cell Tissue Res 279:249–259.

Homberg U, Kingan TG, Hildebrand JG (1987) Immunocytochemistry of GABA in the brain and suboesophageal ganglion of *Manduca sexta*. Cell Tissue Res 248:1–24.

Homberg U, Montague RA, Hildebrand JG (1988) Anatomy of antenno-cerebral pathways in the brain of the sphinx moth *Manduca sexta*. Cell Tissue Res 254:255–281

Honegger KS, Campbell RA, Turner GC (2011) Cellular-resolution population imaging reveals robust sparse coding in the *Drosophila* mushroom body. J Neurosci 31:11772–11785

Hosek JR, Freeman WJ (2001) Osmetic ontogenesis, or olfaction becomes you: The neurodynamic, intentional self and its affinities with the Foucaultian/Butlerian subject. Configurations 9:509–542

Hoskins SG, Homberg U, Kingan TG, et al (1986) Immunocytochemistry of GABA in the antennal lobes of the sphinx moth *Manduca sexta*. Cell Tissue Res 244:243–252

Ian E, Berg A, Lillevoll SC, Berg BG (2016) Antennal-lobe tracts in the noctuid moth, *Heliothis virescens*: new anatomical findings. Cell Tissue Res 366:23–35

Ignell R, Anton S, Hansson BS (2001) The antennal lobe of Orthoptera–anatomy and evolution. Brain Behav Evol 57:1–17

Ignell R, Dekker T, Ghaninia M, Hansson BS (2005) Neuronal architecture of the mosquito deutocerebrum. J Comp Neurol 493:207–240.

Ito I, Bazhenov M, Ong RC, et al (2009) Frequency transitions in odor-evoked neural oscillations. Neuron 64:692–706

Ito K, Shinomiya K, Ito M, et al (2014) A systematic nomenclature for the insect brain. Neuron 81:755–765

Iwama A, Shibuya T (1998) Physiology and morphology of olfactory neurons associating with the protocerebral lobe of the honeybee brain. J Insect Physiol 44:1191–1204.

Iwano M, Hill ES, Mori A, et al (2010) Neurons associated with the flip-flop activity in the lateral accessory lobe and ventral protocerebrum of the silkworm moth brain. J Comp Neurol 518:366–388

Jackman SL, Regehr WG (2017) The mechanisms and functions of synaptic facilitation. Neuron 94:447–464

Jackson FR, Newby LM, Kulkarni SJ (1990) *Drosophila* GABAergic systems: sequence and expression of glutamic acid decarboxylase. J Neurochem 54:1068–1078

Jefferis GSXE, Marin EC, Stocker RF, Luo L (2001) Target neuron prespecification in the olfactory map of *Drosophila*. Nature 414:204–208.

Jefferis GSXE, Potter CJ, Chan AM, et al (2007) Comprehensive maps of *Drosophila* higher olfactory centers: Spatially segregated fruit and pheromone representation. Cell 128:1187–1203.

Jiang X, Breer H, Pregitzer P (2019) Sensilla-specific expression of odorant receptors in the desert locust *Schistocerca gregaria*. Front Physiol 10:1052

Johnston D, Wu S (1994) Extracellular field recordings. In: Foundations of Cellular Neurophysiology. A Bradford Book, The MIT Press, Cambridge, Cambridge, pp 422–439

Joiner WJ, Crocker A, White BH, Sehgal A (2006) Sleep in *Drosophila* is regulated by adult mushroom bodies. Nature 441:757–760.

Jones TA, Donlan NA, O'donnell S (2009) Growth and pruning of mushroom body Kenyon cell dendrites during worker behavioral development in the paper wasp, *Polybia aequatorialis* (Hymenoptera: Vespidae). Neurobiol Learn Mem 92:485–495

Jortner RA, Farivar SS, Laurent G (2007) A simple connectivity scheme for sparse coding in an olfactory system. J Neurosci 27:1659–1669

Joseph J, Dunn FA, Stopfer M (2012) Spontaneous olfactory receptor neuron activity determines follower cell response properties. J Neurosci 32:2900–2910

Kaissling K-E (1971) Insect Olfaction. In: Amoore JE, Beets MGJ, Davies JT, et al. (eds) Olfaction. Springer, Berlin, Heidelberg, pp 351–431

Kanzaki R, Arbas EA, Hildebrand JG (1991a) Physiology and morphology of descending neurons in pheromone-processing olfactory pathways in the male moth *Manduca sexta*. J Comp Physiol A Neuroethol Sens Neural Behav Physiol 169:1–14

Kanzaki R, Arbas EA, Hildebrand JG (1991b) Physiology and morphology of protocerebral olfactory neurons in the male moth *Manduca sexta*. J Comp Physiol A 168:281–298

Kanzaki R, Shibuya T (1992) Long-lasting excitation of protocerebral bilateral neurons in the pheromone-processing pathways of the male moth *Bombyx mori*. Brain Res 587:211–215

Kanzaki R, Soo K, Seki Y, Wada S (2003) Projections to higher olfactory centers from subdivisions of the antennal lobe macroglomerular complex of the male silkmoth. Chem Senses 28:113–130

Kapfer C, Glickfeld LL, Atallah BV, Scanziani M (2007) Supralinear increase of recurrent inhibition during sparse activity in the somatosensory cortex. Nat Neurosci 10:743–753

Karpe SD, Jain R, Brockmann A, Sowdhamini R (2016) Identification of complete repertoire of *Apis florea* odorant receptors reveals complex orthologous relationships with *Apis mellifera*. Genome Biol Evol 8:2879–2895.

Kaupp UB (2010) Olfactory signalling in vertebrates and insects: differences and commonalities. Nat Rev Neurosci 11:188–200.

Kawagishi K, Ando M, Yokouchi K, et al (2014) Stereological quantification of olfactory receptor neurons in mice. Neuroscience 272:29–33.

Kawagishi K, Ando M, Yokouchi K, et al (2015) Stereological estimation of olfactory receptor neurons in rats. Chem Senses 40:89–95.

Kazama H, Wilson RI (2008) Homeostatic matching and nonlinear amplification at identified central synapses. Neuron 58:401–413.

Kazawa T, Namiki S, Fukushima R, et al (2009) Constancy and variability of glomerular organization in the antennal lobe of the silkmoth. Cell Tissue Res 336:119.

Kee T, Sanda P, Gupta N, et al (2015) Feed-forward versus feedback inhibition in a basic olfactory circuit. PLoS Comput Biol 11:e1004531

Keil T A, Hansson BS (Ed) (1999) Morphology and development of the peripheral olfactory organs. In: Insect olfaction. Springer-Verlag Berlin Heidelberg GmbH, pp 5–49

Kenyon FC (1896a) The brain of the bee. A preliminary contribution to the morphology of the nervous system of the arthropoda. J Comp Neurol 6:133–210.

Kenyon FC (1896b) The meaning and structure of the so-called" mushroom bodies" of the hexapod brain. Am Nat 30:643–650

Kido A, Ito K (2002) Mushroom bodies are not required for courtship behavior by normal and sexually mosaic *Drosophila*. J Neurobiol 52:302–311.

Kirby WF (1910) A Synonymic Catalogue of Orthoptera. Vol 3. Orthoptera Saltatoria. Part 2 (Locustidae vel Acrididae). Synonymic Cat Orthoptera Vol 3 Orthoptera Saltatoria Part 2 Locustidae Vel Acrididae

Kirschner S, Kleineidam CJ, Zube C, et al (2006) Dual olfactory pathway in the honeybee, *Apis mellifera*. J Comp Neurol 499:933–952.

Korsching, S.I., 2001. Odor maps in the brain: spatial aspects of odor representation in sensory surface and olfactory bulb. Cellular and Molecular Life Sciences CMLS 58, 520–530.

Kollmann M, Schmidt R, Heuer CM, Schachtner J (2016) Variations on a theme: Antennal lobe architecture across Coleoptera. PloS One 11:e0166253

Komarov M, Stopfer M, Bazhenov M (2017) Olfactory Computation in Insects. In: Aranson IS, Pikovsky A, Rulkov NF, Tsimring LS (eds) Advances in Dynamics, Patterns, Cognition: Challenges in Complexity. Springer International Publishing, Cham, pp 213–225

Komischke B, Sandoz J-C, Lachnit H, Giurfa M (2003) Non-elemental processing in olfactory discrimination tasks needs bilateral input in honeybees. Behav Brain Res 145:135–143

Koontz MA, Schneider D (1987) Sexual dimorphism in neuronal projections from the antennae of silk moths (*Bombyx mori*, *Antheraea polyphemus*) and the gypsy moth (*Lymantria dispar*). Cell Tissue Res 249:39–50.

Kreissl S, Bicker G (1989) Histochemistry of acetylcholinesterase and immunocytochemistry of an acetylcholine receptor-like antigen in the brain of the honeybee. J Comp Neurol 286:71–84

Krieger J, Klink O, Mohl C, et al (2003) A candidate olfactory receptor subtype highly conserved across different insect orders. J Comp Physiol A 189:519–526

Kucharski D, Hall WG (1987) New routes to early memories. Science 238:786–788.

Kucharski D, Hall WG (1988) Developmental change in the access to olfactory memories. Behav Neurosci 102:340–348.

Kuitert LC, Connin RV (1952) Biology of the American grasshopper in the southeastern United States. Fla Entomol 35:22–33

Lai S-L, Awasaki T, Ito K, Lee T (2008) Clonal analysis of *Drosophila* antennal lobe neurons: diverse neuronal architectures in the lateral neuroblast lineage. Development 135:2883–2893

Laissue P p., Reiter C, Hiesinger P r., et al (1999) Three-dimensional reconstruction of the antennal lobe in *Drosophila melanogaster*. J Comp Neurol 405:543–552.

Larsson MC, Domingos AI, Jones WD, et al (2004) Or83b encodes a broadly expressed odorant receptor essential for *Drosophila* olfaction. Neuron 43:703–714

Laurent G (2002) Olfactory network dynamics and the coding of multidimensional signals. Nat Rev Neurosci 3:884–895

Laurent G (1996) Dynamical representation of odors by oscillating and evolving neural assemblies. Trends Neurosci 19:489–496

Laurent G, Davidowitz H (1994) Encoding of olfactory information with oscillating neural assemblies. Science 265:1872–1875

Laurent G, MacLeod K, Stopfer M, Wehr M (1998) Spatiotemporal structure of olfactory inputs to the mushroom bodies. Learn Mem 5:124–132.

Laurent G, Naraghi M (1994) Odorant-induced oscillations in the mushroom bodies of the locust. J Neurosci 14:2993–3004

Laurent G, Wehr M, Davidowitz H (1996) Temporal representations of odors in an olfactory network. J Neurosci 16:3837–3847

Lee JK, Strausfeld NJ (1990) Structure, distribution and number of surface sensilla and their receptor cells on the olfactory appendage of the male moth *Manduca sexta*. J Neurocytol 19:519–538.

Lei H, Anton S, Hansson BS (2001) Olfactory protocerebral pathways processing sex pheromone and plant odor information in the male moth *Agrotis segetum*. J Comp Neurol 432:356–370

Lei Z, Chen K, Li H, et al (2013) The GABA system regulates the sparse coding of odors in the mushroom bodies of *Drosophila*. Biochem Biophys Res Commun 436:35–40.

Leitch B, Laurent G (1996) GABAergic synapses in the antennal lobe and mushroom body of the locust olfactory system. J Comp Neurol 372:487–514

Lerner H, Rozenfeld E, Rozenman B, et al (2020) Differential role for a defined lateral horn neuron subset in naïve odor valence in *Drosophila*. Sci Rep 10:1–17

Li Y, Strausfeld NJ (1997) Morphology and sensory modality of mushroom body extrinsic neurons in the brain of the cockroach, *Periplaneta americana*. J Comp Neurol 387:631–650

Li Y, Strausfeld NJ (1999) Multimodal efferent and recurrent neurons in the medial lobes of cockroach mushroom bodies. J Comp Neurol 409:647–663.

Liang L, Li Y, Potter CJ, et al (2013) GABAergic projection neurons route selective olfactory inputs to specific higher-order neurons. Neuron 79:917–931

Lin AC, Bygrave AM, de Calignon A, et al (2014) Sparse, decorrelated odor coding in the mushroom body enhances learned odor discrimination. Nat Neurosci 17:559–568.

Liu X, Davis RL (2009) The GABAergic anterior paired lateral neuron suppresses and is suppressed by olfactory learning. Nat Neurosci 12:53

Løfaldli BB, Kvello P, Mustaparta H (2010) Integration of the antennal lobe glomeruli and three projection neurons in the standard brain atlas of the moth *Heliothis virescens*. Front Syst Neurosci 4:.

Longair MH, Baker DA, Armstrong JD (2011) Simple Neurite Tracer: open source software for reconstruction, visualization and analysis of neuronal processes. Bioinformatics 27:2453–2454

Louis M, Huber T, Benton R, et al (2008) Bilateral olfactory sensory input enhances chemotaxis behavior. Nat Neurosci 11:187–199.

MacLeod K, Bäcker A, Laurent G (1998) Who reads temporal information contained across synchronized and oscillatory spike trains? Nature 395:693

MacLeod K, Laurent G (1996) Distinct mechanisms for synchronization and temporal patterning of odor-encoding neural assemblies. Science 274:976–979

Mainland JD, Bremner EA, Young N, et al (2002) One nostril knows what the other learns. Nature 419:802–802.

Malun D (1991) Synaptic relationships between GABA-immunoreactive neurons and an identified uniglomerular projection neuron in the antennal lobe of *Periplaneta americana*: a double-labeling electron microscopic study. Histochemistry 96:197–207

Malun D, Waldow U, Kraus D, Boeckh J (1993) Connections between the deutocerebrum and the protocerebrum, and neuroanatomy of several classes of deutocerebral projection neurons in the brain of male *Periplaneta americana*. J Comp Neurol 329:143–162

Mandal S, Dey A, Hazra A (2007) Pictorial handbook on Indian short-horned grasshopper pests (Acridoidea: Orthoptera). Zool Surv India Kolkata

Manor Y, Nadim F, Epstein S, et al (1999) Network oscillations generated by balancing graded asymmetric reciprocal inhibition in passive neurons. J Neurosci 19:2765–2779

Maresh A, Gil DR, Whitman MC, Greer CA (2008) Principles of glomerular organization in the human olfactory bulb–implications for odor processing. PloS One 3:e2640

Martin H (1965) Osmotropotaxis in the honey-bee. Nature 208:59–63

Martin JP, Beyerlein A, Dacks AM, et al (2011) The neurobiology of insect olfaction: sensory processing in a comparative context. Prog Neurobiol 95:427–447

Martini R (1986) Fine structure and development of the large sensilla basiconica on the antennae of sphecid wasps. Tissue Cell 18:143–151

Masson C, Mustaparta H (1990) Chemical information processing in the olfactory system of insects. Physiol Rev 70:199–245

Mauelshagen J (1993) Neural correlates of olfactory learning paradigms in an identified neuron in the honeybee brain. J Neurophysiol 69:609–625.

Mazor O, Laurent G (2005) Transient dynamics versus fixed points in odor representations by locust antennal lobe projection neurons. Neuron 48:661–673

Meisami E, Safari L (1981) A quantitative study of the effects of early unilateral olfactory deprivation on the number and distribution of mitral and tufted cells and of glomeruli in the rat olfactory bulb. Brain Res 221:81–107.

Menzel R, Manz G (2005) Neural plasticity of mushroom body-extrinsic neurons in the honeybee brain. J Exp Biol 208:4317–4332.

Merrick C, Godwin C, Geisler M, Morsella E (2014) The olfactory system as the gateway to the neural correlates of consciousness. Front Psychol 4:1011.

Mishima T, Kanzaki R (1999) Physiological and morphological characterization of olfactory descending interneurons of the male silkworm moth, *Bombyx mori*. J Comp Physiol A 184:143–160.

Mizunami M, Iwasaki M, Okada R, Nishikawa M (1998) Topography of four classes of Kenyon cells in the mushroom bodies of the cockroach. J Comp Neurol 399:162–175.

Mobbs PG (1984) Neural networks in the mushroom bodies of the honeybee. J Insect Physiol 30:43–58.

Mobbs PG, Young JZ (1982) The brain of the honeybee *Apis mellifera*. I. The connections and spatial organization of the mushroom bodies. Philos Trans R Soc Lond B Biol Sci 298:309–354.

Modi MN, Shuai Y, Turner GC (2020) The *Drosophila* mushroom body: From architecture to algorithm in a learning circuit. Annu Rev Neurosci 43:465–484.

Mogily S, VijayKumar M, Sethy SK, Joseph J (2020) Characterization of the olfactory system of the giant honey bee, *Apis dorsata*. Cell Tissue Res 379:131–145

Müller D, Abel R, Brandt R, et al (2002) Differential parallel processing of olfactory information in the honeybee, *Apis mellifera* L. J Comp Physiol A 188:359–370

Murlis J, Elkinton JS, Carde RT (1992) Odor plumes and how insects use them. Annu Rev Entomol 37:505–532

Murlis, J., Jones, C.D., 1981. Fine-scale structure of odour plumes in relation to insect orientation to distant pheromone and other attractant sources. Physiological Entomology 6, 71–86.

Mysore K, Subramanian KA, Sarasij RC, et al (2009) Caste and sex specific olfactory glomerular organization and brain architecture in two sympatric ant species *Camponotus sericeus* and *Camponotus compressus* (Fabricius, 1798). Arthropod Struct Dev 38:485–497

Namiki S, Kanzaki R (2011) Heterogeneity in dendritic morphology of moth antennal lobe projection neurons. J Comp Neurol 519:3367–3386

Namiki S, Takaguchi M, Seki Y, et al (2013) Concentric zones for pheromone components in the mushroom body calyx of the moth brain. J Comp Neurol 521:1073–1092

Namiki S, Wada S, Kanzaki R (2018) Descending neurons from the lateral accessory lobe and posterior slope in the brain of the silkmoth *Bombyx mori*. Sci Rep 8:9663

Neder R (1959) Allomerrisches Wachstum von Hirnteilen bei drei verschieden grossen Schabenarten. Zool Jahrb Anat 4:411–464

Ng M, Roorda RD, Lima SQ, et al (2002) Transmission of olfactory information between three populations of neurons in the antennal lobe of the fly. Neuron 36:463–474.

Nishikawa M, Nishino H, Misaka Y, et al (2008) Sexual dimorphism in the antennal lobe of the ant *Camponotus japonicus*. Zoolog Sci 25:195–204.

Nishino H, Mizunami M (1998) Giant input neurons of the mushroom body: intracellular recording and staining in the cockroach. Neurosci Lett 246:57–60.

Ochieng SA, Hallberg E, Hansson BS (1998) Fine structure and distribution of antennal sensilla of the desert locust, *Schistocerca gregaria* (Orthoptera: Acrididae). Cell Tissue Res 291:525–536

Ochieng SA, Hansson BS (1999) Responses of olfactory receptor neurones to behaviourally important odours in gregarious and solitarious desert locust, *Schistocerca gregaria*. Physiol Entomol 24:28–36

O'Dell KMC, Armstrong JD, Yao Yang M, Kaiser K (1995) Functional dissection of the *Drosophila* mushroom bodies by selective feminization of a genetically defined subcompartments. Neuron 15:55–61.

Okada R, Awasaki T, Ito K (2009) Gamma-aminobutyric acid (GABA)-mediated neural connections in the *Drosophila* antennal lobe. J Comp Neurol 514:74–91.

Okada R, Ikeda J, Mizunami M (1999) Sensory responses and movement-related activities in extrinsic neurons of the cockroach mushroom bodies. J Comp Physiol A 185:115–129.

Okada R, Rybak J, Manz G, Menzel R (2007) Learning-related plasticity in PE1 and other mushroom body-extrinsic neurons in the honeybee brain. J Neurosci 27:11736–11747.

Olsen SR, Wilson RI (2008) Lateral presynaptic inhibition mediates gain control in an olfactory circuit. Nature 452:956–960.

Olshausen BA, Field DJ (2004) Sparse coding of sensory inputs. Curr Opin Neurobiol 14:481–487.

OShea M, Colbert R, Williams L, Dunn S (1998) Nitric oxide compartments in the mushroom bodies of the locust brain. Neuroreport 9:333–336.

Owald D, Felsenberg J, Talbot CB, et al (2015) Activity of defined mushroom body output neurons underlies learned olfactory behavior in *Drosophila*. Neuron 86:417–427.

Papadopoulou M (2010) Gain control and sparse representations in the olfactory system of the locust and fly. California Institute of Technology

Papadopoulou M, Cassenaer S, Nowotny T, Laurent G (2011) Normalization for sparse encoding of odors by a wide-field interneuron. Science 332:721–725.

Park D, Jung JW, Choi B-S, et al (2015) Uncovering the novel characteristics of Asian honey bee, *Apis cerana*, by whole genome sequencing. BMC Genomics 16:1.

Parrish-Aungst S, Shipley MT, Erdelyi F, et al (2007) Quantitative analysis of neuronal diversity in the mouse olfactory bulb. J Comp Neurol 501:825–836.

Peele P, Ditzen M, Menzel R, Galizia CG (2006) Appetitive odor learning does not change olfactory coding in a subpopulation of honeybee antennal lobe neurons. J Comp Physiol A 192:1083–1103.

Perez-Orive J, Bazhenov M, Laurent G (2004) Intrinsic and circuit properties favor coincidence detection for decoding oscillatory input. J Neurosci 24:6037–6047.

Perez-Orive J, Mazor O, Turner GC, et al (2002) Oscillations and sparsening of odor representations in the mushroom body. Science 297:359–365.

Phelps EA (2004) Human emotion and memory: interactions of the amygdala and hippocampal complex. Curr Opin Neurobiol 14:198–202.

Pitman JL, Huetteroth W, Burke CJ, et al (2011) A pair of inhibitory neurons are required to sustain labile memory in the *Drosophila* mushroom body. Curr Biol 21:855–861.

Porter J, Craven B, Khan RM, et al (2007) Mechanisms of scent-tracking in humans. Nat Neurosci 10:27–29.

Pregitzer P, Jiang X, Grosse-Wilde E, et al (2017) In search for pheromone receptors: certain members of the odorant receptor family in the desert locust *Schistocerca gregaria* (Orthoptera: Acrididae) are co-expressed with SNMP1. Int J Biol Sci 13:911.

Preibisch S, Saalfeld S, Tomancak P (2009) Globally optimal stitching of tiled 3D microscopic image acquisitions. Bioinformatics 25:1463–1465.

Rabinovich M, Volkovskii A, Lecanda P, et al (2001) Dynamical encoding by networks of competing neuron groups: winnerless competition. Phys Rev Lett 87:068102.

Rabinovich MI, Huerta R, Volkovskii A, et al (2000) Dynamical coding of sensory information with competitive networks. J Physiol-Paris 94:465–471.

Rajan R, Clement JP, Bhalla US (2006) Rats smell in stereo. Science 311:666–670.

Ramaekers A, Parmentier M-L, Lasnier C, et al (2001) Distribution of metabotropic glutamate receptor DmGlu-A in *Drosophila melanogaster* central nervous system. J Comp Neurol 438:213–225.

Raman B, Joseph J, Tang J, Stopfer M (2010) Temporally diverse firing patterns in olfactory receptor neurons underlie spatiotemporal neural codes for odors. J Neurosci 30:1994–2006.

Rand D, Knebel D, Ayali A (2012) The effect of octopamine on the locust stomatogastric nervous system. Front Physiol 3:288.

Ray S, Aldworth ZN, Stopfer MA (2020) Feedback inhibition and its control in an insect olfactory circuit. Elife 9:e53281.

Richard MB, Taylor SR, Greer CA (2010) Age-induced disruption of selective olfactory bulb synaptic circuits. Proc Natl Acad Sci 107:15613–15618.

Riffell, J.A., Abrell, L., Hildebrand, J.G., 2008. Physical processes and real-time chemical measurement of the insect olfactory environment. Journal of chemical ecology 34, 837–853.

Rø H, Müller D, Mustaparta H (2007) Anatomical organization of antennal lobe projection neurons in the moth *Heliothis virescens*. J Comp Neurol 500:658–675.

Robertson HM, Wanner KW (2006) The chemoreceptor superfamily in the honey bee, *Apis mellifera*: Expansion of the odorant, but not gustatory, receptor family. Genome Res 16:1395–1403.

Robertson HM, Warr CG, Carlson JR (2003) Molecular evolution of the insect chemoreceptor gene superfamily in *Drosophila melanogaster*. Proc Natl Acad Sci 100:14537–14542.

Römer H, Marquart V, Hardt M (1988) Organization of a sensory neuropile in the auditory pathway of two groups of Orthoptera. J Comp Neurol 275:201–215.

Roonwal ML (1952) Variation and post-embryonic growth in the number of antennal segments in the phadka grasshopper (*Hieroglyphus nigrorepletus* bolivar), with remarks on the desert locust and other acrididae (insecta: orthoptera). In: Proceedings of the National Institute of Sciences of India. National Institute of Sciences of India, p 217.

Rospars JP (1983) Invariance and sex-specific variations of the glomerular organization in the antennal lobes of a moth, *Mamestra brassicae*, and a butterfly, *Pieris brassicae*. J Comp Neurol 220:80–96.

Rospars JP, Hildebrand JG (2000) Sexually dimorphic and isomorphic glomeruli in the antennal lobes of the Sphinx moth *Manduca sexta*. Chem Senses 25:119–129.

Rössler W, Zube C (2011) Dual olfactory pathway in Hymenoptera: evolutionary insights from comparative studies. Arthropod Struct Dev 40:349–357.

Royet J-P, Distel H, Hudson R, Gervais R (1998) A re-estimation of the number of glomeruli and mitral cells in the olfactory bulb of rabbit. Brain Res 788:35–42.

Ruta V, Datta SR, Vasconcelos ML, et al (2010) A dimorphic pheromone circuit in *Drosophila* from sensory input to descending output. Nature 468:686–690.

Rybak J (2012) in Honeybee neurobiology and behavior, The digital honey bee brain atlas, eds Galizia CG, Eisenhardt D, Giurfa M (Springer Netherlands, Dordrecht, Netherlands), pp 125–140.

Rybak J, Menzel R (1993) Anatomy of the mushroom bodies in the honey bee brain: the neuronal connections of the alpha-lobe. J Comp Neurol 334:444–465.

Rybak J, Menzel R (1998) Integrative properties of the Pe1 neuron, a unique mushroom body output neuron. Learn Mem 5:133–145.

Sachse S, Galizia CG (2002) Role of inhibition for temporal and spatial odor representation in olfactory output neurons: A calcium imaging study. J Neurophysiol 87:1106–1117.

Sachse S, Krieger J (2017) Olfaction in insects. E-Neuroforum 17:49–60.

Sadd BM, Barribeau SM, Bloch G, et al (2015) The genomes of two key bumblebee species with primitive eusocial organization. Genome Biol 16:76.

Sanda P, Kee T, Gupta N, et al (2016) Classification of odorants across layers in locust olfactory pathway. J Neurophysiol 115:2303–2316.

Sandoz J-C, Menzel R (2001) Side-specificity of olfactory learning in the honeybee: generalization between odors and sides. Learn Mem 8:286–294.

Sanes JR, Hildebrand JG (1976) Acetylcholine and its metabolic enzymes in developing antennae of the moth, *Manduca sexta*. Dev Biol 52:105–120.

Sato K, Pellegrino M, Nakagawa T, et al (2008) Insect olfactory receptors are heteromeric ligand-gated ion channels. Nature 452:1002.

Schäfer S, Bicker G (1986) Distribution of GABA-like immunoreactivity in the brain of the honeybee. J Comp Neurol 246:287–300.

Schäfer S, Bicker G, Ottersen OP, Storm-Mathisen J (1988) Taurine-like immunoreactivity in the brain of the honeybee. J Comp Neurol 268:60–70.

Schenk O (1903) Die antennen Hautsinnesorgane einiger Lepidoptera und Hymenoptera. Zool Jb Anat 17:573–618.

Schildberger K (1984) Multimodal interneurons in the cricket brain: properties of identified extrinsic mushroom body cells. J Comp Physiol A 154:71–79.

Schindelin J, Arganda-Carreras I, Frise E, et al (2012) Fiji: an open-source platform for biological-image analysis. Nat Methods 9:676–682.

Schlief ML, Wilson RI (2007) Olfactory processing and behavior downstream from highly selective receptor neurons. Nat Neurosci 10:623–630.

Schuermann F-W (2016) Fine structure of synaptic sites and circuits in mushroom bodies of insect brains. Arthropod Struct Dev 45:399–421.

Schultzhaus JN, Saleem S, Iftikhar H, Carney GE (2017) The role of the *Drosophila* lateral horn in olfactory information processing and behavioral response. J Insect Physiol 98:29–37.

Schümperli RA (1975) Monocular and binocular visual fields of butterfly interneurons in response to white- and coloured-light stimulation. J Comp Physiol 103:273–289.

Schürmann FW (2000) Acetylcholine, GABA, glutamate and NO as putative transmitters indicated by immunocytochemistry in the olfactory mushroom body system of the insect brain. Acta Biol Hung 51:355–362.

Schürmann FW (1987) The architecture of the mushroom bodies and related neuropils in the insect brain. Arthropod Brain Its Evol Struct Funct 231–264.

Seki Y, Aonuma H, Kanzaki R (2005) Pheromone processing center in the protocerebrum of *Bombyx mori* revealed by nitric oxide-induced anti-cGMP immunocytochemistry. J Comp Neurol 481:340–351.

Shang Y, Claridge-Chang A, Sjulson L, et al (2007) Excitatory local circuits and their implications for olfactory processing in the fly antennal lobe. Cell 128:601–612.

Shields V, Hildebrand JG (1999a) Fine structure of antennal sensilla of the female sphinx moth, *Manduca sexta* (Lepidoptera: Sphingidae). II. Auriculate, coeloconic, and styliform complex sensilla. Can J Zool 77:302–313.

Shields V, Hildebrand JG (1999b) Fine structure of antennal sensilla of the female sphinx moth, *Manduca sexta* (Lepidoptera: Sphingidae). I. Trichoid and basiconic sensilla. Can J Zool 77:290–301.

Shields VDC, Hildebrand JG (2001) Recent advances in insect olfaction, specifically regarding the morphology and sensory physiology of antennal sensilla of the female sphinx moth *Manduca sexta*. Microsc Res Tech 55:307–329.

Shin D, Cho K-H (2013) Recurrent connections form a phase-locking neuronal tuner for frequency-dependent selective communication. Sci Rep 3:1–8.

Shu Y, Hasenstaub A, McCormick DA (2003) Turning on and off recurrent balanced cortical activity. Nature 423:288–293.

Silbering AF, Galizia CG (2007) Processing of odor mixtures in the *Drosophila* antennal lobe reveals both global inhibition and glomerulus-specific interactions. J Neurosci 27:11966–11977.

Sinakevitch I, Bjorklund GR, Newbern JM, et al (2018) Comparative study of chemical neuroanatomy of the olfactory neuropil in mouse, honey bee, and human. Biol Cybern 1–14.

Sinakevitch I, Farris SM, Strausfeld NJ (2001) Taurine-, aspartate- and glutamate-like immunoreactivity identifies chemically distinct subdivisions of Kenyon cells in the cockroach mushroom body. J Comp Neurol 439:352–367.

Singh S, Joseph J (2019) Evolutionarily conserved anatomical and physiological properties of olfactory pathway through fourth-order neurons in a species of grasshopper (*Hieroglyphus banian*). J Comp Physiol A 205:813–838.

Song H (2004) On the origin of the desert locust *Schistocerca gregaria* (Forsk\aal)(Orthoptera: Acrididae: Cyrtacanthacridinae). Proc R Soc Lond B Biol Sci 271:1641–1648.

Song H, Mariño-Pérez R, Woller DA, Cigliano MM (2018) Evolution, diversification, and biogeography of grasshoppers (Orthoptera: Acrididae). Insect Syst Divers 2:3.

Squitier JM, Capinera JL (1996) American grasshopper - *Schistocerca americana* (Drury). http://entnemdept.ufl.edu/creatures/field/american_grasshopper.htm. Accessed 16 Aug 2018.

Stengl M, Homberg U, Hildebrand JG (1990) Acetylcholinesterase activity in antennal receptor neurons of the sphinx moth *Manduca sexta*. Cell Tissue Res 262:245–252.

Stengl M, Zeigelberger G, Boekhoff I, et al (1999) Perireceptor events and transduction mechanisms in insect olfaction. In: Insect Olfaction. Springer-Verlag Berlin Heidelberg GmbH, pp 49–66.

Stocker RF (1994) The organization of the chemosensory system in *Drosophila melanogaster*: a review. Cell Tissue Res 275:3–26.

Stocker RF, Heimbeck G, Gendre N, de Belle JS (1997) Neuroblast ablation in *Drosophila* P [GAL4] lines reveals origins of olfactory interneurons. J Neurobiol 32:443–456.

Stocker RF, Lienhard MC, Borst A, Fischbach KF (1990) Neuronal architecture of the antennal lobe in *Drosophila melanogaster*. Cell Tissue Res 262:9–34.

Stopfer M, Jayaraman V, Laurent G (2003) Intensity versus identity coding in an olfactory system. Neuron 39:991–1004.

Stopfer M, Laurent G (1999) Short-term memory in olfactory network dynamics. Nature 402:664–668

Stopfer M, Wehr M, MacLeod K, Laurent G (1999) Neural dynamics, oscillatory synchronisation, and odour codes. In: Insect olfaction. Springer, pp 163–180.

Strausfeld NJ (2002) Organization of the honey bee mushroom body: Representation of the calyx within the vertical and gamma lobes. J Comp Neurol 450:4–33.

Strausfeld NJ, Hansen L, Li Y, et al (1998) Evolution, discovery, and interpretations of arthropod mushroom bodies. Learn Mem 5:11–37.

Strausfeld NJ, Hildebrand JG (1999) Olfactory systems: common design, uncommon origins? Curr Opin Neurobiol 9:634–639.

Strausfeld NJ, Li Y (1999) Organization of olfactory and multimodal afferent neurons supplying the calyx and pedunculus of the cockroach mushroom bodies. J Comp Neurol 409:603–625.

Strausfeld NJ, Sinakevitch I, Brown SM, Farris SM (2009) Ground plan of the insect mushroom body: Functional and evolutionary implications. J Comp Neurol 513:265–291.

Strausfeld NJ, Sinakevitch I, Vilinsky I (2003) The mushroom bodies of *Drosophila melanogaster*: an immunocytological and golgi study of Kenyon cell organization in the calyces and lobes. Microsc Res Tech 62:151–169.

Strube-Bloss MF, Brown A, Spaethe J, et al (2015) Extracting the behaviorally relevant stimulus: unique neural representation of farnesol, a component of the recruitment pheromone of *Bombus terrestris*. PloS One 10:e0137413.

Strube-Bloss MF, Nawrot MP, Menzel R (2011) Mushroom body output neurons encode odorreward associations. J Neurosci 31:3129–3140.

Suzuki H (1975) Convergence of olfactory inputs from both antennae in the brain of the honeybee. J Exp Biol 62:11–26.

Szyszka P, Ditzen M, Galkin A, et al (2005) Sparsening and temporal sharpening of olfactory representations in the honeybee mushroom bodies. J Neurophysiol 94:3303–3313.

Takahashi N, Katoh K, Watanabe H, et al (2017) Complete identification of four giant interneurons supplying mushroom body calyces in the cockroach *Periplaneta americana*. J Comp Neurol 525:204–230.

Takahashi N, Nishino H, Domae M, Mizunami M (2019) Separate but interactive parallel olfactory processing streams governed by different types of GABAergic feedback neurons in the mushroom body of a basal insect. J Neurosci 39:8690–8704.

Tanaka NK, Awasaki T, Shimada T, Ito K (2004) Integration of chemosensory pathways in the *Drosophila* second-order olfactory centers. Curr Biol 14:449–457.

Tanaka NK, Endo K, Ito K (2012a) Organization of antennal lobe-associated neurons in adult *Drosophila melanogaster* brain. J Comp Neurol 520:4067–4130.

Tanaka NK, Ito K, Stopfer M (2009) Odor-evoked neural oscillations in *Drosophila* are mediated by widely branching interneurons. J Neurosci 29:8595–8603.

Tanaka NK, Suzuki E, Dye L, et al (2012b) Dye fills reveal additional olfactory tracts in the protocerebrum of wild-type *Drosophila*. J Comp Neurol 520:4131–4140.

Tanaka NK, Tanimoto H, Ito KEI (2008) Neuronal assemblies of the *Drosophila* mushroom body. J Comp Neurol 508:711–755.

Turner GC, Bazhenov M, Laurent G (2008) Olfactory representations by *Drosophila* mushroom body neurons. J Neurophysiol 99:734–746.

Varela N, Gaspar M, Dias S, Vasconcelos ML (2019) Avoidance response to CO2 in the lateral horn. PLOS Biol 17:e2006749.

Vijaykumar M, Mogily S, Dutta-Gupta A, Joseph J (2019) Evidence for absence of bilateral transfer of olfactory learned information in Apis dorsata and Apis mellifera. J Exp Biol 222:.

von Hadeln J, Althaus V, Häger L, Homberg U (2018) Anatomical organization of the cerebrum of the desert locust *Schistocerca gregaria*. Cell Tissue Res 374:39–62.

Vosshall LB, Amrein H, Morozov PS, et al (1999) A spatial map of olfactory receptor expression in the *Drosophila* antenna. Cell 96:725–736.

Vosshall LB, Wong AM, Axel R (2000) An olfactory sensory map in the fly brain. Cell 102:147–159.

Waldrop B, Christensen TA, Hildebrand JG (1987) GABA-mediated synaptic inhibition of projection neurons in the antennal lobes of the sphinx moth, *Manduca sexta*. J Comp Physiol A 161:23–32.

Waldrop B, Hildebrand JG (1989) Physiology and pharmacology of acetylcholinergic responses of interneurons in the antennal lobes of the moth *Manduca sexta*. J Comp Physiol A Neuroethol Sens Neural Behav Physiol 164:433–441.

Wang K, Gong J, Wang Q, et al (2014) Parallel pathways convey olfactory information with opposite polarities in *Drosophila*. Proc Natl Acad Sci 111:3164–3169.

Wang Y, Guo H-F, Pologruto TA, et al (2004) Stereotyped odor-evoked activity in the mushroom body of *Drosophila* revealed by green fluorescent protein-based Ca2+ imaging. J Neurosci 24:6507–6514.

Watanabe H, Nishino H, Nishikawa M, et al (2010) Complete mapping of glomeruli based on sensory nerve branching pattern in the primary olfactory center of the cockroach *Periplaneta americana*. J Comp Neurol 518:3907–3930.

Wehr M, Laurent G (1996) Odour encoding by temporal sequences of firing in oscillating neural assemblies. Nature 384:162.

Wehr M, Laurent G (1999) Relationship between afferent and central temporal patterns in the locust olfactory system. J Neurosci 19:381–390.

Weiss MJ (1974) Neuronal connections and the function of the corpora pedunculata in the brain of the American cockroach, *Periplaneta americana* (L.). J Morphol 142:21–69.

Weiss MJ (1981) Structural patterns in the corpora pedunculata of Orthoptera: a reduced silver analysis. J Comp Neurol 203:515–553.

Wicher D, Schäfer R, Bauernfeind R, et al (2008) *Drosophila* odorant receptors are both ligand-gated and cyclic-nucleotide-activated cation channels. Nature 452:1007.

Wilson RI, Laurent G (2005) Role of GABAergic inhibition in shaping odor-evoked spatiotemporal patterns in the *Drosophila* antennal lobe. J Neurosci 25:9069–9079.

Wilson RI, Mainen ZF (2006) Early events in olfactory processing. Annu Rev Neurosci 29:163–201.

Wilson RI, Turner GC, Laurent G (2004) Transformation of olfactory representations in the *Drosophila* antennal lobe. Science 303:366–370.

Witthöft W (1967) Absolute anzahl und verteilung der zellen im him der honigbiene. Z Für Morphol Tiere 61:160–184.

Wong AM, Wang JW, Axel R (2002) Spatial representation of the glomerular map in the *Drosophila* protocerebrum. Cell 109:229–241.

Wu C-L, Shih M-FM, Lee P-T, Chiang A-S (2013) An octopamine-mushroom body circuit modulates the formation of anesthesia-resistant memory in *Drosophila*. Curr Biol 23:2346–2354.

Wu Y, Ren Q, Li H, Guo A (2012) The GABAergic anterior paired lateral neurons facilitate olfactory reversal learning in *Drosophila*. Learn Mem 19:478–486.

Xiang Z, Mita K, Xia Q, The International silkworm genome consortium (2008) The genome of a lepidopteran model insect, the silkworm *Bombyx mori*. Insect Biochem Mol Biol 38:1036–1045.

Yamazaki Y, Nishikawa M, Mizunami M (1998) Three classes of GABA-like immunoreactive neurons in the mushroom body of the cockroach. Brain Res 788:80–86.

Yan Z, Tan J, Qin C, et al (2008) Precise circuitry links bilaterally symmetric olfactory maps. Neuron 58:613–624.

Yasuyama K, Meinertzhagen IA, Schürmann F-W (2002) Synaptic organization of the mushroom body calyx in *Drosophila melanogaster*. J Comp Neurol 445:211–226.

Yasuyama K, Salvaterra PM (1999) Localization of choline acetyltransferase-expressing neurons in *Drosophila* nervous system. Microsc Res Tech 45:65–79.

Zhang K, Guo JZ, Peng Y, et al (2007a) Dopamine-mushroom body circuit regulates saliency-based decision-making in *Drosophila*. Science 316:1901–1904.

Zhang X, Zhang X, Firestein S (2007b) Comparative genomics of odorant and pheromone receptor genes in rodents. Genomics 89:441–450.

Zhao X-C, Chen Q-Y, Guo P, et al (2016) Glomerular identification in the antennal lobe of the male moth *Helicoverpa armigera*. J Comp Neurol 524:2993–3013.

Zheng J, Stevenson RF, Mander BA, et al (2019) Multiplexing of theta and alpha rhythms in the amygdala-hippocampal circuit supports pattern separation of emotional information. Neuron 102:887-898.e5.

Zhou M, Chen N, Tian J, et al (2019) Suppression of GABAergic neurons through D2-like receptor secures efficient conditioning in *Drosophila* aversive olfactory learning. Proc Natl Acad Sci 116:5118–5125.

Zhu JJ, Lo F-S (2000) Recurrent inhibitory circuitry in the deep layers of the rabbit superior colliculus. J Physiol 523:731–740.

Zube C, Kleineidam CJ, Kirschner S, et al (2008) Organization of the olfactory pathway and odor processing in the antennal lobe of the ant *Camponotus floridanus*. J Comp Neurol 506:425–441.

Zwaka H, Bartels R, Grünewald B, Menzel R (2018) Neural organization of A3 mushroom body extrinsic neurons in the honeybee brain. Front Neuroanat 12:57.

Zwaka H, Münch D, Manz G, et al (2016) The circuitry of olfactory projection neurons in the brain of the honeybee, *Apis mellifera*. Front Neuroanat 10:90.

Characterization of the olfactory circuit and computation in an insect Hieroglyphus banian

by Shilpi Singh's Shilpi Singh

Submission date: 31-Dec-2020 04:38AM (UTC+0530)

Submission ID: 1482163707

File name: Shilpi Singh PhD thesis CNCS.pdf (6.18M)

Word count: 38869

Character count: 195436

Characterization of the olfactory circuit and computation in an insect Hieroglyphus banian

ORIGINALITY REPORT

19%

3%

19%

0%

SIMILARITY INDEX

INTERNET SOURCES

PUBLICATIONS

STUDENT PAPERS

PRIMARY SOURCES

Shilpi Singh, Joby Joseph. "Evolutionarily conserved anatomical and physiological properties of olfactory pathway through fourth-order neurons in a species of grasshopper (Hieroglyphus banian)", Journal of Comparative Physiology A, 2019

11%

Publication

Shilpi Singh, Joby Joseph. "Evolutionarily conserved anatomical and physiological properties of olfactory pathway till fourth order neurons in a species of grasshopper ", Cold Spring Harbor Laboratory, 2018

4%

Publication

Publication

"Insect Olfaction", Springer Nature, 1999

<1%

4

thesis.library.caltech.edu

Internet Source

<1%

5

"Olfactory Concepts of Insect Control - Alternative to insecticides", Springer Science

<1%



PLAGIARISM-FREE CERTIFICATE

This is to certify that the similarity index of this thesis (excluding bibliographic content) as checked by the library of University of Hyderabad is 19 %.

Out of this, similarity of 15 % has been found to be identified from the candidate, Shilpi Singh's own publications as first author which forms a part of her thesis. The details of student's publication are as follows:

Singh S, Joseph J (2019) Evolutionarily conserved anatomical and physiological properties of olfactory pathway through fourth-order neurons in a species of grasshopper (*Hieroglyphus banian*). Journal of Comparative Physiology A 205:813–838. **Similarity index: 11** %

Shilpi Singh, Joby Joseph. "Evolutionarily conserved anatomical and physiological properties of olfactory pathway till fourth order neurons in a species of grasshopper", Cold Spring Harbor Laboratory, 2018. (https://doi.org/10.1101/436626) Similarity index: 4 %

About 4 % similarity was identified from external sources, which is in accordance with the norms of the University.

Hence, the present thesis may be considered to be plagiarism free.

Dr. Joby Joseph Supervisor Centre for Neural and Cognitive Sciences University of Hyderabad

ORIGINAL PAPER



Evolutionarily conserved anatomical and physiological properties of olfactory pathway through fourth-order neurons in a species of grasshopper (*Hieroglyphus banian*)

Shilpi Singh¹ • Joby Joseph¹

Received: 4 October 2018 / Revised: 8 August 2019 / Accepted: 4 September 2019 / Published online: 18 September 2019 © Springer-Verlag GmbH Germany, part of Springer Nature 2019

Abstract

Olfactory systems of different species show variations in structure and physiology despite some conserved features. We characterized the olfactory circuit of the grasshopper *Hieroglyphus banian* of family Acrididae (subfamily: Hemiacridinae) and compared it to a well-studied species of locust, *Schistocerca americana* (subfamily: Cyrtacanthacridinae), also belonging to family Acrididae. We used in vivo electrophysiological, immunohistochemical, and anatomical (bulk tract tracing) methods to elucidate the olfactory pathway from the second-order neurons in antennal lobe to the fourth-order neurons in β-lobe of *H. banian*. We observe conserved anatomical and physiological characteristics through the fourth-order neurons in the olfactory circuit of *H. banian* and *S. americana*, though they are evolutionarily divergent (~57 million years ago). However, we found one major difference between the two species—there are four antennal lobe tracts in *H. banian*, while only one is reported in *S. americana*. Besides, we have discovered a new class of bilateral neurons which respond weakly to olfactory stimuli, even though they innervate densely downstream of Kenyon cells.

Keywords Olfactory coding · Schistocerca americana · Comparative neuroanatomy · Mushroom body · Insect brain

Abbreviations		LOG
ACA	Accessory calyx	LFP
AL	Antennal lobe	LN
bLN	β-Lobe neuron	mAL7
CA	Calyx of mushroom body	mlAL
CT	Curved tract	mPN
EPSP	Excitatory postsynaptic potential	MB
FE-SEM	Field-emission scanning electron microscopy	MBE
GGN	Giant GABAergic neuron	OR
IG	Inhibitor of GGN	ORN
IPSP	Inhibitory postsynaptic potential	PSTH
KC	Kenyon cell	PN
IALT	Lateral antennal lobe tract	SL
LH	Lateral horn	tALT
LHN	Lateral horn neuron	TT
		пPN

Electronic supplementary material The online version of this article (https://doi.org/10.1007/s00359-019-01369-7) contains supplementary material, which is available to authorized users.

LFP Local field potential
LN Local neuron
mALT Medial antennal lobe tract
mlALT Mediolateral antennal lobe tract
mPN Multiglomerular projection neuron

Lobus glomerulus

MB Mushroom body
MBEN Mushroom body extrinsic neuron

OR Olfactory receptor
ORN Olfactory receptor neuron
PSTH Peri-stimulus time histogram

PN Projection neuron

SL Soma/cell body layer of mushroom body

tALT Transverse antennal lobe tract

TT Tritocerebral tract

uPN Uniglomerular projection neuron

Introduction

Sensory systems have been well studied across insect species from many orders to elucidate principles underlying their physiology and anatomy. One of the major aims for doing so is to throw light over how the brain represents information



[✓] Joby Joseph

jjcncs@uohyd.ac.in

Centre for Neural and Cognitive Sciences, University of Hyderabad, Hyderabad, India





5th Congress of Federation of Asian-Oceanian Neuroscience Societies

XXVIII Annual Meeting of Indian Academy of Neurosciences

November 25 - 28, 2010, Lucknow, India

The Organizing Committee acknowledges the participation and scientific contribution

Shillipi Singh Hydenobad, India

in the scientific programme of the Congress.

Vivay Kumar Khanna

Vinay K. Khanna **Organizing Secretary**

B.N. Dhawan Chiarman, Organizing Committee

P.K. Seth President, FAONS



Ø

25th Annual Meeting of Society for Neurochemistry, India (SNCI)



and International Symposium on

"Metabolic Signaling in Brain in Health and Diseases" Jan 7th - 9th, 2011

Silver Jubilee Celebrations

Certificate of Participation

We have the	pleasure to	confirm the	e participa	tion of	
r/Mr/Ms	Singh	Shill	wi	114	in the

International Conference and presented Pleany / Invited / Oral /

Poster entitled IMPLICATIONS OF IN NUERONAL SYSTEMS.

Prof. P. Prakash Babu Organizing Secretary



National Brain Research Centre (Doemed University) Maneser 122 050, Haryana

Certificate of Participation

"Fourth DST-SERC School on Systems and Cognitive Neuroscience"

This is to certify that Shilpi Singh, CNCS, University of Hyderabad has participated in the Fourth DST-SERC School on Systems and Cognitive Neuroscience held at NBRC from Feb 21st to March 6th, 2011

Dr Soumya Iyengar Course Co-cordinator Prof Neeraj Jain Course Co-cordinator

Prof Subrata Sinha Director, National Brain Research Centre

Subject Sul



Certificate

This is to certify that Ms. Shilpi Singh attended the IBRO-UNESCO Inter-Regional School on Computational and Theoretical Neuroscience organized by Centre for Neural and Cognitive Sciences, University of Hyderabad from 5th to 21st December 2012.

Date: 21/12/2012

Chairman

International Symposium on Translational Neuroscience and

XXXII Annual Conference of Indian Academy of Neurosciences

Translational Research: Novel Approaches to treat Neurological and Psychiatric disorders

IAN 2014

1st - 3rd November 2014

National Institute of Mental Health and Neuro Sciences (NIMHANS), Bengaluru, India

CERTIFICATE

This is to certify that Prof./Dr./Mr./Ms. Shilpi Singh
has attended the conference as a Key note Speaker / Plenary Speaker / Chairperson /
Symposium Speaker / Delegate and Presented paper (Oral / Poster) during the conference.

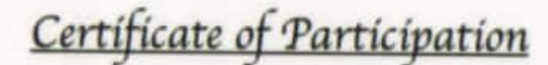
Dr. Laxmi T Rao Scientific Committee, Chairperson Dr. TN Sathyaprabha Joint - Organizing Secretary

Dr. BS Shankaranarayana Rao Organizing Secretary



National Conference on Ethology and Evolution

(39th Annual Meeting of Ethological Society of India)



This is to certify that Ms/Mr/Dr. Shilpi Singh
of. University of Hyderabad participated in the
National Conference on Ethology and Evolution held at
Indian Institute of Science Education and Research Mohali

between 30th October and 1st November 2015.

Secretary, ESI

Organiser, NCEE



भारतीय विज्ञान शिक्षा एवं अनुसंधान संस्थान कोलकाता INDIAN INSTITUTE OF SCIENCE EDUCATION AND RESEARCH KOLKATA

This is to certify that

SHILPI SINGH

affiliated with

UNIVERSITY OF HYDERABAD

has participated in the Workshop on Mathematical and Computational Biology 2016

held on 9 & 10 January 2016 at IISER Kolkata.

Date: January 10, 2016

Organizer WMCB -2016

Place: Mohanpur Campus, IISER Kolkata

